STATE OF CALIFORNIA - NATURAL RESOURCES AGENCY GAVIN NEWSOM, *GOVERNOR*

CALIFORNIA COASTAL COMMISSION
455 MARKET STREET, SUITE 228
SAN FRANCISCO, CA 94105-2219
FAX (415) 904-5400
TDD (415) 597-5885

Th12a

E-00-014-A2 (SONGS)

OCTOBER 13, 2022

CORRESPONDENCE

Received between

September 23, 2022 and October 7, 2022

Table of Contents

E-00-014-A2 (SONGS)

OCTOBER 13, 2022

CORRESPONDENCE:

Letters from Elected

Officials and Organizations

SOUTHERN CALIFORNIA
EDISON
An EDISON INTERNATIONAL℠ Company

Jessica Rankin
Senior Attorney
Jessica.Rankin@sce.com

October 7, 2022

Holly Wyer
Senior Environmental Scientist
Energy, Ocean Resources and Federal Consistency
California Coastal Commission
455 Market Street, Suite 300
San Francisco, CA 94105
EORFC@coastal.ca.gov

Re: CDP E-00-014-A2, Application to Amend the 2001 SONGS NUHOMS ISFSI CDP

Dear Ms. Wyer:

On behalf of Southern California Edison Company (SCE), San Diego Gas & Electric, the City of Anaheim, and the City of Riverside (collectively, the Participants), this letter provides comments on the Staff Report for the Application to Amend the 2001 San Onofre Nuclear Generating Station (SONGS) NUHOMS Independent Spent Fuel Storage Installation (ISFSI) Coastal Development Permit, No. E-00-014-A2 (the CDP Amendment Application).

The Participants appreciate the Coastal Commission staff's detailed review of the CDP Amendment Application. We agree with the analysis, findings and special conditions contained in the Staff Report and offer the following information for consideration by Coastal Commission staff. In addition, the enclosed table (Attachment A) includes minor comments, which are primarily technical corrections and clarifications to the Staff Report.

I. The CDP Amendment is Consistent with All Applicable Coastal Act Policies

The Participants appreciate Coastal Commission staff's thorough analysis of potential impacts on coastal resources, and staff's recommendation that the Coastal Commission find that the CDP Amendment Application is consistent with the relevant policies of the Coastal Act.

As the Staff Report notes, the NUHOMS ISFSI is an existing development that was constructed under the 2001 CDP No. E-00-014 (the 2001 CDP), and no new construction is proposed as part of the CDP Amendment Application. Prior to approving the 2001 CDP, the Coastal Commission undertook a thorough review of the Coastal Act policies and determined that with the incorporated conditions, the NUHOMS ISFSI was consistent with the Coastal Act.

In the two decades since the 2001 CDP was approved, SCE has complied with all Coastal Commission conditions concerning spent fuel storage at SONGS. Since no new construction is proposed as part of the CDP Amendment Application, this approval will not result in any impacts to the following coastal resources previously assessed by the Coastal Commission: public access/recreation, environmentally sensitive habitat areas, visual quality and air quality.[1] In addition, as discussed below and at pages 17-36 of the staff report, Commission staff focused on changed conditions or new information that has come to light since the 2001 CDP and carefully reevaluated potential impacts to geologic and coastal hazards, marine resources and water quality, environmental justice, and visual resources and properly concluded that, as conditioned, the CDP Amendment Application is consistent with the Coastal Act.

Approval of the CDP Amendment Application will also strengthen the special conditions from the 2001 CDP by incorporating conditions from the 2015 Holtec ISFSI CDP (which approved the later-built ISFSI at SONGS), plus a new Special Condition 7, which requires SCE to provide biennial reports on efforts to move the spent fuel offsite. The special conditions provide robust protection for the environment, including coastal resources, particularly considering that no new construction is being proposed.

II. The NUHOMS ISFSI Aging Management Program Will Ensure the Canisters Remain Transportable

One of the new special conditions taken from the 2015 Holtec ISFSI CDP is Special Condition 6, which provides for Coastal Commission staff review of the NUHOMS ISFSI's Aging Management Program (AMP) and implementing procedures. The Participants support Special Condition 6 to ensure that the Coastal Commission is fully informed of the methods for assuring that the spent fuel canisters will remain transportable to an offsite location. As explained in the Staff Report, the AMP and SCE's implementing procedures relate to, among other things, spent fuel canister inspection techniques, physical condition of the canisters, and remediation measures, should any be needed.

At the time of the approval of the 2015 Holtec ISFSI CDP, the Holtec ISFSI did not yet have an AMP in place because the NRC does not require one until license renewal after the first 20 years of service. (See 10 CFR 72.240.) As a result, the 2015 Holtec CDP special condition required SCE to prepare and obtain Coastal Commission approval of an Inspection and Maintenance Program (IMP) designed to provide assurance that the Holtec canisters would remain transportable until the Holtec ISFSI's NRC-approved AMP is in place (*i.e.,* by around 2035). After receiving input from an independent third-party review, the Coastal Commission approved the Holtec IMP in 2020, and it remains in effect today.

In contrast, the NUHOMS ISFSI has been in service for almost 20 years and its NRC-approved AMP, which was provided to Coastal Commission staff by email on September 19, 2022 along with documentation confirming the NRC's approval, is now in place. As implemented at SONGS, the NUHOMS AMP provides the same information the Holtec IMP was designed to provide. Therefore, the Participants agree that it makes sense for Coastal Commission staff to

---

[1] See 2001 NUHOMS ISFSI CDP Final Adopted Findings, a copy of which was submitted with the NUHOMS CDP Amendment Application.

review the NRC-approved AMP and implementing procedures as part of Special Condition 6, rather than a duplicative IMP that would provide the same information.

Through the AMP and SCE's implementing procedures, SCE will conduct frequent and comprehensive inspections of the NUHOMS ISFSI at SONGS. The baseline inspection for the NUHOMS AMP was performed in 2021, and it confirmed that the canisters do not show any signs of degradation. Going forward, two canisters will be inspected every five years, with the next inspection in 2026. Results of the inspections will be reported to the Coastal Commission as described in Special Condition 6.

As part of the upcoming Special Condition 6 review, it is important to note that the NUHOMS ISFSI AMP is not an SCE document – it was approved as part of the NRC license renewal application submitted by the ISFSI vendor TN/Orano, and the AMP remains in effect until the next NRC license period begins in about 2041. However, SCE does have control over the implementing procedures, which describe how SCE will implement the AMP. If, through the Special Condition 6 review process, Coastal Commission staff or its independent reviewer requests changes to the NUHOMS ISFSI aging management program to make it even more conservative than the NRC-approved AMP, SCE would do so by modifying its implementing procedures and would submit the modified procedures to the Executive Director for review and approval.

III. The Location Remains Appropriate Based on a Thorough Scientific Analysis

As discussed in the CDP Amendment Application, the NUHOMS ISFSI location remains appropriate based on the Coastal Commission's previous analyses of the ISFSI site in 2001 and 2015 and current science.

For this application, Coastal Commission reviewed SCE's analysis of the NUHOMS ISFSI site's susceptibility to geologic hazards, including seismic ground shaking, tsunamis, and coastal erosion, as discussed at pages 17-31 of the staff report. Based on a review of the previous CDP conclusions and current science, including sea level rise analysis using the extreme H++ scenario and the 2018 California Ocean Protection Council (OPC) sea level rise guidance, Coastal Commission staff concluded that the ISFSI site remains appropriate.

SCE is aware of recent media coverage that could raise concerns about potential seismic activity at the SONGS site. This media coverage cited research suggesting that the Palos Verdes fault system has more connectivity than was previously known. However, this research does not change the seismic analysis at the SONGS site. The Palos Verdes fault system is well known, and it was considered in the 2010 GeoPentech report[2] cited in SCE's seismic analysis (Coastal Environments Coastal Hazards Analysis at SONGS, Part 2: Geological Hazards, March 2022), which was submitted to Coastal Commission staff on May 13, 2022 in support of this CDP Amendment Application.

SCE's seismic analysis considered very severe earthquakes, and even the recent information regarding the Palos Verdes fault system does not present a more extreme seismic hazard at SONGS.

[2] See GeoPentech, 2010. San Onofre Nuclear Generating Station Seismic Hazard Assessment Program 2010 Probabilistic Seismic Hazard Analysis Report. Prepared for Southern California Edison, December 2010. A copy of the 2010 report is provided to staff via email with this letter.

Primarily, this is because in the area near SONGS, the Palos Verdes fault system is much farther offshore than the Newport-Inglewood-Rose Canyon (NIRC) fault system that is the source of the maximum postulated seismic event at SONGS. As noted in the Staff Report, while "several prominent offshore fault zones" are in the area near SONGS, the NIRC fault system is expected to generate the strongest ground shaking at the ISFSI. This is unchanged.[3]

Because the Palos Verdes fault system is much further offshore than the NIRC system in the area near SONGS, the NIRC fault system remains the source that will generate the largest ground motion at SONGS. Even a theoretical 7.8-magnitude earthquake from the postulated Palos Verdes fault system would generate less ground shaking at SONGS than the potential seismic events already analyzed in the materials submitted in support of the CDP Amendment Application.

As described in those materials, the largest postulated earthquake at the SONGS site would be a 7.6-magnitude earthquake on the NIRC fault system, which is closer to SONGS than the Palos Verdes system.[4] Expert analysis shows that the estimated peak ground acceleration (PGA) at SONGS from a 7.8-magnitude earthquake along the Palos Verdes fault zone, would be 0.19g. That value is less than 40 percent of the PGA estimated for the 7.6-magnitude earthquake scenario modeled along the NIRC system, which was 0.51g. As explained in the CDP Amendment Application materials, which conservatively analyzed that more extreme shaking scenario, the NUHOMS ISFSI would be capable of withstanding the shaking caused by such an event. Please see Attachment B to this letter for additional information explaining why the recent information regarding the Palos Verdes fault system does not alter the conclusions regarding seismic risks to SONGS.

The same holds true for the tsunami analysis. Expert analysis confirms that, as described in the tsunami hazards report submitted in support of the CDP Amendment Application,[5] the Eastern Aleutian tsunami risk remains the most extreme tsunami risk at SONGS, and is bounding compared to any tsunami risk from the Palos Verdes fault system.[6]

IV. SCE Continues to Advance its Strategic Plan for Relocating SONGS Spent Fuel Offsite

While SCE is committed to safely storing spent nuclear fuel in the NUHOMS and Holtec ISFSIs, SCE also continues to actively pursue avenues to relocate SONGS spent fuel offsite. Under federal law, the ultimate disposition of spent nuclear fuel for all commercial nuclear power plants is the responsibility of the U.S. Department of Energy (DOE). SONGS spent fuel is expected to remain in dry storage at SONGS until the federal government identifies a facility and establishes a program for the fuel's offsite storage and/or disposal (or some other licensed offsite interim storage facility becomes operational).

In the interim, SCE is being proactive in identifying alternatives for the relocation of the SONGS spent fuel. Information regarding SCE efforts to assess the feasibility of relocating the

---

[3] See Attachment B to this letter, Coastal Environments October 6, 2022 letter to Ronald Pontes (SCE) re Geological and Tsunami Hazards / Palos Verdes Fault Zone.
[4] See Coastal Environments, Coastal Hazards Analysis at SONGS, Part 2: Geological Hazards, March 2022.
[5] See Coastal Environments, Coastal Hazards Analysis at SONGS, Part 3: Tsunami Hazards, March 2022.
[6] See Attachment B, Coastal Environments October 6, 2022 letter.

SONGS spent fuel to a licensed and commercially reasonable offsite facility is described in the Strategic Plan for the Relocation of SONGS Spent Nuclear Fuel to An Offsite Storage Facility or a Repository, and the Conceptual Transportation Plan, which were released in 2021.[7]

SCE has begun implementing actions from the Strategic Plan. For example, heeding a recommendation made by the Coastal Commission during the Holtec ISFSI CDP review, SCE has established a coalition called Action for Spent Fuel Solutions Now (the "Coalition") to advocate for solutions. The Coalition includes representatives from over 200 entities, including private industry, organized labor, environmental groups, government, and Native American tribes. In addition, SONGS has hosted members of Congress and the Secretary of Energy to discuss solutions. Recent developments are encouraging: the DOE has restarted efforts to find a suitable location for a federal storage facility using a consent-based approach, and federal legislation has been circulated that would authorize work on a permanent geologic repository for spent fuel and create a single-purpose agency to take over the spent fuel management program from the DOE.

In September 2022, SCE and a representative of the Coalition provided an update to the Coastal Commission on the efforts to move the SONGS spent fuel. The materials SCE provided to the Coastal Commission at that meeting are attached as Attachment C.

V. Conclusion

Thank you for considering these comments on the Staff Report. The Participants appreciate the diligent work of the Coastal Commission staff on this CDP Amendment Application, and we respectfully request that the Commission approve the CDP Amendment Application.

Very truly yours,

Jessica Rankin

Jessica Rankin

cc: David Asti
Linda Anabtawi
Robert Pontelle

Attachments

---

[7] Copies of these plans are available on the SONGS Community website, https://www.songscommunity.com/strategic-plan-for-relocating-spent-fuel/spent-nuclear-fuel-solutions-a-fresh-approach. The Strategic Plan for the Relocation of SONGS Spent Nuclear Fuel to An Offsite Storage Facility or a Repository is available at https://s3.amazonaws.com/cms.ipressroom.com/339/files/20213/SONGS+SP+Final+3-15-21+1.pdf, and the Conceptual Transportation Plan is available at https://www.songscommunity.com/_gallery/get_file/?file_id=604d0feeb3aed3384873372a&ir=1&file_ext=.pdf.

Attachment A

Attachment A

SONGS NUHOMS ISFSI CDP Amendment Application Staff Report – SCE Comments

No.	Staff Report Page(s)	Suggested Edits to Staff Report Text	SCE Comment
1.	1	Southern California Edison (SCE), on behalf of itself and the other ~~co-owners~~co-participants of the San Onofre Nuclear Generating Station (SONGS), San Diego Gas and Electric, the City of Anaheim, and the City of Riverside, requests an amendment to Coastal Development Permit (CDP) No. E-00-014.	The City of Anaheim is no longer an owner of SONGS, but it does still participate in all decommissioning and remaining spent fuel storage issues. We have been using the term "participants" to include the City of Anaheim in this applicant group.
2.	13	In total, the NUHOMS waste storage facility has a capacity under its current build-out for 63 steel reinforced spent fuel storage modules on top of ~~three~~two steel-reinforced concrete pads.	Although CDP No. E-00-014 provided for a maximum of three concrete pads, only two were constructed.
3.	13	The concrete pads are reinforced with rebar and are a minimum of three feet thick, with the top being at existing grade elevation, approximately 20 ft mean lower low water (MLLW), and are approximately 43 ft and 60 ft wide, respectively.	The two concrete pads are not identical in size, so SCE suggests minor edits to reflect the appropriate dimensions of the two pads.
4.	14	Each spent fuel storage module houses an NRC-licensed stainless steel canister that ~~may~~ contains either GTCC or spent fuel assemblies. For example, a typical Unit 2/3 canister contains up to 24 spent fuel assemblies. A Unit 2/3 fuel assembly consists of 236 zircalloy metal tubes approximately 12.8 ft long and 3/8 inch in diameter, in which ceramic uranium dioxide fuel pellets are placed. Known as fuel pins, the tubes are completely sealed with welded end plugs. Each fuel assembly has an overall length of about 15 ft and weighs approximately 1,500 lbs.	The fuel assemblies used at SONGS Unit 1 were slightly different in size and arrangement from the assemblies used in SONGS Units 2 and 3. SCE suggests a minor edit to clarify that the description in the Staff Report refers to the size and composition of the Units 2 and 3 assemblies, which although different in specific details from those in the Unit 1 assemblies, are representative of the size and contents of the canisters in the NUHOMS ISFSI.
5.	17	SCE ~~is in the process of applying for an extension of the grant of easement from the Navy~~has submitted an application to the Navy to extend the current easement.	SCE suggests this edit to reflect that an application for extension of the existing easement has already been filed and is under review by the Navy.

Attachment A
SONGS NUHOMS ISFSI CDP Amendment Application Staff Report – SCE Comments

No.	Staff Report Page(s)	Suggested Edits to Staff Report Text	SCE Comment
6.	24-25	The worst-case hypothetical far-field tsunami would come from a M9.5 earthquake in the eastern Aleutians. In the worst-case scenario, which would include 2.8 ft of sea level rise (H++ projection for 2050), the maximum potential water elevation at the waste storage facility would be 29.8 ft MLLW, with a water depth above ground surface of 9.1 ft around the NUHOMS waste storage facility. This would be below the top of the NUHOMS waste storage facility concrete module height of ~~32.5~~40.3 ft MLLW, and much lower than the waste storage facility water submergence design depth of 50 ft.	The top of the NUHOMS concrete modules is 40.3 ft MLLW. This number is calculated by adding the elevation of the top of the NUHOMS ISFSI pad (19.75 ft MLLW) to the height of the NUHOMS module (20.6 ft). The top of the module is 19.75 ft + 20.6 ft = 40.3 ft MLLW. The corrections are provided for accuracy only; they do not change the analysis/conclusions in any way.
7.	26	All of these inundation depths are below the concrete module height of ~~32.5~~40.3 ft, and are much lower than the waste storage facility submergence design of 50 ft.	Same comment as above.
8.	29	~~The remainder of the SONGS facilities are~~The Units 2 and 3 portion of the SONGS site is currently in the process of being decommissioned. Once the Units 2 and 3 decommissioning is complete in approximately 2028, the only above-grade structures aside from the two dry storage facilities that will remain on site are the revetment, walkway, seawall, and electrical switchyard.	SCE suggests edits to clarify the elements of the existing SONGS site that will remain after the current decommissioning project is complete.
9.	34-35	SCE also works closely with unions such as Laborers International Union of North America and Valentine ("Val") Macedo, LiUNA Local 89, Business Manager, to ensure that on-site workers at SONGS receive updates on decommissioning and other relevant activities.	SCE suggests this edit to clarify Mr. Macedo's full name and position.

Attachment A

SONGS NUHOMS ISFSI CDP Amendment Application Staff Report – SCE Comments

No.	Staff Report Page(s)	Suggested Edits to Staff Report Text	SCE Comment
10.	35	Once the decommissioning process for Units 2 and 3 is complete in approximately 2028, the only above-grade structures aside from the two dry storage facilities that will remain on the site are the revetment, walkway, seawall, and electrical switchyard.	SCE suggests this edit to clarify that under the current decommissioning project plan being undertaken pursuant to CDP No. 9-19-0194, some below-grade structures may remain in place.

Attachment B

CE Coastal Environments, Inc.
Oceanographic and Coastal Services

6 October 2022

Ronald Pontes
Southern California Edison
2244 Walnut Grove Avenue
Rosemead, CA 91770

Subject: Geological and Tsunami Hazards / Palos Verdes Fault Zone

Dear Mr. Pontes,

Below is our response to your question regarding seismic and tsunami hazards considering the recent paper regarding the Palos Verdes fault zone.

Question:

In light of the recent paper by Wolfe et al. (2022) entitled "Origin of the Palos Verdes Restraining Bend and Its Implications for the 3 D Geometry of the Fault and Earthquake Hazards in Los Angeles, California" (Wolfe Paper) about the Palos Verdes fault zone, do the seismic and tsunami analyses prepared for the NUHOMS ISFSI CDP remain valid?

Answer:

The Wolfe Paper does not alter the conclusions in the seismic and tsunami reports submitted in support of the NUHOMS CDP Amendment Application. The postulated seismic and tsunami hazards from the Palos Verdes fault zone would not exceed those identified in the seismic and tsunami reports.

1. Seismic Hazards

The seismic hazards identified in the Wolfe Paper do not present a greater seismic hazard at SONGS than the greatest postulated seismic event discussed in the geological hazards report submitted in support of the NUHOMS CDP Amendment Application.

The Palos Verdes fault zone has been identified and mapped by numerous investigators for decades, including scientists at the US Geological Survey, California Geological Survey, and Southern California Earthquake Center. The Wolfe Paper presents a revised model of the Palos Verdes fault zone that emphasizes the complex mapped fault patterns that could combine to produce large earthquakes, Mw 7.4 - 7.8, during multi-segment ruptures.

The overall length of the revised model of the Palos Verdes fault zone is estimated to be 110 km, reaching from the Santa Monica fault near Point Dume in Santa Monica Bay to the northern end of the San Diego Trough. The maximum magnitude potential identified in the revised model requires rupture of all the combined fault segments and branches in an extreme earthquake.

Ground shaking hazard, measured by the horizontal Peak Ground Acceleration (PGA), is estimated using Ground Motion Prediction Equations such as the GK15 version that was used to estimate shaking hazards for SONGS. The estimated PGA at SONGS from a Mw7.8 earthquake along the Palos Verdes fault zone, including the Lasuen Knoll segment (which is the closest portion of the Palos Verdes fault zone, at 28 km from SONGS), would be **0.19g**. That value is less than 40 percent of the **0.51g** PGA estimated for the Mw7.6 earthquake scenario along the Coastal Fault System that includes Newport-Inglewood, Rose Canyon and linked faults from Newport Beach to La Jolla (Coastal Environments, 2022a). The Mw7.6 Coastal Fault System earthquake was the largest postulated earthquake modeled in the seismic report submitted in support of the NUHOMS ISFSI CDP Amendment Application.

2. Tsunami Hazards

Potential tsunamis from the revised model also would not present a greater tsunami hazard at SONGS than the greatest tsunami event discussed in the tsunami hazards report submitted in support of the NUHOMS ISFSI CDP Amendment Application.

Tsunami runup along a coastal site depends on 1) the seafloor displacement during the source (earthquake for this study), 2) the distance from the seafloor displacement to the site, 3) the configuration of the seafloor displacement (elongate, irregular with high-slip patches, etc.), and 4) seafloor morphology (bathymetry) that may focus or dissipate tsunami wave energy along the source-to-site propagation path.

In light of the Wolfe Paper, the following discussion compares tsunami hazards identified in the tsunami report submitted in support of the NUHOMS ISFSI CDP Amendment Application (i.e., from a) an Eastern Aleutian source, which is the largest tsunami overall, and b) the Coastal Fault System), against c) a postulated tsunami generated from revised model of the Palos Verdes fault zone. As described below, the largest postulated tsunami is from an Eastern Aleutian source, which was already considered in the tsunami report.

a. Eastern Aleutian Subduction Zone

The Eastern Aleutian subduction zone would produce the largest potential tsunami at SONGS. This is because of factors 1, 3 and 4 described above. For the Eastern Aleutian zone, the seafloor displacement would be very large. Fault displacement of 33.25 m, based on a maximum postulated earthquake of Mw9.5, would produce 4.5 - 5.0 m tsunami amplitude at the source. The configuration is broad (1500 km) and its east-west orientation focuses the wave energy southeast toward Southern California, and the seafloor morphology contributes to the severity of the tsunami as it approaches the Southern California coast. Although the distance from the Eastern Aleutian subduction zone to SONGS is more than two thousand miles (about 4000 km), much farther than the other two systems below, these three factors overcome the distance and make it the largest potential tsunami threat.

The Eastern Aleutians worst-case model (EA-sc3) would produce a maximum wave amplitude offshore SONGS of 7.77 m, with runup of 8.67 m NAVD88 at SONGS.

b. Coastal Fault System – Newport-Inglewood, Rose Canyon, San Mateo, San Onofre, Carlsbad fault Sections

The Coastal Fault System (Newport-Inglewood, Rose Canyon, San Mateo, San Onofre, Carlsbad fault sections) is the closest to SONGS of all tsunami sources, with Newport-Inglewood fault segment located about 7 km from SONGS.

The largest postulated earthquake of Mw7.62 for this system involves a 9-segment earthquake rupture that stretches about 92 km along the Southern California coast from Encinitas to Newport Beach. The model includes a 2-segment San Mateo Thrust source located about 15 km offshore. The modeled fault displacements of 4.0 m and 8.0 m for the San Mateo fault segments would produce seafloor uplift ranging from +6.91 m to -1.10 m peak-to-trough amplitude, which would produce runup of 6.75 m NAVD88 at SONGS. Therefore, the largest tsunami from the Coastal Fault System would be smaller than the Eastern Aleutian worst-case model above, but would still be larger than the largest tsunami from the postulated Palos Verdes fault zone scenario, discussed below.

c. Palos Verdes Fault Zone – Lasuen Knoll Section

The largest postulated earthquake from the Palos Verdes fault zone that has been modeled as the potential source of a tsunami at the SONGS site is a 3-segment source from the Lasuen Knoll section (Borrero et al, 2004). The Lasuen Knoll section at the southern end of the Palos Verdes fault zone is farther offshore than the Coastal Fault System, and is located about 28 km from SONGS. This modeled earthquake was an earthquake of Mw7.1, with average fault displacement of 4.0 m (5.0 m maximum). The maximum seafloor uplift (initial wave peak-to-trough) would range from +1.74 m to -1.20 m. The tsunami runup estimated at SONGS would be 3.75 m NAVD88.

Even assuming a worst-case Mw7.8 earthquake rupture from Santa Monica Bay to Lasuen Knoll (as postulated in the revised model), it would be a long, complex source that will focus tsunami energy shoreward in Santa Monica and San Pedro Bays, and offshore to the west, with local tsunami energy from the Lasuen Knoll segment directed to SONGS. The Palos Verdes source includes the Palos Verdes Hills, where the greatest uplift would be expected, but this would be located above sea level and would not contribute to tsunami generation. The seafloor uplift from the submerged areas in Santa Monica Bay, San Pedro Bay and San Pedro Basin would have lower wave amplitudes and would be expected to produce two major wave fronts, north and south of the Palos Verdes Peninsula. This pattern would resemble the model for the Mw7.6 Catalina tsunami scenario (Legg et al. 2004) which would produce a maximum runup at SONGS of about 3.75 m NAVD88.

The Palos Verdes largest postulated tsunami runup values are lower than the Mw7.62 Coastal Fault System tsunami and the Eastern Aleutians worst-case model (EA-sc3). In summary, the Eastern Aleutians subduction zone represents the most severe tsunami potential at SONGS, with 7.7 m tsunami elevation offshore and 8.67 m runup NAVD88.

Sincerely,

Hany Elwany, Ph.D.
Coastal Environments Inc.

REFERENCES:

Borrero, J.C., M.R. Legg, and C.E. Synolakis, 2004. Tsunami sources in the southern California Bight. *Geophysical Research Letters*, 31(13), L13211.

Coastal Environments, 2022a. Coastal Hazard, Step by step description of the modeling to evaluate the potential ground-shaking intensity associated with nine segments. Letter submitted to SCE dated 26 August 2022.

Coastal Environments, 2022b. Coastal Hazard Analysis At San Onofre Nuclear Generating Station, Tsunami Hazards, Submitted to Southern California Edison, 31 March, CE Ref. No. 22-04. 68 pp plus 1 Appendix.

Legg, M. R., C. E. Synolakis, and J. Borrero, 2004, Tsunami hazards associated with the Catalina Fault in southern California, *EERI Spectra, 20(3),* 1-34.

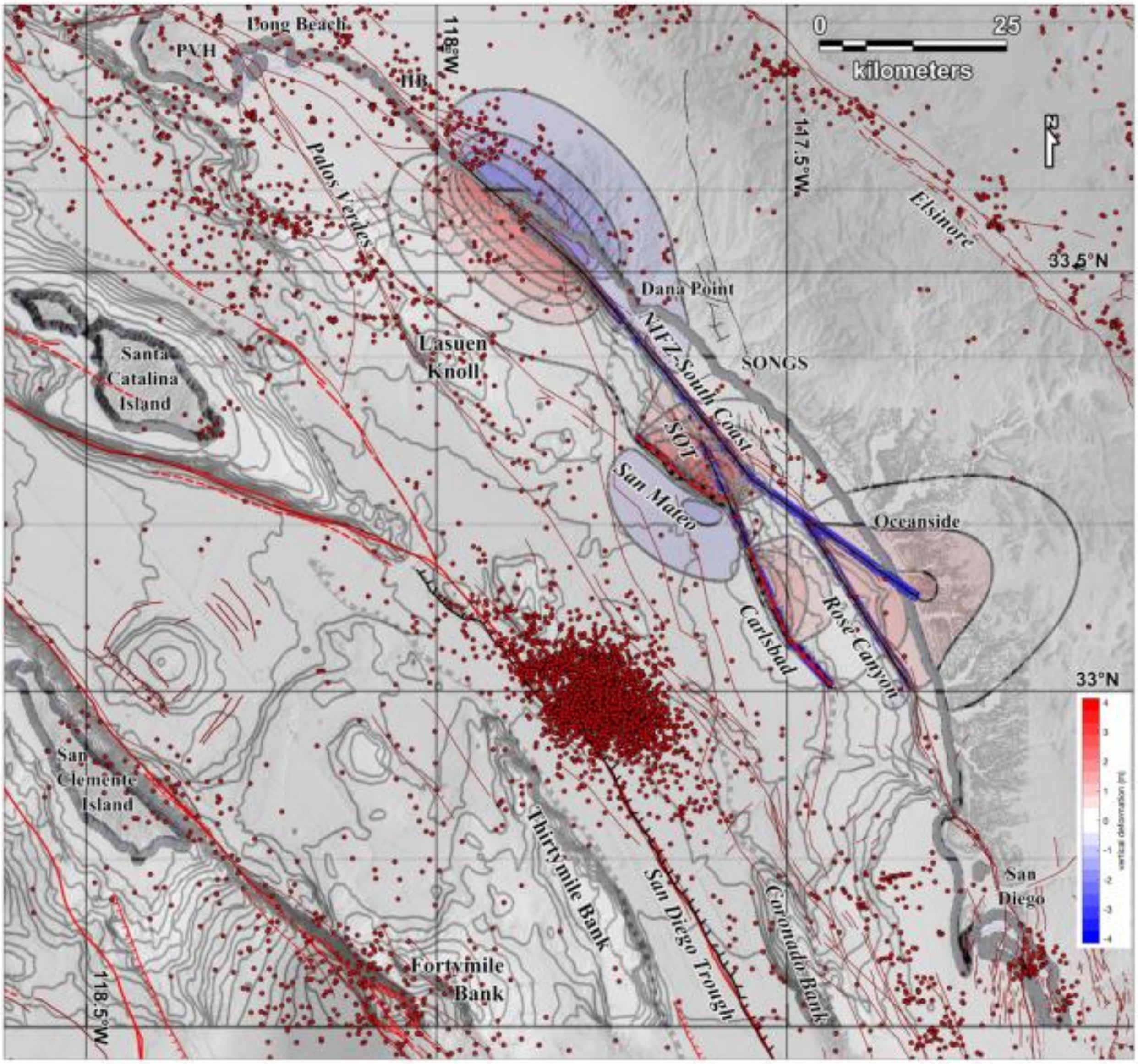

Figure 1. **Map showing seafloor deformation produced by local tsunami source 1 with all nine fault segments, bathymetry and relocated seismicity (M > 2, 1981-2019; Hauksson et al., 2012, 2019 update). Palos Verdes Fault is show including Lasuen Knoll. From Coastal Environments (CE, 2022b)**

Attachment C

ACTION FOR SPENT FUEL SOLUTIONS NOW

Action for Spent Fuel Solutions Now is a new group of local governments, elected officials, utilities, environmental groups, labor leaders, Native American leaders, business organizations and other community members who support the relocation of spent nuclear fuel to a federally licensed facility away from our coastline. This is the first step forward to take action. Our founding members include representatives from the County of Orange, County of San Diego, Southern California Edison (SCE), San Diego Gas & Electric and the City of Riverside.

WHAT WE DO

Our goal is to encourage the federal government to provide off-site storage and/or permanent disposal solutions for the spent nuclear fuel at the San Onofre Nuclear Generating Station (SONGS) and other nuclear sites across the state and nation, with input from stakeholders and engaged communities. SCE retired SONGS in 2013, but spent nuclear fuel continues to be stored on site with nowhere to send it.

WHY ACTION IS NEEDED

Under the Nuclear Waste Policy Act, the federal government was required by law and executed contracts with nuclear power providers to begin taking possession of and disposing spent nuclear fuel back in 1998. Today – more than two decades later – it has not yet fulfilled its legal and contractual obligations. Spent nuclear fuel can be safely stored on site at SONGS for decades, but SCE cannot complete decommissioning of the plant and restore the land until the federal government takes action to facilitate an off-site solution.

100%
of SONGS spent fuel in canisters designed for storage and transportation

102 of 123
spent fuel canisters at SONGS ready for transport now

4
spent nuclear fuel dry storage sites in California

19
on-site dry storage facilities at retired U.S. nuclear power plants

35
states with at least some spent fuel stored at plant sites

Take action today! Join the coalition at **spentfuelsolutionsnow.com**.

COALITION LEADERSHIP

Executive Board

Our Executive Board sets the coalition's goals, directs efforts and oversees activities to support the removal of spent fuel from SONGS and other sites to a federally licensed offsite facility. Executive Board members include local governments and the SONGS plant owners.

Supervisor Lisa Bartlett, County of Orange (Co-Chair)

Supervisor Jim Desmond, County of San Diego (Co-Chair)

Mayor Patricia Lock Dawson, City of Riverside

Caroline Choi, Senior Vice President of Corporate Affairs, Southern California Edison

Estela de Llanos, Vice President of Energy Procurement & Sustainability, San Diego Gas & Electric

Advisory Council

Action for Spent Fuel Solutions Now's Advisory Council provides the Executive Board with recommendations and advice related to coalition strategy and activities. Membership includes stakeholders representing diverse interests such as environmental organizations, labor unions, industry experts, community leaders, Native American leaders, and business groups.

Members

Garry Brown, Orange County Coastkeeper

Valentine "Val" Macedo, LiUNA Local 89

Aaron McCall, California Environmental Voters

Rachel Norton, California State Parks Foundation

Jerry Sanders, San Diego Regional Chamber of Commerce

Captain Mel Vernon, San Luis Rey Band of Mission Indians

Dr. David Victor, SONGS Community Engagement Panel/ UC San Diego/ Scripps Institution of Oceanography

Advisor

Tom Isaacs, Independent Strategic Advisor to SCE for Nuclear Waste Management/Former Director, Office of Nuclear Waste Policy within the U.S. Department of Energy

CONTACT US

info@spentfuelsolutionsnow.com

(858) 290-1373

SUPPORTING MEMBERS

Our Supporting Members include organizations and individuals committed to the relocation of spent nuclear fuel at SONGS to a federally licensed offsite consolidated interim storage facility or permanent geologic repository.

Elected officials and local governments

ORANGE COUNTY BOARD OF SUPERVISORS

Supervisor Doug Chaffee, Chair, Orange County
Supervisor Donald P. Wagner, Vice Chair, Orange County
Supervisor Andrew Do, Orange County
Supervisor Katrina Foley, Orange County
Supervisor Lisa Bartlett, Orange County

SAN DIEGO COUNTY BOARD OF SUPERVISORS

Supervisor Nathan Fletcher, Chair, County of San Diego
Supervisor Nora Vargas, Vice Chair, County of San Diego
Supervisor Joel Anderson, County of San Diego
Supervisor Terra Lawson-Remer, County of San Diego
Supervisor Jim Desmond, County of San Diego

RIVERSIDE COUNTY BOARD OF SUPERVISORS

Supervisor Karen Spiegel, Chair, County of Riverside
Supervisor Jeff Hewitt, Vice Chair, County of Riverside
Supervisor Kevin Jeffries, County of Riverside
Supervisor Chuck Washington, County of Riverside
Supervisor V. Manuel Perez, County of Riverside

CALIFORNIA STATE LEGISLATURE

Senator Pat Bates, California State Senate, 36th District
Senator Brian Jones, California State Senate, 38th District
Assemblymember Randy Voepel, California State Assembly, 71st District

CITY OF BUENA PARK

Councilmember Connor Traut

CITY OF BREA

Councilmember Steve Vargas

CITY OF CARLSBAD

Mayor Matt Hall

CITY OF CHULA VISTA

Mayor Mary Salas
Councilmember Andrea Cardenas

CITY OF DANA POINT

Mayor Joe Muller
Mayor Pro Tem Mike Frost
Councilmember Richard Viczorek
Councilmember Jamey Federico
Councilmember Michael Villar

CITY OF EL CAJON

Councilmember Phil Ortiz

CITY OF ESCONDIDO

Councilmember Michael Morasco

CITY OF HUNTINGTON BEACH

Mayor Barbara Delgleize
Mayor Pro Tem Mike Posey

CITY OF LA MESA

Mayor Mark Arapostathis
Vice Mayor Jack Shu
Councilmember Bill Baber
Councilmember Laura Lothian
Councilmember Colin Parent

CITY OF NATIONAL CITY

Councilmember Jose Rodriguez

CITY OF NEWPORT BEACH

Mayor Kevin Muldoon
Mayor Pro Tem Noah Blom
Councilmember Brad Avery
Councilmember Joy Brenner
Councilmember Diane B. Dixon
Councilmember Duffy Duffield
Councilmember Will O'Neill

CITY OF OCEANSIDE

Mayor Esther C. Sanchez
Deputy Mayor Ryan Keim
Councilmember Kori Jensen
Councilmember Christopher Rodriguez
Councilmember Peter Weiss

CITY OF SAN CLEMENTE

Mayor Gene James
Mayor Pro Tem Chris Duncan
Councilmember Laura Ferguson
Councilmember Steve Knoblock
Councilmember Kathleen Ward

CITY OF SAN DIEGO

Mayor Todd Gloria

CITY OF SAN JUAN CAPISTRANO

Councilmember John Taylor

CITY OF SAN MARCOS

Mayor Rebecca Jones

CITY OF STANTON

Mayor David Shawver

CITY OF VISTA

Mayor Judy Ritter
Deputy Mayor John Franklin

FORMER ELECTED OFFICIALS

Shirley Dettloff, Former Mayor, City of Huntington Beach
Diane Harkey, Former California State Board of Equalization Member

Environmental groups and advocates

Marni Magda, CEP Member
President Gayle Waite, Laguna Canyon Conservancy
Bolsa Chica Conservancy
California Environmental Voters
California State Parks Foundation
Friends of Harbors, Beaches and Parks
Industrial Environmental Association
Orange County Coastkeeper

Labor unions

LiUNA Local 89
Orange County Professional Firefighters Association, Local 3631

School districts

Capistrano Unified School District

Emergency responders

Sheriff Don Barnes, Orange County
Former Sheriff Bill Gore, County of San Diego
Orange County Fire Authority

Business and industry groups

Anaheim/Orange County Hotel and Lodging Association
Apartment Association of Orange County
California Apartment Association – Orange County
Carlsbad Chamber of Commerce
Costa Mesa Chamber of Commerce
Dana Point Chamber of Commerce
East County Chamber of Commerce
Greater Irvine Chamber of Commerce
La Mesa Chamber of Commerce
Laguna Beach Chamber of Commerce
Laguna Niguel Chamber of Commerce
National City Chamber of Commerce
Newport Beach Chamber of Commerce
North Orange County Chamber of Commerce
North San Diego Business Chamber
Oceanside Chamber of Commerce
Orange County Association of REALTORS
Orange County Business Council
Orange County Taxpayers Association
Otay Chamber of Commerce
Poway Chamber of Commerce
San Clemente Chamber of Commerce
San Diego County Taxpayers Association
San Diego Military Advisory Council
San Diego North Economic Development Council
San Diego Port Tenants Association
San Diego Regional Chamber of Commerce
San Diego Regional Economic Development Corporation
San Diego Restaurant Association
San Juan Capistrano Chamber of Commerce
San Ysidro Chamber of Commerce
South Orange County Economic Coalition
Vista Chamber of Commerce

Government agencies and organizations

Association of California Cities - Orange County
Orange County Council of Governments

CONTACT US

info@spentfuelsolutionsnow.com
(858) 290-1373

SAN ONOFRE NUCLEAR GENERATING STATION
SEISMIC HAZARD ASSESSMENT PROGRAM
2010 PROBABILISTIC SEISMIC HAZARD ANALYSIS REPORT

Prepared for
Southern California Edison

December 2010

PROBABILISTIC SEISMIC HAZARD ANALYSIS OUTLINE

1.0 INTRODUCTION

1.1 Purpose

A seismic hazard analysis update was performed for the San Onofre Nuclear Generating Station (SONGS) to evaluate if the most recent or current available seismic, geologic, and ground motion information in the vicinity of SONGS has affected the seismic hazard at SONGS. The analysis specifically included the Uniform California Earthquake Rupture Forecast, Version 2 (UCERF 2) by the 2007 Working Group on California Earthquake Probabilities (WGCEP, 2008), which is the joint product of the Southern California Earthquake Center (SCEC), the California Geological Survey (CGS) and the United States Geological Survey (USGS).

1.2 Site Information

SONGS is located on the west coast of southern California in San Diego County, approximately 80 kilometers (km) northwest of the City of San Diego and 97 km southeast of Los Angeles, as seen in the map on Figure 1-1. The plant is located entirely within the Camp Pendleton Marine Corps Base (Base) near the northwest end of the Base's shoreline. Figure 1-1 also shows the general configuration of SONGS. The plant is currently operating Units 2 and 3, which, as seen on Figure 1-1, occupy about 21 hectare (ha) of the approximately 34 ha facility. The power block for both Units 2 and 3, and the station's switchyard cover about 11 ha with the remaining 10 ha providing parking, access areas, and other miscellaneous facilities.

Approximately 6 ha of SONGS, northwest of Unit 2, were previously occupied by Unit 1; the last of Unit 1 facilities was removed in 2008. This area is now called the "North Industrial Area," as shown on Figure 1-1.

1.3 Approach

This evaluation of the seismic hazard at SONGS utilizes a probabilistic seismic hazard analysis (PSHA) approach. The PSHA was used on the plant's established ground motion criteria to evaluate the implications of alternative active fault models based on the most recent or current seismic, geologic, and ground motion information in the vicinity of SONGS.

The analysis uses UCERF 2 (WGCEP, 2008), the National Seismic Hazards Mapping Program (NSHMP) (USGS, 2008), the current USGS implementation of UCERF 2 seismic source characterization (USGS, 2009, personal communication [PC]), and more recently available information regarding both the regional faults and the Newport-Inglewood/Rose Canyon (NI/RC) Fault Zone. The current USGS seismic source characterization roughly corresponds to the initial seismic source characterization used in the plant's licensing and in its two follow-on PSHAs (SCE, 1995 and 2001). These earlier seismic source characterizations and that used by the USGS (2008) lead to the conclusion that the active, right-lateral, strike-slip NI/RI Fault Zone is the largest contributor to the seismic hazard at SONGS.

A postulated active, regional low-angle thrust fault (the Oceanside Blind Thrust [OBT]) was proposed to extend beneath the coastline under SONGS and from offshore of Dana Point to the U.S./Mexican border by Rivero et al. (2000), Rivero (2004), Rivero and Shaw (2005), and Rivero and Shaw (2010, in press). The implication of this hypothesized OBT on SONGS' seismic hazard was first evaluated as part of the

SCE (2001) study through a PSHA approach using published and unpublished information available in 2001.

For this updated 2010 PSHA for SONGS, both a strike-slip end-member model, which includes the NI/RC Fault Zone source, and a blind thrust end-member model, which includes the OBT Fault source, were incorporated to reflect current alternative interpretations of the seismic source characteristics of active faults in the Inner Continental Borderland (ICB) near SONGS. For incorporation into this 2010 PSHA, a relative contribution, or relative weight, was assigned to each of these end-member models based on an assessment of the technical community's consensus on interpretation of data available in relevant publications and ongoing research.

The Next Generation Attenuation (NGA) relationships (NGA, 2008) were used in performing this PSHA. This seismic hazard evaluation was limited to annual frequencies of exceedance greater than 10^{-4}. A 10^{-4} annual frequency of exceedance is equivalent to a return period (RP) of 10,000 years. At annual frequencies of exceedance lower than 10^{-4}, some issues are to be addressed that potentially could affect the calculated seismic hazard results. These issues consist of those associated with dispersions, such as epistemic and aleatory uncertainties in seismic source characterization and ground motion characterization models including the ground motion predictive equation (GMPE) epistemic uncertainty, and those associated with nonlinear behavior of soils at the site. These issues will be addressed as part of the SONGS ongoing seismic hazard program.

In presenting the results of this SONGS seismic hazards analysis, this report is organized into six sections and two appendices.

Section 1 is this introductory section.

Section 2 describes the seismic source characterization used in this PSHA.

Section 3 presents a more detailed discussion of the methodology used in conducting the PSHA and the results of the PSHA.

Section 4 provides our conclusions regarding the SONGS seismic hazards assessment.

Section 5 lists the relevant references.

Section 6 provides a glossary.

The two appendices are:

A. Seismic Source Characteristics, which provides a detailed summary of the currently available information regarding these seismic source characteristics including references and abstracts of the key sources of information (Attachment A-1).

B. PSHA – Selected Issues, which provides a detailed summary of the methodology used and key issues with this current PSHA.

1.4 Acknowledgements

The overall project was sponsored by Southern California Edison (SCE). GeoPentech's effort was managed by Mr. John Barneich with the seismic source characterization work led by Mr. S. Thomas Freeman and the PSHA evaluation by Dr. Yoshi Moriwaki. Other GeoPentech team members were geoscientists Mr. Steven Duke (seismic source characterization support); Ms. Phuong Chau and Ms. Alexandra Sarmiento (geologic support); and engineers Dr. Phalkun Tan (PSHA) and Mr. Andrew Dinsick (logic tree development). Geoscientists Dr. Philip Hogan and Mr. Steven Varnell of Fugro West provided input on offshore fault characteristics from evaluations of available geophysical marine seismic surveys and other relevant sources of information. Ms. Kathryn Hanson of AMEC Geomatrix provided input, guidance, and reviews to the seismic source characterization effort, and Dr. Robert Youngs, also from AMEC Geomatrix, provided early input to the PSHA evaluation.

Mr. Freeman, Dr. Hogan, and Ms. Hanson served as a seismic source characterization integrator team in compiling the seismic source characterization models for the offshore area and ultimately developed the relative weights for these models that were used in this PSHA.

Several consultants were involved in the project, including Dr. John Shaw and Dr. Andreas Plesch of the Department of Earth and Planetary Sciences, Harvard University, who provided helpful input and reviews on the characteristics of the blind thrust fault models. Dr. Thomas Rockwell of San Diego State University contributed fault characterization input for the strike-slip fault model and provided helpful reviews. Dr. Peter Shearer and Dr. Neil Driscoll of the University of California at San Diego Scripps Institute, Dr. Lisa Grant of University of California at Irvine, and Dr. Roy Shlemon also provided timely input, guidance, and reviews on the source characterization effort.

Dr. Holly Ryan and Dr. Dan Ponti from the USGS are acknowledged for meeting with the seismic source characterization technical integrator team and sharing pre-publication data and information on the offshore faults and the onshore NI Fault, respectively, as well as providing helpful review comments.

Lastly, acknowledgement is given to the members of the Seismic Technical Advisory Board (STAB) for their comments and recommendations on the methods and presentation of this report: Dr. Clarence Allen, California Institute of Technology emeritus; Dr. Kevin Coppersmith, Coppersmith Consulting; Dr. Jan Rietman, consultant; Mr. Lloyd Cluff, consultant; Dr. Steven Day, San Diego State University; Dr. I.M. Idriss, consultant; and Dr. Norman Abrahamson, consultant.

GeoPentech Geotechnical & Geoscience Consultants	SAN ONOFRE NUCLEAR GENERATING STATION SEISMIC HAZARD ASSESSMENT PROGRAM	SITE LOCATION MAP AND APPROXIMATE STATION LAYOUT	FIGURE 1-1

2.0 SEISMIC SOURCE CHARACTERIZATION

Two variations have been proposed on the tectonic model explaining the crustal deformation currently occurring in the ICB offshore adjacent to SONGS.

One variation of the model, which has substantial support in the technical community (e.g., Moore, 1972; Fischer and Mills, 1991; Legg, 1991; Wright, 1991), assumes that active high-angle, right-lateral strike-slip faults, similar to what is observed on land, extend to seismogenic depth and are the primary source of large offshore earthquakes that might affect the plant. Figures 2-1a through 2c show the mapped surface traces of the active, right-lateral strike-slip faults and recorded earthquakes in the region surrounding SONGS. The closest of these right-lateral strike-slip faults to SONGS is the NI/RC Fault Zone, located 8 km offshore.

In this right-lateral strike-slip model, nearby shallow-dipping, active and non-active, normal, oblique, reverse, and thrust faults are subsidiary to the high-angle strike-slip fault (i.e., the NI/RC Fault Zone). The UCERF 2 (WGCEP, 2008) seismic source characterization model and the seismic source characterization model used in the 2008 National Seismic Hazard Mapping Program (USGS, 2008) and the current implementation of UCERF 2 by the USGS (2009, PC) are based on this strike-slip model. For this PSHA, a logic tree for the NI/RC Fault Zone was developed based on WGCEP (2008) and USGS (2008 and 2009, PC).

A brief overview of the seismic characteristics of the strike-slip dominated tectonic model used in this 2010 PSHA is provided in the following Section 2.1 with particular emphasis on the NI/RC Fault Zone, which is the closest fault source to SONGS. In addition, Dr. Tom Rockwell provides a more thorough discussion of the current understanding of the seismic characteristics of the NI/RC Fault Zone in Appendix A, Attachment A-2.

The other variation of the tectonic model was proposed by Rivero et al. (2000) in which regional blind thrust faults (reactivated Miocene detachment surfaces) also represent regional-scale active faults. These regionally extensive blind thrusts are inferred to interact at depth with high angle, strike-slip or oblique-slip faults, such as the NI/RC Fault Zone, yielding segmented fault geometries. This alternative model was further developed and described by Rivero (2004), Rivero and Shaw (2005), and Rivero and Shaw (2010, in press). Figure 2-2 provides a copy of the Community Fault Model (CFM) developed by Plesch et al. (2007), which illustrates the blind thrust faults included in this variation of the tectonic model. These postulated blind thrust fault sources were described in UCERF 2 (WGCEP, 2008) as being considered for future deformation model development, but they are not included in the current USGS source characterization model (USGS, 2009, PC).

Section 2.2 presents a brief overview of the seismic characteristics of the blind thrust variation to the tectonic model, in particular the OBT, the closest inferred blind thrust to SONGS. For this PSHA, Dr. Shaw and Dr. Plesch (2010, Appendix A, Attachment A-3) developed logic trees and segmentation models to assign seismic source characterization parameters for fault sources based on the blind thrust variations of the tectonic model as outlined by Rivero et al. (2000), Rivero (2004), Rivero and Shaw (2005), and Rivero and Shaw (2010, in press).

There are significant differences in the characterization of fault sources in the vicinity of SONGS based on these two variations of the tectonic model. As such, the alternative seismic source characterizations that stem from these two models are considered end-member assessments, referred to as: (1) the strike-slip end-member seismic source characterization model and (2) the blind thrust end-member seismic source characterization model. Based on recent and ongoing interpretations of offshore and nearby onshore seismic and geologic data, other researchers (e.g., Grant et al., 2002; Grant and Rockwell, 2002; Grant and Shearer, 2004) have suggested modifications to the blind thrust model presented by Rivero et al. (2000) and Rivero (2004). The results of more recent studies (e.g., Ponti and Ehman, 2009; Ryan et al., 2009; Sorlien et al., 2009a; Conrad et al., 2010; Rockwell, 2010; and Rentz, 2010), which were not available or had not undergone sufficient peer-review at the time of preparing UCERF 2 (WGCEP, 2008), were incorporated in this study.

The seismic sources included in the PSHA for this current study are outlined in the following sections:

Section 2.1 provides an updated description of the NI/RC Fault Zone and its seismic source characterization parameters as part of the strike-slip end-member model.

Section 2.2 provides a summary of the seismic characterization parameters for alternative fault sources based on the blind thrust end-member seismic source characterization model.

Section 2.3 presents the time-independent seismic source characteristics of the more distant regional faults that were used in USGS (2009, PC) source characterization. These more distant faults in the region are included in both of the end-member models.

Section 2.4 provides discussions regarding the weights assigned to the two alternative end-member seismic source characterization models for incorporation in the PSHA based on information from previous studies and using more recent published and unpublished studies by other researchers in the technical community.

Summaries of the key publications and results and observations from past, recently completed, and ongoing research in the California Continental Borderland offshore SONGS that were used in this evaluation are provided in Attachment A-1 of Appendix A.

2.1 Strike-slip Seismic Source Characterization Model

In the strike-slip end-member seismic source characterization model used in this 2010 PSHA, the offshore portion of the high-angle, right-lateral NI/RC Fault Zone is the closest fault source to SONGS. The onshore NI/RC Fault Zone, including its numerous oil fields, has been extensively studied (Moody and Hill, 1956; Wilcox et al., 1973; Harding, 1973; and Yeats, 1973). These authors concluded that the subsidiary faulting is mechanically consistent with, and causally related to, dominant strike-slip faulting, and, parenthetically, the evidence is sufficiently strong that NI/RC Fault Zone has been sometimes cited as one of the classic examples of this so-called wrench tectonics mode of deformation. This theory explains and is compatible with the presence of shorter, shallower dipping, normal, and thrust subsidiary faults in a system dominated by a high-angle, through-going primary strike-slip fault.

During the 1970s, SCE, with the assistance of firms such as Fugro West, Western Geophysical, Woodward-Clyde Consultants, and other independent consultants, completed rigorous onshore and offshore investigations to evaluate the seismic source characteristics of the NI/RC Fault Zone. The conclusion from this work was that the faulting offshore of San Diego County is a continuation of the strike-slip dominated wrench faulting tectonics reflected in the northern onshore portion of the NI/RC

Fault Zone in the Los Angeles Basin. The characterization of the NI/RC Fault Zone as a strike-slip fault was the basis of deterministic ground motion analyses completed for the licensing of SONGS Units 2 and 3 and documented in the plant's Updated Final Safety Analysis Report (SCE, UFSAR). Little has changed in the geoscience community's overall understanding of the NI/RC Fault Zone's offshore characteristics since the original investigations for SCE's UFSAR. Some refinements were made in the mapped offshore traces of the fault by Fischer and Mills (1991), and slip rate estimates were improved for the on-shore portions of the NI/RC Fault Zone in Huntington Beach by Freeman et al. (1992), Law/Crandall, Inc. (1993), Grant et al. (1997), Shlemon et al. (1995), Franzen et al. (1998), and in Rose Canyon by Lindvall and Rockwell (1995). These changes in the NI/RC Fault Zone's seismic characteristics were incorporated in the source models used in the PSHAs for SONGS by SCE in 1995 and 2001, as well as in UCERF 2 (WGCEP, 2008), the NSHM (USGS, 2008), and in the current USGS implementation of UCERF 2 (2009, PC).

Further support for the strike-slip end-member model, with the high–angle NI/RC Fault Zone as the primary source fault closest to SONGS includes more recent research by Grant and Shearer (2004); Fisher (2009); Fisher et al. (2009a, 2009b); Lee et al. (2009); Ryan et al. (2009); Rockwell (2010); additional proprietary work completed offshore by Fugro West for the oil industry; and work currently underway by Dr. Dan Ponti of the USGS (Ponti, 2010, PC) along subsidiary traces of the onshore NI Fault north of Long Beach. The work completed by Ryan et al. (2009) is essentially an independent assessment of the available data reviewed during SCE's earlier work on the characteristics of the faults located offshore of SONGS, complemented by more recent seismic reflection data. Some of the proprietary marine geophysical survey data recently obtained by the USGS from WesternGeco and used by Ryan et al. (2009) was purchased by SCE years ago (Western Geophysical Company, 1972). Ryan (2010, PC) indicated that the results of the USGS independent assessment of the data are in general agreement with the results of SCE's previous investigations and analysis of the faulting offshore of SONGS.

UCERF 2 (WGCEP, 2008), the USGS (2008), and the current USGS implementation of UCERF 2 (2009, PC) characterize the NI/RC Fault Zone as a high-angle, right-lateral, strike-slip, primary seismic source, with relatively minor alternatives to its geometry onshore north of Long Beach. The map and logic tree used by the USGS (2008) for the NI/RC Fault Zone, with some minor changes to the seismic source characteristics based on USGS (2009, PC), are shown on Figures 2-3, 2-4, and 2-5. The same logic tree was utilized to represent the NI/RC seismic source model in this PSHA for SONGS.

Figures 2-3, 2-4, and 2-5 are an interpreted version of UCERF 2 (WGCEP, 2008), USGS (2008), and the current USGS implementation of UCERF 2 (2009, PC) seismic characterization of the NI/RC Fault Zone with a corresponding logic tree for that fault source. Further details regarding the earthquake recurrence model for the NI/RC Fault Zone used in this 2010 PSHA are presented in Section 3.1.3.3 of this report. Supporting the viability of the strike-slip end-member model is the possibility that the onshore and offshore segments of the NI/RC Fault Zone may be connected and capable of slipping together producing a significant magnitude earthquake. The sense of motion in the ICB offshore SONGS is dominantly NW-directed right-lateral shear at about 6 millimeters per year (mm/yr) based on recent global positioning system (GPS) data (Appendix A, Figure A-3), as discussed in more detail in Section 2.4. The dominance of right-lateral shear in the ICB has been in existence over the past approximately 20 Million Years (Ma) (Nicholson et al., 1994) as evidenced by the 250 km of strike-slip offsets of the Eocene Poway conglomerates from San Diego to the west end of the Channel Islands (Kies and Abbott, 1983; and Rockwell, 2010, PC). The initiation of this offset predates the inception of the San Andreas Fault (~5 Ma; Atwater, 1998). Furthermore, considering the kinematic motions in northern Baja

California, which projects into to ICB, there currently should be a small component of divergence in the Borderland offshore San Diego (Rockwell, 2010, PC). Observations of marine terraces along the coast of San Diego County and northern Baja California indicate that the uplift along this portion of the coast (~ 0.13 mm/yr) is regional in character, evenly distributed, and most likely driven by rift-shoulder uplift caused by the spreading of the Gulf of California (Mueller et al., 2009; and Rockwell, 2010, PC). This interpretation as to the cause of the evenly distributed, regionally persistent, uplifted terraces along the San Diego County/northern Baja California coast is further supported by the lack of folding in the Tertiary rocks beneath the terraces, except locally at the steps and bends in the strike-slip fault systems, such as the NI/RC Fault Zone through San Diego County and the Agua Blanca Fault in northern Baja California (Rockwell, 2010, PC).

Attachment A-2 of Appendix A presents Dr. Tom Rockwell's summary of current information concerning the NI/RC Fault Zone. This and other information form the basis for the weighting of the strike-slip end-member seismic source characterization model used in this study as discussed below in Section 2.4.

2.2 Blind Thrust Seismic Source Characterization Model

Reactivated Miocene detachment surfaces are the key elements of this blind thrust seismic source characterization model with the OBT being closest to SONGS. The OBT Fault was first proposed by Rivero et al. (2000) as an alternative primary active fault that could explain some of the deformation in the ICB region commonly associated with the strike-slip NI/RC Fault Zone. Rivero (2004) completed further assessments of the blind thrust fault systems (including the OBT and Thirtymile Bank Thrust Fault, TMBT) in his Ph.D. research, which was supervised by Professor John Shaw at Harvard University. Rivero et al. (2000), Rivero (2004), Rivero and Shaw (2005), and Rivero and Shaw (2010, in press) provide overviews of the evidence for active folding and blind-thrust faults induced by basin inversion processes in the southern ICB region and characterization of the OBT and TMBT as active fault sources. The OBT and TMBT are included in the CFM, developed by Dr. Andreas Plesch (a Research Associate at Harvard University) (Plesch et al., 2007). However, as noted above, the hypothesized active OBT and TMBT faults are not presently included as fault sources in UCERF 2 (WGCEP, 2008) or the USGS current implementation of UCERF 2 (2009, PC) seismic source characterization model. A focused summary of the seismic source characteristics of these postulated blind thrust fault sources and alternative models to explain the structural relationships among the active blind thrusts and strike-slip faults in the ICB region was prepared for SCE by Drs. Shaw and Plesch (2010, Appendix A, Attachment A-3), to reflect their current interpretation of the fault sources in the vicinity of SONGS.

The basis behind the OBT Fault model is Rivero's interpretation of paper copies of 1980s vintage oil industry digital deep-penetration 2D marine seismic reflection records (see Figures 2-6 and 2-7). Many of these records were proprietary at the time of Rivero's analyses, but have subsequently been released to the public and are being currently used by other researchers (e.g., Sorlien et al., 2009b and Ryan, 2010, PC).

Rivero et al. (2000) and Rivero (2004) formulated the models and sub-models presented on Figures 2-8, 2-9, and 2-10 and in Attachment A-3 of Appendix A based on the following:

- Based on balanced and restored cross-sections of the seismic reflection data, the recognition that compression has resulted in significant shortening of Plio-Pleistocene sediments into folds and faults;

- The 1986 Oceanside and Coronado Bank earthquake sequences;
- Regional uplift as evidenced by elevated onshore marine terraces; and
- To a very limited extent, GPS data.

Utilizing this data, Shaw and Plesch characterized the blind thrust fault sources (i.e., the OBT and TMBT) and their associated hanging wall and footwall subsidiary faults. Possible structural scenarios that represent potential interactions between the steeply-dipping strike-slip faults and the low-angle blind thrust fault sources are outlined in Figure A3-2A. Steeply-dipping, right-lateral strike-slip faults, such as the NI and RC, are incorporated into the blind thrust seismic source characterization model by Rivero (2004) and Rivero and Shaw (2010, in press). Preferred models for the interaction of these faults suggest that the strike-slip faults are segmented and offset at depth under the argument that continuous, through-going, strike-slip faults, as primary fault sources, are not kinematically compatible with the large amount of shortening documented on the OBT fault.

Shaw and Plesch (2010, Appendix A, Attachment A-3) qualitatively assigned weights to the four alternative models as shown on Figure 2-9 based on their observations and confidence in the available data. Utilizing the information developed by Rivero (2004), Rivero and Shaw (2005), and Rivero and Shaw (2010, in press), Shaw and Plesch (2010, Appendix A, Attachment A-3) developed the simplified rupture segmentation models as depicted on Figure 2-11 and depicted in the logic tree shown on Figure 2-12.

The map on Figure 2-11 and the logic tree on Figure 2-12 reflect the complex alternatives of the OBT Fault as the closest hypothesized fault to SONGS in the blind thrust fault end-member model. All of the alternative geometries of the OBT Fault with their single and combined segment rupture possibilities are addressed in this logic tree. The earthquake recurrence rates for these alternatives were calculated using the identified slip rates on Figure 2-12, and are discussed further in Section 3.1.3.3. Refer to the complete discussion by Shaw and Plesch (2010) in Appendix A, Attachment A-3 for additional details.

2.3 Base-case Regional Fault Sources and Background Source Zones

The more distant (with respect to SONGS) regional faults and background source zones used in the strike-slip and blind thrust end-member seismic source characterization models used in this 2010 PSHA are referred to as the base-case model. These base-case regional fault sources are shown on Figure 2-3 and their closest distances from the plant are listed in Table 2-1. The information presented in Table 2-1 is based on the time-independent characteristics of these seismic source faults used in the current implementation of UCERF 2 model provided by the USGS (2009, PC). Table 2-1 also lists non-designated faults (i.e., faults not presently included as seismic sources, but faults that WGCEP [2008] targeted for future consideration).

The use of time-independent characterization of seismic source faults in the PSHA for SONGS is justified by the observations that the seismic sources amenable to time-dependent modeling (such as the San Andreas Fault) are distant sources that are not the controlling sources for seismic hazard at SONGS, and there are uncertainties involved in evaluating time-dependency.

Following UCERF 2 (WGCEP, 2008), the seismic sources provided by the USGS (2009, PC) are designated as either a Type-A fault, a Type-B fault, or a Type-C zone, depending on the level of knowledge tied to the specific seismic source. Type-A faults have known slip rates and paleoseismic recurrence interval estimates; Type-B faults have observed slip rates; and Type-C zones are areas of crustal shear that lack sufficient detailed knowledge to apportion slip onto specific faults. In southern California, Type-A faults include the San Andreas, San Jacinto, Elsinore, and Garlock faults. All other fault sources in southern California represented by the USGS (2009, PC) and used in this SONGS PSHA are designated Type-B faults. The Type-C zones in southern California include the Mojave or Eastern California shear zone, the San Gorgonio zone or “knot,” and the Brawley zone, or Imperial Valley zone (WGCEP, 2008; USGS, 2008). Figures 2-5 and 2-12 provide the key source characterization parameters for regional fault sources included in the SONGS PSHA. At a distance of about 38 km to the northeast, the Elsinore Fault is the Type-A designated fault closest to SONGS. The closest Type-B designated fault is the NI/RC Fault Zone, which lies about 8 km offshore to the west of SONGS. The characterization of the NI/RC Fault Zone source as a primary strike-slip fault end-member model is described in Section 2.1. Alternative geometries and slip rate estimates for the NI/RC Fault Zone source based on the blind thrust fault end-member model are presented in Section 2.2.

The next closest Type-B designated fault in UCERF 2 (WGCEP, 2008) is the Palos Verdes/Coronado Bank Fault, which is about 32 km west of SONGS. The San Diego Trough and San Clemente Faults, which lie at closest distances of 46 km and 94 km, respectively, are not presently characterized as fault sources by the USGS (2009, PC). The potential contribution of these faults to the seismic shaking hazard along the onshore portions of southern California, including SONGS, is judged to be negligible for several reasons including, but not exclusively, their location farther offshore, as shown on Figure 2-3, and their relatively low slip rates. These faults were included as faults sources in the SCE (1995, 2001) PSHA, and the results of these studies showed that neither the San Diego Trough nor San Clemente faults contribute significantly to the hazard at SONGS; thus these faults are not included in the PSHA for this study.

Of the three Type-C zones in southern California, the Eastern California Shear zone and Brawley zone are not significant contributors to the SONGS PSHA, due to their distances from SONGS (greater than 100 km), and thus were not included in the PSHA for this study. The San Gorgonio Type-C zone through Banning Pass, as shown on Figure 2-1b, is incorporated in the USGS (2009, PC) characterization as shown on Figure 2-3, as a low slip rate segment of the San Andreas Fault; this approach was followed in this PSHA.

The more distant regional faults listed in Table 2-1a, are included in both end-member seismic source characterization models for this PSHA. In the strike-slip end-member seismic source characterization model, the NI/RC Fault Zone, as characterized by UCERF 2 and USGS (2009, PC), is used; in the blind thrust end-member seismic source characterization model, the OBT and alternative characterizations of the NI and RC faults as defined by Shaw and Plesch (2010, Appendix A, Attachment A-3) are used.

In both end-member seismic source characterization models, the current SONGS PSHA incorporates a background seismicity zone(s) to account for additional seismicity not modeled by the seismic source faults using procedures similar to UCERF 2 (WGCEP, 2008) and the USGS’ current implementation of UCERF 2 (2009, PC).

2.4 Weighting of Alternative Models

Figures 2-1b, 2-2, 2-3, 2-6, and 2-8 in this report, and Figures A-7a through A-7f and A-17 in the accompanying Appendix A, present maps of the more recent alternative interpretations of the faulting in the ICB offshore of SONGS, as discussed above and in Appendix A. Figures 13a shows the nearby location of the marine seismic reflection geophysical survey records that follow in Figures 13b through 13h. These geophysical records were used, in part, by Ryan et al. (2009), Sorlien et al. (2009b), and Rivero and Shaw (2010, in press) in their interpretations of the faulting offshore of SONGS. This sequence of figures is used to illustrate the similarity in these geophysical records and to illustrate the similarities and differences in these different researcher's interpretations of these records. This was accomplished by superimposing Ryan et al. (2009) and Rivero and Shaw (2010, in press) records over the Sorlien et al. (2009b) record, in both opaque and transparent overlays.

Generally, this exercise demonstrates that these different researchers are observing essentially the same geophysical record, but offer different interpretations as to what these records illustrate in regard to the location, geometry, and style of faulting in this area. Figure 14 is a consolidated sketch of the interpreted geophysical records based on Ryan et al. (2009), Sorlien et al. (2009b), and Rivero and Shaw (2010, in press). This sketch, and the following simplified sketches in Figure 15 of the two end-member fault models, illustrates the uncertainties in the different interpretations of these marine geophysical records. First, it is unclear how the principal faults interact with each other at depths greater than approximately 4 km. This uncertainty results in the question as to whether the blind thrust end-member model or the strike-slip end-member model is the primary nearby fault source to SONGS. Second, the apparent vertical displacement of the geophysical marker horizons across the inferred faults on these records may not reflect the actual slip and resulting slip rate across the faults in either of the two end-member models. For example, the apparent displacements of geophysical marker horizons inferred to be the top of the Pliocene, Pico or Repetto formations or the top of the basement rocks, across apparent faults, such as the San Mateo Thrust (SMT) Fault, may not reflect the amount of lateral displacement and thus not entirely representing the total amount and direction of slip across the fault. Further, in the area offshore of SONGS, the range in depth and age estimates placed on geophysical marker horizons, such as these, remains broad. This introduces uncertainty in estimates of the level of activity and slip rates on these faults based solely on the geophysical records, particularly uncertainty in the late Quaternary level of activity on these faults. This limitation in the geophysical survey records results in the need for a careful assessment of all available relevant information and the development of reasonable weightings, based on that information, as to which end-member fault model is the more likely the case driving the PSHA for SONGS.

2.4.1 Discussion of Alternative Models

The weights assigned to the two end-member alternative models for potential fault sources that pose the most significant seismic hazard to SONGS (i.e., the OBT and the NI/RC models) are based on available relevant evidence and information regarding their seismogenic potential. The data include their geometry and level of activity, as well as geologic and geodetic evidence that pertains to the style and rate of crustal deformation occurring in the present tectonic environment. The references utilized in this weighting assessment are summarized in Attachment A-1 of Appendix A.

The evidence supporting both the reactivation of parts of the Oceanside detachment (i.e., compressional folding and thrust/reverse faulting) and high-angle, right-lateral strike-slip along the NI/RC Fault Zone is generally unequivocal in the technical community. There is general agreement that detachment faults are present in eastern California, the Transverse Ranges, and portions of the Los Angeles Basin, and ICB. Fisher et al. (2009a) summarize the technical community's current understanding of the paleotectonics of southern California's Continental Borderland, stating: *"A significant complication for hazards research is that during late Mesozoic and Cenozoic time, three* *successive tectonic episodes affected this plate-boundary zone. Each episode imposed its unique structural imprint such that early-formed structures controlled, or at least influenced, the location and development of later ones."* Each episode was driven by changes in tectonic plate motion. During the first episode, in the Mesozoic, thrust faults developed in an accretionary wedge above an east-directed subduction zone. The second episode, during the Miocene, was transtensional in nature, resulting in the development of extensional detachment and normal faults concurrently with rotation and northward translation of the Western Transverse Ranges. The third episode, in Pliocene through Holocene time, was primarily transpressional, resulting in structural inversion of some of the Miocene normal faults as oblique reverse/strike-slip faults, and localized re-activation of low-angle detachment faults as thrust faults.

There is no direct evidence that clearly demonstrates that the Miocene detachment faults have been reactivated as blind thrust faults on a regional scale off of the San Diego County coast. At this time, based on more recent re-evaluations of existing data and more recently collected data, the specific characteristics and the seismogenic potential of these Miocene detachment faults remain in discussion. This led to conservatively considering both end-member seismic source characterization models as contributing to the ground motion hazard at SONGS rather than limiting the evaluation to a single dominate model. In accordance with Senior Seismic Hazard Analysis Committee (SSHAC) guidelines (Budnitz et al., 1997), the weighting of these two end-member seismic source models (i.e., dominated by the high-angle, strike-slip NI/RC or the low-angle OBT) is based on an assessment of the extent of the evidence supporting the respective interpretations and the current understanding of the technical community's judgment regarding the tectonic setting of the region.

A low-angle detachment fault is visible in the marine seismic reflection records and has been recognized by the technical community as an east-northeast-dipping geologic structure beneath the ICB west of the mapped traces of the NI-RC Fault Zone (Bohannon and Geist, 1998; Crouch and Suppe, 1993; Ryan et al., 2009; Sorlien et al., 2009a, 2009b). Some geoscientists have interpreted this fault as having been reactivated on a regional scale in Pliocene through Holocene time as the OBT (Rivero 2004; Shaw and Plesch, 2010, Appendix A, Attachment A-3). However, their research by itself does not entirely resolve discrepancies between the strike-slip and blind thrust end-member models. The structural interaction of the detachment and high-angle faults cannot be resolved based on currently available marine seismic reflection records. More recent marine seismic reflection, coastal geomorphic, paleoseismic, and seismological research, previously not available to Rivero et al. (2000) and Rivero (2004), offer alternative interpretations of the lateral and down-dip extent of the OBT. Further, although the marine seismic reflection data supports Miocene extensional detachments and localized Pliocene through Holocene compressional activity, there is no direct evidence that clearly demonstrates Pleistocene or Holocene activity on the OBT as a major regional through-going thrust fault. Appropriate weight is given in this PSHA to the possibility that the OBT may be a capable seismic source based on the following data, observations, and interpretations:

- The wedge/thrust model developed by Rivero et al. (2000), Rivero and Shaw (2001), and Rivero (2004) to explain fold deformation along southern California's offshore region is based on a systematic analysis and review of an extensive set of seismic data.

- This model provides an alternative explanation of the apparent discontinuity of post-Upper Miocene faulting in this region and explains the significant amounts of Pliocene and post-Pliocene crustal shortening exhibited by the folded strata at and seaward of the shelf break.

- Available seismic reflection data cannot resolve whether the high-angle, strike-slip faults along the NI/RC Fault Zone displace the postulated OBT.

The activity and seismogenic potential of the OBT, however, is not definitive. The evidence cited by Rivero et al. (2000), Rivero and Shaw (2001), and Rivero (2004) is based on their interpretation of:

- Geophysical evidence of post-Pliocene folding and faulting in the offshore region;
- A structural relationship between the San Joaquin Hills and a similar wedge/thrust structure in the offshore;
- Association of the 1986 Oceanside earthquake with a component of the ICB thrust belt system (the Thirtymile Bank blind thrust);
- Regional coastal uplift; and
- Geodetic measurement of contractional crustal strain.

Each of these items of evidence may have some viability for indicating the seismogenic capacity of the OBT, but, as noted below, they are also consistent with a predominantly strike-slip regime.

A stronger case is made in support of the model that characterizes the NI/RC Fault Zone as part of a system of through-going strike-slip faults. The primary data, observations, and interpretations supporting a higher weight given to the strike-slip model are:

- The dominance of strike-slip motions that has occurred on the faults in ICB since the Eocene.
- Marine 2D seismic reflection geophysical records, similar and is some cases the same as those used by Rivero et al. (2000) and by Rivero (2004), led to alternate interpretations by Moore (1972), Western Geophysical (1972), Fischer and Mills (1991), Sliter et al. (2001), Crouch and Suppe (1993), and more recently Legg et al. (2007), Ryan et al. (2009), Sorlien et al. (2009b), and Ryan (2010, PC) as to the relatively continuous zone of recently active en echelon fault traces offshore of southern Orange County and San Diego County linking the onshore traces of the NI Fault and RC Fault, and alternate configurations of the faults further offshore to the west.
- Evidence to support reactivation of the entire OBT in the current tectonic environment is not conclusive. Recent re-analysis of available deep seismic reflection data acquired in the 1970s (Ryan et al., 2009; Sorlien et al., 2009b) provides alternative interpretations that the OBT is not a continuous active tectonic structure, but is composed of smaller, separate segments, not all of which are active.
- Alternatively, late Pleistocene/Holocene faults and associated folding used to support the regionally continuous blind thrust model can also be explained by strain partitioning and contraction in the right-lateral NI/RC Fault Zone, in particular at en echelon left steps or bends in the fault trace. In addition, some compressional elements apparent in the available marine seismic reflection records may be relics of earlier Pliocene compression. Further, local apparent compressional folds and/or discontinuities evident in these marine seismic reflection records

also may be due to translation of sediments over inherited basement protrusions, as suggested by Wright (1991).

- Clockwise rotation of crustal blocks in the ICB, which was postulated in SCE (2001), has been emphasized by Ryan et al. (2009). Rotation of a large crustal block would be consistent with the local reactivation of northern portions of the OBT (i.e., late Quaternary compression on subsidiary reverse faults beneath the continental slope offshore of San Mateo Point west of the NI/RC Fault Zone), but would not require reactivation or rupture of the entire length or depth of the detachment. Late Quaternary inactivity of the OBT further south offshore of Carlsbad and extensional subsidiary fault activity on continental slopes west of the NI/RC between Carlsbad and La Jolla, as suggested by Sorlien et al. (2009b), are consistent with this block rotation model. Geodetic data on the neighboring Peninsula Range block shows similar clockwise rotation as detailed in Appendix A.

- Based on their analysis of the tectonics surrounding the Agua Blanca Fault in Baja California, Wetmore et al. (2010, in review) document evidence that the Agua Blanca Fault becomes transtensive as it transitions offshore into the Borderland. This interpretation is consistent with a current tectonic environment of transtension in the Borderlands offshore of southern California, and suggests that the current kinematic framework offshore is principally transtensional in nature. They state that "Major late Miocene normal faults form an important kinematic component of deformation in the southern half of the central domain, but extreme crustal thinning is partially compensated by north-south shortening associated with detachment folds and conjugate-slip faults." This suggests that the regionally extensive thrust faults in the southern portions of the Peninsular Ranges and the ICB inferred by Rivero et al (2000) may be inherited from the Pliocene before development of the through-going strike-slip faults of the Peninsular Ranges, such as the San Jacinto, Elsinore and NI/RC faults. However, the presence of local compressional folds and faults is not precluded (Rockwell, 2010, PC).

- Seismicity data show that the NI and RC faults are capable strike-slip faults (Hauksson, 1987; Hauksson and Gross, 1991; Astiz and Shearer, 2000; and Grant and Shearer, 2004). Based on discussions with Dr. Ryan of the USGS (2010, PC) regarding her recent assessment of high-resolution seismic reflection data (Conrad et al., 2010) and refined epicenter locations/focal mechanism analyses by Astiz and Shearer (2000), an alternate interpretation for the source behind the thrust mechanism of the 1986 Oceanside earthquake is strain partitioning and contraction in the a left-step in the right-lateral strike-slip San Diego Trough Fault. This interpretation further indicates that strike-slip faults extend to seismogenic depths and are the major seismic source faults in the ICB.

- Paleoseismic data demonstrates that the onshore NI and RC faults are strike-slip faults (Rockwell et al., 1991, 1992; Ponti and Ehman, 2009; Ponti, 2010, PC; and Rockwell, 2010, PC). A dominate long and continuous primary thrust fault between these two northern and southern right-lateral fault sections appears inconsistent with the current dominate tectonic framework of the Peninsular Ranges and the ICB, however, the local presence of blind thrust faults cannot be refuted.

- Regional coastal uplift, which is cited by Rivero et al. (2000) to indicate that the Oceanside and Thirtymile Bank thrusts are active over a region larger than the San Joaquin Hills (Grant et al., 1999 and 2002) or Mount Soledad, (Rockwell, 2010) may be attributed to a large degree to other processes (e.g., rift shoulder thermal isostasy). Studies by Mueller et al. (2009) suggest that the uniform regional uplift observed in southern California may reflect the far-field effect of unloading and rift shoulder development associated with lithospheric thinning in the northern Gulf of California and the Salton Trough.

- There is no marked change in the pattern of coastal uplift across the segmentation boundary between the more shallow dipping northern OBT and the steeper dipping southern OBT as proposed by Rivero (2004), Rivero and Shaw (2010, in press), and Shaw and Plesch (2010, Appendix A, Attachment A-3). This suggests that either the coastal uplift is not directly linked to slip on the OBT, or the southern segment has a lower slip rate. Dr. T. Rockwell notes that there is no evidence for tilting or significant differential uplift along the coast as recorded by the Quaternary marine terraces and underlying Tertiary bedrock (Kern and Rockwell, 1992; Rockwell, 2001, PC and 2010, PC).

- The initiation of structural inversion and thrust faulting in the offshore, which is inferred to have begun in the Pliocene (Crouch and Suppe, 1993; Rivero et al., 2000; and Rivero and Shaw, 2001; Rivero, 2004; Rivero and Shaw, 2010, in press; and Shaw and Plesch, 2010, Appendix A, Attachment A-3), may significantly predate the initiation of coastal uplift as noted above. This suggests that coastal uplift is not directly linked with movement on the ICB thrust system. However, age estimates and correlation of stratigraphy across the fold belts in the offshore are not well constrained due to the paucity of offshore well control. Consequently, the initiation of folding could have been later than previously estimated.

- Geodetic data, as presented in Appendix A, shows that strain in the southern ICB is dominated by northwest directed shear subparallel to the overall North American/Pacific plate motion. Little or no convergence across the ICB normal to the plate boundary is observed in the vicinity of SONGS as detailed in Appendix A. In particular, the lack of significant convergence in the regional signal to the east of the OBT suggests there is not a regional “driving” force that would reactivate a through going seismogenic thrust (SCE, 2001).

- Some of the contractional deformation observed in the ICB could have occurred during the Pliocene or early Quaternary within a different stress regime. Based on geologic evidence that suggests coastal uplift in the San Diego region, as well as activity on the Elsinore Fault, was initiated approximately 0.9 to 1.0 Ma, Dr. Rockwell (2001, PC and 2010, PC) suggests that a reorientation of the plate vector may have occurred in the region during early to middle Quaternary. Dr. Ponti (2001 and 2010, PC) also suggests a change in the tectonic stress regime in that same time frame based on evidence for decreasing Late Quaternary slip rates compared to longer-term rates for some blind thrusts in the Los Angeles basin (e.g., the Compton-Los Alamitos and Las Cienegas faults).

2.4.2 Assigned Weights

Based on these observations and qualitative judgments, weights were assigned to the two alternative end-member seismic source fault characterization models by the seismic source characterization integrator team. The weights assigned reflect the team’s professional geoscience judgment as to the extent to which each end-member source fault model would find support from the currently available scientific evidence and best fit the engineering and scientific technical community’s current understanding of the tectonic environment surrounding southern California, including SONGS. A 90% weight was assigned by two of the team members and a 85% weight was assigned by the third member to the strike-slip seismic source characterization model, which includes the through-going high-angle, right-lateral strike-slip, NI/RC Fault Zone as the nearest primary active fault system in the ICB offshore of SONGS. The blind thrust seismic source characterization model, which includes the postulated, regionally extensive OBT as the nearest primary fault system in the ICB offshore of SONGS, was assigned the remaining weight of 10 or 15%, respectively. For use in the 2010 PSHA, the weights assigned by the seismic source integrator team were numerically equal to 88% for the strike-slip end-member model and 12% for the blind thrust end-member model.

This weighting is supported by the following key points. First, there is little empirical evidence available to support that oblique slip with the ratio of strike-slip to dip-slip suggested by the available information regarding the OBT would occur on a fault plane dipping between 14 and 24 degrees. Second, recent assessments of offshore earthquakes relative to new mapped fault locations and geometry raise questions as to whether thrust focal mechanisms from recent earthquakes are tied to regionally persistent blind thrust faults or are generated by more local subsidiary blind thrust faults driven by strain partitioning in contractional left-steps or bends in the more dominate right-lateral strike-slip fault system. Finally, more current GPS records do not support a regionally persistent blind thrust model that would extend the full distance of the San Diego County coast line. Locally, there does appear to be indications of reactivation of low-angle Miocene detachment surfaces as thrust faults since late Pliocene time, but in the present tectonic environment, these thrust faults do not appear to make up a continuous, active tectonic structure on a regional scale.

Table 2-1a: Type-A Faults and Type-B Faults

	Fault Name	Closest Distance from SONGS to Rupture Plane Rrup (km)(5)
Type-A Faults(1)	San Andreas(3)	92
	San Jacinto(3)	70
	Elsinore(3)	38
Type-B Faults(1)	Newport-Inglewood/Rose Canyon (NI/RC)(3)	8
	Palos Verdes/Coronado Bank(3)	32

Table 2-1b: Non-Designated Faults

	Fault Name	Closest Distance from SONGS to Rupture Plane Rrup (km) (5)
Non-Designated Faults(2)	Oceanside Blind Thrust (OBT)(4)	7
	San Diego Trough	46
	San Clemente	94

(1) "Type" designated fault; parameters for fault listed in Table 1 of Appendix A in UCERF 2 and used in the current USGS implementation of UCERF 2 (2009, PC) and in this PSHA.
(2) Non-designated fault; parameters for fault being considered for development by WGCEP (2008) as presented in Table 2 of Appendix A in UCERF 2.
(3) Relevant faults models by the current USGS implementation of UCERF 2 (2009, PC) and used in this PSHA.
(4) OBT Fault as hypothesized by Rivero et al. (2000) and Rivero (2004).
(5) Distances taken from Figure 2-3.

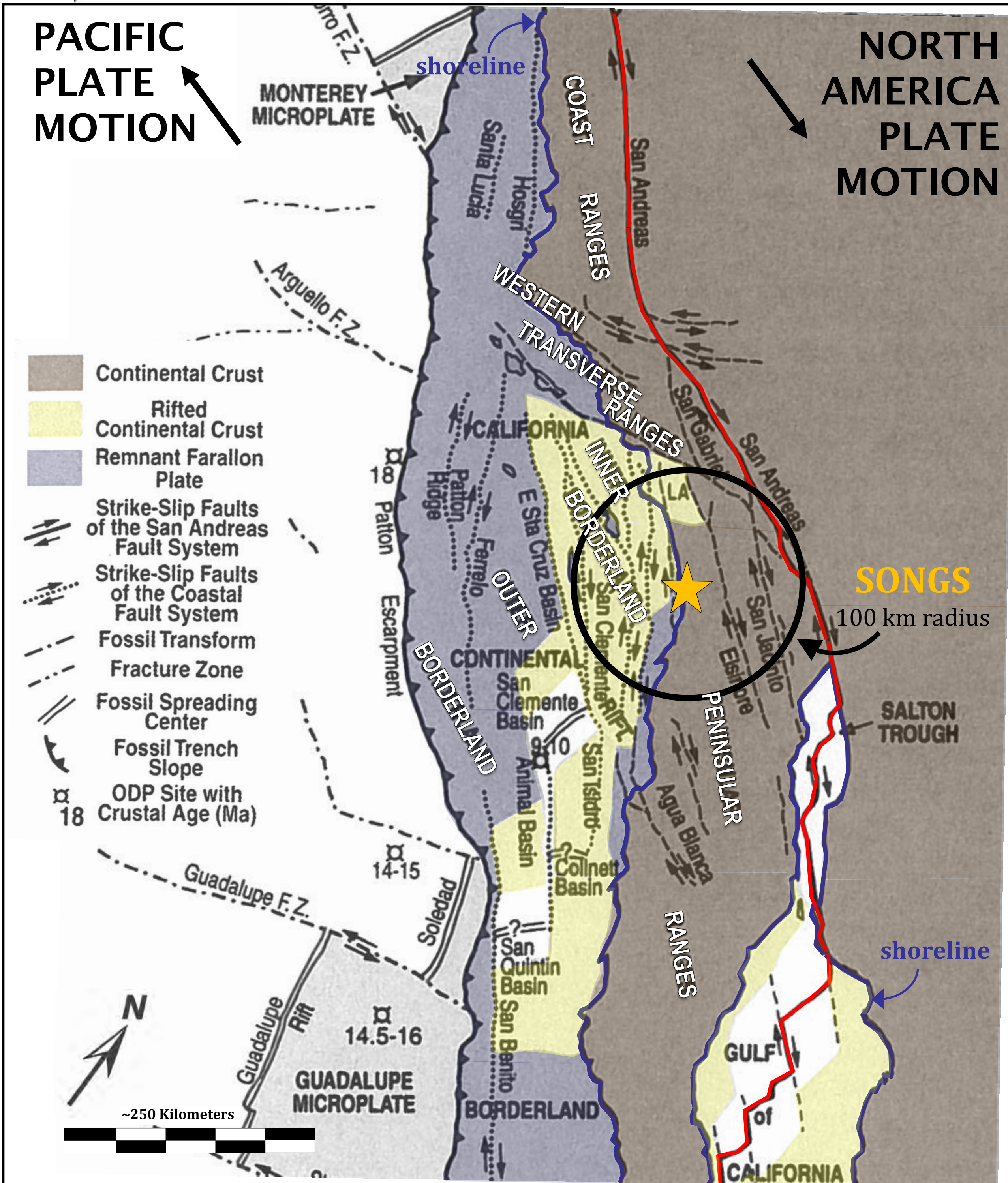

Modified from Legg et al. (2004). Plate motion vectors from Argus and Gordon (1991).

GeoPentech Geotechnical & Geoscience Consultants

REGIONAL MAP SHOWING TECTONIC BLOCKS OF SOUTHERN CALIFORNIA

FIGURE 2-1a

SAN ONOFRE NUCLEAR GENERATING STATION

SEISMIC HAZARD ASSESSMENT PROGRAM

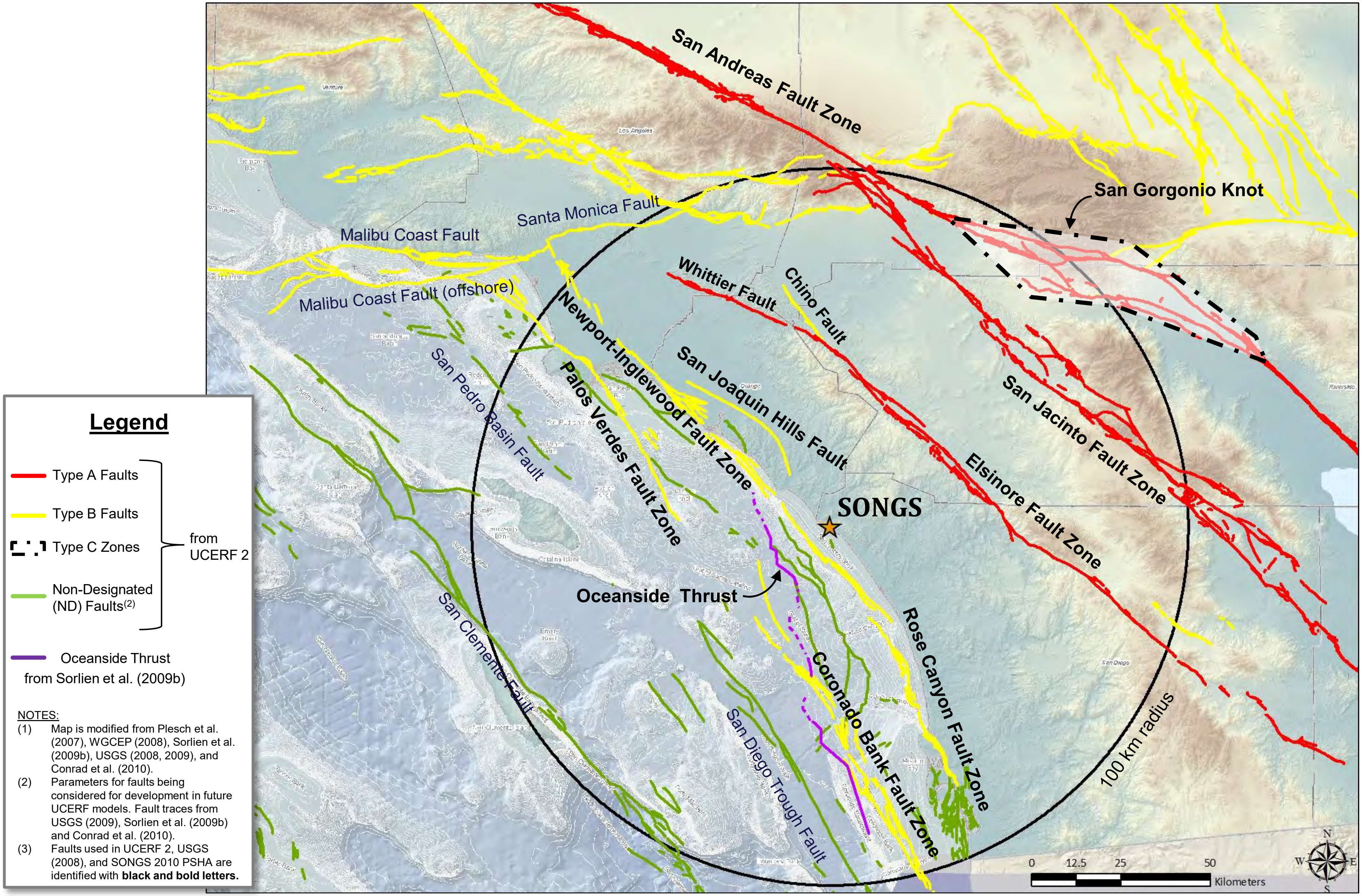

GeoPentech Geotechnical & Geoscience Consultants

SAN ONOFRE NUCLEAR GENERATING STATION
SEISMIC HAZARD ASSESSMENT PROGRAM

POTENTIAL SEISMIC SOURCES

FIGURE 2-1b

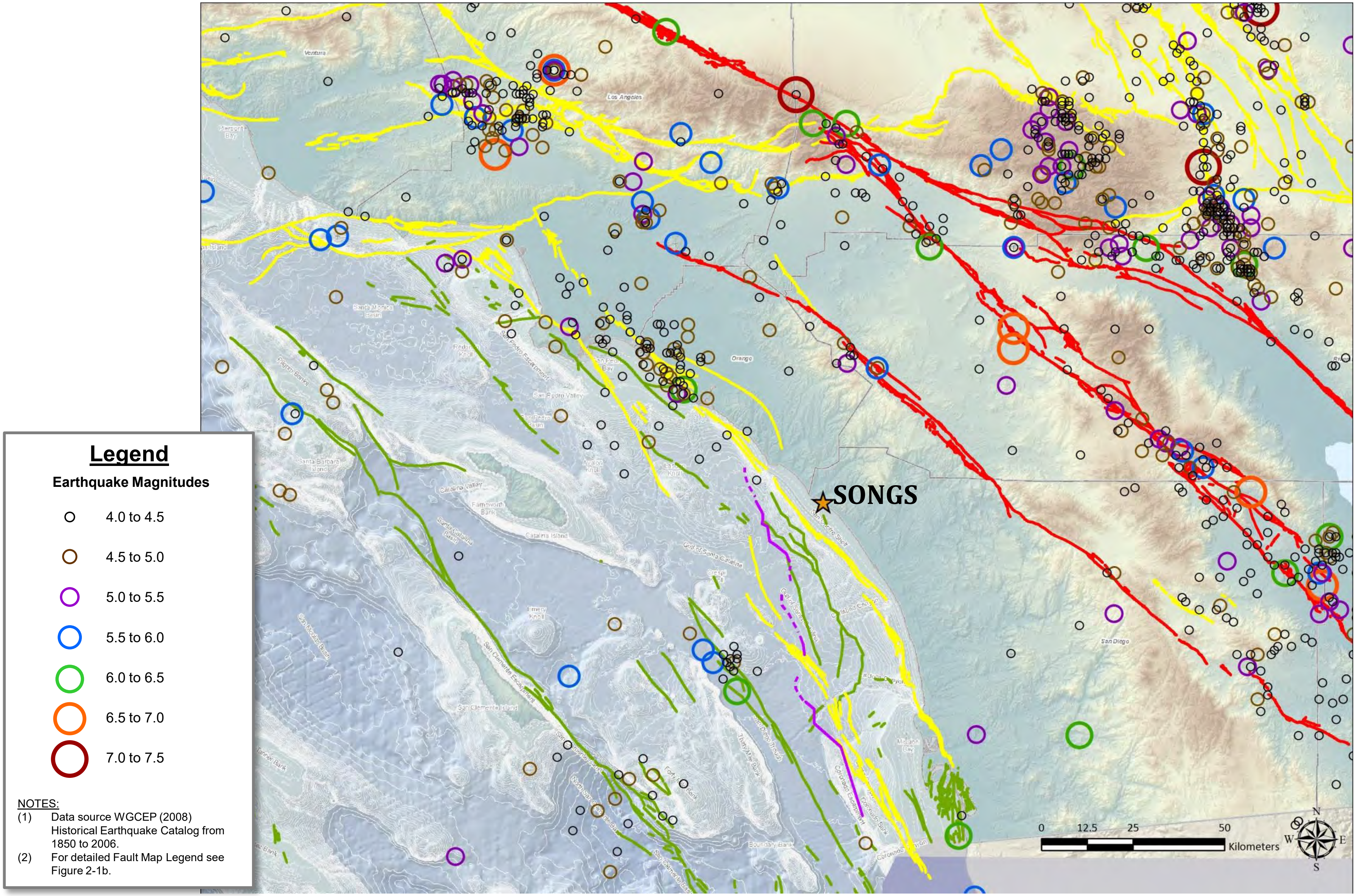

GeoPentech
Geotechnical & Geoscience Consultants

SAN ONOFRE NUCLEAR GENERATING STATION
SEISMIC HAZARD ASSESSMENT PROGRAM

EPICENTERS OF MAINSHOCK AND AFTERSHOCK EARTHQUAKES

FIGURE 2-1c

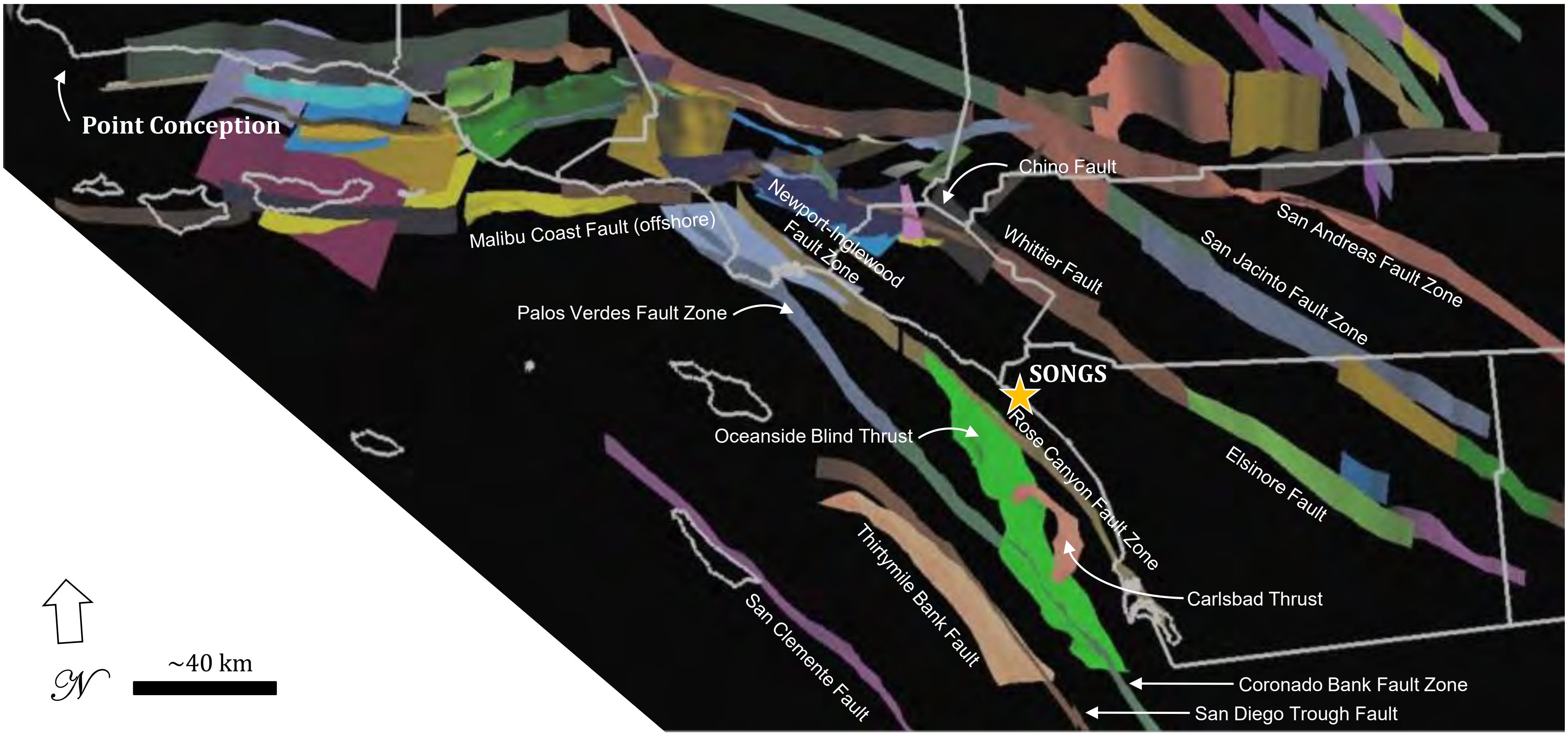

Modified from CFM (Plesch et al., 2007)

GeoPentech Geotechnical & Geoscience Consultants	SAN ONOFRE NUCLEAR GENERATING STATION SEISMIC HAZARD ASSESSMENT PROGRAM	POTENTIAL SEISMIC SOURCES FROM THE COMMUNITY FAULT MODEL (CFM)	FIGURE 2-2

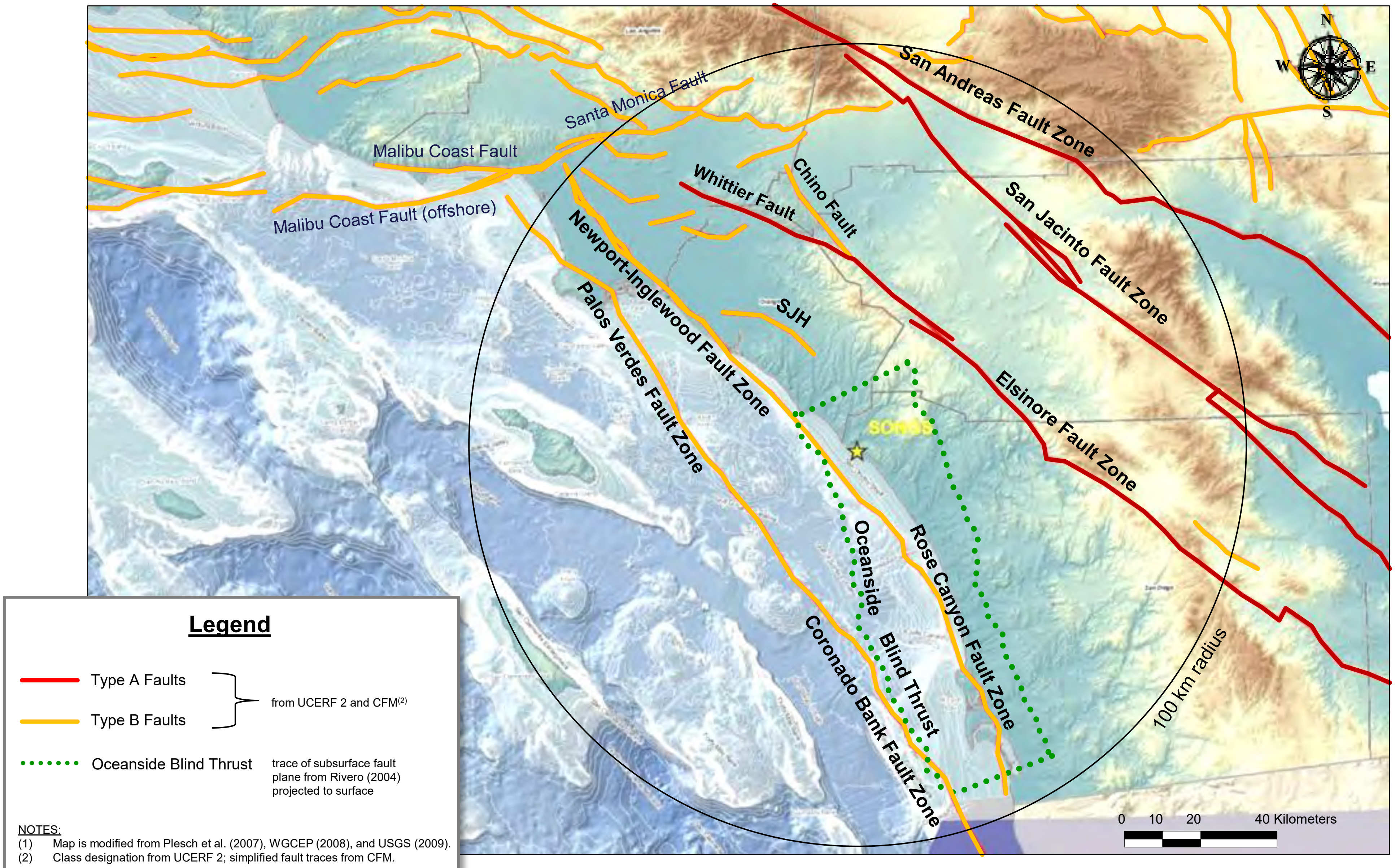

GeoPentech
Geotechnical & Geoscience Consultants

SAN ONOFRE NUCLEAR GENERATING STATION
SEISMIC HAZARD ASSESSMENT PROGRAM

SEISMIC SOURCES CONSIDERED IN HAZARD ANALYSIS

FIGURE 2-3

Notes:

[1] Assuming 5km to 17km Seismogenic Depth

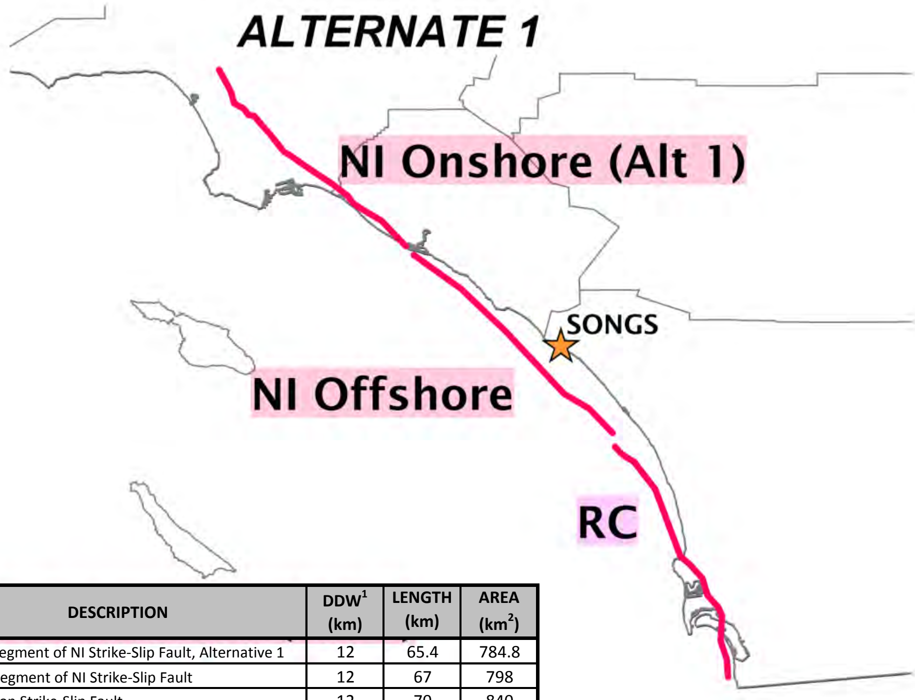

SEGMENT LABEL	DESCRIPTION	DDW[1] (km)	LENGTH (km)	AREA (km^2)
NI Onshore (Alt 1)	Onshore Segment of NI Strike-Slip Fault, Alternative 1	12	65.4	784.8
NI Offshore	Offshore Segment of NI Strike-Slip Fault	12	67	798
RC	Rose Canyon Strike-Slip Fault	12	70	840

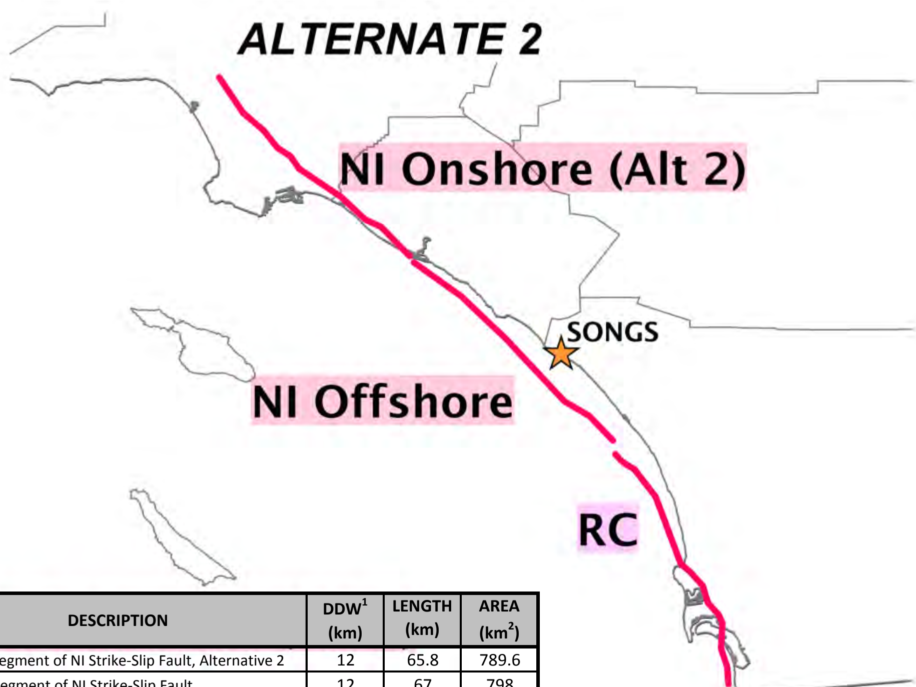

SEGMENT LABEL	DESCRIPTION	DDW[1] (km)	LENGTH (km)	AREA (km^2)
NI Onshore (Alt 2)	Onshore Segment of NI Strike-Slip Fault, Alternative 2	12	65.8	789.6
NI Offshore	Offshore Segment of NI Strike-Slip Fault	12	67	798
RC	Rose Canyon Strike-Slip Fault	12	70	840

GeoPentech
Geotechnical & Geoscience Consultants

SIMPLIFIED GEOMETRY AND SEGMENTATION FOR STRIKE-SLIP END-MEMBER MODEL

FIGURE 2-4

SAN ONOFRE NUCLEAR GENERATING STATION

SEISMIC HAZARD ASSESSMENT PROGRAM

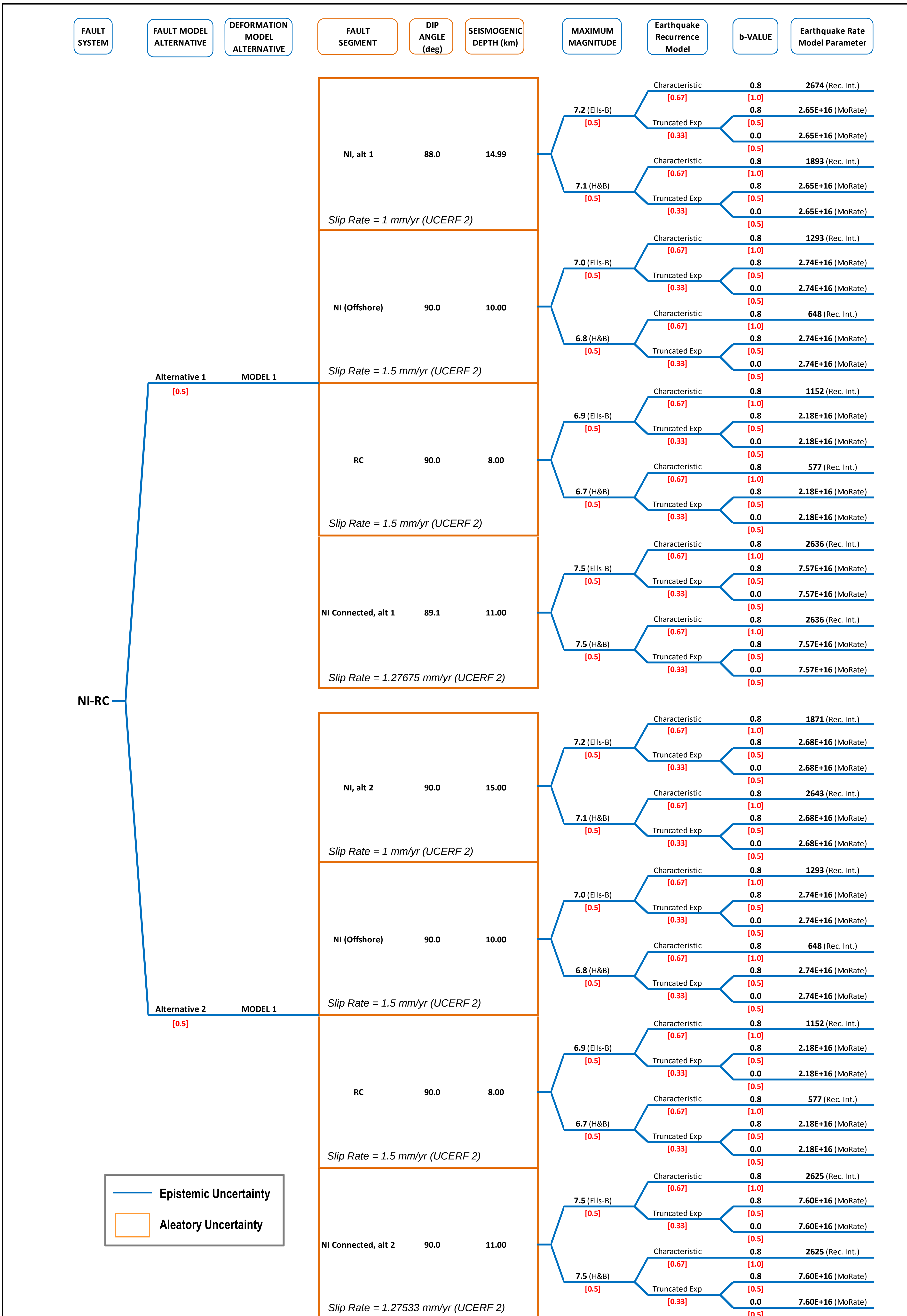

GeoPentech
Geotechnical & Geoscience Consultants

NIRC 'LOGIC TREE' – 8 COMBINATIONS OF FAULT SEGMENT RUPTURE

FIGURE 2-5

SAN ONOFRE NUCLEAR GENERATING STATION

SEISMIC HAZARD ASSESSMENT PROGRAM

Seismic Reflection Data from Harvard University

Original data compiled from several petroleum industry sources

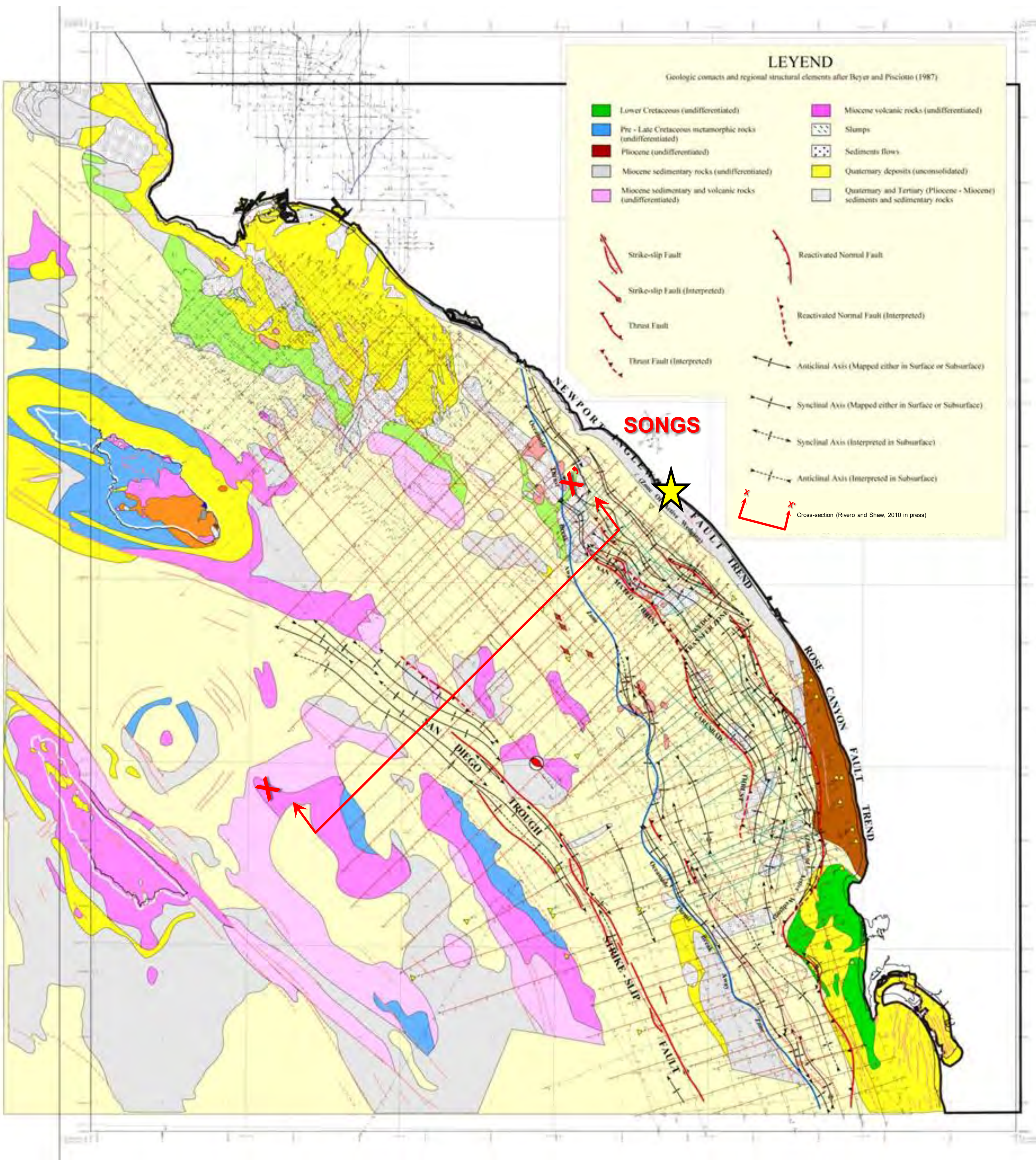

Modified from Rivero (2004)

GeoPentech Geotechnical & Geoscience Consultants	MARINE GEOLOGIC MAP	FIGURE 2-6
	SAN ONOFRE NUCLEAR GENERATING STATION SEISMIC HAZARD ASSESSMENT PROGRAM	

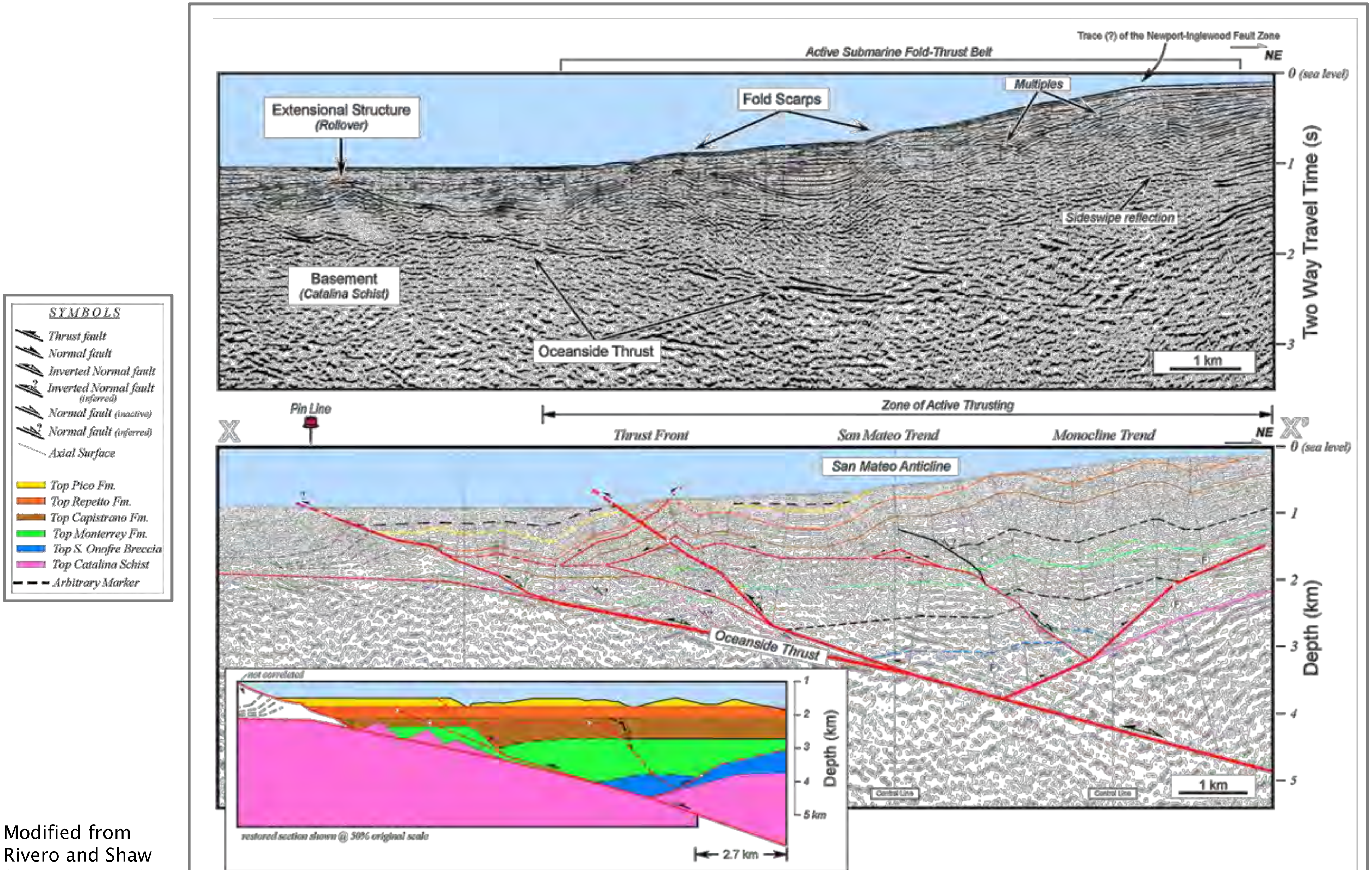

Modified from Rivero and Shaw (2010, in press)

GeoPentech
Geotechnical & Geoscience Consultants

SAN ONOFRE NUCLEAR GENERATING STATION
SEISMIC HAZARD ASSESSMENT PROGRAM

RECORD AND INTERPRETATION

FIGURE 2-7

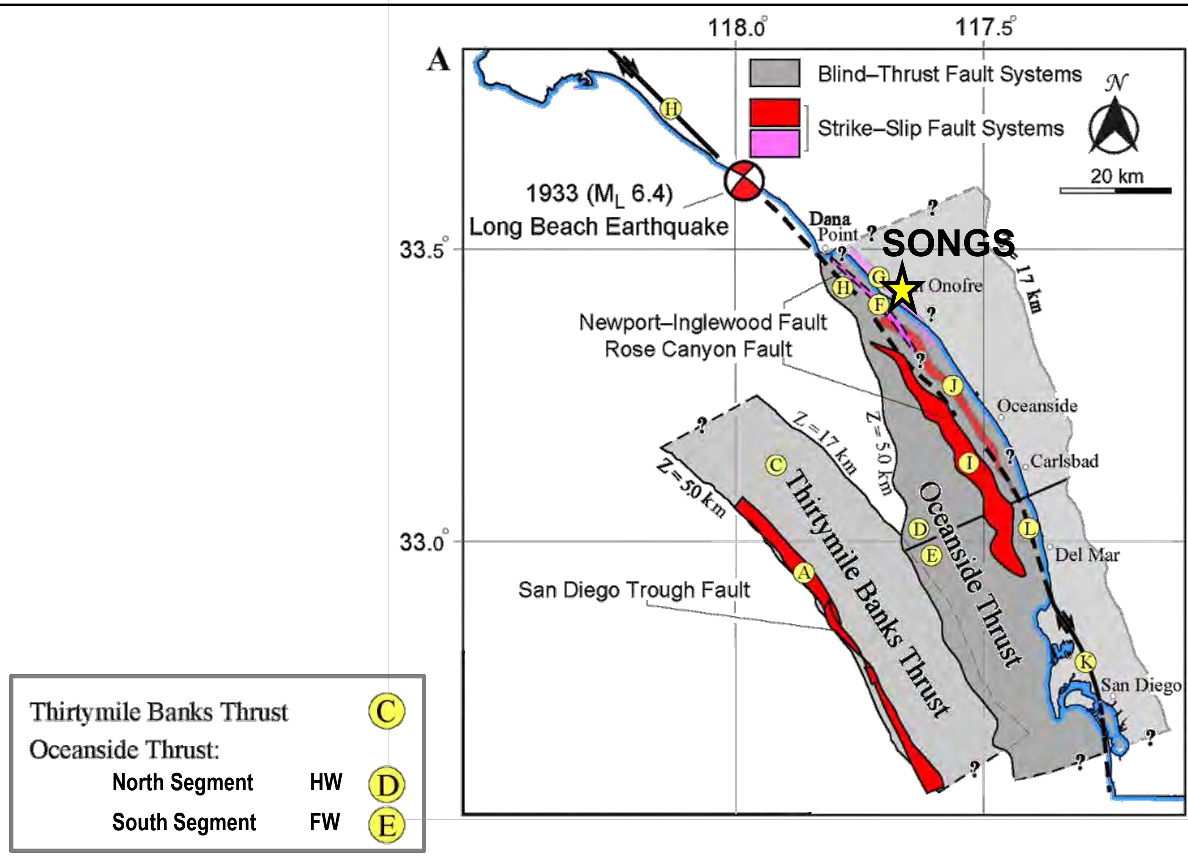

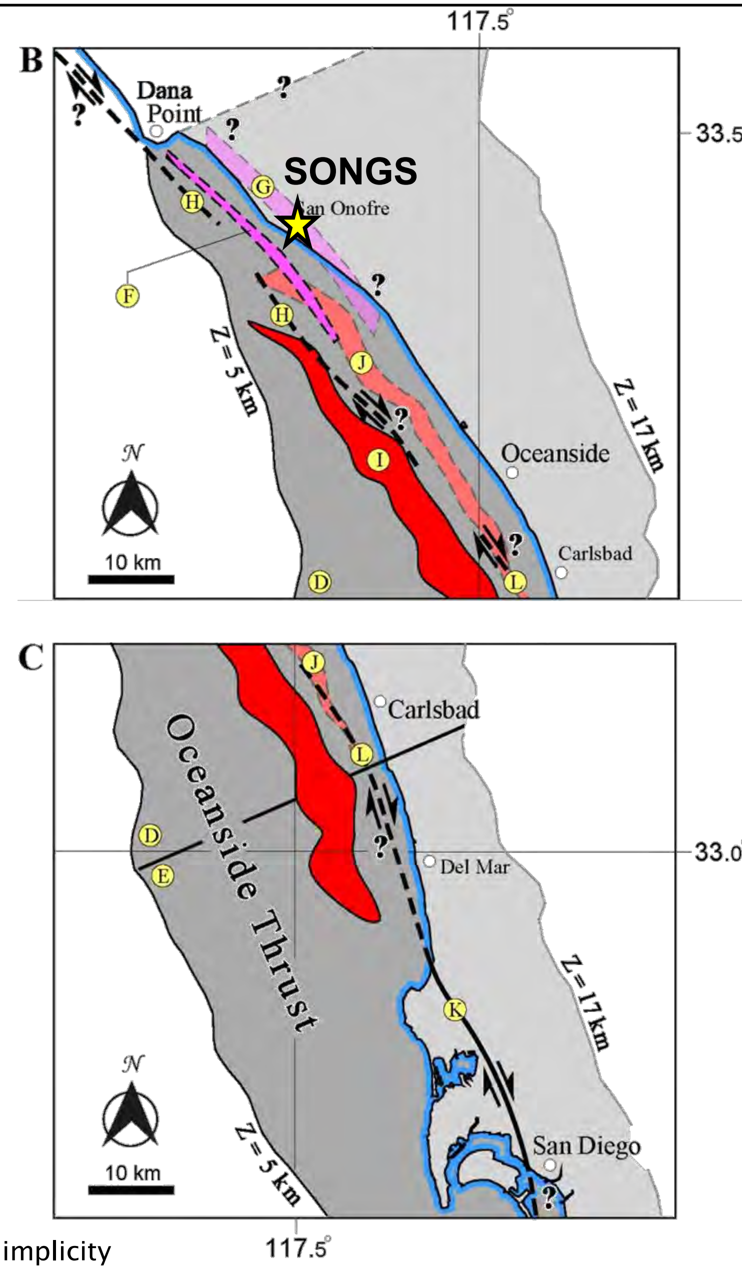

FAULT SEGMENTS	LOCATION	CODE
San Diego Trough Strike–Slip Fault	HW–FW	A – B
Offshore Newport–Inglewood Strike–Slip Fault	HW–FW	F – G
Onshore Newport–Inglewood Strike–Slip Fault	HW–FW	H
Offshore Rose Canyon Fault (mapped)	HW–FW	I – J
Onshore Rose Canyon Strike–Slip Fault	HW–FW	K
Offshore Rose Canyon Strike–Slip Fault	HW–FW	L

NOTES: (1) Modified from Rivero (2004)
(2) Footwall segment of the San Diego Strike-Slip Trough Fault B is not shown for simplicity
(3) Latitude and longitude approximate

GeoPentech
Geotechnical & Geoscience Consultants

SAN ONOFRE NUCLEAR GENERATING STATION
SEISMIC HAZARD ASSESSMENT PROGRAM

HYPOTHESIZED OBT FAULT SYSTEM

FIGURE 2-8

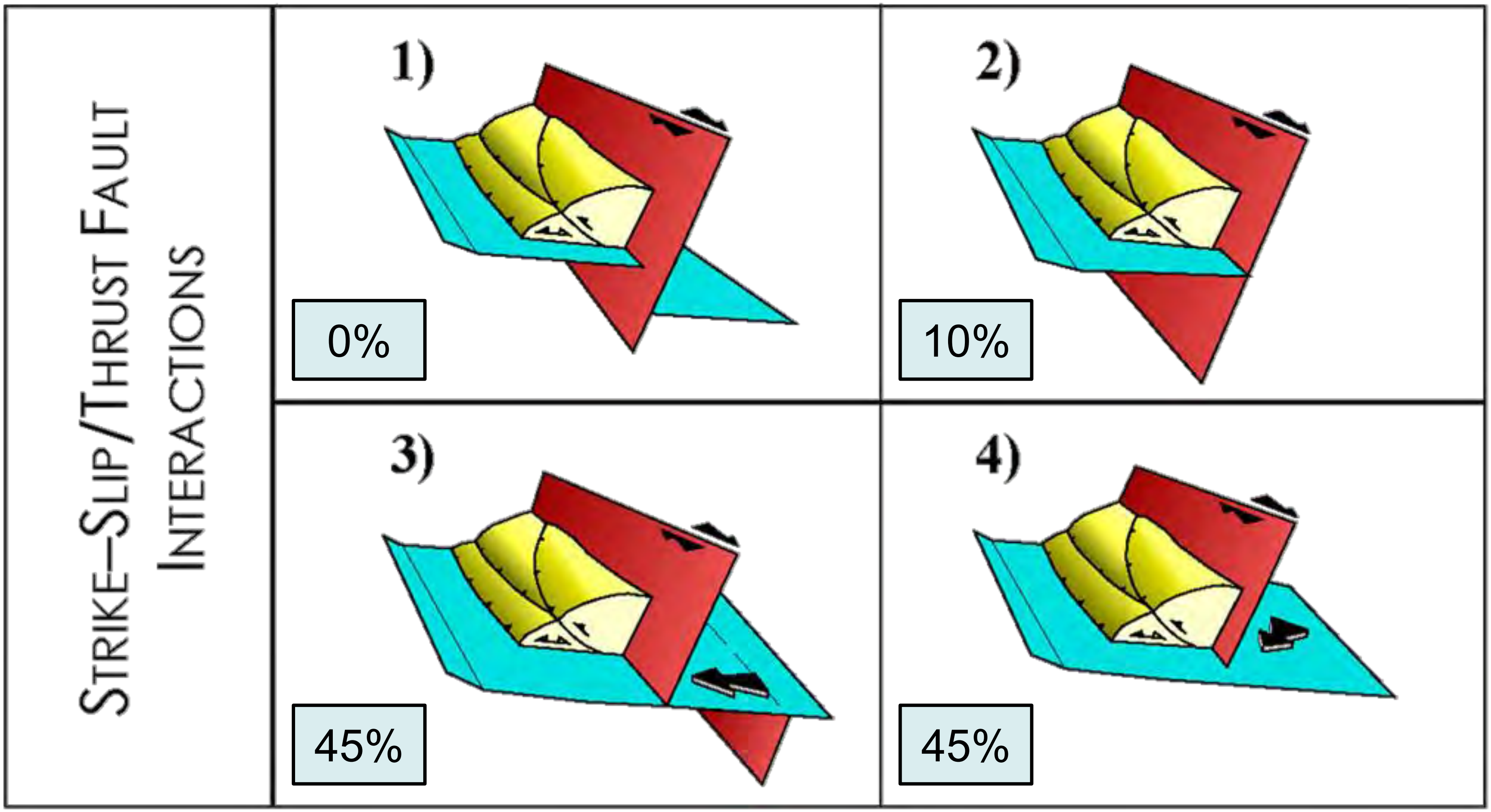

Modified from Rivero (2004)

GeoPentech Geotechnical & Geoscience Consultants	**SAN ONOFRE NUCLEAR GENERATING STATION** SEISMIC HAZARD ASSESSMENT PROGRAM	**HYPOTHESIZED OBT FAULT SYSTEM MODEL CONFIGURATIONS WITH EPISTEMIC 'WEIGHTS'**	FIGURE 2-9

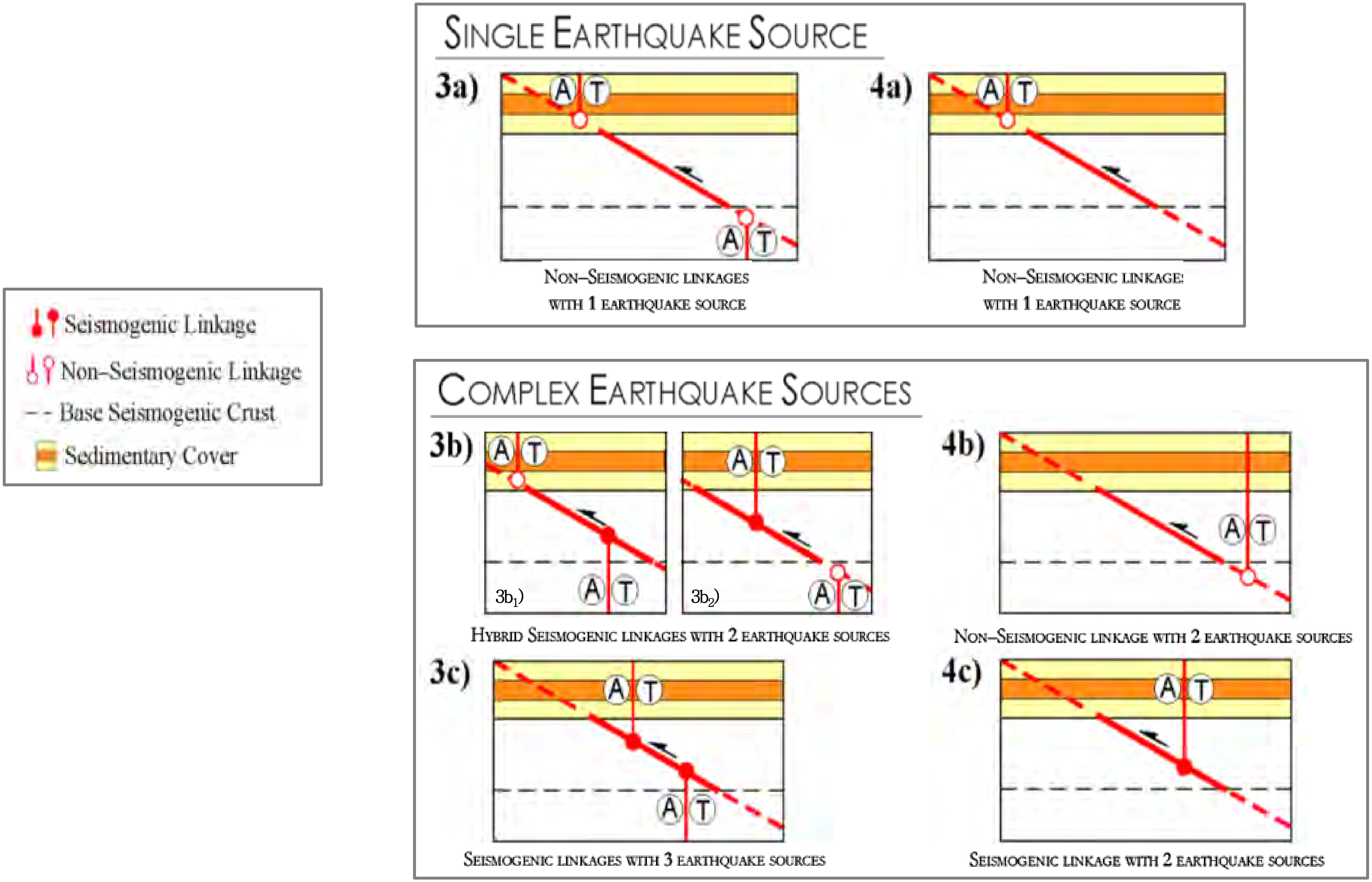

Modified from Rivero and Shaw (2010, in press)

GeoPentech Geotechnical & Geoscience Consultants	SAN ONOFRE NUCLEAR GENERATING STATION SEISMIC HAZARD ASSESSMENT PROGRAM	EPISTEMIC ALTERNATIVES TO HYPOTHESIZED OBT FAULT SYSTEM MODEL CONFIGURATIONS 3 AND 4	FIGURE 2-10

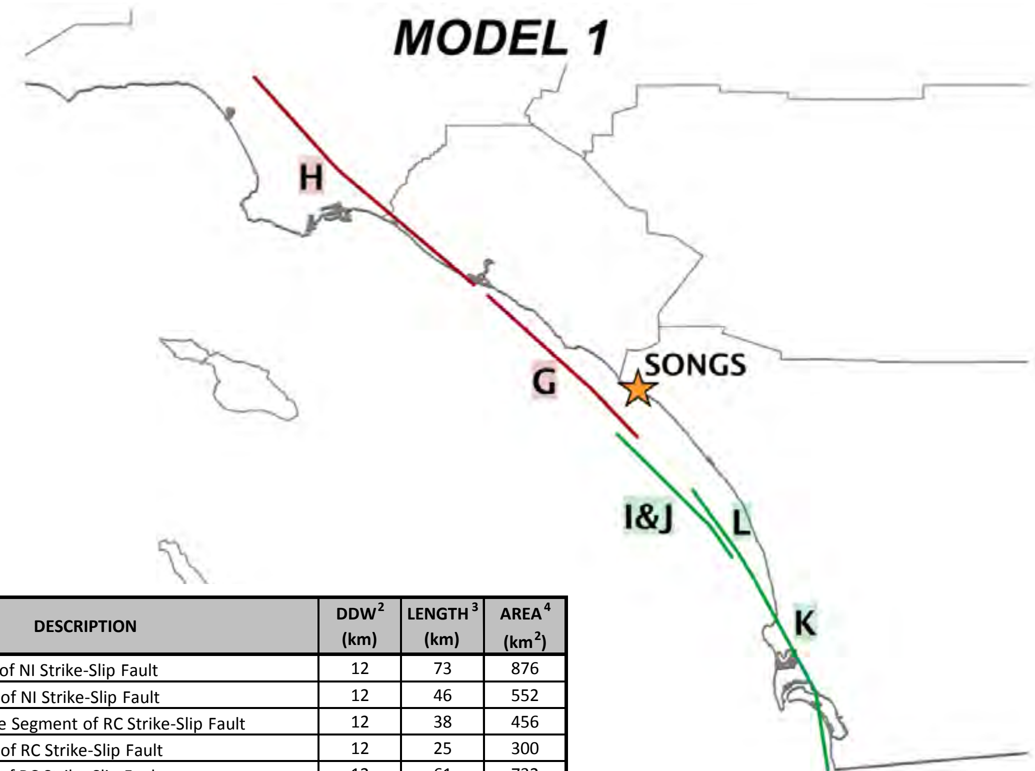

SEGMENT LABEL[1]	DESCRIPTION	DDW[2] (km)	LENGTH[3] (km)	AREA[4] (km^2)
H	Onshore Segment of NI Strike-Slip Fault	12	73	876
G	Offshore Segment of NI Strike-Slip Fault	12	46	552
I&J	"Mapped" Offshore Segment of RC Strike-Slip Fault	12	38	456
L	Offshore Segment of RC Strike-Slip Fault	12	25	300
K	Onshore Segment of RC Strike-Slip Fault	12	61	732

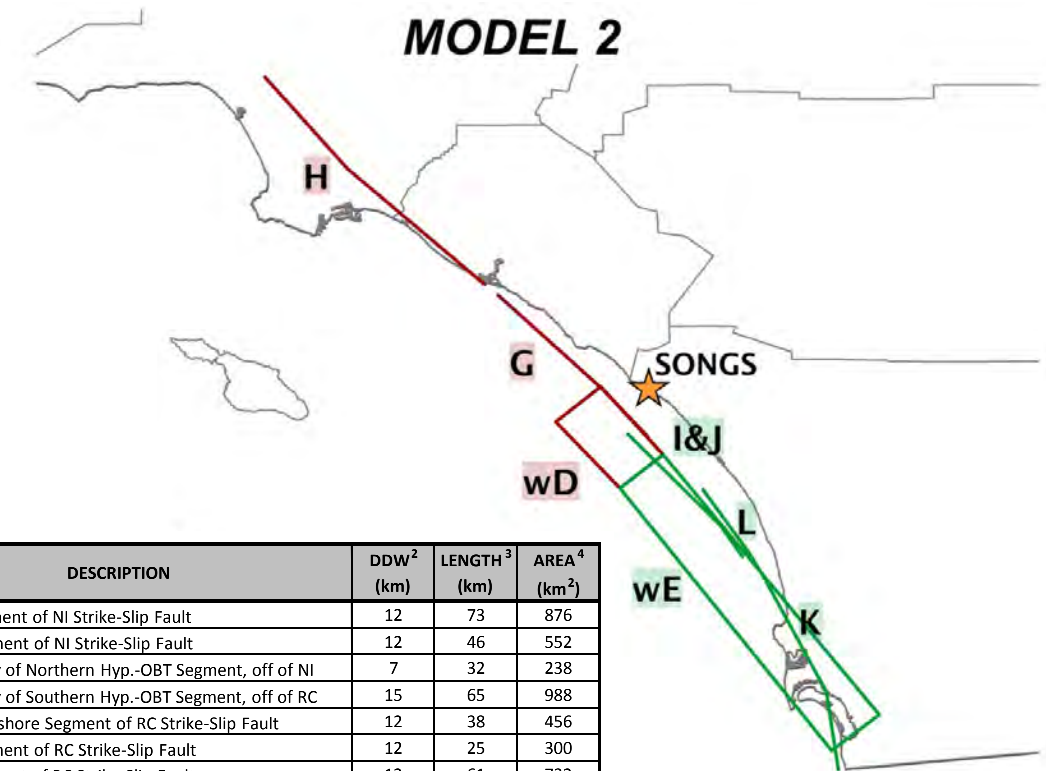

SEGMENT LABEL[1]	DESCRIPTION	DDW[2] (km)	LENGTH[3] (km)	AREA[4] (km^2)
H	Onshore Segment of NI Strike-Slip Fault	12	73	876
G	Offshore Segment of NI Strike-Slip Fault	12	46	552
wD	Western Splay of Northern Hyp.-OBT Segment, off of NI	7	32	238
wE	Western Splay of Southern Hyp.-OBT Segment, off of RC	15	65	988
I&J	"Mapped" Offshore Segment of RC Strike-Slip Fault	12	38	456
L	Offshore Segment of RC Strike-Slip Fault	12	25	300
K	Onshore Segment of RC Strike-Slip Fault	12	61	732

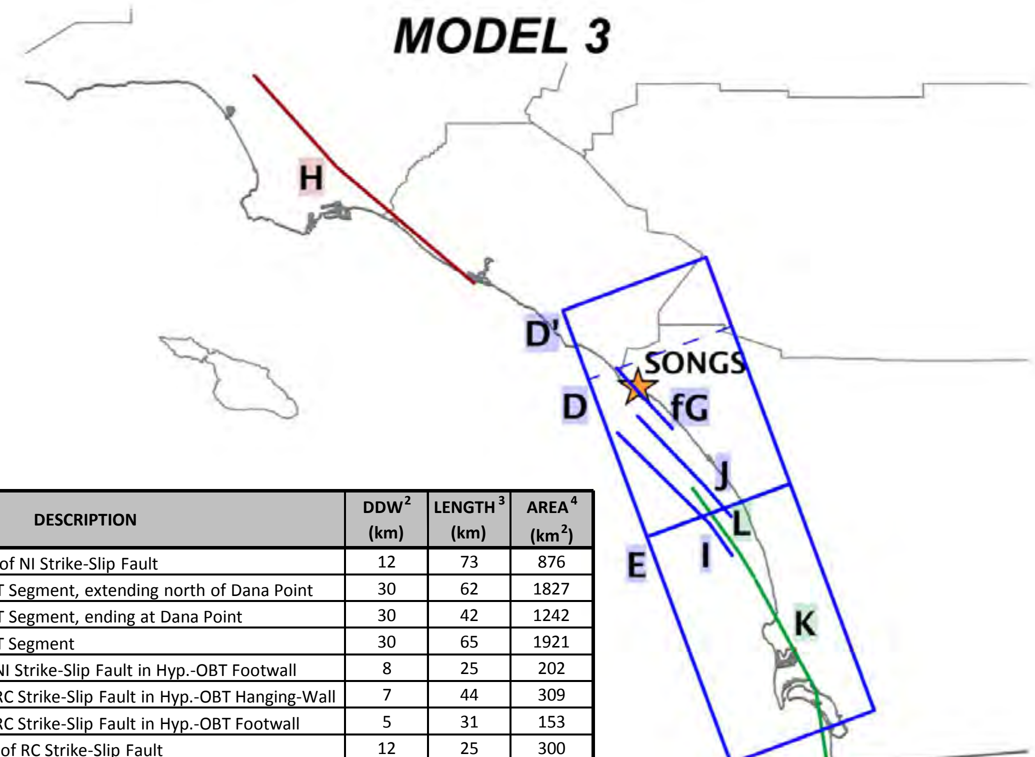

SEGMENT LABEL[1]	DESCRIPTION	DDW[2] (km)	LENGTH[3] (km)	AREA[4] (km^2)
H	Onshore Segment of NI Strike-Slip Fault	12	73	876
D'	Northern Hyp.-OBT Segment, extending north of Dana Point	30	62	1827
D	Northern Hyp.-OBT Segment, ending at Dana Point	30	42	1242
E	Southern Hyp.-OBT Segment	30	65	1921
fG	Offshore Splay of NI Strike-Slip Fault in Hyp.-OBT Footwall	8	25	202
I	Offshore Splay of RC Strike-Slip Fault in Hyp.-OBT Hanging-Wall	7	44	309
J	Offshore Splay of RC Strike-Slip Fault in Hyp.-OBT Footwall	5	31	153
L	Offshore Segment of RC Strike-Slip Fault	12	25	300
K	Onshore Segment of RC Strike-Slip Fault	12	61	732

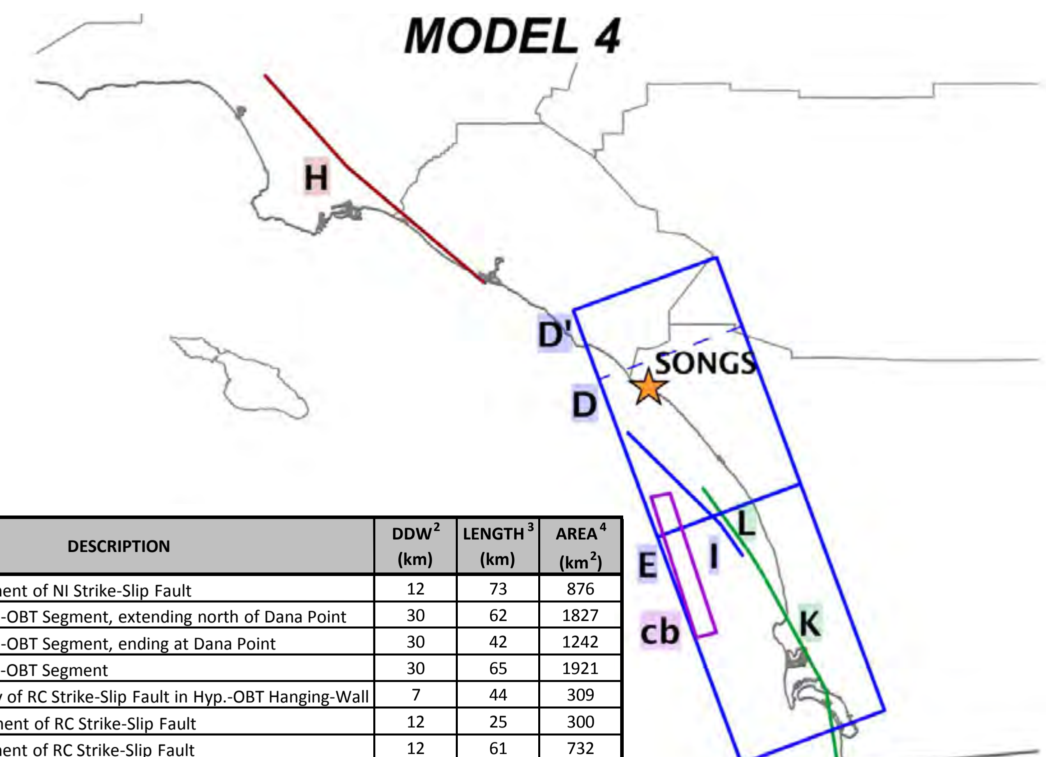

SEGMENT LABEL[1]	DESCRIPTION	DDW[2] (km)	LENGTH[3] (km)	AREA[4] (km^2)
H	Onshore Segment of NI Strike-Slip Fault	12	73	876
D'	Northern Hyp.-OBT Segment, extending north of Dana Point	30	62	1827
D	Northern Hyp.-OBT Segment, ending at Dana Point	30	42	1242
E	Southern Hyp.-OBT Segment	30	65	1921
I	Offshore Splay of RC Strike-Slip Fault in Hyp.-OBT Hanging-Wall	7	44	309
L	Offshore Segment of RC Strike-Slip Fault	12	25	300
K	Onshore Segment of RC Strike-Slip Fault	12	61	732
cb	Carlsbad Blind Thrust Fault	20	12	241

Notes:

[1] Labels modified from Figure A-2-1

[2] Assuming 5km to 17km Seismogenic Depth

[3] Based on Rivero (2004)

[4] Calculated based on DDW and Length

[5] See Appendix A, Attachment A-3 for details

GeoPentech
Geotechnical & Geoscience Consultants

SAN ONOFRE NUCLEAR GENERATING STATION

SEISMIC HAZARD ASSESSMENT PROGRAM

SIMPLIFIED GEOMETRY AND SEGMENTATION FOR OBT FAULT SYSTEM MODEL CONFIGURATIONS

FIGURE 2-11

FAULT SYSTEM	KINEMATIC MODEL	SEISMIC SOURCE	OBT LIMIT	LINKAGE	SEGMENTATION	FAULT SEGMENT COMBINATION	DISTRIBUTION OF SEGMENT RUPTURE	LONG-TERM SLIP RATE (mm/yr)	RECURRENCE MODEL [1]	
OBT System [2]	Model 1 (0.00)	NI Strike-Slip			Single	G	25%	1.5+/-0.5	Characteristic	Trunc G-R
					Single	H	50%	1.0+/-0.5	Characteristic	Trunc G-R
					Multi	G + H	25%	1.0+/-0.5	Characteristic	Trunc G-R
		RC Strike-Slip			Single	I&J	10%	1.07+/-0.03	Characteristic	Trunc G-R
					Single	K	20%	1.07+/-0.03	Characteristic	Trunc G-R
					Single	L	20%	1.07+/-0.03	Characteristic	Trunc G-R
					Multi	I&J + K	10%	1.07+/-0.03	Characteristic	Trunc G-R
					Multi	K + L	20%	1.07+/-0.03	Characteristic	Trunc G-R
					Multi	I&J + L	10%	1.07+/-0.03	Characteristic	Trunc G-R
					Multi	I&J + K + L	10%	1.07+/-0.03	Characteristic	Trunc G-R
	Model 2 (0.10)	NI Strike-Slip			Single	G&wD	25%	1.02+/-0.14	Characteristic	Trunc G-R
					Single	H	50%	1.0+/-0.5	Characteristic	Trunc G-R
					Multi	G&wD + H	25%	1.02+/-0.14	Characteristic	Trunc G-R
		RC Strike-Slip			Single	I&J&wE	10%	0.82+/-0.12	Characteristic	Trunc G-R
					Single	K	20%	1.07+/-0.03	Characteristic	Trunc G-R
					Single	L	20%	1.07+/-0.03	Characteristic	Trunc G-R
					Multi	I&J&wE + K	10%	0.82+/-0.12	Characteristic	Trunc G-R
					Multi	K + L	20%	1.07+/-0.03	Characteristic	Trunc G-R
					Multi	I&J&wE + L	10%	0.82+/-0.12	Characteristic	Trunc G-R
					Multi	I&J&wE + K + L	10%	0.82+/-0.12	Characteristic	Trunc G-R
	Model 3 (0.45)	NI Strike-Slip			Single	H	100%	1.0+/-0.5	Characteristic	Trunc G-R
		RC Strike-Slip			Single	K	33%	1.07+/-0.03	Characteristic	Trunc G-R
					Single	L	33%	1.07+/-0.03	Characteristic	Trunc G-R
					Multi	K + L	33%	1.07+/-0.03	Characteristic	Trunc G-R
		Oceanside Thrust	Stops at DP (0.50)	Linkage 3a (0.30)	Single	D	33%	1.02+/-0.14	Characteristic	Trunc G-R
					Single	E	33%	0.82+/-0.12	Characteristic	Trunc G-R
					Multi	D + E	33%	1.02+/-0.14	Characteristic	Trunc G-R
				Linkage 3b1 (0.20)	Single	D&fG	33%	1.02+/-0.14	Characteristic	Trunc G-R
					Single	E&J	33%	0.82+/-0.12	Characteristic	Trunc G-R
					Multi	D&fG + E&J	33%	1.74+/-0.2	Characteristic	Trunc G-R
				Linkage 3b2 (0.30)	Single	D	33%	1.02+/-0.14	Characteristic	Trunc G-R
					Single	E&I	33%	0.82+/-0.12	Characteristic	Trunc G-R
					Multi	D + E&I	33%	1.74+/-0.2	Characteristic	Trunc G-R
				Linkage 3c (0.20)	Single	D&fG	33%	1.02+/-0.14	Characteristic	Trunc G-R
					Single	E&I&J	33%	0.82+/-0.12	Characteristic	Trunc G-R
					Multi	D&fG + E&I&J	33%	1.74+/-0.2	Characteristic	Trunc G-R
			Extends North of DP (0.50)	Linkage 3a (0.30)	Single	D'	33%	1.02+/-0.14	Characteristic	Trunc G-R
					Single	E	33%	0.82+/-0.12	Characteristic	Trunc G-R
					Multi	D' + E	33%	1.02+/-0.14	Characteristic	Trunc G-R
				Linkage 3b1 (0.20)	Single	D'&fG	33%	1.02+/-0.14	Characteristic	Trunc G-R
					Single	E&J	33%	0.82+/-0.12	Characteristic	Trunc G-R
					Multi	D'&fG + E&J	33%	1.74+/-0.2	Characteristic	Trunc G-R
				Linkage 3b2 (0.30)	Single	D'	33%	1.02+/-0.14	Characteristic	Trunc G-R
					Single	E&I	33%	0.82+/-0.12	Characteristic	Trunc G-R
					Multi	D' + E&I	33%	1.74+/-0.2	Characteristic	Trunc G-R
				Linkage 3c (0.20)	Single	D'&fG	33%	1.02+/-0.14	Characteristic	Trunc G-R
					Single	E&I&J	33%	0.82+/-0.12	Characteristic	Trunc G-R
					Multi	D'&fG + E&I&J	33%	1.74+/-0.2	Characteristic	Trunc G-R
	Model 4 (0.45)	NI Strike-Slip			Single	H	100%	1.0+/-0.5	Characteristic	Trunc G-R
		RC Strike-Slip			Single	K	33%	1.07+/-0.03	Characteristic	Trunc G-R
					Single	L	33%	1.07+/-0.03	Characteristic	Trunc G-R
					Multi	K + L	33%	1.07+/-0.03	Characteristic	Trunc G-R
		Oceanside Thrust	Stops at DP (0.50)	E Linkage 4b (0.50)	Single	D	25%	1.02+/-0.14	Characteristic	Trunc G-R
					Single	E	25%	0.82+/-0.12	Characteristic	Trunc G-R
					Single	I	25%	1.07+/-0.03	Characteristic	Trunc G-R
					Multi	D + E	25%	1.02+/-0.14	Characteristic	Trunc G-R
				E Linkage 4c (0.50)	Single	D	33%	1.02+/-0.14	Characteristic	Trunc G-R
					Single	E&I	33%	0.82+/-0.12	Characteristic	Trunc G-R
					Multi	D + E&I	33%	1.74+/-0.2	Characteristic	Trunc G-R
			Extends North of DP (0.50)	E Linkage 4b (0.50)	Single	D'	25%	1.02+/-0.14	Characteristic	Trunc G-R
					Single	E	25%	0.82+/-0.12	Characteristic	Trunc G-R
					Single	I	25%	1.07+/-0.03	Characteristic	Trunc G-R
					Multi	D' + E	25%	1.02+/-0.14	Characteristic	Trunc G-R
				E Linkage 4c (0.50)	Single	D'	33%	1.02+/-0.14	Characteristic	Trunc G-R
					Single	E&I	33%	0.82+/-0.12	Characteristic	Trunc G-R
					Multi	D' + E&I	33%	1.74+/-0.2	Characteristic	Trunc G-R
		Carlsbad			Single	cb	100%	0.25+/-0.08	Characteristic	Trunc G-R

Epistemic Uncertainty

Aleatory Uncertainty

Notes:
[1] Recurrence based on 2/3 Characteristic Model and 1/3 Truncated Gutenberg-Richter Distribution
[2] See Appendix A, Attachment A-3 for details

GeoPentech
Geotechnical & Geoscience Consultants

HYPOTHESIZED - OBT 'LOGIC TREE' –
73 COMBINATIONS OF FAULT SEGMENT RUPTURE

FIGURE
2-12

SAN ONOFRE NUCLEAR GENERATING STATION

SEISMIC HAZARD ASSESSMENT PROGRAM

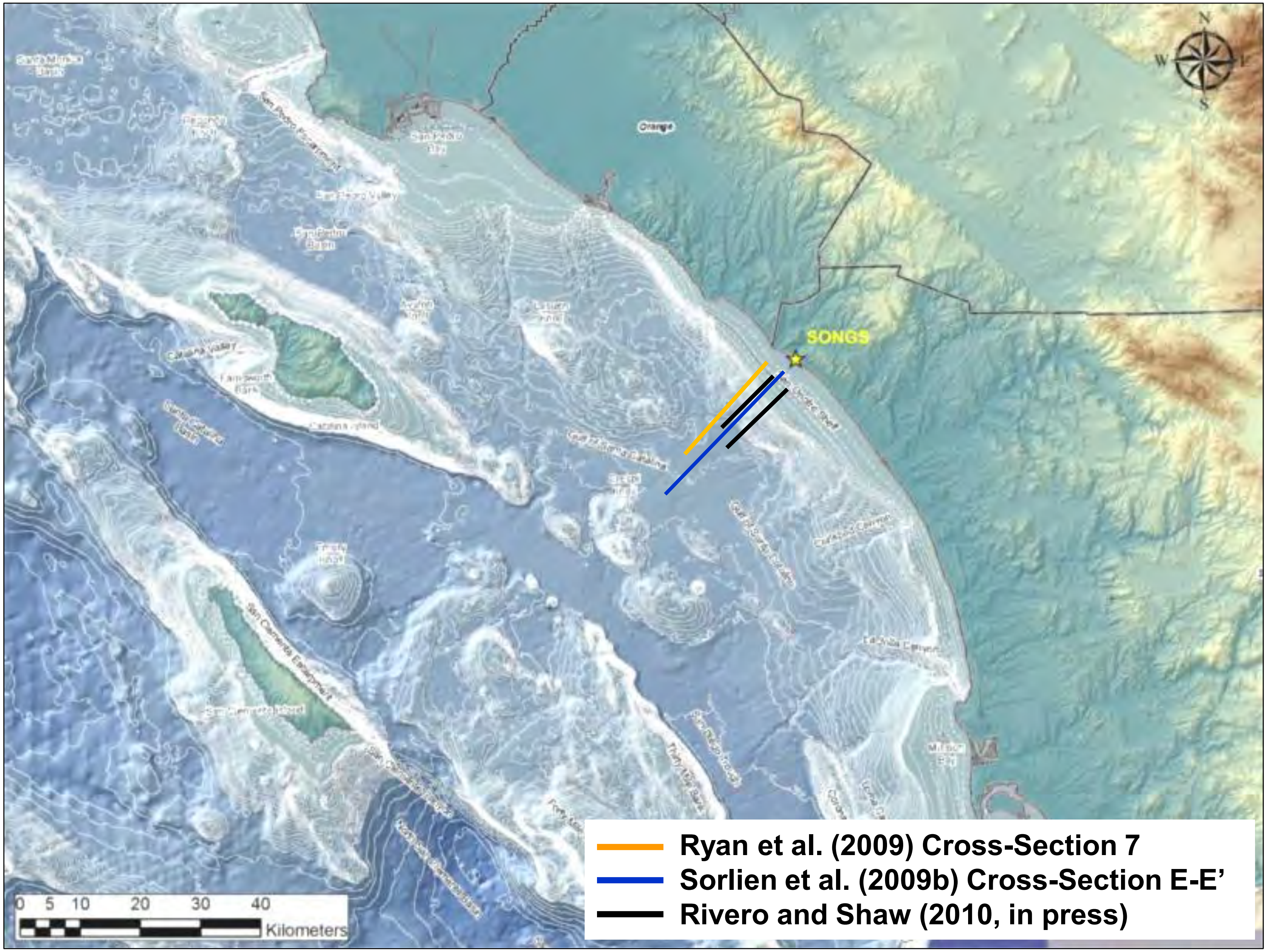

GeoPentech
Geotechnical & Geoscience Consultants

SAN ONOFRE NUCLEAR GENERATING STATION
SEISMIC HAZARD ASSESSMENT PROGRAM

COMPARISON OF SEISMIC REFLECTION LINES

FIGURE 2-13a

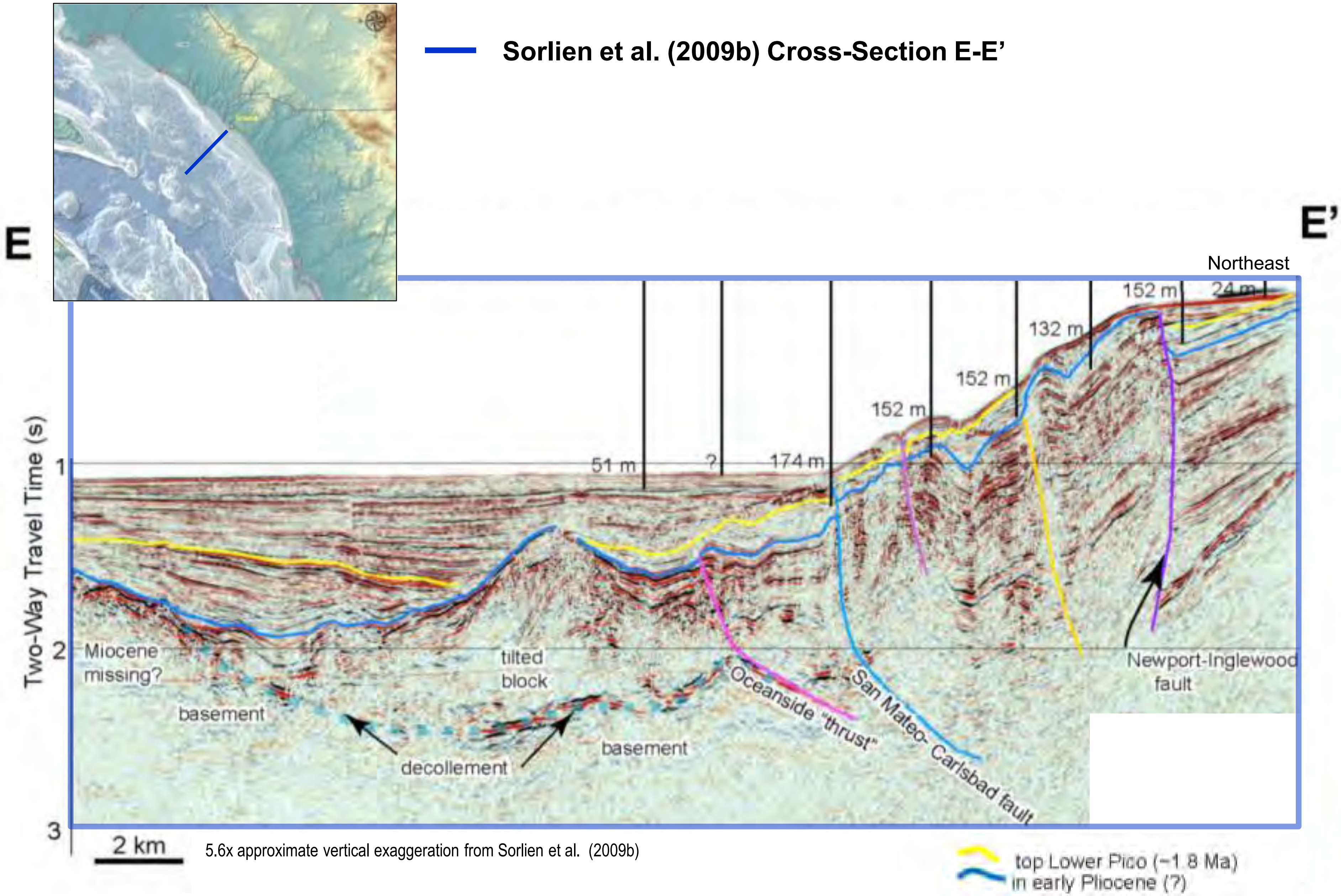

5.6x approximate vertical exaggeration from Sorlien et al. (2009b)

GeoPentech Geotechnical & Geoscience Consultants	SAN ONOFRE NUCLEAR GENERATING STATION SEISMIC HAZARD ASSESSMENT PROGRAM	COMPARISON OF SEISMIC REFLECTION LINES	FIGURE 2-13b

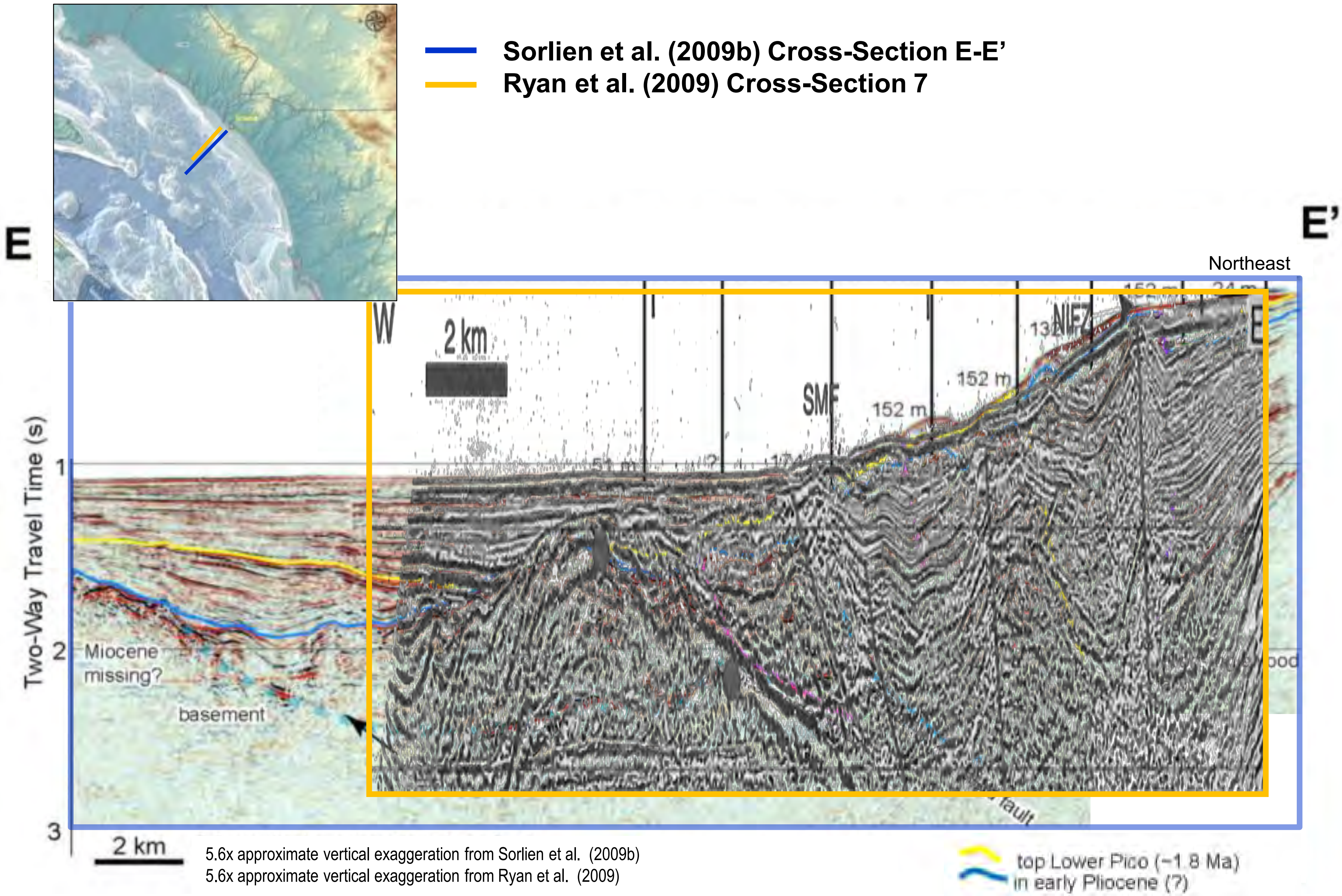

5.6x approximate vertical exaggeration from Sorlien et al. (2009b)
5.6x approximate vertical exaggeration from Ryan et al. (2009)

GeoPentech
Geotechnical & Geoscience Consultants

SAN ONOFRE NUCLEAR GENERATING STATION
SEISMIC HAZARD ASSESSMENT PROGRAM

COMPARISON OF SEISMIC REFLECTION LINES

FIGURE 2-13c

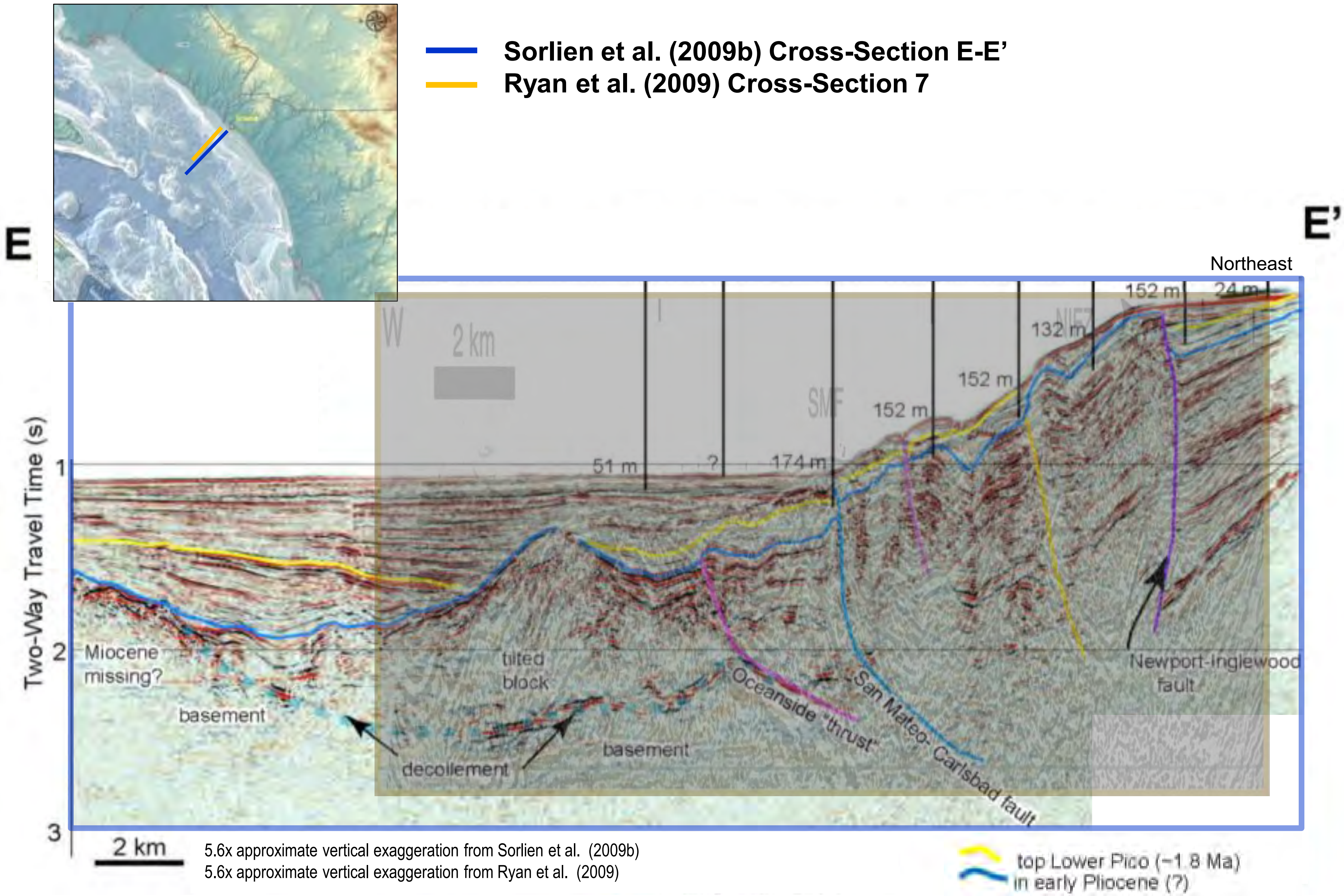

5.6x approximate vertical exaggeration from Sorlien et al. (2009b)
5.6x approximate vertical exaggeration from Ryan et al. (2009)

GeoPentech
Geotechnical & Geoscience Consultants

SAN ONOFRE NUCLEAR GENERATING STATION
SEISMIC HAZARD ASSESSMENT PROGRAM

COMPARISON OF SEISMIC REFLECTION LINES

FIGURE 2-13d

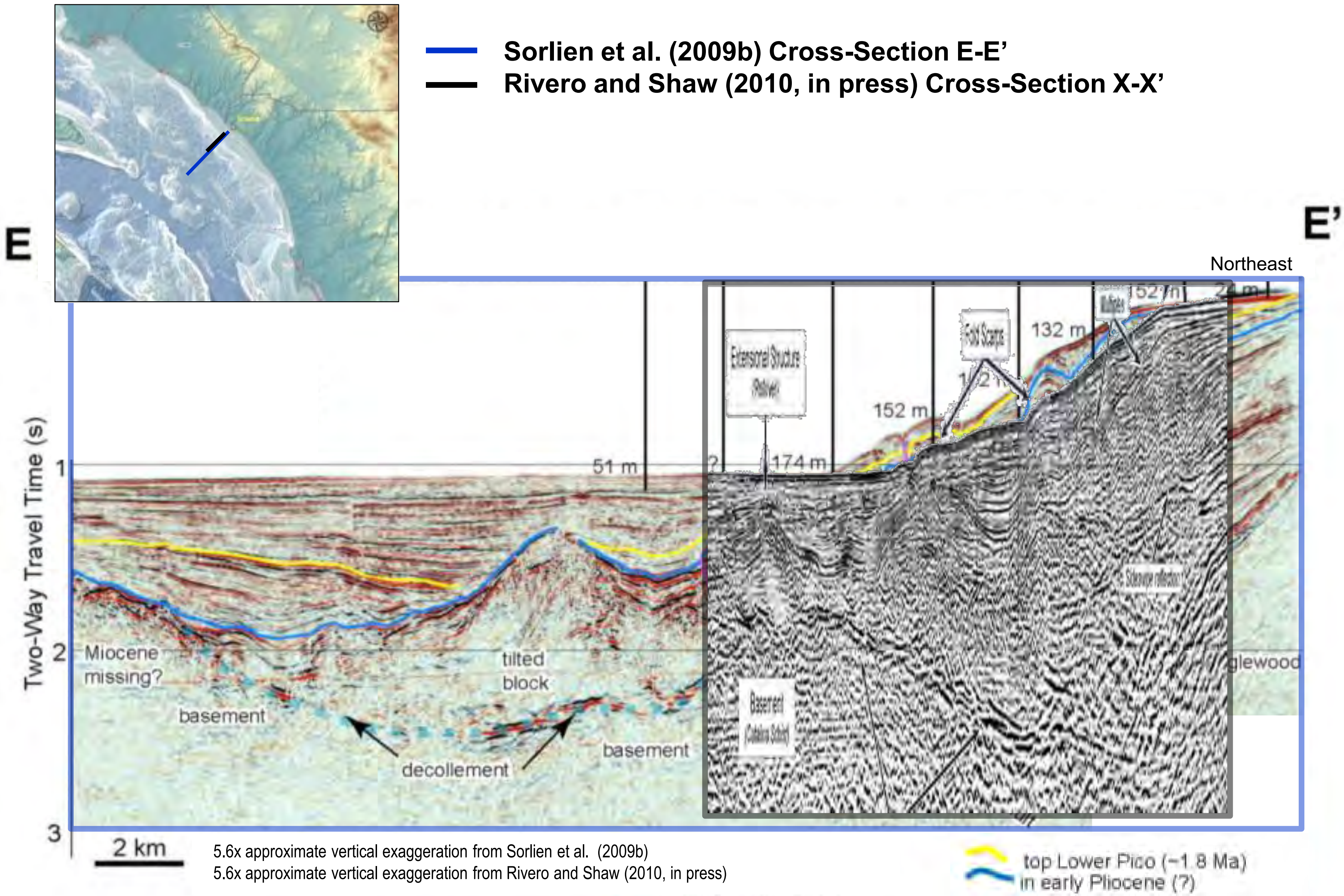

5.6x approximate vertical exaggeration from Sorlien et al. (2009b)
5.6x approximate vertical exaggeration from Rivero and Shaw (2010, in press)

GeoPentech Geotechnical & Geoscience Consultants	SAN ONOFRE NUCLEAR GENERATING STATION SEISMIC HAZARD ASSESSMENT PROGRAM	COMPARISON OF SEISMIC REFLECTION LINES	FIGURE 2-13e

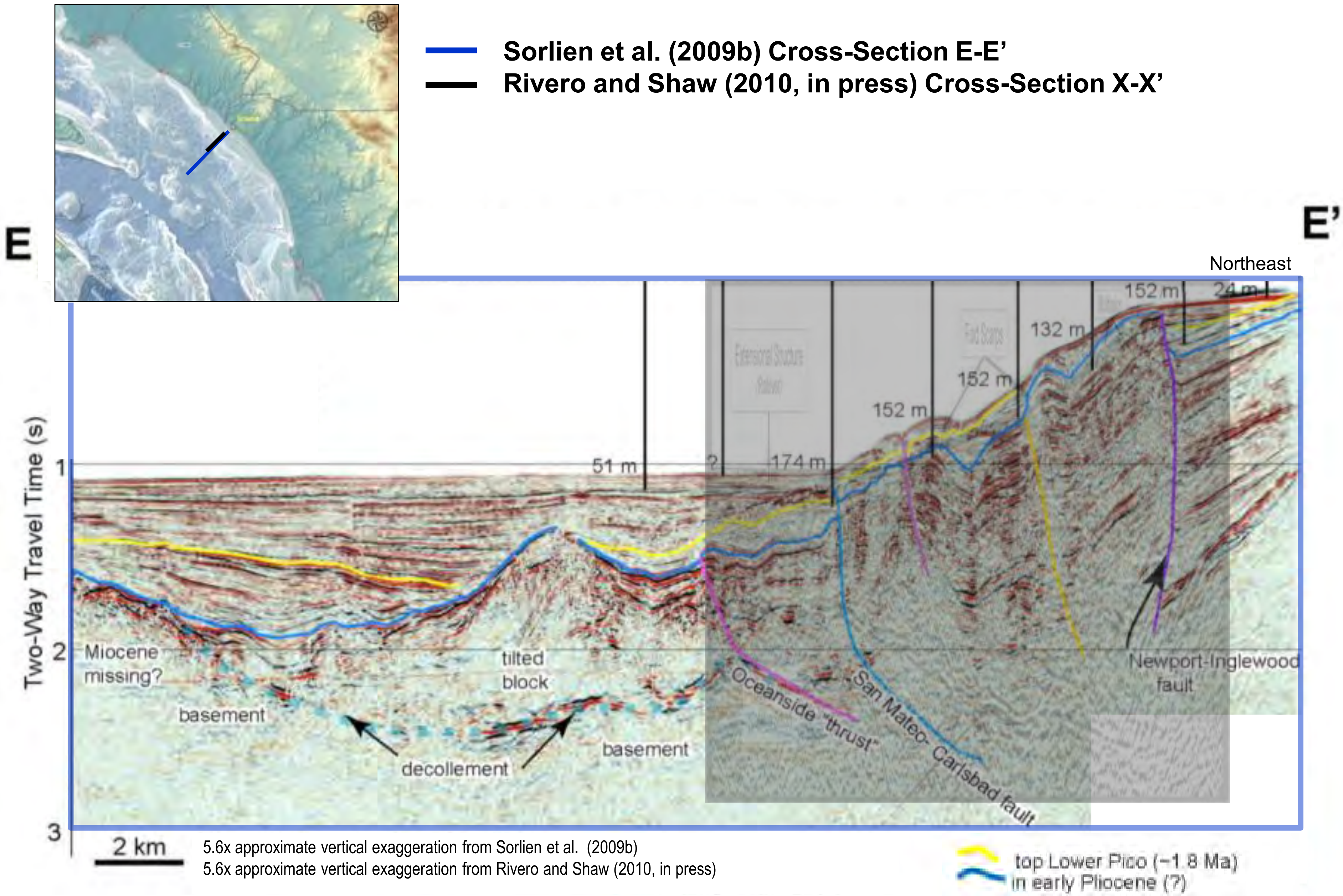

GeoPentech
Geotechnical & Geoscience Consultants

SAN ONOFRE NUCLEAR GENERATING STATION
SEISMIC HAZARD ASSESSMENT PROGRAM

COMPARISON OF SEISMIC REFLECTION LINES

FIGURE 2-13f

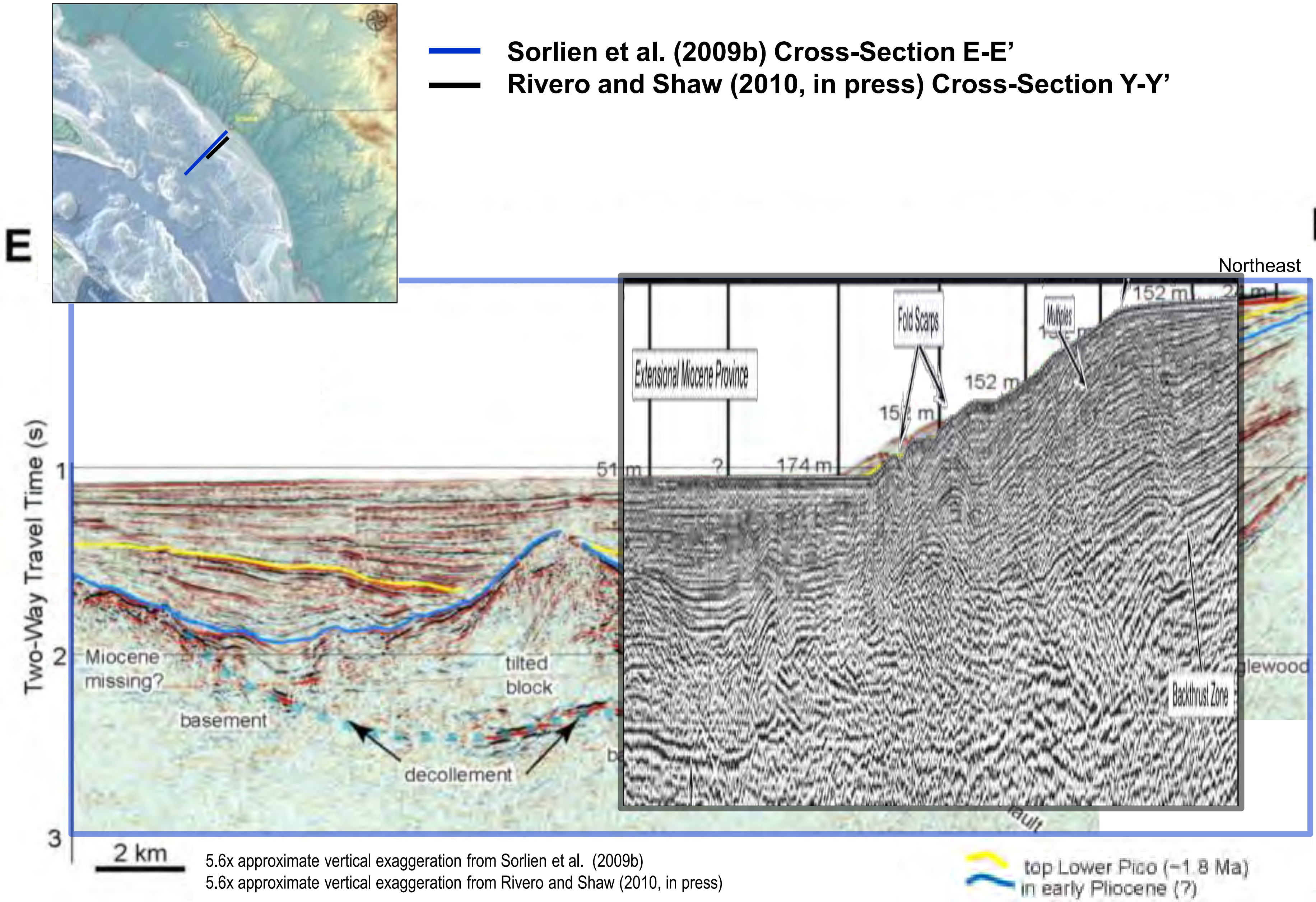

5.6x approximate vertical exaggeration from Sorlien et al. (2009b)
5.6x approximate vertical exaggeration from Rivero and Shaw (2010, in press)

GeoPentech
Geotechnical & Geoscience Consultants

SAN ONOFRE NUCLEAR GENERATING STATION
SEISMIC HAZARD ASSESSMENT PROGRAM

COMPARISON OF SEISMIC REFLECTION LINES

FIGURE 2-13g

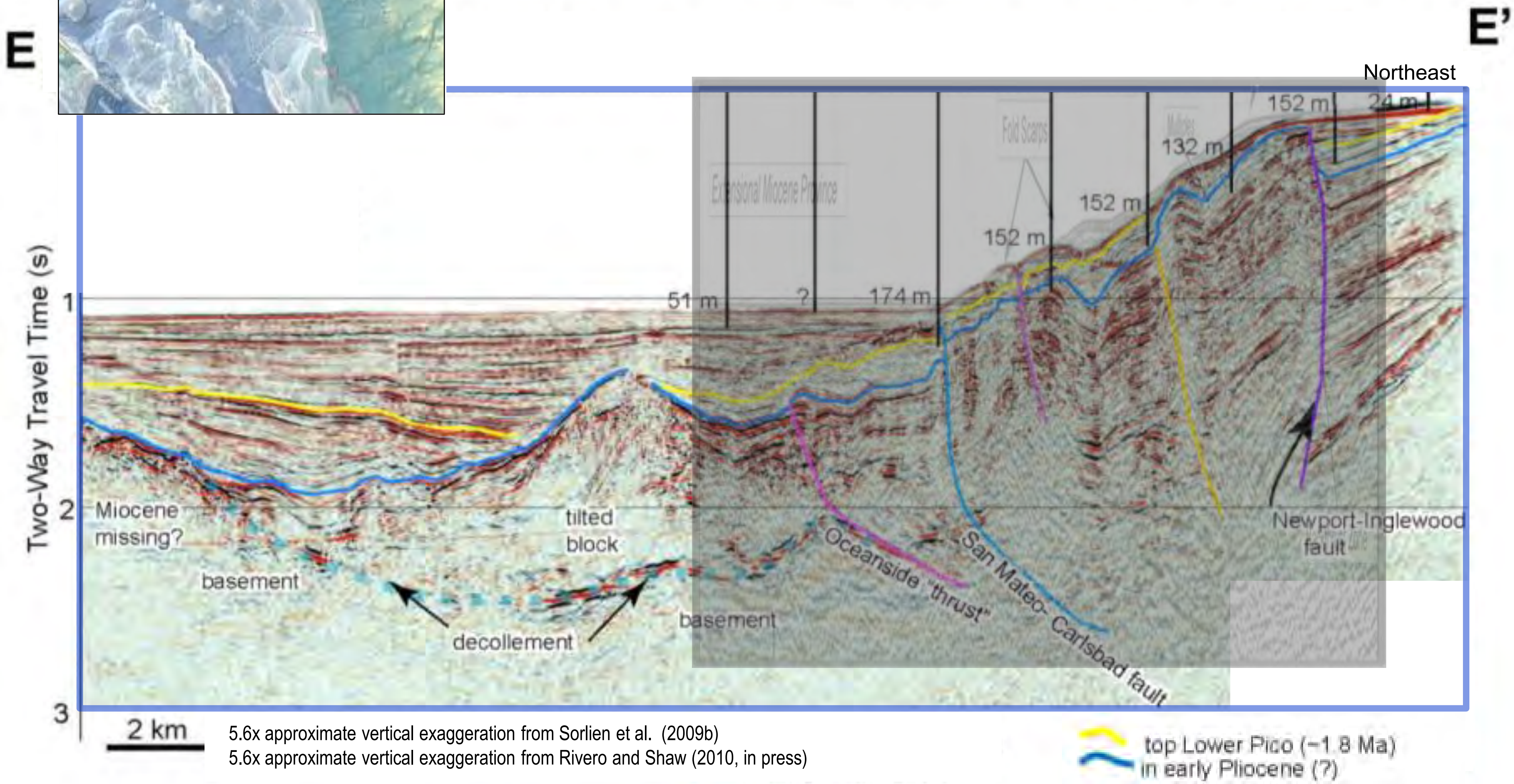

5.6x approximate vertical exaggeration from Sorlien et al. (2009b)
5.6x approximate vertical exaggeration from Rivero and Shaw (2010, in press)

GeoPentech Geotechnical & Geoscience Consultants	SAN ONOFRE NUCLEAR GENERATING STATION SEISMIC HAZARD ASSESSMENT PROGRAM	COMPARISON OF SEISMIC REFLECTION LINES	FIGURE 2-13h

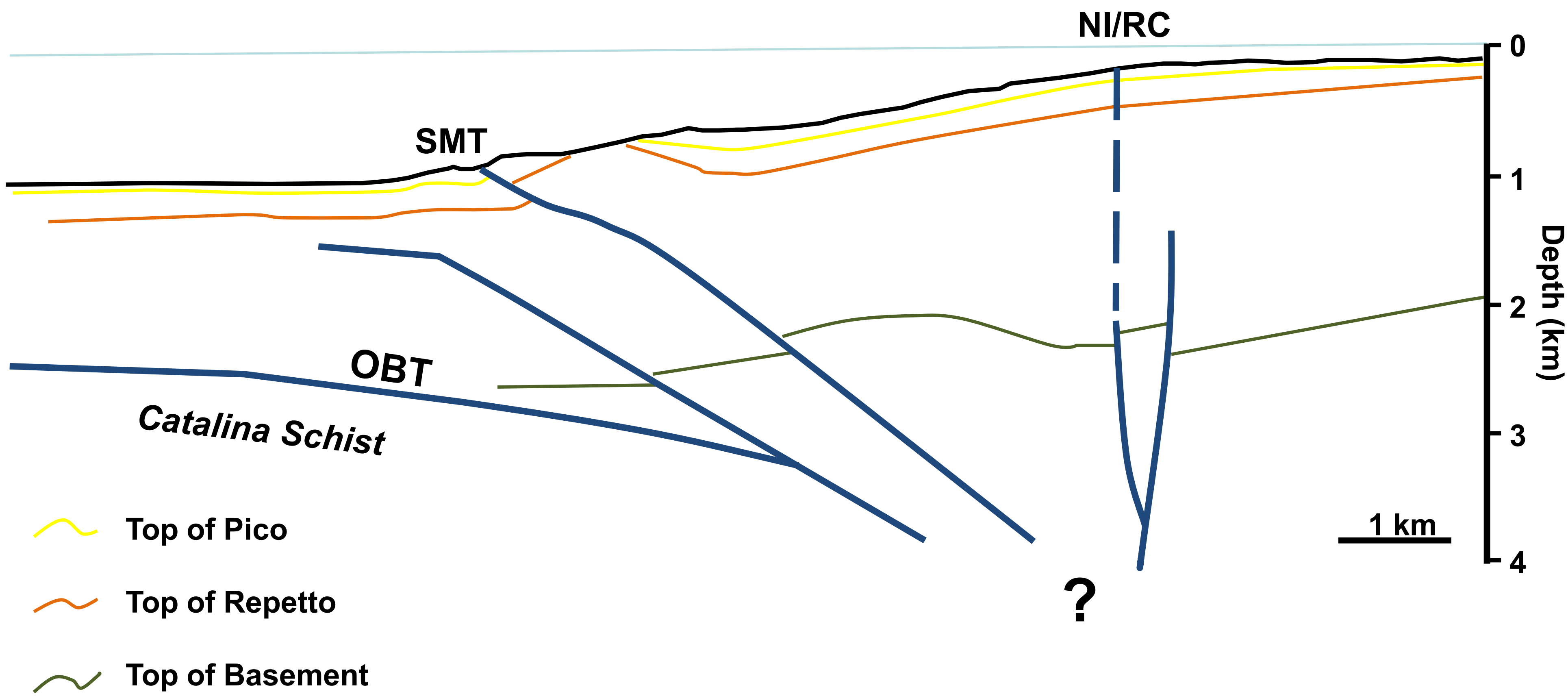

GeoPentech
Geotechnical & Geoscience Consultants

SAN ONOFRE NUCLEAR GENERATING STATION
SEISMIC HAZARD ASSESSMENT PROGRAM

SKETCH OF THE SAN MATEO THRUST, NI/RC FAULT ZONE AND OBT WITH OFFSET STRATIGRAPHY

FIGURE 2-14

BLIND THRUST END MEMBER MODEL

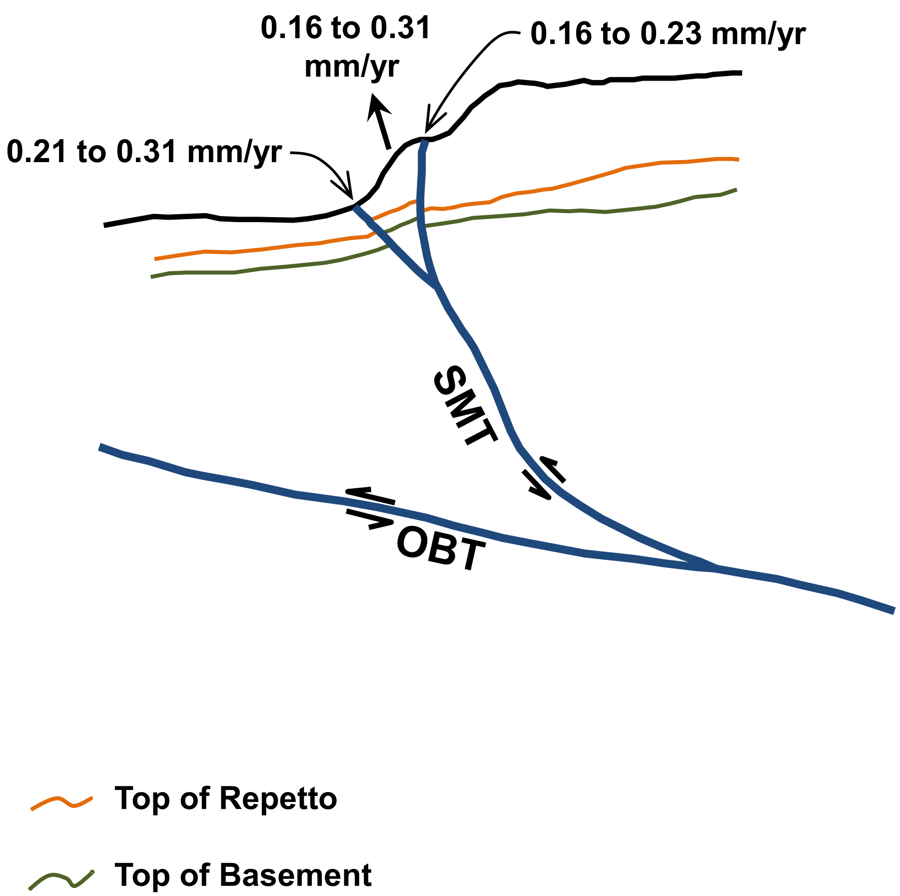

STRIKE-SLIP END MEMBER MODEL

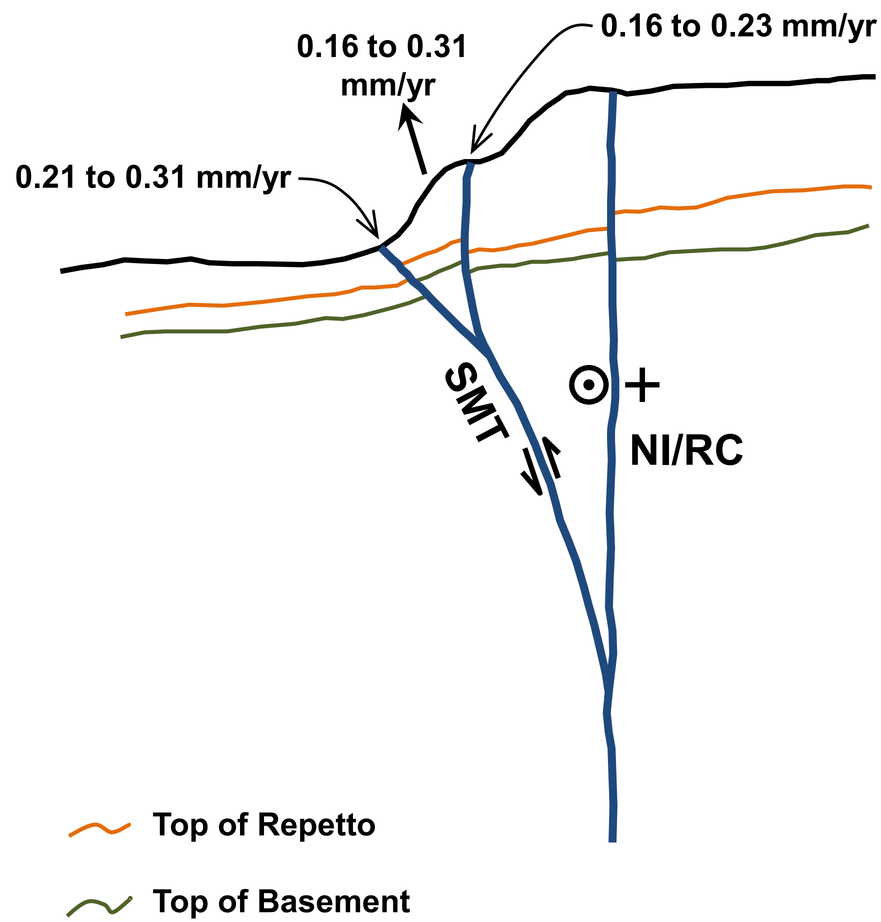

GeoPentech Geotechnical & Geoscience Consultants	SAN ONOFRE NUCLEAR GENERATING STATION SEISMIC HAZARD ASSESSMENT PROGRAM	SKETCH SHOWING FAULT CONFIGURATIONS AND OFFSET STRATIGRAPHY FOR END MEMBER MODELS	FIGURE 2-15

3.0 PROBABILISTIC SEISMIC HAZARD ANALYSIS

Spectral acceleration values for SONGS were obtained from the PSHA using the seismic sources discussed in Section 2.0. This SONGS 2010 PSHA followed the methods of the 1995 PSHA (SCE, 1995) and the 2001 PSHA (SCE, 2001). The 2001 PSHA results included both response spectral values and time histories, reflecting the effects of near-fault directivity and fling step. Unlike the 2001 PSHA results, the PSHA results reported here focus mainly on high frequency spectral accelerations and do not reflect the effects of near-fault directivity or fling step, which were found to be insignificant for SONGS. Based on the 2001 PSHA, the near-fault directivity and the fling steps only affect the low frequency range below about 1.5 Hertz (Hz), which is outside the frequencies of interest for structures and components at SONGS.

3.1 PSHA Methodology

3.1.1 General

The basic result of PSHA is a relationship between a ground motion parameter *"Z"* (peak ground acceleration [PGA] and spectral acceleration herein) and the mean number of seismic events per year in which *"Z"* at the site exceeds a specified value *"z"*. This relationship is called a "hazard curve." The mean number of seismic events per year is referred to as "annual frequency of exceedance" and designated "$v(Z \geq z)$". The inverse of this number is called the "return period" (RP) and is expressed in years. Once the relationships between appropriate parameters and annual frequency of exceedance are obtained, various probabilistic calculations can be made assuming a Poisson process. Details of PSHA are available elsewhere (e.g., SSHAC, 1997: http://www.ce.memphis.edu/7137/). Apart from the general discussions below, only the key pertinent topics will be discussed here with some further details presented in Appendix B.

The five major components in PSHA consist of the following:

- Characterization of Seismogenic Sources. The location, geometry, and characteristics of seismic sources (or earthquake generating faults) relative to the site are evaluated and specified. This component is addressed in Section 2.0
- Specification of Recurrence Relationship. In the PSHA, one of the most important characteristics of a seismic source is its recurrence relationship or the relationship showing the annual recurrence of earthquakes of various magnitudes up to the "maximum" magnitude. The recurrence relationship is used to provide the mean number of earthquakes per year having a particular magnitude "m_j" on a given seismic source, "$\dot{N}_s(m_j)$". Two types of recurrence relationships were used: the characteristic and the truncated exponential (Youngs and Coppersmith, 1985). These two recurrence models were selected to be consistent with the UCERF 2 (WGCEP, 2008).
- Evaluation of Probability of Distance to Rupture. Assuming that the typical earthquake generating fault rupture can occur anywhere along the plane of an active fault with an equal probability, the conditional probability is computed so that the rupture plane is at a specified distance, r_k, from the site for the given m_j. This probability is evaluated by considering the rupture plane's dimensions and the distance definition used in the particular attenuation relationship being used.

- Calculation of Exceedance Using Attenuation Equation. The conditional probability that the ground motion parameter "Z" from the earthquake of a certain magnitude "m_j" occurring at a certain distance "r_k" on a particular seismic source fault will exceed a specified level "z" at the site is calculated based on the median and standard deviation of the ground motion given by the attenuation relationship.

- Calculation of Probabilistic Seismic Hazard. By combining the rate of occurrence of earthquakes of a given magnitude with the two conditional probability functions associated with steps 2 through 4 above, for each seismic source fault, the mean number of events per year (annual frequency of exceedance) resulting in "Z" being greater than "z" ($v(Z \geq z)$) at the site is computed for that particular seismic source fault. This process was repeated for each seismic source fault, and the contributions are added to obtain the total seismic hazard at the site for a given z. The complete hazard curve is obtained by repeating these computations for several levels of ground motion parameter z.

Once this mean number of events per year (annual frequency of exceedance) $v(Z \geq z)$ has been determined, the probability of the level of the seismic ground motion parameter being exceeded over a specified time period, t, is calculated by the following equation assuming the Poisson model for the earthquake occurrence:

$$Pr(Z \geq z) = 1 - \exp[-\nu(Z \geq z) \cdot t] \qquad \textbf{(3-1)}$$

The results of the SONGS 2010 PSHA are presented here in terms of the mean number of events per year or annual frequency of exceedance, $v(Z \geq z)$. The results are presented from an annual frequency of exceedance of 10^{-2} to 10^{-4} corresponding to a RP of 100 to 10,000 years. The computer program Haz4.2 developed by Abrahamson (2010, PC) was used in completing this PSHA. The results of quality assurance/quality control (QA/QC) work performed on the program are summarized in Appendix B.

3.1.2 Attenuation Relationships

The attenuation relationships from the NGA project, which are now called GMPEs, were used in this PSHA and are listed in Table 3-1 along with key parameter values. These attenuation relationships are referred to herein as the "NGA relationships" and consist of the following:

- Abrahamson and Silva (2008)
- Boore and Atkinson (2008)
- Campbell and Bozorgnia (2008)
- Chiou and Youngs (2008)
- Idriss (2008)

Further details of these NGA relationships are provided in Appendix B.

3.1.3 Uncertainties

Two major types of uncertainties are addressed in PSHA. They are as follows:

- Aleatory Uncertainty. Uncertainties in the earthquake recurrence process and in the attenuation of ground motion are the major sources of the aleatory uncertainty in PSHA. This uncertainty is a reflection of the "randomness" inherent to the natural phenomenon of earthquake generation and ground motions. This uncertainty may be based in part on the limited scientific understanding of the natural phenomenon of earthquake generation and seismic wave propagation. This type of uncertainty, in theory, cannot be reduced when additional data or understanding of earthquakes and their effects become available.

- Epistemic Uncertainty. This uncertainty reflects limited available data, limited scientific understanding, and/or limitations in the utility of modeling earthquake and related processes. This type of uncertainty, in theory, can be reduced when additional data or understanding of earthquakes and their effects become available.

The PSHA methodology includes probability models for these two major types of uncertainty. For example, both aleatory uncertainty and epistemic uncertainty are reflected in the logic tree provided for the OBT seismic source fault shown on Figure 2-12 in Section 2.0. Two specific epistemic uncertainties considerations were addressed because of their pertinence to the current PSHA: one is associated with the GMPEs and the other is the NI/RC Fault Zone versus the OBT Fault as the primary seismic source fault.

3.1.3.1 GMPE Uncertainty

In using attenuation relationships, their epistemic uncertainty should be considered. In the past, this epistemic uncertainty was often accommodated by using multiple attenuation relationships. However, given the coordinated process used to develop the NGA relationships, it may not be adequate to address this epistemic uncertainty by just using multiple NGA relationships.

On the basis of the evaluation results presented in Appendix B, an epistemic GMPE uncertainty in addition to the five NGA relationships was used in the current PSHA. This additional uncertainty represents the difference between the GMPE uncertainty that the USGS (2008) is currently using with only three NGA relationships in their seismic hazard mapping program for the building code purposes and the epistemic uncertainty covered by the five NGA relationships and the GMPE uncertainty used in this PSHA.

3.1.3.2 Uncertainty Regarding Strike-slip and Blind Thrust Sources

As discussed in Sections 1 and 2, the seismic sources used in this PSHA consisted of the pertinent time-independent portion of the seismic source fault characterization in UCERF 2 (WGCEP, 2008). For SONGS, the most important seismic source fault in this PSHA's base case set is the NI/RC source, which was also reflected in the 1995 PSHA (SCE, 1995) and a weighted NI/RC and OBT in the 2001 PSHA (SCE, 2001). Since the 2001 PSHA, the OBT has been re-characterized, and new weights have been assigned to the NI/RC (strike-slip) and OBT (blind thrust) models as recommended by the seismic source integration team. Based on the evaluation of the uncertainties associated with both models as discussed in Section 2, the numerically calculated average weights applied to the NI/RC model and the OBT model for use in the PSHA are: 88% and 12% for the strike-slip model and blind thrust end-member models, respectively. The PSHA utilized the above weights applied to the logic trees developed for the NI/RC model as shown on Figure 2-5 and for the OBT as shown on Figure 2-12. These analysis results are, therefore, provided for a single case and referred to as the "2010 PSHA" results.

3.1.3.3 Recurrence Relationships

The recurrence relationships used for the NI/RC source followed UCERF 2 (WGCEP, 2008) and involved using the characteristic recurrence relationship of Youngs and Coppersmith (1985) with a 2/3 weight and the truncated exponential relationship of Molnar (1979) and Anderson (1979) with a 1/3 weight. For the hypothesized OBT source, a comparison of the recurrence model with the available seismicity data presented in Appendix B indicates that using only the characteristic recurrence relationship is more appropriate.

3.2 PSHA Results

The 2010 PSHA results are presented in terms of hazard curves relating spectral acceleration to annual frequency of exceedance on Figure 3-1 for PGA, 25 Hz, 10 Hz, and 5 Hz; similar results are presented on Figure 3-2 for 3.33 Hz, 2.5 Hz, 2 Hz, and 1 Hz. The 2010 PSHA results are also listed in Table 3-2.

3.2.1 Effects of Seismic Sources

The contributions to the total seismic hazard at the SONGS site from various seismic sources are presented for the 2010 PSHA results on Figures 3-3 and 3-4 corresponding to PGA and 1 Hz, respectively.

As shown on Figures 3-3 and 3-4 for the 2010 PSHA results, the NI/RC-OBT source contributes the most to the total hazard for annual frequency of exceedance less than about 10^{-3} for PGA and 1 Hz. For the higher annual frequency of exceedance, the San Jacinto source, the Southern San Andreas source, and, to a lesser degree, the Elsinore source start to contribute more than the NI/RC source.

3.2.2 Deaggregation Results

Figure 3-5 shows the results of deaggregation for the 2010 PSHA results for a RP of 475 years at PGA and 1 Hz; similarly, Figure 3-6 shows the results of deaggregation for a RP of 2,475 years at PGA and 1 Hz. The RP values of 475 and 2,475 years were selected to correspond to numbers often used in current building codes. For the 2010 PSHA results at 475 year RP, the PGA shaking at SONGS is primarily associated with the NI/RC-OBT source with moment magnitude falling in the 6.5 to 7.5 bin at a distance falling in the 5 to 10 km bin, whereas the 1 Hz shaking is somewhat more controlled by the San Jacinto, South San Andreas, and Elsinore faults with moment magnitude falling in the 7 to 8 bin at a distance falling in the 30 to 100 km bin. At 2,475 year RP, however, the ground motion at the SONGS site is dominated by the NI/RC-OBT source with moment magnitude falling in the 6.5 to 7.5 bin at a distance falling in the 5 to 10 km bin.

3.2.3 Comparison with 1995 PSHA Results

The “weighted hazard curve,” presented previously (SCE, 1995 and 2001), shows the relationship between the weighted spectral acceleration values and annual frequency of exceedance. At each annual frequency of exceedance value evaluated, the weighted spectral values were obtained as follows: spectral accelerations at frequencies 1 Hz and 10 Hz are multiplied by ½ and added to the sum of spectral accelerations at frequencies 5 Hz and 2.5 Hz with the resulting sum divided by 3.

The weighted hazard curves corresponding to the 2010 PSHA and 1995 PSHA results are presented on Figure 3-7. The results shown on Figure 3-7 indicate that the 2010 PSHA results are lower compared to the 1995 PSHA results throughout the range shown. These weighted hazard curves are also tabulated in Table 3-3.

Table 3-1: NGA Relationships and Related Parameters used in PSHA

NGA	Epistemic Weight	Subsurface Parameters†		
		V_{s30}*	$Z_{1.0\text{-km/s}}$**	$Z_{2.5\text{-km/s}}$***
Abrahamson & Silva (2008)	0.20	500-m/s****	0.31-km	3.35-km
Boore & Atkinson (2008)	0.20			
Campbell & Bozorgnia (2008)	0.20			
Chiou & Youngs (2008)	0.20			
Idriss (2008)	0.20			

Notes:

† Used as needed in each NGA relationship.

* V_{s30} is the average shear wave velocity in the upper 30 meters of a soil profile.

** $Z_{1.0\text{-km/s}}$ is the depth at which the shear wave velocity is 1.0 kilometers per second (km/s).

*** $Z_{2.5\text{-km/s}}$ is the depth at which the shear wave velocity is 2.5 km/s.

**** m/s is meters per second.

Table 3-2: Mean Horizontal Ground Motions (g) at Various Frequencies of Exceedance for 2010 PSHA

Annual Frequency of Exceedance	Average Return Period	Spectral Acceleration - g*								
		PGA	25-Hz	10-Hz	5-Hz	3.33-Hz	2.5-Hz	2-Hz	1-Hz	Weighted**
1.00E-04	10,000	0.778	0.936	1.489	1.895	1.832	1.673	1.456	0.852	1.579
2.00E-04	5,000	0.618	0.736	1.178	1.477	1.413	1.284	1.131	0.661	1.227
5.00E-04	2,000	0.430	0.510	0.813	1.019	0.970	0.875	0.776	0.463	0.844
1.00E-03	1,000	0.318	0.372	0.593	0.746	0.716	0.638	0.576	0.353	0.619
2.00E-03	500	0.233	0.269	0.426	0.542	0.525	0.476	0.422	0.266	0.455
5.00E-03	200	0.152	0.176	0.272	0.356	0.348	0.314	0.280	0.176	0.298
1.00E-02	100	0.108	0.124	0.191	0.251	0.248	0.223	0.198	0.123	0.211
2.11E-03	475	0.227	0.263	0.415	0.530	0.515	0.464	0.413	0.261	0.444
4.04E-04	2,475	0.472	0.554	0.895	1.111	1.056	0.949	0.849	0.501	0.920

Notes: * Spectral Accelerations were interpolated at the provided annual frequencies of exceedance

** Weighted Spectral Acceleration (Sa) is determined as follows:

Weighted Sa = $(0.5*Sa_{10\text{-}Hz} + Sa_{5\text{-}Hz} + Sa_{2.5\text{-}Hz} + 0.5*Sa_{1\text{-}Hz})/3$

where $Sa_{x\text{-}Hz}$ is the spectral acceleration at x-Hz

Table 3-3: Comparison of Weighted Hazard Curves 2010 PSHA and 1995 PSHA

Annual Frequency of Exceedance*	Average Return Period	Weighted Spectral Acceleration – g**	
		2010 PSHA	1995 PSHA***
1.00E-04	10,000	1.579	1.656
2.00E-04	5,000	1.227	1.407
5.00E-04	2,000	0.844	1.015
1.00E-03	1,000	0.619	0.884
2.00E-03	500	0.455	0.675
5.00E-03	200	0.298	0.430
1.00E-02	100	0.211	0.310
2.11E-03	475	0.444	0.655
4.04E-04	2,475	0.920	1.077

Notes:

* Spectral Accelerations were interpolated at the provided annual frequencies of exceedance

** Weighted Spectral Acceleration (Sa) is determined as follows:

Weighted Sa = $(0.5*Sa_{10\text{-}Hz} + Sa_{5\text{-}Hz} + Sa_{2.5\text{-}Hz} + 0.5*Sa_{1\text{-}Hz})/3$

where $Sa_{x\text{-}Hz}$ is the spectral acceleration at x-Hz

*** Spectral Acceleration not calculated for annual frequency of exceedance greater than 1.00E-02 in 1995 results.

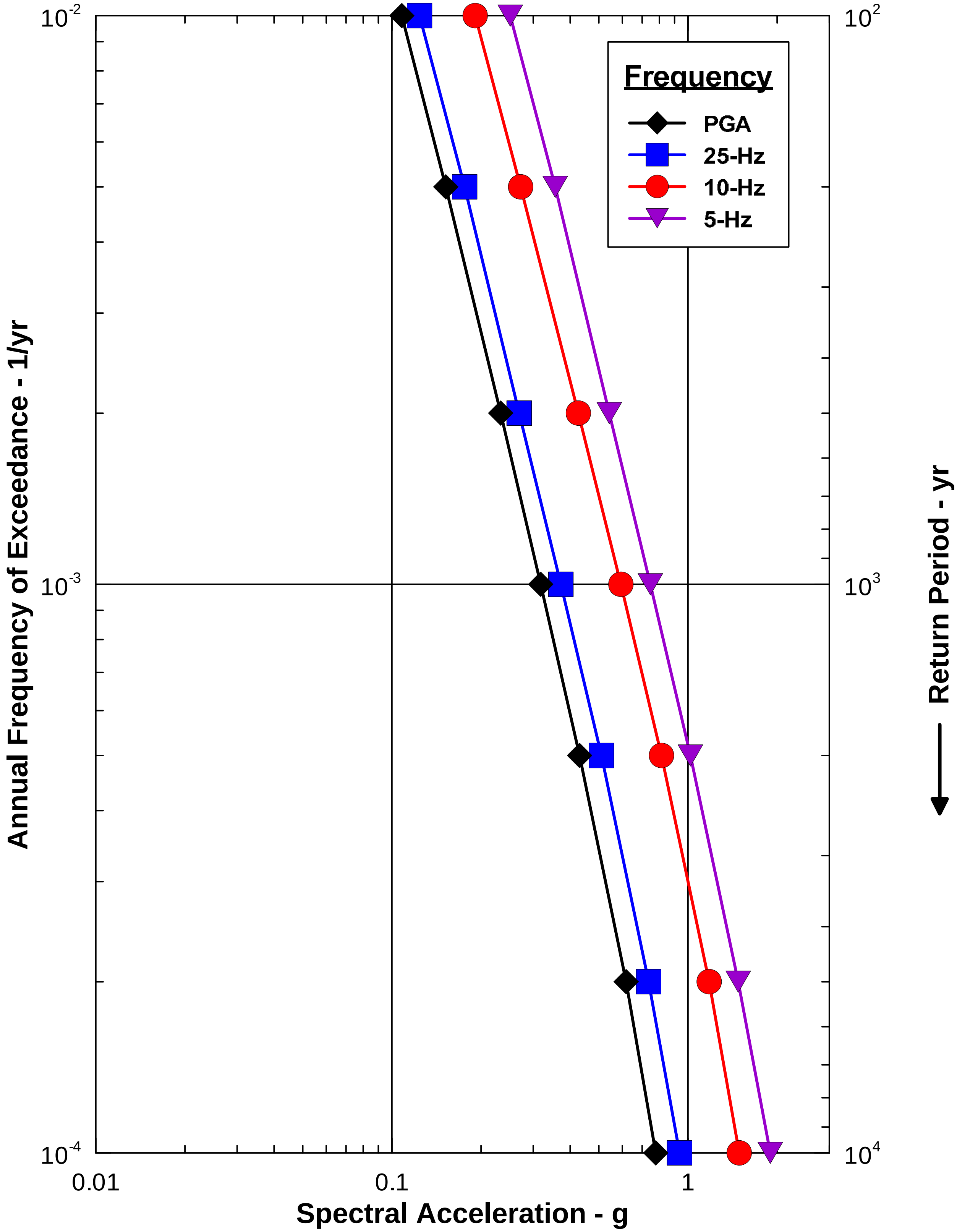

GeoPentech
Geotechnical & Geoscience Consultants

2010 PSHA HAZARD CURVES

FIGURE 3-1

SAN ONOFRE NUCLEAR GENERATING STATION

SEISMIC HAZARD ASSESSMENT PROGRAM

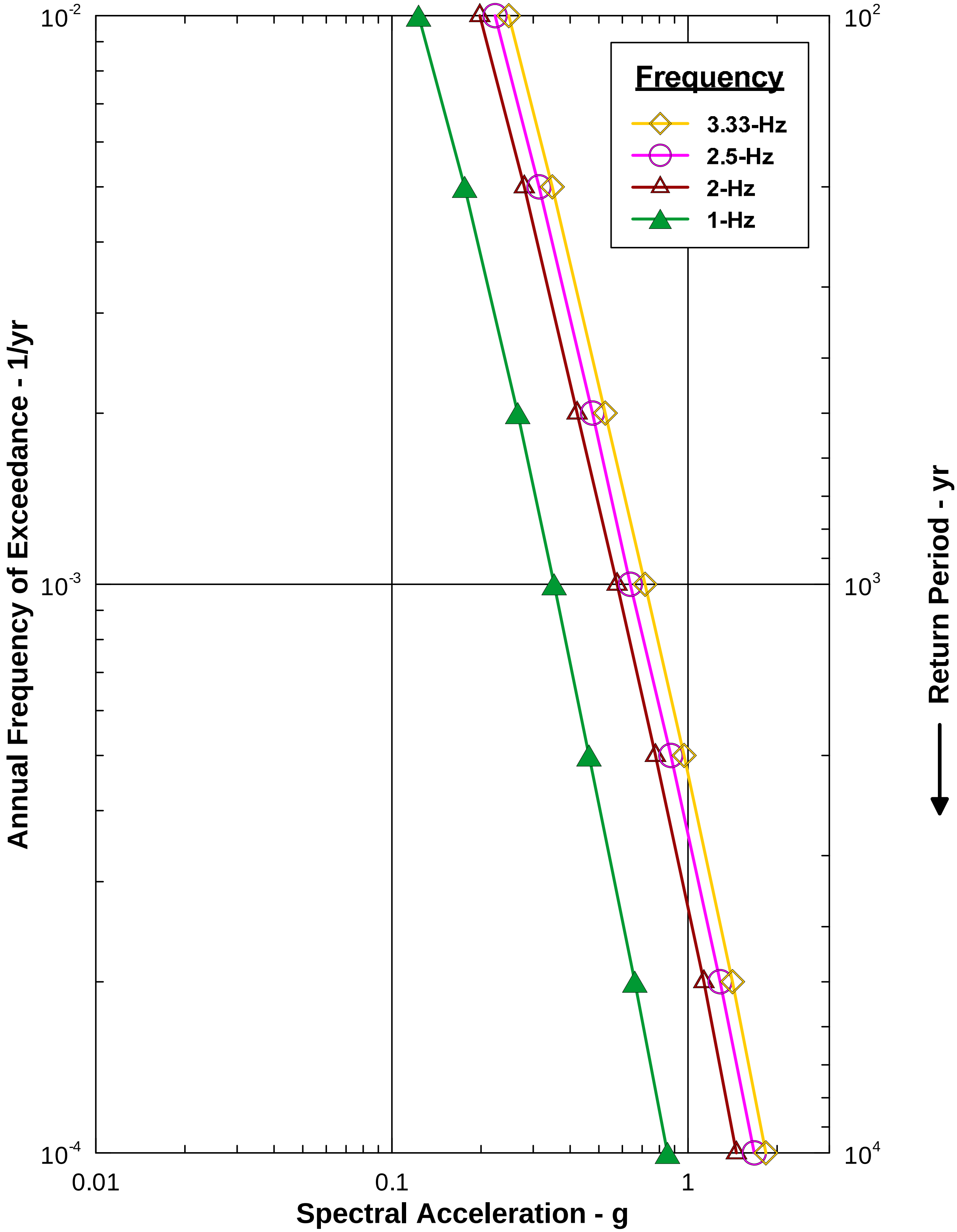

GeoPentech
Geotechnical & Geoscience Consultants

2010 PSHA HAZARD CURVES

FIGURE
3-2

SAN ONOFRE NUCLEAR GENERATING STATION

SEISMIC HAZARD ASSESSMENT PROGRAM

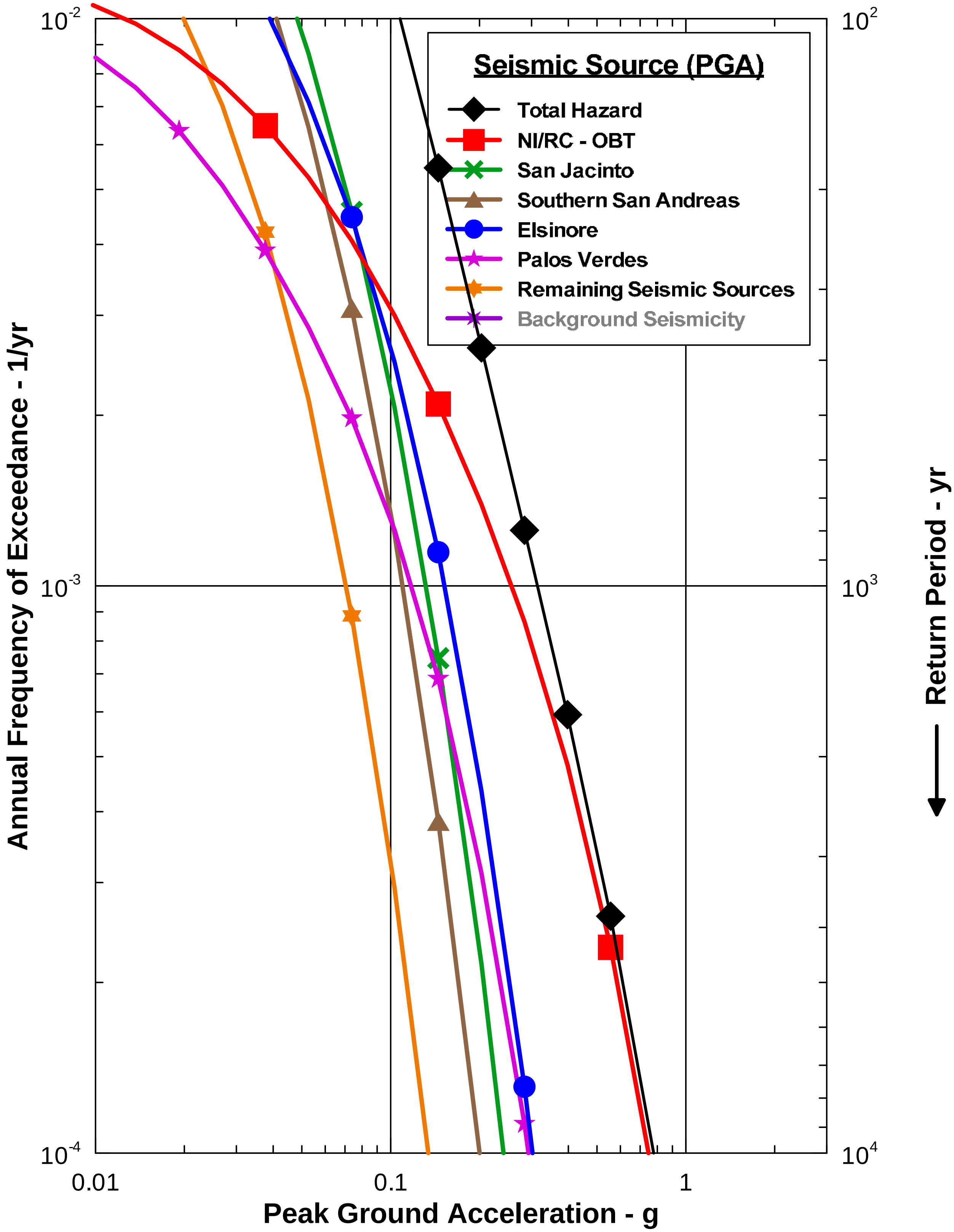

2010 PSHA - PGA SEISMIC SOURCE CONTRIBUTIONS

FIGURE 3-3

GeoPentech
Geotechnical & Geoscience Consultants

SAN ONOFRE NUCLEAR GENERATING STATION

SEISMIC HAZARD ASSESSMENT PROGRAM

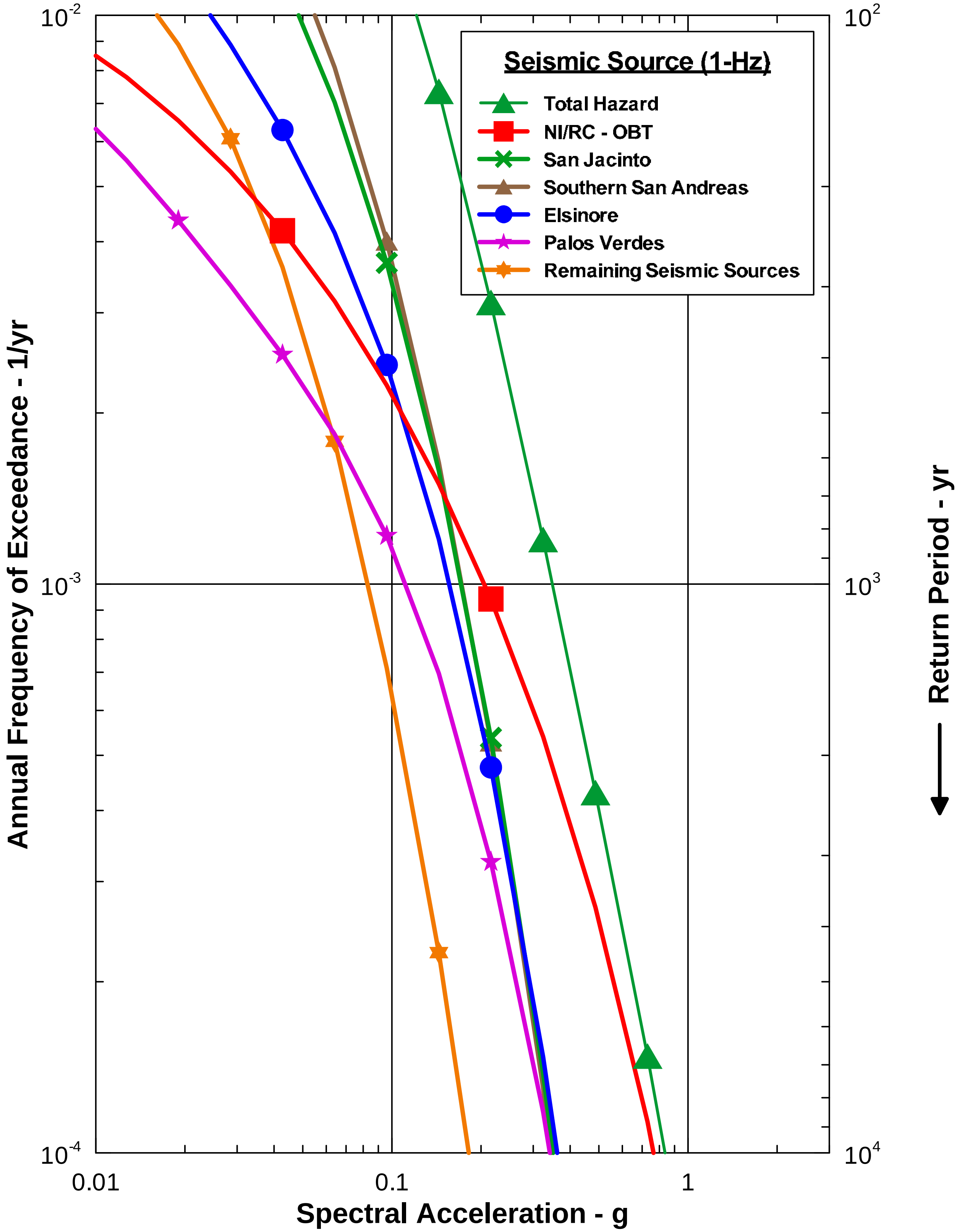

GeoPentech
Geotechnical & Geoscience Consultants

2010 PSHA - 1-Hz SEISMIC SOURCE CONTRIBUTIONS	FIGURE 3-4
SAN ONOFRE NUCLEAR GENERATING STATION SEISMIC HAZARD ASSESSMENT PROGRAM	

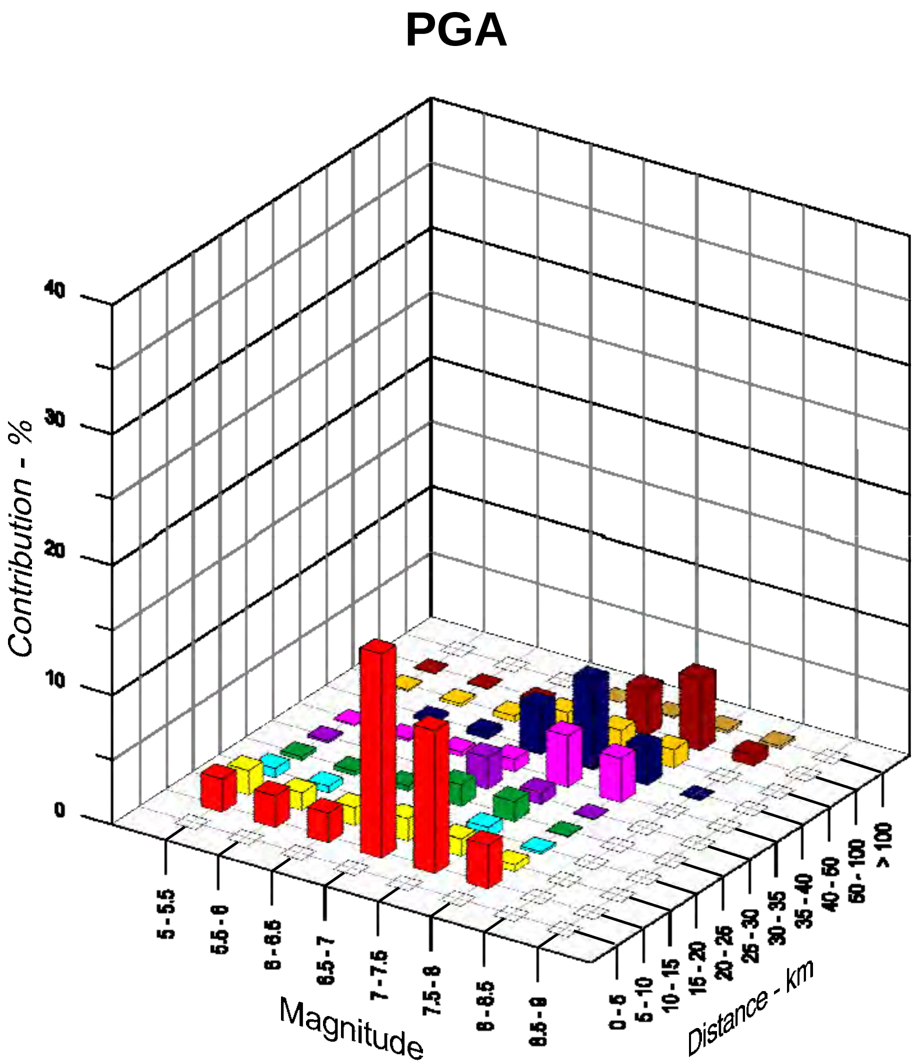

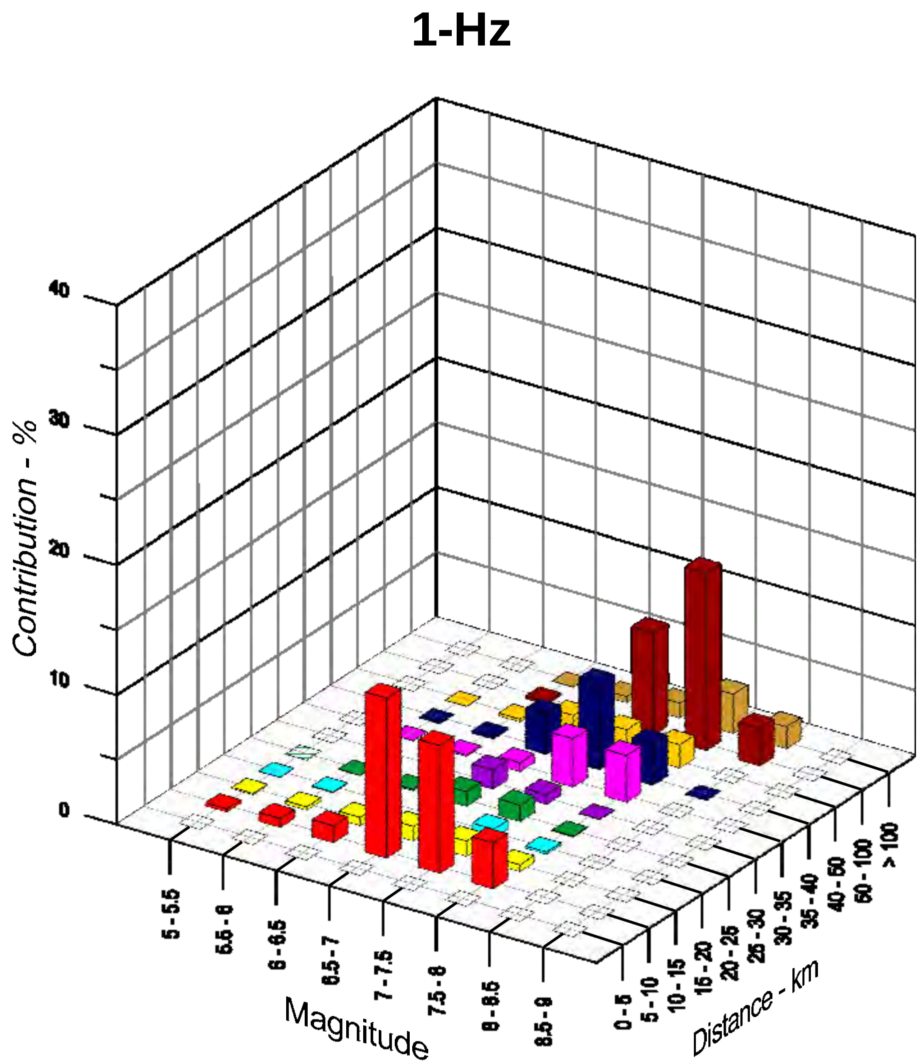

GeoPentech Geotechnical & Geoscience Consultants	**SAN ONOFRE NUCLEAR GENERATING STATION** SEISMIC HAZARD ASSESSMENT PROGRAM	HAZARD DEAGGREGATION 2010 PSHA FOR 475-yr ARP at PGA and 1-Hz	FIGURE 3-5

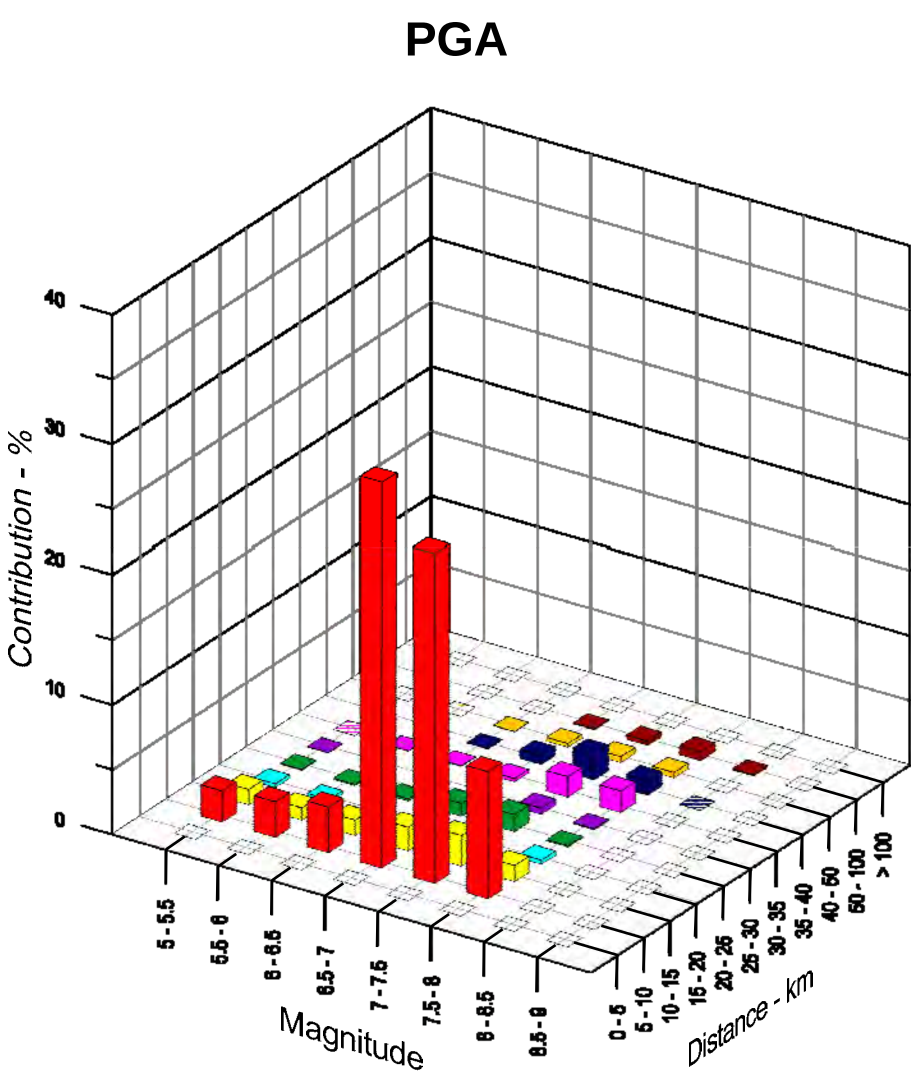

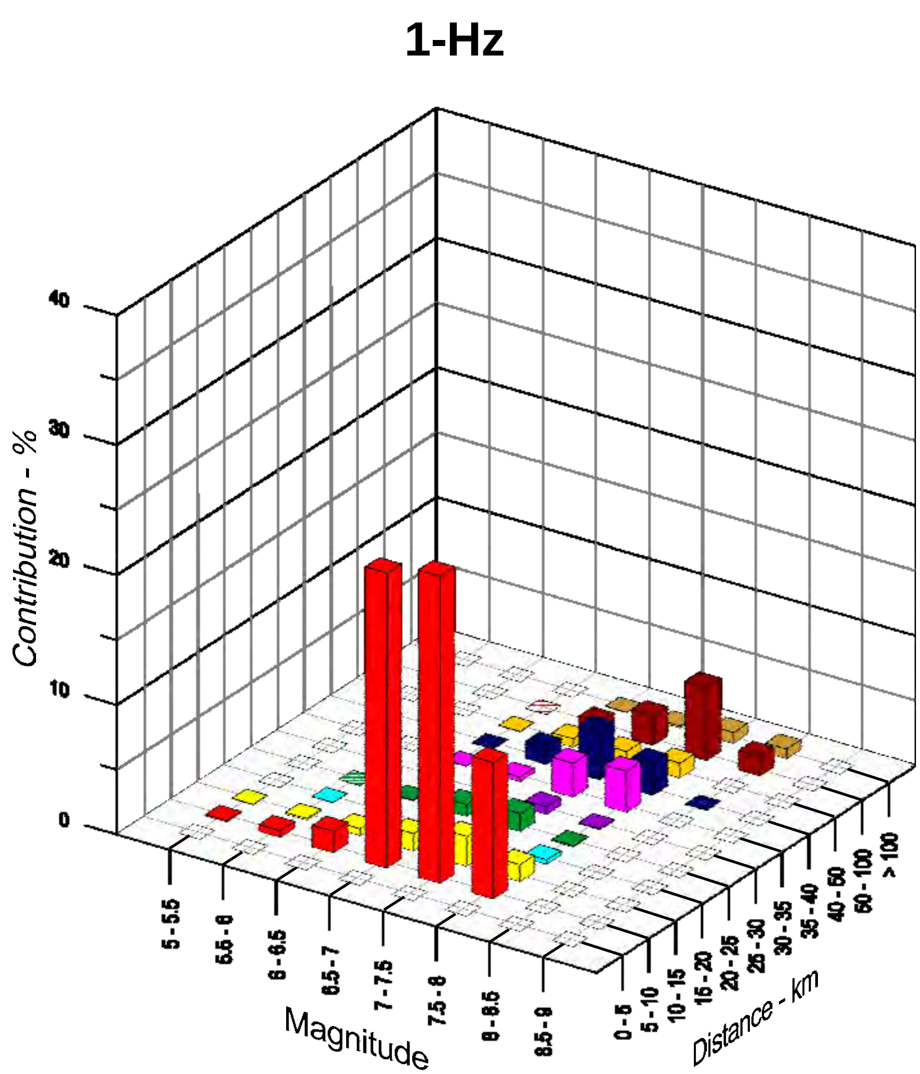

GeoPentech Geotechnical & Geoscience Consultants	**SAN ONOFRE NUCLEAR GENERATING STATION** SEISMIC HAZARD ASSESSMENT PROGRAM	HAZARD DEAGGREGATION OF 2010 PSHA FOR 2475-yr ARP at PGA and 1-Hz	FIGURE 3-6

T:_2009 Projects\09024A SONGS Seismic Hazard Plan\REPORT\Reliability\Section 3 Appendix B

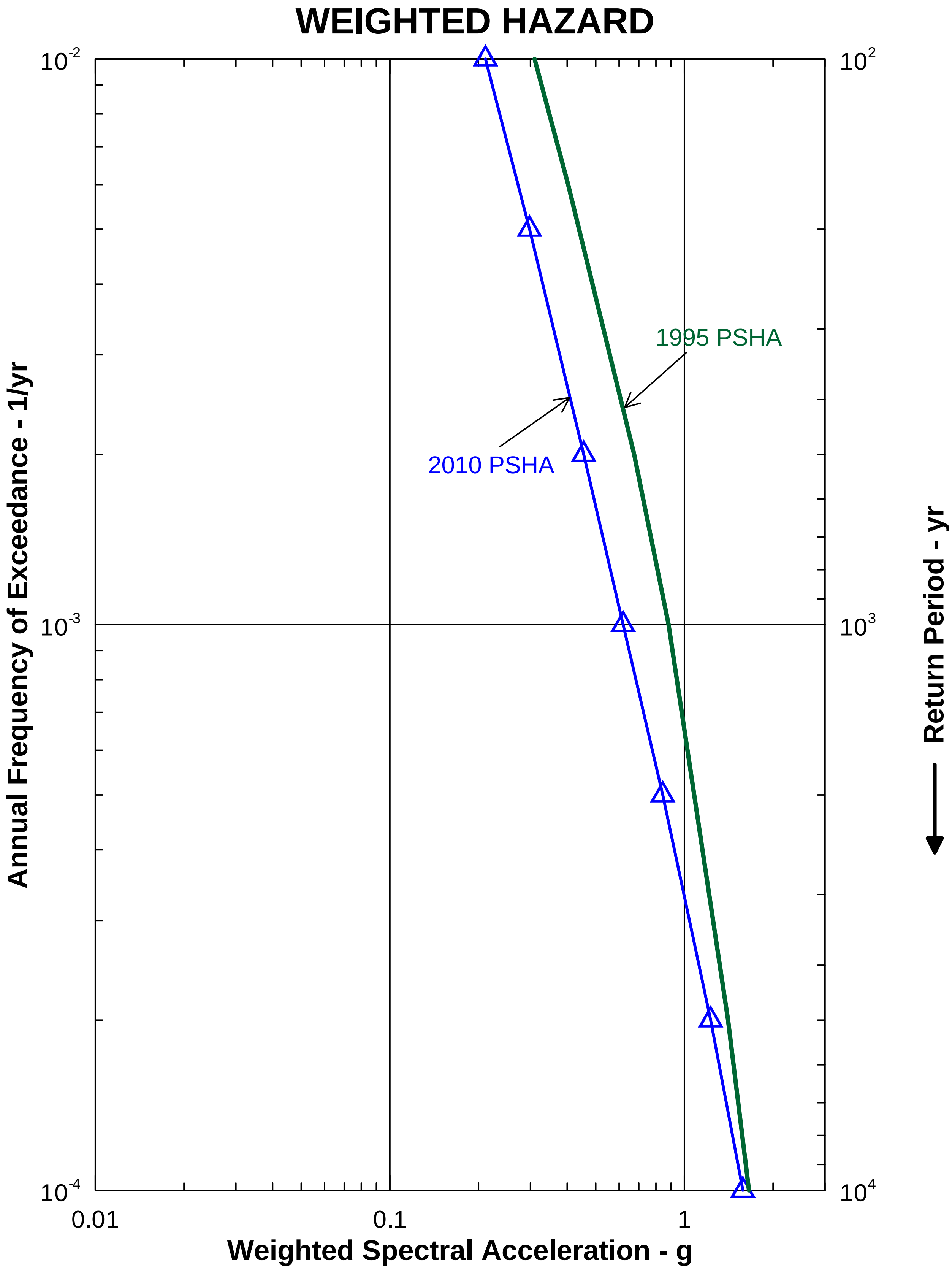

GeoPentech
Geotechnical & Geoscience Consultants

COMPARISON OF WEIGHTED HAZARD CURVES
2010 PSHA AND 1995 PSHA

FIGURE
3-7

SAN ONOFRE NUCLEAR GENERATING STATION

SEISMIC HAZARD ASSESSMENT PROGRAM

4.0 SUMMARY AND CONCLUSIONS

This seismic hazard assessment was completed to evaluate if recent available information has affected the seismic hazard at SONGS. A PSHA was performed utilizing available and regionally relevant seismic geology and seismology information (in particular, the recently released UCERF 2 [WGCEP, 2008], as well as discussions with current academic and USGS researchers) and the recently released five "Next Generation of Ground-Motion Attenuation Models" (NGA, 2008).

On the basis of this analysis, the following conclusions were reached:

- The two fault sources that contribute most to the ground motion hazard at SONGS are the NI/RC Fault Zone, which was the primary source fault governing the licensing of SONGS in the early 1980s, and the recently hypothesized OBT Fault of Rivero et al. (2000) and Rivero (2004). To appropriately represent the generally accepted NI/RC Fault Zone and the recently hypothesized OBT Fault in the 2010 PSHA, the end-member models associated with the NI/RC Fault Zone and OBT were evaluated as described in Section 2 of the report. The relative weights of 88% and 12% were assigned to the NI/RC Fault Zone and the hypothesized OBT, respectively, by the seismic source integration team. The weights are based on the consideration of a number of technical arguments given in the text.

- The mean seismic hazard curves presented on Figures 3-1 and 3-2 are assigned to the combined strike-slip and blind thrust end-member models. The NGA relationships (NGA, 2008) were used in performing this PSHA. This seismic hazard evaluation was limited to annual frequencies of exceedance greater than 10^{-4}. A 10^{-4} annual frequency of exceedance is equivalent to a RP of 10,000 years. At annual frequencies of exceedance lower than 10^{-4}, some issues are to be addressed that potentially could affect the calculated seismic hazard results. These issues consist of those associated with dispersions, i.e., epistemic and aleatory uncertainties in seismic source characterization and ground motion characterization models including the GMPE epistemic uncertainty; and those associated with nonlinear behavior of soils at the site. These issues will be addressed as part of the SONGS on-going seismic hazard program.

- The weighted hazard curves shown on Figure 3-7 indicate that the 2010 PSHA results are lower compared to the 1995 PSHA results throughout the range shown. These weighted hazard curves are also tabulated in Table 3-3.

5.0 REFERENCES

5.1 Publicly Available Publications and Data

Annotated bibliographies of pertinent publications provided in Appendix A, Attachment A-1, are denoted with an asterisk.

Abrahamson, N. and Silva, W., 2008, Summary of the Abrahamson & Silva NGA ground-motion relations: Earthquake Spectra, v. 24, no. 1, p. 67-97.

Allmendinger, R.W., 1998, Inverse and forward numerical modeling of trishear fault-propagation folds: Tectonics, v. 17, no, 4, p. 640-656.

Anderson, J.G., 1979, Estimating the seismicity from geological structure for seismic risk studies: Bulletin of the Seismological Society of America, v. 69, p. 135-158.

Argus, D.F., and Gordon, R.G., 1991, Current Sierra Nevada-North America motion from very long baseline interferometry: implications for the kinematics of the western United States: Geology, v. 19, p. 1085-1088.

*Astiz, L., and Shearer, P.M., 2000, Earthquake locations in the Inner Continental Borderland, offshore Southern California: Bulletin of the Seismological Society of America, v. 90, no. 2, p. 425-449.

Atwater, T., 1998, Plate tectonic history of southern California with emphasis on the western Transverse Ranges and Santa Rosa Island, *in* Weigand, P. W., ed., Contributions to the geology of the Northern Channel Islands, Southern California: American Association of Petroleum Geologists, Pacific Section, MP 45, p. 1-8.

Atwater, T., and Stock, J., 1998, Pacific-North America plate tectonics of the Neogene southwestern United States–an update: International Geological Review, v. 40, p. 375-402.

Axen, G J., and Fletcher, J.M., 1998, Late Miocene-Pleistocene extensional faulting, northern Gulf of California, Mexico and Salton Trough, California: International Geological Review, v. 40, p. 217-244.

Barrows, A.G., 1974, A review of the geology and earthquake history of the Newport–Inglewood Structural Zone, southern California, California Division of Mines and Geology, Special Report 114, 115 pp.

*Bender, E.E., 2000, Late Quaternary uplift and earthquake potential of the San Joaquin Hills, southern Los Angeles basin, California – COMMENT: Geology, v. 28, no. 4, p. 383.

Bennett, R.A., Rodi, W., and Reilinger, R.E., 1996 Global Positioning System constraints on fault slip rates in southern California and northern Baja, Mexico: Journal of Geophysical Research, v. 101, p. 21,943 – 21,960.

*Bohannon, R.G., and Geist, E., 1998, Upper crustal structure and Neogene tectonic development of the California Continental Borderland: Geological Society of America Bulletin, v. 110, n. 6, p. 779-800.

Boore, D.M., and Atkinson, G.M., 2008, Ground-motion prediction equations for the average horizontal component of PGA, PGV, and 5%-damped PSA at spectral periods between 0.01 s and 10.0 s: Earthquake Spectra, v. 24, no. 1, p. 99-138.

Budnitz, R.J., Apostolakis, G., Boore, D.M., Cluff, L.S., Coppersmith, K.J., Cornell, C.A., and Morris, P.A., 1997, Recommendations for Probabilistic Seismic Hazard Analysis: Guidance on Uncertainty and Use of Experts, Report NUREG/CR-6372, Lawrence Livermore National Laboratory, sponsored by the US Nuclear Regulatory Commission, US Department of Energy, and Electric Power Research Institute, 888 pp.

California Geological Survey (CGS), 2002a, California fault parameters-Interactive fault parameter map of California, [http://www.consrv.ca.gov/cgs/rghm/psha/fault_parameters/htm/Pages/index.aspx].

California Geological Survey (CGS), 2002b, California geomorphic provinces, Note 36, December 2002, 4 pp.

California Spatial Information Library (CaSIL), 2006, 1° x 1° Topography DEMs, [http://www.atlas.ca.gov/download.html] extract 1 March 2010.

California State University Monterey Bay (CSUMB), 2010, Seafloor Mapping Lab data library, accessed June 2010 from SFML website, [http://seafloor.csumb.edu/SFMLwebDATA.htm].

Campbell, K.W., and Bozorgnia, Y., 2008, NGA ground motion model for the geometric mean horizontal component of PGA, PGV, PGD and 5% damped linear elastic response spectra for periods ranging from 0.01 to 10 s: Earthquake Spectra, v. 24, no. 1, p. 139-171.

*Campbell, B.A., Sorlien, C.C., Cormier, M., and Alward, W.S., 2009, Quaternary deformation related to 3D geometry of the Carlsbad fault, offshore San Clemente to San Diego [abstract]: Southern California Earthquake Center Proceedings and Abstracts, 12–16 September 2009, v. 19, p. 263.

Cande, S.C., and Kent, D.V., 1995, Revised calibration of the geomagnetic polarity timescale for the late Cretaceous and Cenozoic: Journal of Geophysical Research, v. 100, no. B4, p. 6093-6095.

Cao, T., Bryant, W.A., Rowshandel, B., Branum, D., and Wills, C.J., 2003, The revised 2002 California probabilistic seismic hazard maps June 2003: California Geological Survey, [http://www.consrv.ca.gov/cgs/rghm/psha/fault_parameters/pdf/2002_CA_Hazard_Maps.pdf].

Chiou, B.S.-J., and Youngs, R.R., 2008, An NGA model for the average horizontal component of peak ground motion and response spectra: Earthquake Spectra, v. 24, no. 1, p. 173-215.

Clark, M.M., 1972, Surface rupture along the Coyote Creek Fault: US Geological Survey Professional Paper 787, p. 55-86.

Clark, D.H., Hall, N.T., Hamilton, D.H., and Heck, R.G., 1991. Structural analysis of late Neogene deformation in the central offshore Santa Maria Basin, California: Journal of Geophysical Research, v. 96, no.B4, p. 6435–6457.

*Conrad, J.E., Ryan, H.F., and Sliter, R.W., 2010, Tracing active faulting in the Inner Continental Borderland, Southern California, using new high-resolution seismic reflection and bathymetric data [abstract]: Seismological Society of America 2010 Annual Meeting, Seismological Research Letters, v.81, no. 2, p. 347.

*Crouch, J.K., and Suppe, J., 1993, Late Cenozoic tectonic evolution of the Los Angeles basin and Inner California Borderland: A model for core complex-like crustal extension: Geological Society of America Bulletin, v. 105, p. 1415-1434.

Dames & Moore, 1970, Seismic and foundation studies, proposed units 2 and 3, San Onofre Nuclear Generating Station, for Southern California Edison, 15 April 1970.

DeMets, C., and Dixon, T.H., 1999, New kinematic models for Pacific-North America motion from 3 Ma to present, I: evidence for steady motion and biases in the NUVEL-1A model: Geophysical Research Letters, v. 26, no. 13, p. 1921-1924.

Dorsey, R.J., and Janecke, S.U., 2002, Late Miocene to Pleistocene West Salton detachment fault and basin evolution, southern California: new insights [abstract]: Geological Society of America Abstracts with Programs, v. 34, no. 248.

*Ehlig, P.L., 1977, Geologic report on the area adjacent to the San Onofre Nuclear Generating Station northwestern San Diego County, CA, for Southern California Edison Company, 31 September 1977, 32 pp.

Erslev, E., 1991, Trishear fault-propagation folding: Geology, v. 19, p. 617-620.

Fialko, Y., 2006, Interseismic strain accumulation and the earthquake potential on the southern San Andreas fault system: Nature, v. 441, p. 968- 971, doi: 10.1038/nature04797.

*Fischer, P.J. and Mills, G.I., 1991, The offshore Newport-Inglewood – Rose Canyon fault zone, California: structure, segmentation and tectonics *in* Abbott, P.L., and Elliott, W.J., eds., Environmental Perils San Diego Region: San Diego, San Diego Association of Geologists, p. 17-36.

Fisher, M.A., 2009, Introduction to geologic hazards of offshore southern California *in* Lee, H.J., and Normark, W.R., eds., Earth and Science in the Urban Ocean: The Southern California Continental Borderland: Geological Society of America Special Paper 454, p. 227-228, doi: 10.1130/2009.2454(4.1).

Fisher, M.A., Langenheim, V.E., Nicholson, C., Ryan, H.F., and Sliter, R.W., 2009a, Recent developments in understanding the tectonic evolution of the southern California offshore area: implications for earthquake-hazard analysis *in* Lee, H.J., and Normark, W.R., eds., Earth and Science in the Urban Ocean: The Southern California Continental Borderland: Geological Society of America Special Paper 454, p. 229-250, doi: 10.1130/2009.2454(4.2).

Fisher, M.A., Sorlien, C.C., and Sliter, R.W., 2009b, Potential earthquake faults offshore southern California, from the eastern Santa Barbara Channel south to Dana Point *in* Lee, H.J., and Normark, W.R., eds., Earth and Science in the Urban Ocean: The Southern California Continental Borderland: Geological Society of America Special Paper 454, p. 271-290, doi: 10.1130/2009.2454(4.4).

Franzen, S., Lew, M., and Elliott, P.J., 1998, Multiple investigation methods for fault rupture hazard evaluation, *in* Robertson, and Mayne, eds., Geotechnical Site Characterization, Balkema, Rotterdam, ISBN 90 5410 939 4, p. 139-144.

Freeman, T.S., Heath, E.G., Guptill, P.D., and Waggoner, J.T., 1992, Seismic hazard assessment, Newport-Inglewood fault zone, *in* Engineering Geology Practice in Southern California, Special Publication, no. 4, Association of Engineering Geologists, Southern California Section, p. 211-231.

Glover, E.S., 1876, Bird's Eye View of San Diego, California. Map published by Schneider and Kueppers, San Diego.

*Grant, L.B., and Shearer, P.M., 2004, Activity of the offshore Newport-Inglewood Rose Canyon Fault Zone, coastal southern California, from relocated microseismicity: Bulletin of the Seismological Society of America, v. 94, no. 2, p. 747-752.

*Grant, L.B., and Rockwell, T.K., 2002, A northward propagating earthquake sequence in coastal southern California?: Seismological Research Letters, v. 73, no. 4, p. 461-469.

*Grant, L.B., Ballenger, L.J., and Runnerstrom, E.E., 2002, Coastal uplift of the San Joaquin Hills, southern Los Angeles basin, California, by a large earthquake since A.D. 1635: Bulletin of the Seismological Society of America, v. 92, no. 2, p. 590-599.

*Grant, L.B., Mueller, K.J., Gath, E.M., and Munro, R., 2000, Late Quaternary uplift and earthquake potential of the San Joaquin Hills, southern Los Angeles basin, California – REPLY: Geology, v. 28, no. 4, p. 384.

*Grant, L.B., Mueller, K.J., Gath, E.M., Cheng, H., Edwards, R.L., Munro, R., and Kennedy, G., 1999, Late Quaternary uplift and earthquake potential of the San Joaquin Hills, southern Los Angeles basin, California: Geology, v. 27, p. 1031-1034.

Grant, L.B., Waggoner, J.T., Rockwell, T.K., and von Stein, C., 1997, Paleoseismicity of the north branch of the Newport-Inglewood fault zone in Huntington Beach, California, from Cone Penetrometer Test data: Bulletin of the Seismological Society of America, v. 94, no. 2, p. 277-293.

Greene, H.G., Bailey, K.A., Clarke, S.H., Ziony, J.I., and Kennedy, M.P., 1979, Implications of fault patterns of the Inner California Continental Borderland between San Pedro and San Diego *in* Abbott, P.L., and Elliott, W.J., eds., Earthquakes and Other Perils, San Diego Region, San Diego Association of Geologists, p. 21-29.

Hanks, T.C., and Kanamori, H., 1979, A moment magnitude scale: Journal of Geophysical Research, v. 84, no. B5, p. 2348-2350.

Hanson, K.L., Angell, M., Foxall, W., and Rietman, J., 2002, Evaluation of seismic source characterization of models for the inner borderlands of southern California [abstract]: Eos (Transactions, American Geophysical Union) v. 83, no. 47, Fall Meeting Supplement, abstract S21A-0973, p. F1067.

Harding, T.P., 1973, Newport-Inglewood trend, California – an example of wrenching style of deformation: American Association of Petroleum Geologists Bulletin, v. 57, no. 1, p. 97-116.

*Hauksson, E., 1987, Seismotectonics of the Newport-Inglewood fault zone in the Los Angeles basin, southern California: Bulletin of the Seismological Society of America, v. 77, no. 2, p. 539-561.

*Hauksson, E., and Gross, S., 1991, Source parameters of the 1933 Long Beach earthquake: Bulletin of the Seismological Society of America, v. 81, no. 1, p. 81-98.

Hauksson, E., and Jones, L.M., 1988, The July 1986 Oceanside (M_L = 5.3) earthquake sequence in the Continental Borderland, southern California: Bulletin of the Seismological Society of America, v. 76, no. 6, p. 1885-1906.

Idriss, I.M., 2008, An NGA empirical model for estimating the horizontal spectral values generated by shallow crustal earthquakes: Earthquake Spectra, v. 74, no. 1, p. 217-242.

Jennings, C.W., 1994, Fault activity map of California and adjacent areas with location and ages of recent volcanic eruptions: California Department of Conservation, Division of Mines and Geology, Geologic Data Map Series, Map No. 6 , map with explanatory text, 92 pp., scale 1:750,000.

Kamerling, M.J., and Luyendyk, B.P., 1985, Paleomagnetism and Neogene tectonics of the northern Channel Islands, California: Journal of Geophysical Research, v. 90, p. 12,485-12,502.

Kamerling, M.J., and Luyendyk, B.P., 1979, Tectonic rotations of the Santa Monica Mountains region, western Transverse Ranges, California, suggested by paleomagnetic vectors: Geological Society of America Bulletin, part I, v. 90, p. 331-337.

Kennedy, M.P. and Clarke, S.H., 1996, Analysis of late Quaternary faulting in San Diego Bay and hazard to the Coronado Bridge, prepared for California Department of Transportation (Caltrans).

Kern, J.P., 1977, Origin and history of upper Pleistocene marine terraces, San Diego, California, Geological Society of America Bulletin, v. 88, p. 1553-1566.

*Kern, J.P., and Rockwell, T.K., 1992, Chronology and deformation of Quaternary marine shorelines, San Diego County, California *in* Kern, J.P., and Rockwell, T.K., eds., Quaternary Coasts of the United States: Marine and Lacustrine Systems, Special Publication no. 48, Society for Sedimentary Geology, 377-382.

*Kier, G., and Mueller, K., 1999, Flexural modeling of the northern Gulf of California Rift: relating marine terrace uplift to the forebulge on a subsiding plate: Southern California Earthquake Center 1999 internship final report, 11 pp., [http://www.scec.org/education/college/internships/1999/99grant.pdf].

Kies, R.P. and Abbott, P.L., 1983, Rhyolite clast populations and tectonics in the California continental borderland: Journal of Sedimentary Research, v. 53, no. 2, p. 461-475.

Klinger, R.E. and Rockwell, T.K., 1989, Flexural-slip folding along the eastern Elmore Ranch fault in the Superstition Hills earthquake sequence of November 1987: Bulletin of the Seismological Society of America, v. 79, no. 2, p. 297-303.

Lajoie, K.R., Ponti, D.J., Powell, C.L., Mathieson, S.A., and Sarna-Wojcicki, A.M., 1992, Emergent marine strandlines and associated sediments, coastal California: A record of Quaternary sea- level fluctuations, vertical tectonic movements, climatic changes and coastal processes, *in* Heath, E., and Lewis, L., eds., The regressive Pleistocene shoreline in southern California: Santa Ana, California, South Coast Geological Society annual Field Trip guidebook 20, p. 81-104.

Law/Crandall, Inc., 1993, Report of potential fault displacements Wastewater Treatment Plant Number 2 Huntington Beach, California for County Sanitation Districts of Orange County, 2661.30140.0001, 16 September 1993, 10 pp, 7 plates.

Lee, H.J., Greene, G.H., Edwards, B.D., Fisher, M.A., and Normark, W.R., 2009, Submarine landslides of the southern California Borderland Point *in* Lee, H.J. and Normark, W.R., eds., Earth and Science in the Urban Ocean: The Southern California Continental Borderland: Geological Society of America Special Paper 454, p. 251-269, doi: 10.1130/2009.2454(4.3).

*Legg, M.R., 1991, Developments in understanding the tectonic evolution of the California Continental Borderland: Special Publication no. 46, Society for Sedimentary Geology, p. 291-312.

*Legg, M.R., Goldfinger, C., Kamerling, M.J., Chaytor, J.D., and Einstein, D.E., 2007, Morphology, structure and evolution of California Continental Borderland restraining bends *in* Cunningham, W.D., and Mann, P., eds., Tectonics of Strike-Slip Restraining and Releasing Bends: Geological Society, London, Special Publications, 290, p. 143-168, doi: 10.1144/SP290.3.

Legg, M.R., Kamerling, M.J., and Francis, R.D., 2004, Termination of strike-slip faults at convergence zones within continental transform boundaries: examples from the California Continental Borderland in Grocott, J., McCaffrey, K.J.W., Taylor, G., and Tikoff, B., eds., Vertical Coupling and Decoupling in the Lithosphere, Geological Society of London, p. 65-82.

Leon, L.A., Dolan, J.F., Shaw, J.H., and Pratt, T.L., 2009, Evidence for large Holocene earthquakes on the Compton thrust fault, Los Angeles, California: Journal of Geophysical Research, v. 114, no. B12305, 14 pp., doi: 10.1029/2008JB006129.

Lindvall, S.C., and Rockwell, T.K., 1995, Holocene activity of the Rose Canyon fault zone in San Diego, California: Journal of Geophysical Research, v. 100, no. B12, p. 24,121-24,132.

Lutz, A.T.; Dorsey, R.J.; Housen, B.A.; and Janecke, S.U., 2006, Stratigraphic record of Pleistocene faulting and basin evolution in the Borrego Badlands, San Jacinto fault zone, southern California: Geological Society of America Bulletin, v. 118, p. 1377-1397.

Medwedeff, D., 1992, Geometry and kinematics of an active, laterally propagating wedge thrust, Wheeler Ridge, California, *in* Mitra, S., and Fischer, G. W., eds., Structural geology of fold and thrust belts: Baltimore, Maryland, Johns Hopkins University Press, p 3-28.

Minerals Management Services (MMS), 2001, Oil and gas resources in the Pacific outer continental shelf as of January 1, 1999: an expanded update to the 1995 National Assessment of United States Oil and Gas Resources: US Department of the Interior Minerals Management Services OCS Report MMS 2001-014, February 2001, 21 pp.

Molnar, P., 1979, Earthquake recurrence intervals and plate tectonics: Bulletin of the Seismological Society of America, v. 69, p. 115-133.

Morton, D.M., and Matti, J.C., 1993, Extension and contraction within an evolving divergent strike-slip fault complex: the San Andreas and San Jacinto fault zones at their convergence in southern California. *in* Powell, R.E. Weldon, R.J., and Matti, J.C., eds., The San Andreas Fault system: displacement, palinspastic reconstruction, and geologic evolution, Geological Society of America Memoirs, v. 178, p. 217-230.

Moody, J.D., and Hill, M.J., 1956, Wrench-fault tectonics: Geological Society of America Bulletin, v. 67, p. 1207-1246.

*Moore, G.W., 1972, Offshore extension of the Rose Canyon fault, San Diego, California: US Geological Survey Professional Paper 800-C, C113-C116.

Moriwaki, Y., Tan, P., and Barneich, J.A., 2002, Evaluation of alternative seismic source models using SCIGN data [abstract]: Eos (Transactions, American Geophysical Union) v. 83, no. 47, Fall Meeting Supplement, 19 November 2002.

Mount, V., Suppe, J., and Hook, S., 1990, A forward modeling strategy for balancing cross sections: American Association of Petroleum Geologist Bulletin, v. 74, p. 521-531.

*Mueller, K., Kier, G., Rockwell, T., and Jones, C.H., 2009, Quaternary rift flank uplift of the Peninsular Ranges in Baja and southern California by removal of mantle lithosphere: Tectonics, v. 28, TC5003, doi:10.1029/2007TC002227.

Mueller, K.J., Grant, L.B., and Gath, E., 1998, Late Quaternary growth of the San Joaquin Hills anticline—a new source of blind thrust earthquakes in the Los Angeles basin [abstract]: Seismological Society of America 1998 Annual Meeting, Seismological Research Letters, v. 69, no. 2, p. 161-162.

NOAA, 2008, Geophysical Data System (GEODAS) bathymetry points, Volume 1, Version 5.0.11.

NOAA, 2001, Geophysical Data System (GEODAS) bathymetry points, Volume 1, Version 4.1.

NGA, 2008, Earthquake Spectra, v. 24, no. 1, p. 1-341.

Nicholson, C., Sorlien, C.C., Atwater, T., Crowell, J.C., and Luyendyk, B.P., 1994, Microplate capture, rotation of the western Transverse Ranges, and initiation of the San Andreas transform as a low-angle fault system: Geology, v. 22, p. 491-495.

Petersen, M.D., Bryant, W.A., Cramer, C.H., Cao, T., and Reichle, M., 1996, Probabilistic seismic hazard assessment for the State of California: U.S. Geological Survey Open File Report 96-706, 19 pp.

Plesch, A., Shaw, J.H., Benson, C., Bryant, W.A., Carena, S., Cooke, M., Dolan, J., Fuis, G., Gath, E., Grant, L., Hauksson, E., Jordan, T., Kamerling, M., Legg, M., Lindvall, S., Magistrale, H., Nicholson, C., Niemi, N., Oskin, M., Perry, S., Planansky, G., Rockwell, T., Shearer, P., Sorlien, C., Suss, M. P., Suppe, J., Treiman, J., and Yeats, R., 2007, Community Fault Model (CFM) for southern California: Bulletin of the Seismological Society of America, v. 97, no. 6, p. 1793-1802.

Ponti, D.J., 2010, USGS investigations of stratigraphy and neotectonics of the Los Angeles basin [abstract]: US Geological Survey, 5 pp.

*Ponti, D.J., 2001, Changing deformation rates through time: insights from new Quaternary stratigraphic studies in the Los Angeles basin, California [abstract]: American Geophysical Union 2001 Fall Meeting, 10–14 December 2001, abstract #S12E-11.

*Ponti, D.J., and Ehman, K.D., 2009, A 3-D sequence-based structural model for the Quaternary Los Angeles basin, California [abstract]: Southern California Earthquake Center Proceedings and Abstracts, 12–16 September 2009, vol. 19, p. 262-263.

Rentz, P, 2010, The influence of tectonics, sea level, and sediment supply on coastal morphology in the Oceanside littoral cell, CA, unpublished M.S. Thesis: University of California, San Diego.

*Rivero, C.A., 2004, Origin of active blind-thrust faults in the southern Inner California Borderlands, unpublished Ph.D. Dissertation: Harvard University, 146 pp.

*Rivero, C., and Shaw, J.H., 2010, in press, Active folding and blind-thrust faulting induced by basin inversion processes, Inner California Borderlands: Tectonics, submitted for consideration of publication 2010, 45 pp.

*Rivero, C., and Shaw, J.H., 2005, Fault-related folding in reactivated offshore basins, California *in* Interpretations of Contractual Fault-Related Folds, An American Association of Petroleum Geologists Seismic Atlas, Studies in Geology, No. 53, Department of Earth and Planetary Sciences: Harvard University, Cambridge, MA, 3 pp.

*Rivero, C., and Shaw, J.H., 2001, 3D geometry and seismogenic potential of the Inner California Borderland blind thrusts system [abstract]: Southern California Earthquake Center Proceedings and Abstracts, 23–26 September 2001, p. 105-106.

*Rivero, C., Shaw, J.H., and Mueller, K., 2000, Oceanside and Thirtymile Bank blind thrusts: implications for earthquake hazards in coastal southern California: Geology, v. 28, no. 10, p. 891-894.

Rockwell, T., 2010a, The Rose Canyon Fault Zone in San Diego; Proceeding of Fifth International Conference on Recent Advances in Geotechnical Earthquake Engineering and Soil Dynamics and Symposium in Honor of Professor I.M. Idriss; Paper No. 7.06c, 9pgs.

Rockwell, T., 2010b, The non-regularity of earthquake recurrence in California: Lessons from long paleoseismic records from the San Andreas and San Jacinto faults in southern California, and the north Anatolian fault in turkey, Proceeding of Fifth International Conference on Recent Advances *in* Geotechnical Earthquake Engineering and Soil Dynamics and Symposium in Honor of Professor I.M. Idriss, Paper No. EQ 5, 9 pp.

Rockwell, T., 2010c, Fault hazard characterization for a transportation tunnel project in Coronado, California *in* Geotechnical Earthquake Engineering and Soil Dynamics and Symposium in Honor of Professor I.M. Idriss, Paper No. 7.02c, 13 pp.

Rockwell, T.K. and Murbach, M., 1999, Holocene earthquake history of the Rose Canyon fault zone. USGS Award No. 1434-95-G-2613 Final Technical Report 36 pp (plus appendix).

*Rockwell, T.K., Lindvall, S.C., Haraden, C.C., Hirabayashi, C.K., and Baker, E., 1992, Minimum Holocene slip rate for the Rose Canyon fault in San Diego, California, *in* Heath, E.G., and Lewis, W.L., eds., The Regressive Pleistocene Shoreline Coastal Southern California: South Coast Geological Society, Inc., 1992 Annual field Trip Guide Book No. 20, p. 55-64.

Rockwell, T.K., Lindvall, S.C., Haraden, C.C., Hirabayashi, C.K., and Baker, E., 1991, Minimum Holocene slip rate for the Rose Canyon fault in San Diego, California *in* Abbott, P.L., and Elliott, W.J., eds., Environmental Perils San Diego Region: San Diego, San Diego Association of Geologists, p. 37-46.

*Ryan, H.F., Legg, M.R., Conrad, J.E., and Sliter, R.W., 2009, Recent faulting in the Gulf of Santa Catalina: San Diego to Dana Point *in* Lee, H.J., and Normark, W.R., eds., Earth and Science in the Urban Ocean: The Southern California Continental Borderland: Geological Society of America Special Paper 454, p. 291-315, doi: 10.1130/2009.2454(4.5).

SCE, UFSAR, San Onofre Nuclear Generating Station, Units 2 & 3, Updated Final Safety Analysis Report, submitted to the U.S. Nuclear Regulatory Commission (NRC).

SCE, 2001, San Onofre Nuclear Generating Station Units 2 and 3 Seismic Hazard Study of Postulated Blind Thrust Faults, prepared by Geomatrix Consultants, GeoPentech, and Southern California Edison for the Nuclear Regulatory Commission, 26 December 2001, 165 pp.

SCE, 1995, Seismic Hazard at San Onofre Nuclear Generating Station, prepared by Risk Engineering, Inc. for Southern California Edison Co., 2244 Walnut Grove Avenue, Rosemead, California 91770, 25 August 1995, 340 pp.

SCE, 1979, Report of the Evaluation of Maximum Earthquake and Site Ground Motion Parameters Associated with the Offshore Zone of Deformation San Onofre Nuclear Generating Station, prepared by Woodward-Clyde Consultants for Southern California Edison, P.O. Box 800, Rosemead, California 91770, June 1979, 243 pp.

SSHAC, 1997, Recommendations for probabilistic seismic hazard analysis: Guidance on uncertainty and use of experts, prepared by Senior Seismic Hazard Analysis Committee, Lawrence Livermore National Laboratory, Volume 1, Main Report, NUREG/CR-6372, UCRL-ID-122160, 280 pp.

Schneider, C.L., Hummon, C., Yeats, R.S., and Huftile, G.L., 1996, Structural evolution of the northern Los Angeles basin, California, based on growth strata: Tectonics, v. 15, no. 2, p. 341-355.

Scripps Orbit and Permanent Array Center (SOPAC), 2010, SOPAC refined velocities, accessed June 2010, from SOPAC website, [http://sopac.ucsd.edu/cgi-bin/refinedModelVelocities.cgi].

Seeber, L, and Sorlien, C.C., 2000, Listric thrusts in the western Transverse Ranges, California: Geological Society of America Bulletin, v. 112, p. 1067-1079.

Shaw, J., and Suppe, J., 1996, Earthquake hazards of active blind-thrust faults under the central Los Angeles basin, California: Journal of Geophysical Research, v. 101, no. B4, p. 8623-8642.

Shlemon, R.J., 1987, The Cristianitos fault and Quaternary geology, San Onofre State Beach, California *in* Geological Society of America Continental Field Guide—Cordilleran Section, p. I126-I129.

Shlemon, R.J., 1978, Late Quaternary rates of deformation Laguna Beach–San Onofre State Beach Orange and San Diego Counties, California, prepared by Roy J. Shlemon & Assoc. for Southern California Edison Company and San Diego Gas & Electric Company, October 1978, 31 pp.

Shlemon, R.J., Elliott, P., and Franzen, S., 1995, Holocene displacement history of the Newport-Inglewood, north branch fault splays, Santa Ana River floodplain, Huntington Beach, California [abstract]: Geological Society of America Abstracts with Programs 1995 Annual Meeting, 6–9 November 1995, v. 27, no. 6, p. A-375.

*Sliter, R.W., Ryan, H.F., and Normark, W.R., 2001, Does recent deformation at the base of slope provide evidence of a connection between the Newport-Inglewood and the Rose Canyon fault zones offshore southern California? [abstract]: American Geophysical Union 2001 Fall Meeting, 10–14 December 2001, abstract #S11A-0531.

*Sorlien, C.C., Campbell, B.A., Alward, W.S., Seeber, L., Legg, M.R., and Cormier, M., 2009a, Transpression along strike-slip restraining segments vs. regional thrusting in the Inner California Continental Borderland [abstract]: Southern California Earthquake Center Proceedings and Abstracts, 12–16 September 2009, v. 19, p. 264.

*Sorlien, C.C., Campbell, B.A., and Seeber, L., 2009b, Geometry, kinematics, and activity of a young mainland-dipping fold and thrust belt: Newport Beach to San Clemente, California, USDI/USGS Award No. 08HQGR0103 Final Technical Report, 25 pp.

Sorlien, C.C., Kamerling, M.J., and Mayerson, D., 1999, Block rotation and termination of the Hosgri strike-slip fault system, California, from 3-D map restoration: Geology, v. 27, p. 1039-1042.

Suppe, J., 1983. Geometry and kinematics of fault bend folding: American Journal of Science, v. 283, p. 684–721.

Suppe, J., and Medwedeff, D.A., 1990, Geometry and kinematics of fault-propagation folding: *Eclogae* Geologicae Helvetiae., v. 83, p. 409-454.

Thomas, P., Wong, I., and Abrahamson, N., 2010, Verification of probabilistic seismic hazard analysis computer programs: PEER Report 2010/106, Pacific Earthquake Engineering Research Center, College of Engineering, University of California, Berkeley, May 2010, 176 pp.

Treiman, J., 1993, The Rose Canyon fault zone, southern California: California Division of Mines and Geology, Open File Report 93-02, 45 pp.

USGS, 2009, Quaternary fault and fold database for the United States, accessed 25 October 2010, from USGS website, [http//earthquakes.usgs.gov/regional/qfaults/].

USGS, 2008, Documentation for the 2008 update of the United States National Seismic Hazard Maps, prepared by Petersen, M. D., Frankel, A. D., Harmsen, S. C., Mueller, C. S., Hallar, K. M., Wheeler, R. L.,

Wesson, R. L., Zeng, Y., Boyd, O. S., Perkins, D. M., Luco, N., Field, E. H., Wills, C. J., and Rukstales, K. S., U.S. Geological Survey Open File Report 2008-1128, 128 pp.

WGCEP, 2008, The Uniform California Earthquake Rupture Forecast, Version 2 (UCERF 2), prepared by 2007 Working Group on California Earthquake Probabilities: US Geological Survey Open File Report 2007-1437 and California Geological Survey Special Report 203, [http://pubs.usgs.gov/of/2007/1497/].

WGCEP, 1995, Seismic hazards in southern California: probable earthquakes, 1994-2024: Bulletin of the Seismological Society of America, v. 85, p. 379-439.

Weichert, D.H., 1980, Estimation of the earthquake recurrence parameters for unequal observation periods for different magnitudes: Bulletin of the Seismological Society of America, v. 70, no. 4, p. 1337-1346.

Wells, D.L., and Coppersmith, K. J., 1994, New empirical relationships among the magnitude, rupture length, rupture width, rupture area, and surface displacement: Bulletin of the Seismological Society of America, v. 84, p. 974-1002.

Wentworth, C.M., 1990, Structure of the Coalinga region and thrust origin of the earthquake, in The Coalinga, California earthquake of May 2, 1983: US Geological Survey Professional Paper 1487, p. 41-68.

Wesnousky, S.G., 2008, Displacement and geometrical characteristics of earthquake surface ruptures: Issues and implications for seismic-hazard analysis and the process of earthquake rupture: Bulletin of the Seismological Society of America, v. 98, p. 1609-1632.

Western Geophysical Company, 1972, Final Report: San Onofre Offshore Investigations, *in* SCE, 2001, SONGS Units 2 and 3 Seismic Hazard Study of Postulated Blind Thrust Faults, offshore marine reflection seismic data, Plate 2-3, 26 December 2001.

Weston Geophysical, 1971, Seismic Velocity Measurements, San Onofre Nuclear Generating Station, *in* Woodward-McNeill and Associates, 1972, Material Property Studies, San Onofre Nuclear Generating Station, Appendix C, 15 March 1972.

*Wetmore, P.H., Malservisi, R., Fletcher, J., Alsleben, H., Callihan, S., Springer, A., and González-Yajimovich, O., 2010, in review, Transtension within a restraining bend domain of a transform plate boundary: the role of block rotations and the reactivation of preexisting crustal structures: Geological Society of America Lithosphere, submitted for consideration of publication 2010, 17 pp.

Wilcox, R.E., Harding, T.P., Seely, D.R., 1973, Basic Wrench Tectonics: American Association of Petroleum Geologists Bulletin, v. 57, no.1, p. 74-96.

Woodward-Clyde Consultants, 1980, Response to NRC Questions San Onofre 2 & 3, Question 361.61, 4 pp., 3 figures, April 1980.

Woodward-McNeill and Associates, 1972, Material Property Studies, San Onofre Nuclear Generating Station, Appendix E, 15 March 1972, 8 pp.

*Wright, T.L., 1991, Structural geology and tectonic evolution of the Los Angeles basin, California *in* Biddle, K.T., ed., Active margin basins: American Association of Petroleum Geologists Memoir 52, p. 35–134.

Yeats, R.S., 1987, Late Cenozoic structure of the Santa Susana fault zone, California: U.S. Geological Survey Professional Paper 1339, p. 137-160.

Yeats, R.S., 1973, Newport-Inglewood fault zone, Los Angeles basin, California: American Association of Petroleum Geologists Bulletin, v. 57, no. 1, p. 117-135.

Yerkes, R.F., 1990, Tectonic setting, in The Coalinga, California earthquake of May 2, 1983: US Geological Survey Professional Paper 1487, p. 13-22.

Youngs, R.R., and Coppersmith, K.J., 1985, Implications of fault slip rates and earthquake recurrence models to probabilistic seismic hazard analysis: Bulletin of the Seismological Society of America, v. 75, no. 4, p. 939-964.

5.2 Personal Communication

Details of personal communication summarized in Appendix A, Attachment A-1, are denoted with an asterisk.

Abrahamson, N., 2010, personal communication.

*Ponti, D., 2010, personal communication.

*Rockwell, T., 2010, personal communication.

Rockwell, T., 2001, personal communication.

*Ryan, H., 2010, personal communication.

USGS, 2009, Harmsen, S., personal communication on 20 October 2009.

USGS, 2007, Kendrick, C., personal communication.

6.0 GLOSSARY

ALEATORY UNCERTAINTY: Uncertainty arising from or associated with the inherent, irreducible, natural randomness of a system or process

ANNUAL FREQUENCY OF EXCEEDANCE: Mean number of seismic events per year exceeding a specified value

BASE: United States Marine Corps Base at Camp Pendleton

CFM: Community Fault Model of southern California developed by Plesch et al. (2007)[1]

CGS: California Geological Survey

CPT: Cone Penetration Test

dgnd: The median or spectral acceleration uncertainty for any given attenuation relationship

EPISTEMIC UNCERTAINTY: Uncertainty associated with a model of a system or process and its parameters that arises from limitations of the data available or on causal understanding

GMPEs: Ground motion prediction equations

GPS: Global Positioning System

HAZ4.2: PSHA computer program developed by Dr. Norman Abrahamson (2010, PC)[1]

HAZARD CURVE: Plot of the relationship between a ground motion parameter and the mean number of seismic events per year in which the ground motion parameter at the site exceeds a specified value; herein, the ground motion parameters of interest are the peak ground acceleration and spectral acceleration

HECTARE: Unit of surface area equal to 10,000 square meters (i.e., 100 meters by 100 meters); also equal to 2.47 acres

Hz: Hertz

ICB: Inner Continental Borderland

InSAR: Interferometric Synthetic Aperture Radar

ka: Thousand years ago

km: Kilometers

km/s: Kilometers per second

Ma: Million years ago

MIS 5e/5a: Marine Isotope Stages 5e/5a; part of a series of stages 1 through 6

MMS: Minerals Management Services

mm/yr: Millimeters per year

m_j: A variable used in PSHA calculations representing an earthquake of a particular magnitude

m/s: Meters per second

M: A quantity characteristic of the total energy released by an earthquake

M_L: Local magnitude scale developed by Richter in the 1930s

Mw: Moment magnitude scale as presented by Hanks and Kanamori (1979)[1]

NGA: Next Generation Attenuation relationships presented as part of the NGA Relations Project, a five year research program designed to improve earthquake ground motion attenuation relationships for shallow crustal earthquakes in the western United States[1]

NI: Newport-Inglewood (Fault)

NI/RC: Newport-Inglewood/Rose Canyon Fault Zone

NSHM: National Seismic Hazard Maps as presented by USGS (2008; 2009, PC)[1]

$\dot{N}_s(m_j)$: A variable used in PSHA calculations representing the mean number of earthquakes per year having an earthquake magnitude m_j

OBT: Oceanside Blind Thrust Fault as characterized by Rivero et al. (2000)[1], Rivero and Shaw (2001)[1], Rivero (2004)[1], Rivero and Shaw (2005)[1], and Rivero and Shaw (2010, in press)[1]

OZD: Offshore Zone of Deformation

PC: Personal communication

PEER: Pacific Earthquake Engineering Research

PGA: Peak ground acceleration

PSHA: Probabilistic Seismic Hazard Analysis

POISSON PROCESS: A random function which describes the number of random events in a specified interval of time or space; the random events have the following properties: (i) the probability of more than one event during the specified time interval is negligible; (ii) the probability of an event during the specified time interval does not depend on what happened prior to the specified time

QA/QC: Quality Assurance/Quality Control

RC: Rose Canyon (Fault)

RP: Return Period in years; inverse of annual frequency of exceedance value

RECURRENCE RELATIONSHIP: Relationship showing the annual recurrence of earthquakes of various magnitudes up to a maximum magnitude; used to determine the mean number of earthquakes per year

r_k: A variable used in PSHA calculations representing the distance between the site and a fault rupture plane

SA: Spectral Acceleration

SCE: Southern California Edison

SCOZD: South Coast Offshore Zone of Deformation

SDT: San Diego Trough

SONGS: San Onofre Nuclear Generating Station

SOPAC: Scripps Orbit and Permanent Array Center

SSHAC: Senior Seismic Hazard Analysis Committee

STAB: Seismic Technical Advisory Board for SONGS Seismic Hazard Analysis

TMBT: Thirtymile Bank Blind Thrust Fault as characterized by Rivero (2004)[1] and Plesch et al. (2007)[1]

TECHNICAL COMMUNITY: As used in this report, this term refers to geoscientists and engineers that have demonstrated expertise in relevant ground motion and seismotectonic fields of study in the area around SONGS

TYPE-A FAULT: Seismic sources with detailed earthquake recurrence models where the timing of past events and event displacements are available; earthquakes on Type-A Faults are modeled as characteristic earthquakes; faults as presented by WGCEP (2008)[1] and USGS (2008)[1]

TYPE-B FAULT: Seismic sources with measurable slip rates but lacking information of the timing of past events, fault segmentation, and/or event displacements; earthquakes on Type-B Faults are modeled as characteristic earthquakes that rupture the full fault length; faults as presented by WGCEP (2008)[1] and USGS (2008)[1]

TYPE-C ZONE: Regions of distributed shear in which overall rate and style of deformation are unknown; zones as presented by WGCEP (2008)[1] and USGS (2008)[1]

UCERF 2: Uniform California Earthquake Rupture Forecast, Version 2 as developed by the 2007 WGCEP (WGCEP, 2008)[1]

UFSAR: Updated Final Safety Analysis Report

V_{S30}: A variable used in the NGA relationships for the average shear wave velocity from the ground surface to a depth of 30 m

$v(Z \geq z)$: A function used in PSHA calculations representing the annual frequency of exceedance

USGS: United States Geological Survey

WGCEP: Working Group(s) on California Earthquake Probabilities

WEIGHTS: A weight as used in this report is a number between zero and one assigned to a branch of logic trees in such a way that the sum of the weights assigned to the branches associated with any single branching point (a point from which all the branches under considerations are shown) is one. A weight assigned to a branch usually represents the assigner's or assigners' combined judgment regarding how that branch should be counted with respect to the other branches associated with that branching point in the analysis of the probabilistic model represented by the entire logic tree.

Z: A variable used in PSHA calculations representing the ground motion parameters peak ground acceleration (PGA) and spectral acceleration (SA)

z: A variable used in PSHA calculations representing a specified ground motion parameter threshold

$Z_{1.0}$: A variable used in the NGA relationships for the approximate depth to 1.0 km/s shear wave velocity material

$Z_{2.5}$: A variable used in the NGA relationships for the approximate depth to 2.5 km/s shear wave velocity material

[1] Citation contained in Section 5.0 References

APPENDIX A
SEISMIC SOURCE CHARACTERIZATION

APPENDIX A OUTLINE

APPENDIX A

SEISMIC SOURCE CHARACTERIZATION

A1.0 INTRODUCTION

This Appendix provides additional background information to support the judgments regarding the weights assigned to the alternative strike-slip and blind thrust end-member seismic source characterization models discussed in Section 2.0 of the main report. Brief summaries of key seismic hazard assessments that have been conducted specifically for the SONGS Units 2 and 3 and of the current community seismic source characterization model are given in Section A-2. Section A-3 outlines the geologic and tectonic setting and history of the study region. Sections A-4 and A-5 provide additional discussion of the data and studies supporting the strike-slip fault source model (NI/RC as the primary fault source) and the blind thrust fault source model (OBT as the primary fault source), respectively. The following three Attachments are included in this Appendix and provide additional background information:

A-1 Annotated Bibliographies, which contain abstract summaries of selected references.

A-2 Seismic Source Characterization of Onshore RC Fault by Dr. Thomas Rockwell of San Diego State University.

A-3 Seismic Source Characteristics of Inner California Borderland's Blind Thrust Fault Systems by Dr. John Shaw and Dr. Andreas Plesch of Harvard University.

A2.0 CHRONOLOGY OF PREVIOUS RELEVANT SEISMIC HAZARD ASSESSMENTS

During the 1970s and early 1980s, SCE, with the assistance of firms such as Dames & Moore, Fugro, Western Geophysical, Woodward-Clyde Consultants, and several independent consultants completed rigorous onshore and offshore investigations to identify and characterize nearby fault sources and to evaluate their impact on potential earthquake ground motion and tsunami hazards for licensing SONGS Units 2 and 3 (SCE, UFSAR). During these SCE licensing investigations, what was referred to then as the Offshore Zone of Deformation (OZD), was part of a system of faults that included the onshore NI to the north, the offshore South Coast Offshore Zone of Deformation (SCOZD) in the middle, and the RC Fault to the south as illustrated on Figure A-1a. The SCOZD, the closest of these OZD source faults, is located offshore about 8 km southwest of SONGS. This system of faults was identified as the controlling earthquake source in the deterministic assessment of earthquake ground motions completed at that time.

The Cristianitos Fault, which is the closest mapped fault (refer to Figures A-1a, b, and c), is exposed in the sea cliff 915 m southeast of SONGS. Based on this exposure, the Cristianitos Fault was found by SCE (UFSAR) and Shlemon (1987) to have not displaced a 125 ka old marine terrace platform. Therefore, the Cristianitos Fault was not considered to be a fault source in the licensing earthquake ground motion assessment (SCE, UFSAR).

Other fault sources considered during the licensing of Units 1 and 2 to be capable of producing significant earthquake ground motions at SONGS included the onshore San Andreas, San Jacinto, and the Elsinore fault zones, and the offshore Palos Verdes, Coronado Banks, Santa Catalina, San Diego Trough, and San Clement faults, as illustrated in Figures A-1a and b.

An updated seismic hazard assessment was conducted by SCE in 1995, with the assistance of Geomatrix Consultants, Risk Engineering, and Woodward-Clyde Consultants. During the 1995 PSHA (SCE, 1995), offshore and onshore data relevant to the OZD, in particular the SCOZD, that had become available since the preparation of the SCE UFSAR, were evaluated. The results of a PSHA, which was completed in this study, also showed that the NI, the SCOZD, and the RC fault sources were the controlling sources for seismic hazard at SONGS.

In 2001, with the assistance of Fugro West, Geomatrix Consultants, and GeoPentech, SCE completed a re-assessment of the seismic source characteristics of the NI/SCOZD/RC and conducted a PSHA that specifically addressed the newly postulated blind fault sources in the vicinity of SONGS. Alternative source characterizations for this 2001 seismic hazard analysis were developed to capture the range of plausible fault geometries and interactions between postulated thrusts, including the OBT (Rivero et al., 2000) and the San Joaquin Hills Blind Fault (SJBF) (Grant et al., 1999 and 2000), and strike-slip faults, including the NI/SCOZD/RC faults. Analysis of geodetic GPS data conducted as part of this assessment showed relative motion more consistent with north-northwest shear with little or no convergence across the ICB Province, or evidence of a regional “driving” force that would reactivate a large seismogenic thrust fault (SCE, 2001; Hanson et al., 2002; Moriwaki et al., 2002). Quaternary slip rates assigned to offshore blind thrust fault sources were modified from postulated higher long-term post-Pliocene slip rates (Rivero et al., 2000) to reflect constraints provided by the geodetic data and coastal marine terrace uplift rates.

UCERF 2, which was published by the 2007 WGCEP in 2008, represents the USGS current seismic source model for the southern California region. UCERF 2 primarily updated the state of knowledge on the southern California portion of the San Andreas Fault and the San Jacinto and Elsinore faults over what had previously been reported by a WGCEP in 1995. Postulated onshore blind thrust faults, such as the SJBF (Grant et al., 1999) were included in UCERF 2. However, postulated blind thrust faults in the ICB Province are not included in the source model used in UCERF 2, but were flagged by the authors of UCERF 2 as potential sources for future consideration.

There is ongoing debate within the technical community (e.g., Rivero and Shaw, 2001; Grant et al., 2002; Grant and Rockwell, 2002; Rivero, 2004; Grant and Shearer, 2004; Rivero and Shaw, 2005; Ryan et al., 2009; Sorlien et al., 2009b; Rentz, 2010; Rivero and Shaw, 2010, in press; and many others) as to whether high-angle strike-slip faults or low angle reverse or thrust faults are the primary tectonic structures or faults accommodating the crustal motions in the vicinity of SONGS. The present study utilizes two end-member tectonic structural models (referred to as the strike-slip and blind thrust system models) to facilitate the characterization of the closest offshore faults that have been demonstrated to dominate the earthquake shaking hazard for SONGS. UCERF 2 was selected as the basis or reference for one end-member model because it represents the most recent technical community’s consensus seismic source characterization model for California faults. In this strike-slip end-member model, the NI/RC Fault Zone is characterized as the closest, active, primary strike-slip fault to SONGS. The source parameters from UCERF 2 used to characterize the NI/RC Fault Zone in the USGS (2008) and USGS (2009, PC) seismic hazard mapping studies are used in this study. For the blind thrust end-member model, the OBT is characterized as the primary contributing seismic source for SONGS. The OBT is included in the CFM (Plesch et al., 2007) and is identified in UCERF 2 as a potential fault source that should be given future consideration.

A3.0 TECTONIC AND GEOLOGIC SETTING

Southern California is divided into several physiographic regions, or provinces based on the makeup of their geologic and tectonic characteristics. Refer to Figure 2-1 in the main portion of this report and Figures A-2a, b, c, and d for the location of these provinces relative to SONGS and illustrations of their long and complex tectonic evolution. SONGS is located in the Peninsular Ranges Province, just east of its boundary with the ICB Province and to the south of the Transverse Ranges Province.

A summary of the geologic and tectonic characteristics of these physiographic provinces (Section A3.1) and a tectonic history that outlines the development of their key geologic and tectonic structures (Section A3.2 and Figures A-2a, b, c, and d) provide additional perspectives on the relationships between strike-slip and thrust faults in the region.

A3.1 Physiographic Provinces in the Study Region

As seen on Figure A-2a, the Peninsular Ranges Province extends from Colorado Desert Province in Coachella/Imperial Valley on the east, well into Baja California on the south, and to the Transverse Ranges Province on the north. To the west, the ICB Province is almost entirely offshore, including Santa Catalina and San Clemente Islands. This province also includes the Palos Verdes Peninsula and the western portion of the Los Angeles (LA) Basin. Similar to the Peninsular Ranges Province, the ICB Province is also bounded on the north by the Transverse Ranges Province and also extends to the south offshore of Baja California. The Outer Continental Borderland Province (MMS, 2001 and Crouch and Suppe, 1993) bounds the ICB Province on the west.

The Peninsular Ranges and ICB provinces are dominated by northwest-southeast trending mountain ranges and intervening basins that extend from within Baja California to the southern border of the Transverse Ranges Province (CGS, 2002b). The Transverse Ranges province is dominated by east-west trending mountain ranges and intervening basins that extend from the Twenty-Nine Palms/Palm Springs area on the east to offshore of Point Conception and the Channel Islands on the west. The basins and ranges in the Peninsular Ranges, ICB, and Transverse Ranges Provinces are commonly separated by fault zones that trend parallel to the ranges and valleys. The LA Basin, located at the juncture of these three physiographic provinces, includes faults and folds with differing orientations resulting from the complex interaction between the northwest-trending Peninsular Ranges and ICB Provinces and the east-west-trending Transverse Ranges Provinces.

As mentioned above, the physiography of both the ICB and the Peninsular Ranges provinces are composed of generally similar northwest-oriented faulted ridges and basins, with relatively steep slopes on the flanks of the uplifted ridges. However, there are distinct differences between the ICB and Peninsular Ranges provinces in their underlying basement rock composition and their structural relief their overlying sedimentary rocks, which suggest that it is appropriate to keep these two provinces separated. The ICB Province is underlain by the Catalina Schist basement rock complex and the Peninsular Ranges Province is underlain by a batholithic and older basement rock complex, as illustrated on Figures A-2c and A-2d. The ICB Province is bounded on the east by the NI/RC Fault Zone near the coast. The East Santa Cruz Basin Fault bounds the ICB Province on the west. The Peninsular Ranges

Province is bound on the west by the NI/RC Fault Zone and on the east by the Coachella and Imperial valleys with their San Andreas Fault System (refer to Figures A-2a and A-3).

A3.2 Tectonic History of the Inner Continental Borderland and Transverse Ranges

Southern California's current complex tectonic and geologic setting resulted from a long and complicated history in crustal plate interaction that has culminated in today's San Andreas Fault being the dominate player in the predominate right-lateral strike-slip boundary between the Pacific and North American crustal plates (Figures A-2b and 2c) (Atwater, 1998; Nicholson et al., 1994; Bohannon and Geist, 1998; Fisher 2009; and Fisher et al., 2009a). This complex deformational history and resulting tectonic setting form the basis for interpreting the stratigraphy, faults and folds, and present seismotectonic setting of the Peninsular Ranges and ICB provinces in the area around SONGS. Essentially, there have been three different phases of the crustal deformation, each with a distinct style and pattern of deformation and resulting geology.

A3.2.1 Phase 1 - Collision and Subduction

In the Cretaceous and early Tertiary, the western side of the Continental Borderland was a convergent (subduction) plate boundary (Figure A-2b). During Cretaceous and Paleogene time (>24 Ma), the oceanic Farallon plate was subducting beneath the continental crust of western North America, resulting in a continental margin arc-trench system. The subduction-related geology of California, when reconstructed, includes the Sierra Nevada granitic batholith that formed the roots of a magmatic arc, the metamorphic rocks along the arc front that form the foothills belt of the Sierra Nevada, the Great Valley Sequence of marine sedimentary rocks formed in the submarine fore-arc basin, the Coast Range ophiolite that was the oceanic floor of the fore-arc basin, and the Franciscan complex of accreted terrain metamorphic rocks formed in the accretionary wedge at the subduction front. These major geologic units are still recognizable in southern California, but, as illustrated on Figures A-2c and 2d, they have been broken up and re-organized by subsequent tectonic events (Atwater, 1998; Nicholson et al., 1994; Bohannon and Geist, 1998; Fischer, 2009; and Fisher et al., 2009a).

A3.2.2 Phase 2 - Oblique Extension

Beginning in the late Oligocene and early Miocene (17 to 24 Ma), subduction gradually ceased along the western margin of North America when the East Pacific Rise (source of the Farallon and Pacific Plates) encountered the continental margin and, along with the Farallon Plate, was, in turn, subducted beneath North America (Figure A-2b). A new plate boundary configuration resulted with the Pacific Plate in direct contact with the North American Plate along the strike-slip San Andreas Fault. The relative motion between the Pacific and North American Plates was no longer convergent, but rather largely right-lateral translational in nature.

During the Miocene (5 to 24 Ma), various crustal blocks along the North American margin became attached to the northward-moving Pacific Plate (Atwater, 1998). This microplate capture led to extensional deformation of the upper plate of the subduction zone, rotation and translation of large crustal blocks, normal faulting, widespread Middle Miocene Volcanism, and a zone of oblique extension (transtension) in the Borderland (Kamerling and Luyendyk, 1979 and 1985; Wright, 1991; Nicholson et al., 1994; Fisher, 2009; and Fisher et al., 2009a). This oblique extension continued into the middle Pliocene (~4 Ma) and caused extensive ridge and basin (horst and graben) morphology (similar to block faulting in the Basin and Range Province) to occur in the ICB. This formed many of the generally northwest-trending basins and ridges of the ICB that are apparent today.

As schematically illustrated by Nicholson et al. (1994) in the sequence of maps shown on Figure A-2b, the western Transverse Ranges Province was one of these several captured rotating crustal blocks. These blocks, while simultaneously being translated northward, were also rotated as much as 90 to 110 degrees in a clockwise direction (also refer to Figure A-2c) forming the east-west trending, western portion of the Transverse Ranges Province (Kamerling and Luyendyk, 1985; Crouch and Suppe 1993; and Bohannon and Geist, 1998). As the Transverse Ranges Province moved northward and rotated into its present position and the transform plate boundary continued to develop along the eastern edge of the rotating block, significant extension occurred in the Los Angeles Basin and ICB Province resulting in rapid basin subsidence and sedimentation accumulation during the Miocene and early Pliocene. Approximately 4 to 5 Ma (during the early Pliocene), another reorientation of the plate boundary in southern California and northern Mexico occurred. The plate boundary south of the Borderland and west of Baja California migrated eastward, splitting Baja California and coastal southern California off from the rest of North America, attaching these crustal blocks to the Pacific Plate (Figure A-2b). Since that time (about 5 Ma), the relative plate motion vector between the North American and Pacific Plates has been oriented approximately N37°W (Cande et al., 1995; Atwater and Stock, 1998). The southern San Andreas Fault was the manifestation of this new shift eastward of the plate boundary in southern California. The southern San Andreas and the northern San Andreas are now connected through the well-known, large left restraining bend in the fault trace, (now referred to as the Mojave segment) thereby producing convergence across a wide area of the southern California, expressed most proximately in the Transverse Ranges Province (Clark et al., 1991; Wright, 1991; Schneider et al., 1996; Sorlien et al., 1999; and Seeber and Sorlien, 2000).

Thus, overall, the tectonic setting in this portion of southern California changed in the Pliocene from predominately transtensional to predominately transpressional. The increased convergence commonly resulted in diversely-striking Miocene normal faults being reactivated as reverse faults, and inversion of half-graben basins into anticlines (Yeats, 1987; Clark et al., 1991; Seeber and Sorlien, 2000). Significant transpression occurred across the newly-developing Transverse Ranges and portions of the LA Basin on numerous oblique reverse and blind faults, many of which are inverted normal faults (Pasadenan orogeny). Large scale, rapid uplift of crustal blocks north of the LA Basin occurred concurrently with gradual uplift of the Palos Verdes Peninsula and the San Joaquin Hills, and subsidence and rapid sedimentation in the LA Basin (Wright, 1991).

A3.2.3 Phase 3 - Transform Plate Boundary (Present)

The present-day Pacific-North American Plate boundary south of the Transverse Ranges Province in southern California is dominated by a broad zone of distributed right-lateral strike-slip motion. This motion affects an area extending from the San Andreas Fault in the east to the offshore San Clemente Fault in the west (Figure A-1a).

Various studies have estimated that approximately 48 to 52 millimeters per year (mm/yr) of right-lateral shear occurs across southern California (Bennett et al., 1996; DeMets and Dixon, 1999). The San Andreas Fault and several other strike-slip fault zones accommodate most of the slip across the plate boundary (Jennings, 1994; Petersen et al., 1996). The Eastern California Shear Zone (east of San Andreas Fault) is believed to accommodate about 10 mm/yr of right-lateral slip (Bennett et al., 1996). The slip rate on the San Andreas Fault is variable, but ranges from about 10 to 35 mm/yr in southern California. The most recent information from paleoseismic studies suggests that the San Jacinto Fault has a slip rate of about 15 to 20 mm/yr (C. Kendrick, USGS, 2007, PC), which exceeds the 12 mm/yr reported by the CGS and the SCEC. Geologic data suggest that the Whittier-Elsinore, NI onshore, and Palos Verdes faults have slip rates of about 5, 1, and 3 mm/yr, respectively (Cao et al., 2003).

Quaternary to Holocene offsets on the major fault zones within the Continental Borderland are interpreted to be primarily right-lateral strike-slip faults with a lesser vertical slip component, commonly referred to as oblique-slip faults. The San Pedro Basin Fault and the San Clemente Fault are two of the most active faults in the Borderland, but their slip-rates are largely unknown. Based on regional slip budgets and offsets of Miocene volcanic rocks, estimates of the slip-rates of the key faults in the ICB are as follows: the San Pedro Basin Fault has a slip-rate of 1 to 2 mm/yr and individual splays of the San Clemente Fault Zone (including the Santa Cruz-Catalina Ridge and Pilgrim Banks-Santa Barbara Island faults) have slip-rates of 1 to 4 mm/yr. GPS observations between 1986 and 1995 indicate that the total relative slip between the North American and Pacific plates is 49 ± 3mm/yr. The estimated total relative slip-rate between the North American and Pacific Plates is reported by DeMets and Dixon (1999) to be about 52 mm/yr. While there are no permanent GPS stations on the eastern edge of the Pacific Plate, stations on Santa Catalina, San Clemente and San Nicolas Islands have shown 45.5, 47.5 and 48.5 mm/yr of slip with respect to stable North America, respectively (SOPAC, 2010). As shown in Figure A-3, the station on San Clemente Island, ***scip,*** is moving at a rate of 6 mm/yr with an azimuth of 41 degrees west of north relative to station, ***scms,*** in San Clemente (11 miles northeast of SONGS). These GPS velocities would suggest that the upper limit of postulated slip-rates for the offshore right-lateral strike-slip faults is slightly overestimated.

Using this more regional perspective and stepping closer to the area surrounding SONGS, two end models were utilized to facilitate the characterization of the closest offshore faults that have been demonstrated to dominate the seismic shaking hazard for SONGS. In this regard, UCERF 2 was selected as the basis for reference because it represents the most recent regionally documented seismic source characterization for California faults. Therefore, for the first end-member model, the NI/RC Fault Zone was selected because it was the only UCERF 2 model utilized by the USGS (2008) and USGS (2009, PC) in developing the seismic hazard maps for the building code that applies to the area near SONGS. Similarly, the other end-member model selected was the OBT because of its postulated ability to generate large magnitude earthquakes on a fault plane that was proposed to extend eastward, under the coastline and beneath SONGS.

A4.0 DATA AND OBSERVATIONS SUPPORTING THE NI/RC AS THE PRIMARY FAULT SOURCE

This section provides more detailed discussion of the available and relevant structural, geomorphology, paleoseismicity, seismology and GPS information that have been used to identify and characterize the NI/RC Fault Zone as a predominantly high-angle, right-lateral, strike-slip fault. The NI/RC Fault Zone is the closest primary seismic source fault to SONGS in the strike-slip end-member seismic source model included in this 2010 PSHA. Attachment A-2 presents Dr. Tom Rockwell's summary of current information concerning the NI/RC Fault Zone.

A4.1 Geometry and Structural Analyses

The geometry of a fault, as well as its flanking lithology, provide the geologic and tectonic structural information for estimating how that fault will rupture in the future; this information in turn is needed to model the resulting earthquake ground motions that will impact facilities, such as SONGS. In addition to geometry and structural geologic information about the San Andreas Fault and other active strike-slip faults in the world, subsurface data from the oil fields under the LA Basin along the onshore NI portion of the NI/RC Fault Zone lead to the development of the classic theory of wrench fault tectonics (Moody and Hill, 1956; Wilcox et al., 1973; Harding, 1973; Yeats, 1973; Barrows, 1974; Harding 1985). In simplistic terms, as illustrated on Figure A-4a, the primary principal behind wrench fault theory is that, as high-angle, crustal-through-going, strike-slip faults progressively propagate through overlying more recently deposited sediments, they initially form a broad, near-surface zone of subsidiary faults in a flower-like pattern (refer to Figure A-4b). The orientation of these subsidiary faults is at oblique angles to the primary strike-slip fault and the direction of crustal deformation. These conjugate subsidiary faults vary in their geometry and style of faulting (i.e., normal, reverse, thrust, strike-slip, or oblique-slip) depending on their orientations relative to the strike and dip of the primary strike-slip fault. As the displacement of these more recently deposited sediments increases, the broad, flower-like pattern progressively narrows into the primary trace of the fault. The subsidiary fault patterns are most prominent in en echelon step-overs or bends in the trace of the primary, high-angle, strike-slip fault. As illustrated on Figures A-4a and A-4b, for right-lateral strike-slip faults right step-overs produce localized zones of tension expressed in subsiding blocks bracketed by normal or transtensional oblique slip faults. Examples of the en echelon right step-overs along the NI/RC Fault Zone are the subsiding San Diego Bay and Bolsa Chica and Anaheim Bay wetlands. Left step-overs produce localized zones of compression expressed in rising blocks bracketed by thrust, reverse, or transpressional oblique slip faults. Examples of these left step-overs along the NI/RC Fault Zone are Mount Soledad, Signal Hill, Domingues Hills, and Baldwin Hills.

SCE (UFSAR), with the assistance of Woodward-Clyde Consultants (1980), completed a thorough re-analysis of the oil well records and available geologic data from the oil fields between Newport Beach and Westwood (an example is provided on Figure A-5). This independent assessment concluded that the oil field data supported the wrench fault model and that a high-angle, right-lateral strike-slip fault dominated by the NI Fault Zone, and estimated that the long term slip rate on the fault was about 0.5 mm/yr. More recent work in examining oil well and groundwater well data from western Los Angeles County by Dr. Dan Ponti of the USGS (2010, PC) further supports the dominance of the high-angle strike-slip fault in the NI Fault Zone as illustrated in Figure A-6.

Data supporting the characteristics of the offshore part of the NI/RC Fault Zone are more limited. The continuity of the NI/RC Fault Zone, between its southern onshore trace near La Jolla and its onshore traces north of Newport Beach was first suggested by Moore (1972). SCE (UFSAR), through Western Geophysical Company, completed rigorous offshore marine seismic reflection surveys to assess potential faulting offshore of SONGS (Western Geophysical Company, 1972). Track lines of these surveys and their interpreted faults are shown on Figure A-7a. This offshore work supported the conclusion that the closest primary seismic source fault to SONGS is the offshore continuation of the high-angle, right-lateral, strike-slip NI/RC Fault Zone, whose characteristics are reflected in the wrench fault style of tectonics present in the northern and southern onshore portions of the fault zone.

Little has changed in the geoscience community's overall assessment of the NI/RC Fault Zone characterization as a strike-slip fault zone since the SCE's original investigations were completed. Some refinements were made in the mapped offshore traces of the faults by Fischer and Mills (1991) (Figure A-7b); Ryan et al. (2009) (Figure A-7c); Sorlien et al. (2009b) (Figure A-7d); and Conrad et al. (2010) (Figure A-7e). Figure A-7f illustrates a map containing the USGS (2009) Quaternary Fault and Fold

Database in the ICB. The changes in the NI/RC Fault Zone's seismic characteristics by Fischer and Mills (1991) were incorporated in the source models used in SCE (1995 and 2001) and those by Ryan et al. (2009), Sorlien et al. (2009b), and Conrad et al. (2010) were considered in this PSHA. Other research, including Grant and Shearer (2004), Fisher (2009), Fisher et al. (2009a), Fisher et al. (2009b), Lee et al. (2009), Rockwell (2010a and 2010c), proprietary work completed by Fugro, Inc., and work currently underway by Dr. Dan Ponti of the USGS along the onshore NI Fault and its subsidiary traces north of Long Beach, further supports the weights assigned herein to a high-angle, strike-slip characterization of the NI/RC Fault Zone as the closest primary source fault to SONGS in the strike-slip end-member model incorporated into this PSHA.

Most notable of this more recent research is the work completed by Ryan et.al. (2009), which essentially is an independent assessment of the available data reviewed during SCE's earlier work (Western Geophysical Company, 1972) on the characteristics of the faults located offshore of SONGS. Some of the proprietary marine geophysical survey data recently obtained by the USGS from WesternGeco and used by Ryan et al. (2009) was purchased by SCE years ago. Ryan (2010, PC) indicated that the results of the USGS's independent assessment of the data are in general agreement with the results of SCE's previous investigations and analysis of the faulting off-shore of SONGS, as seen by comparing Figure A-7a and A-7c.

USGS (2009) considers the NI/RC Fault Zone to be a primary, high-angle, right-lateral, strike-slip seismic source fault, with relatively minor alternatives to its most northern on-shore geometry.

A4.2 Evidence for Activity

A4.2.1 Paleoseismicity

The results of the SCE (UFSAR) (Woodward-Clyde) analysis of the oil field data (see example on Figure A-5 from Freeman et al., 1992) showed that, although the quality of the data varied between the different oil fields, the best fit of that data indicated about 0.5 mm/yr of strike-slip displacement across the main trace of the NI Fault. Slip rate estimates for the northern on-shore part of the NI/RC Fault Zone have been made by Fischer and Mills (1991), Freeman et al. (1992), Law/Crandall, Inc. (1993), Shlemon et al. (1995), Grant et al. (1997), and Franzen and Elliott (1998). In combination, these estimates suggest a wide range in slip-rate between 0.4 to 3.0 mm/yr for the onshore RC segment. More thorough and extensive paleoseismic investigations conducted by Lindvall and Rockwell (1995) and Rockwell (2010a and 2010c) support seismic source characteristics assigned to the southern onshore portion of the NI/RC Fault Zone in the San Diego area (summarized in Attachment A-2). Detailed 3D fault trenching in that work further supports the dominate high-angle, right-lateral, strike-slip style of faulting along the NI/RC Fault Zone with slip-rates estimated to be between 1.5 and 2.5 mm/yr. Offshore the paleoseismic data along the NI/RC Fault Zone has been more limited. Fischer and Mills (1991), based on their re-assessment of seismic reflection data available at that time, estimated a slip-rate of about 0.8 mm/yr, but were careful to qualify their estimate based on the limitations of their available data. Recent, high resolution marine geophysical surveys, like the USGS (Conrad et al., 2010) survey over the San Diego Trough Fault and the Rentz (2010) survey off the coast over the inner shelf between Dana Point and Carlsbad (refer to Figure A-8a), are providing more useable data to assess the paleoseismic record beneath the ICB.

High-resolution seismic data on the inner shelf has been used to constrain the recency of displacement on the Cristianitos Fault. Using this data, which is illustrated on Figure 8b, Rentz (2010) notes that what subtle surface relief is observed locally on the inner shelf is of eroded, partially buried, bedrock remnants of "…adjacent geologic formations with different erosive properties." As Rentz (2010) suggests, "this differential erosion may be responsible for the trend of the San Mateo promontory, the highstand relief in the seismic profiles, and the ~9.6 km wide shelf," off of the coast between Dana Point and Carlsbad. Further, they conclude that in the area of their survey, "There is no observed offset of the overlying Holocene sediment packages, which would be expected if deformation was ongoing"; further supporting the SCE (UFSAR) conclusion that the Cristianitos Fault is inactive.

A4.2.2 Geomorphology

The geomorphology along the onshore parts of the NI/RC Fault Zone clearly supports the dominance of a high-angle strike-slip fault. As Dr. Rockwell presents in more detail in Attachment A-2, displaced stream channels in RC Fault are predominately offset right-laterally. Although the location and geomorphology defined by the NI/RC Fault Zone is less obvious in other parts of San Diego due to urban development, Dr. Rockwell presents in Attachment A-2, a late 19th century cartographer's sketch that shows a linear topographic lineament, which correlates with the present known location of the NI/RC Fault Zone. The pattern of this lineament across San Diego's hilly terrain supports the presence of an active near-vertical, right-lateral fault plane along this trace of the NI/RC Fault Zone.

The linear surface trace of the NI/RC Fault Zone through the western part of the LA Basin, particularly between Newport Beach and Long Beach, and the presence of localized uplifted hills and plateaus and intervening subsiding lowlands and wetlands is consistent with the presence of an underlying strike-slip dominated wrench fault system.

Between Newport Beach and La Jolla, the onshore geomorphology is characterized by a flight of emergent marine terraces (Figure A-9). The relatively uniform altitude of these surfaces suggests uniform uplift that does not appear to be consistent with the varying dips and long-term rates of slip postulated for the OBT. The sequence of emergent marine terraces have been mapped and described by Shlemon (1978), Kern and Rockwell (1992), Lajoie et al. (1992), and Grant et al. (1999) (refer to Figure A-9). Dating of the emergent MIS 5e/5a marine terraces at 125/80 ka by these authors, suggests regionally uniform coast uplift at a rate of about 0.13 to 0.14 mm/yr. Along the coastal San Joaquin Hills, the uplift rate may be as high as 0.21 to 0.27 mm/yr (Grant et al., 1999).

The presence and regionally persistent elevations of these onshore marine terraces, which are subparallel with the trend of the NI/RC Fault Zone, are more in concert with a nearby strike-slip faulting rather than a regionally persistent underlying thrust fault with changing dip angles, as proposed by Rivero et al. (2000) and Rivero (2004). As suggested by Mueller et al. (2009), the uniform uplift of these late Pleistocene uplifted marine terraces is more likely tied to regional tilting or "flexure of the crust driven largely by heating and thinning of the upper mantle beneath the Gulf of California and eastern Peninsular Ranges." Locally, this regional uplift is amplified by transpressional bends and en echelon step overs in the NI/RC Fault Zone leading to the higher uplift rates such as those tied of the San Joaquin Hills (Grant et al., 1999, 2000, and 2002) and Mount Soledad (Rockwell, 2010).

A relatively low-relief offshore continental shelf and the consistent 400-foot depth of its shelf break, is evident in the bathymetry extending along the coast between Palos Verde Peninsula to the Mexican Border, as illustrated in Figure A-10. This geomorphology also is inconsistent with a regionally persistent underlying thrust fault with changing dip angles, as proposed by Rivero et al. (2000) and Rivero (2004).

This uniform low-relief surface, which correlates to the last glacial maximum sea level low-stand at approximately 19 to 21 ka, is more consistent with a through-going strike-slip fault, such as the NI/RC.

Recent marine geophysical surveys along this shelf by Rentz (2010) are consistent with this conclusion by associating the wider shelf offshore between Dana Point and Carlsbad Canyon, in contrast to the width of the rest of the self between Newport Beach and Dana Point and between Carlsbad Canyon and La Jolla, to more erosion resistant bedrock formations. However, agreeing that the width of the shelf is at least in part is controlled by erosion patterns, based on new multibeam data acquired by the USGS in November 2010, Dr. Ryan (2010, PC) notes that there are major changes in erosion patterns across the San Mateo Point area and suggest that the San Mateo fold and thrust belt, located to the west of the NI/RC Fault Zone, does contributes to the shelf width. She also noted that the shelf morphology would be primarily controlled by sea level cycles, especially considering the low slip rate estimates for the offshore reverse and thrust faults.

A4.2.3 Seismology

Seismology data from the ICB, as a tool to help resolve the location and geometry of faults in this province, has limitations due to the paucity of nearby stations, limited azimuthal coverage, and uncertainties in the underlying velocity structure. Recognizing these limitations, Astiz and Shearer (2000) used improved methods to refine the locations of earthquakes that occurred in the Borderland between 1981 and 1997. Rivero et al. (2000) and Rivero (2004) utilized Astiz and Shearer (2000), in particular the 1986 M_L 5.3 Oceanside Earthquake, to support the offshore thrust fault models as discussed below in Section A-5.

Grant and Shearer (2004) also re-analyzed the 1981 M <3.0 cluster of earthquakes located about 10 km northwest of Oceanside and a 2,000 cluster of seismic events offshore of Newport Beach (refer to Figure A-11). Their work, especially the analysis of earthquakes northwest of Oceanside, supports a high-angle fault plane at depths of 12.5 to 13 km, This orientation of hypocenters and the their depth suggest the presence of a deep-rooted, high-angle, strike-slip fault (i.e., the NI/RC Fault Zone), rather than a low-angle reverse or thrust fault (i.e., the OBT). This supports the high-angle, strike-slip, end-member model containing the NI/RC Fault Zone as the closest primary seismic source fault to SONGS.

The 2,000 cluster of earthquakes offshore of Newport Beach also indicate a high-angle fault, such as the NI/RC Fault Zone, but this cluster is located west of the surface trace of the NI/RC Fault Zone and occurs at a depth of 6.5 to 7 km. The shallow depth of these earthquakes, however, does not preclude the possible presence of a seismogenic thrust fault plane passing beneath the high-angle structure.

Marrying the epicenter data from the M 5.3, 1986 Oceanside Earthquake with the new trace of the San Diego Trough Fault, recently re-located by new USGS offshore marine geophysical surveys (Conrad et al., 2010 and Ryan, 2010, PC) is in contrast with the thrust mechanism of that event being correlated with the Thirtymile Bank Blind Thrust (TMBT) as suggested by Rivero et al. (2000) and Rivero (2004). As seen on Figure A-12, the Oceanside event occurred near the San Diego Trough Fault at a left bend in that fault's trace. This relationship supports the occurrence of a thrust event within a high-angle, right-lateral, strike-slip fault system and not the occurrence of a thrust event on a regionally persistent underlying blind thrust fault.

A4.2.4 GPS

Clockwise rotation of crustal blocks in the ICB Province, suggested in SCE (2001), has been emphasized by Ryan et al. (2009). The rotating block proposed by Ryan et al. (2009) has been plotted along with geodetic data on Figure A-13 to qualitatively analyze whether geodetic data collected in southern California supports possible block rotation. Figure A-13 shows the best estimate of long-term velocities for permanent continuous GPS stations with respect to station ID ***scms*** in San Clemente. As shown on Figure A-13, stations in the southern portion of the Peninsula Range crustal block (shown in purple) appear to show slight clockwise rotation about the ***scms*** reference station. It is noted that the velocity vectors are presented in an exaggerated scale (1 inch equals 15 mm/yr) for effect. The tension and compression caused by this block rotation would likely lead to the reactivation of some portions of the Oceanside detachment as thrust faults and some portions as normal faults. Some portions would likely remain inactive, making it kinematically incompatible with the postulated through-going, regional thrust model. Conversely, Late Quaternary inactivity of the OBT fault offshore of Carlsbad and La Jolla, as suggested by Sorlien et al. (2009b), is consistent with this block rotation model.

Similarly, a qualitative analysis of geodetic data was prepared with respect to San Clemente Island as previously shown in Figure A-3. The visual trend of the relative velocities presented on Figure A-3 is in strong agreement with the strike-slip end-member seismic source characterization model for the ICB Province. It is noted that the velocities are presented in a smaller scale than in the previous figure (1 inch equals 5 mm/yr). In a qualitative sense, no tension or compression is observed in the relative velocities between Santa Catalina or San Clemente Islands and the Peninsula Range as would be expected in the blind thrust end-member model. The geodetic data (velocities and uncertainties) presented on Figures A-3 and A-13 are based on the public archive preserved by the Scripps Orbit and Permanent Array Center (SOPAC) and includes all permanent continuous GPS stations installed in southern California between 1995 and 2008 with at least 1.5 years of data collected.

A5.0 DATA AND OBSERVATIONS SUPPORTING THE OBT AS THE PRIMARY FAULT SOURCE

This section provides more detailed discussion of the available and relevant structural, geomorphology, paleoseismicity, seismology and GPS information that have been used to identify and characterize the OBT as the closest primary seismic source fault to SONGS. This summary is based primarily on Rivero (2004), Rivero and Shaw (2005), and Rivero and Shaw (2010, in press). Attachment A-3 presents Dr. John Shaw’s and Dr. Andreas Plesch’s assessment of the seismic source characteristics and current information concerning the OBT Fault based primarily on the work summarized in these publications. Figures A-14 through A-27 present illustrations supporting the data and observations described in this section of Appendix A. This information forms the basis for the blind thrust seismic source characterization end-member model used in the 2010 PHSA.

The OBT model is based on recognition of an extensive offshore low-angle fault by previous workers (Fischer and Mills, 1991; Crouch and Suppe, 1993; Rivero et al., 2000; Rivero and Shaw, 2010, in press). Rivero et al. (2000) first postulated that regional offshore thrust faults are primary, regional-scale active faults. These workers suggest that Mesozoic subduction zones (Phase 1) were reactivated as detachment surfaces during rotation of the Transverse Ranges in the Miocene (Phase 2), and that subsequent transpression in the Pliocene and Quaternary has resulted in structural inversion (Phase 3). According to Rivero et al. (2000) the OBT forms a regionally continuous fault extending from Laguna Beach to at least the US-Mexican Border. Fault rupture scenarios by Rivero et al. (2000) suggest the potential to generate large (M_W 7.1-7.6) earthquakes that would control seismic hazards in the adjacent coastal area.

These regionally extensive blind thrusts are inferred to interact at depth coevally with displaced high angle, strike-slip or oblique-slip faults, such as the NI/RC Fault Zone and the other high-angle, strike-slip faults in the ICB, which are illustrated in Figure A-14. This blind thrust system model was further developed and described by Rivero (2004), Rivero and Shaw (2005), and Rivero and Shaw (2010, in press). Figure 2-2 in the main text provides a copy of the CFM developed by Plesch et al. (2007), which illustrates the OBT and TMBT fault sources included in this alternative seismic source model. These postulated blind thrust fault sources were addressed in UCERF 2 (WGCEP, 2008) as being considered for future deformation model development, but they are not in the current USGS source characterization model (USGS, 2009, PC).

Utilizing available seismic data Rivero and Shaw (2010, in press) and Shaw and Plesch (Attachment A-3) characterized the blind thrust fault sources (i.e., the OBT and TMBT) and associated hanging wall and footwall subsidiary faults. Possible structural scenarios that represent potential interactions between the steeply-dipping strike-slip faults and the low-angle blind thrust fault sources are outlined in Figure A3-2. Steeply-dipping, right-lateral strike-slip faults, such as the NI and RC, are incorporated into Rivero's (2004) blind thrust seismic source characterization model as highly segmented and offset faults under the argument that continuous, through-going, strike-slip faults, as primary fault sources are not kinematically compatible with the several km of shortening documented on the OBT Fault.

The key data and analyses that Rivero (2004), Rivero and Shaw (2005), and Rivero and Shaw (2010, in press) present in support of the OBT as a primary regional-scale active blind thrust are discussed in the following sections.

A5.1 Geometry and Structural Analysis

A5.1.1 Geometry

The geometry and style of faulting associated with the OBT are less well understood than for many other faults in southern California. Until recently, studies of blind faults and large oblique reverse faults in southern California focused primarily on the Transverse Ranges Province and the LA Basin where higher rates of contractional strain were expected. The work of Shaw and Suppe (1996) identified the Compton blind thrust as part of an active regional fault bend fold system in the western LA Basin. The OBT may be inferred to be an analog and possible extension of this system further to the southeast into the ICB Province. Although the offshore setting of the ICB Province poses challenges to the identification and characterization of blind thrust faults, the Oceanside detachment surface that is interpreted to be the OBT is clearly imaged in many offshore seismic reflection profiles.

The prominent reflector in the seismic data, now interpreted to be the OBT, originally was mapped by Western Geophysical Company (1972). Western Geophysical mapped a regional unconformity or disconformity at the top of acoustical basement, and mapped faults in 'cover sediments' offsetting upper Miocene strata above this surface (Figure A-7a). Subsequent studies described the regional disconformity as an extensional breakaway detachment fault surface (Figure A-2a-d), and identified it throughout much of the ICB Province (e.g., Crouch and Suppe, 1993 and Bohannon and Geist, 1998). The exposed detachment surface became an erosional unconformity that was subsequently covered by Miocene and younger sediments.

Rivero (2004) presents a detailed map (Figure 2-6) showing the locations of seismic profile data used to constrain the location and geometry of the OBT as developed by Rivero et al. (2000) and described by Rivero and Shaw (2005), and Rivero and Shaw (2010, in press). More than 10,000 km of industry seismic reflection profiles, well data, seismicity, and seafloor geologic maps were analyzed. The structural analysis employed kinematic and forward modeling techniques based on quantitative structural relationships between fold shape and fault geometry (Suppe, 1983; Suppe and Medwedeff, 1990; Mount et al., 1990; Erslev, 1991; and Almendinger, 1998). Advanced three–dimensional modeling techniques were used to generate full representations of fault surfaces and key stratigraphic markers. The lateral extent and geometric segmentation of the active blind–thrust ramps were determined by mapping of direct fault plane reflections and associated fold trends throughout the basin areas covered by the seismic grid. The three–dimensional modeling also was used to quantify the distribution of dip slip on the active fault system, and to further constrain the geometrical analysis (Rivero, 2004).

The geometry of the two segments of the OBT as represented in the CFM (Plesch et al., 2007), which is used to characterize the OBT for this study, therefore, is based on a systematic and comprehensive analysis of offshore deep seismic reflection data.

The geometry of the OBT as mapped by Rivero and Shaw consists of two segments of differing sizes and dips. The OBT has been mapped over an area of more than 1800 km^2, and extends to the south beyond the mapped limits of the fault at the US-Mexican Border. The northern segment averages 14 degree dip, and the southern segment averages 25 degree dip (Rivero et al., 2000). The geometry of the OBT is described in greater detail in Attachment A-3 and Rivero (2004).

A5.1.2 Structural Analysis

Rivero (2004) presents a comprehensive structural analysis of faults in the ICB, focusing on the tectonic reactivation of the Oceanside and Thirtymile detachments as blind–thrust faults. As an outgrowth of the studies presented in Rivero et al. (2000), this analysis generated more precise three–dimensional representations of the faults and estimates of long–term slip rates. More advanced three–dimensional modeling techniques and fault–related fold theories were employed to identify and to describe active blind–thrust faulting and folding induced by the reactivation of the OBT and the TMBT in the Dana Point, Carlsbad and TMBT regions. Over 10,000 km of industry seismic reflection profiles, well data, seismicity, and geologic maps were used. Rivero (2004) performed kinematic and forward modeling structural analysis techniques based on quantitative structural relationships between fold shape and fault geometry. He also used advanced 3D modeling techniques to generate full representations of fault surfaces and key stratigraphic horizons, and provided evidence for present day strain partitioning produced by the interaction of the low-angle thrusts and vertical strike-slip faults (Figures A-16, A-18 through A-20, A-22, and A-26).

The structural analysis led Rivero and Shaw to postulate Pliocene and Quaternary oblique compression and structural reactivation processes as the originating mechanism of the regional blind–thrust fault system (Rivero and Shaw, 2010, in press). This reactivation generated regional structural wedges cored by faulted basement blocks that inverted sedimentary basins (Figures A-15 and A-16) in the hanging wall of the Miocene detachments (Rivero, 2004). The Miocene detachment break-away zone and Pliocene through Quaternary reactivated blind thrust, as well as emergent thrust faults such as the San Onofre Thrust, located in the hanging wall of the OBT, were mapped (Figures A-17 through A-20). From these results, earthquake scenarios based on the structural interaction of active blind–thrust faults and major strike–slip faults were developed for the ICB Province (see discussion in Attachment A-3). By defining new long–term slip rates, Rivero (2004) concluded that simple and complex earthquake sources could produce large earthquakes (M 7.0 to M 7.6) with recurrence intervals from 970 to 1,810 years (Attachment A-3).

Rivero (2004) notes that it is not possible to directly measure the long–term amount of contractional slip on the OBT because it is generally blind. However, since the location of the OBT is constrained in the region, he used area balancing methods to constrain fault slip. He also evaluated alternative slip values derived from balanced structural interpretations located across several of the major contractional trends observed in the study area as an additional constraint. Excess–area balancing methods were modified and used to invert for the amount of contractional slip consumed by the OBT (Figures A-24 and A-25), since the spatial location and geometry (dip value) of this fault were assumed by Rivero 2004 to be well–known in the study region.

Balanced and restored cross sections based on available seismic data and well data suggest approximately 2.2 to 2.7 km of shortening across the OBT during the last 1.8 to 2.4 Ma (Rivero and Shaw, 2010, in press; Attachment A-3). This suggests an average slip rate of about 1 mm/yr on the OBT, although shortening rate estimates vary significantly along strike (Figures A-24 and A-25).

A5.2 Evidence for Activity

Blind thrusts by definition do not extend to the surface and thus cannot be observed directly. Secondary deformation related to folding and faulting in the hanging wall of the blind thrust is used to identify and characterize recent movement on such fault sources. The following two subsections (4.2.1 Paleoseismicity and 4.2.2 Geomorphology) describe evidence and methods used to evaluate evidence for activity and provide constraints slip rates for the OBT and related structures.

A5.2.1 Paleoseismicity

Fault trenching or other paleoseismic data are not available for the OBT. The offshore location of the near-surface projected traces of the main thrust and back thrusts mapped by Rivero (2004) precludes direct observation of the surface deformation that may be associated with these tectonic structures. The Compton blind thrust, which is postulated to be an onshore equivalent of the OBT, may provide an analog to the OBT.

Leon et al. (2008) employed a multidisciplinary methodology that uses a combination of high-resolution seismic reflection profiles and borehole excavations to suggest a link between blind faulting on the Compton thrust at seismogenic depths directly to near-surface folding. They concluded from these studies that the Compton blind thrust fault is active and has generated at least six large-magnitude earthquakes (M_W 7.0 to 7.4) during the past 14,000 years that deformed the Holocene strata record. Growth strata (discrete sequences that thicken sequentially across a series of buried fold scarps) are interpreted to be associated with uplift events on the underlying Compton thrust ramp.

Rivero et al. (2000) interpret the San Joaquin Hills Blind Thrust (SJHBT) as a backthrust to the OBT. Rivero (2004) estimates that M 7.1 and M 7.3 events would occur on average every 1,070 to 1,430 and 1,480 to 1,960 years, respectively, on the OBT where the SJHBT is linked with the OBT. Grant et al. (1999) also suggest that a backthrust that soles into the OBT is a viable structural model, although less preferred than one in which movement of the SJHB is the product of partitioned strike-slip and compressive shortening across the NI/RC Fault Zone. They calculated average recurrence times of 1,650 to 3,100 years for moderate-magnitude earthquakes (based on an average uplift event of 1.3 m; Grant et al., 2002).

A5.2.2 Geomorphology

Rivero et al. (2000) provides a viable structural model that explains the localized uplift of the San Joaquin Hills as a backthrust in the hanging wall of the OBT (Figure A-21). They interpret an offshore extension of this structure that is imaged in seismic data as forming above a shallow blind thrust ("Shelf Monocline Trend" on Figure A-21) with an average southwest dip value of 23 degrees. This shallow fault is restricted to the hanging wall of the OBT at depth, and they interpret that this shallow fault soles into the OBT forming a structural wedge (Medwedeff, 1992; Mueller et al., 1998 and Rivero, 2004) (Figure A-21 and A-26). Quaternary uplift of the San Joaquin Hills as manifested by emergent marine terraces, therefore, is interpreted as evidence of Quaternary reactivation of the OBT (Figure A-23).

On a more regional scale, Rivero and Shaw suggest that emergent marine terraces along the entire coast between southern Orange County and northern Baja California show evidence for regional uplift of approximately 0.13 to 0.14 mm/yr (Kern and Rockwell, 1992), and may be the surface manifestation of Quaternary uplift in the hanging wall to the OBT (Rivero et al., 2000 and Rivero, 2004; Attachment A-3).

Seafloor fold and fault scarps associated with the OBT (Figures A-4b, A-16, A-18, A-19, and A-20) also suggest recent contractional activity (Rivero et al., 2000 and Rivero, 2004). Structural inversion and associated reactivation of normal faults commonly produce broad regions of positive structural relief characterized by the development of broad anticlines located directly on top of extensional rollovers and syn-extensional stratigraphic wedges (Figure A-15). Rivero (2004) concludes that thrust motion on the OBT generated four prominent contractional fold trends. Three of these trends are foreland–directed structures, namely the San Mateo, the San Onofre and the Carlsbad trends (Figures A-17 through A-20). These active structures are characterized by thrust sheets that extend laterally for 10 to 20 km, and produce prominent fold and fault scarps on the sea floor. The fourth trend is characterized by hinterland thrusting, which is manifested in a laterally continuous monocline that controls the relief and bathymetric expression of the continental shelf. This monocline is interpreted to result from the interaction between a shallow west–dipping back thrust system and the deep–seated, east–dipping OBT.

Geomorphically, youthful seafloor scarps and folds above fault tiplines have been documented on multibeam bathymetry data and seismic reflection data. Growth folding and offset of Late Quaternary strata are locally apparent on the seismic records, documenting active seafloor uplift on the continental slope in the vicinity of the San Mateo, San Onofre, and Carlsbad faults (Sorlien et al., 2009b; Ryan et al., 2009 and Rivero and Shaw, 2010, in press).

A5.2.3 Seismology

Seismicity in the offshore region is generally diffuse and scattered as compared to more spatially correlated patterns associated with many strike-slip active faults in the Peninsular Ranges on the mainland (Astiz and Shearer, 2000). The focal mechanism of the 1986 M_L 5.6 Oceanside event suggests that the main shock during that event had reverse motion (Hauksson and Jones, 1988). Most importantly, Astiz and Shearer (2000) document a shallow, east-dipping plane of seismicity at a depth of between 10 and 15 km beneath the continental slope and shelf west of San Diego based on relocation of

1981–1997 earthquakes (Figure A-27). The standard errors associated with these earthquake locations are less than 1.5 km. Astiz and Shearer (2000) suggest that these focal mechanisms document the existence of an active, low-angle east-dipping fault in the Coronado Banks Region that may be part of a larger system of offshore thrust faults like the OBT. Rivero (2004) cites this low angle plane of seismicity as evidence for contractional activity on the OBT.

A5.2.4 GPS

As previously noted, the geodetic data (velocities and uncertainties) presented on Figures A-3 and A-13 are based on the public archive preserved by the Scripps Orbit and Permanent Array Center (SOPAC) and includes all permanent continuous GPS stations installed in southern California between 1995 and 2008 with at least 1.5 years of data collected. The GPS data collected to date generally does not support regional compression or extension normal to the postulated OBT. However, it is noted that the current status of geodetic data can be considered inconclusive due to the following:

- Data reduction has quantitative limitations due to the uncertainty caused by locking effects that are dependent upon the characterization of major strike-slip faults in the Continental Borderlands.

- Currently, GPS stations in the vicinity of SONGS are either located on what would be the locked part of the OBT where resolution of low postulated slip rates are within the uncertainty of the GPS measurements or they are located too close to the Elsinore Fault to show any gradient of shortening across the area in question.

- There are very few GPS stations in the vicinity of SONGS and even fewer in the offshore region of the Continental Borderlands; one continuous station exists on San Clemente Island and two on Catalina Island.

- There are many sources with unknown slip-rates in the ICB Province making it difficult to resolve the low magnitude of slip postulated on either the OBT or the NI/RC Fault Zone system.

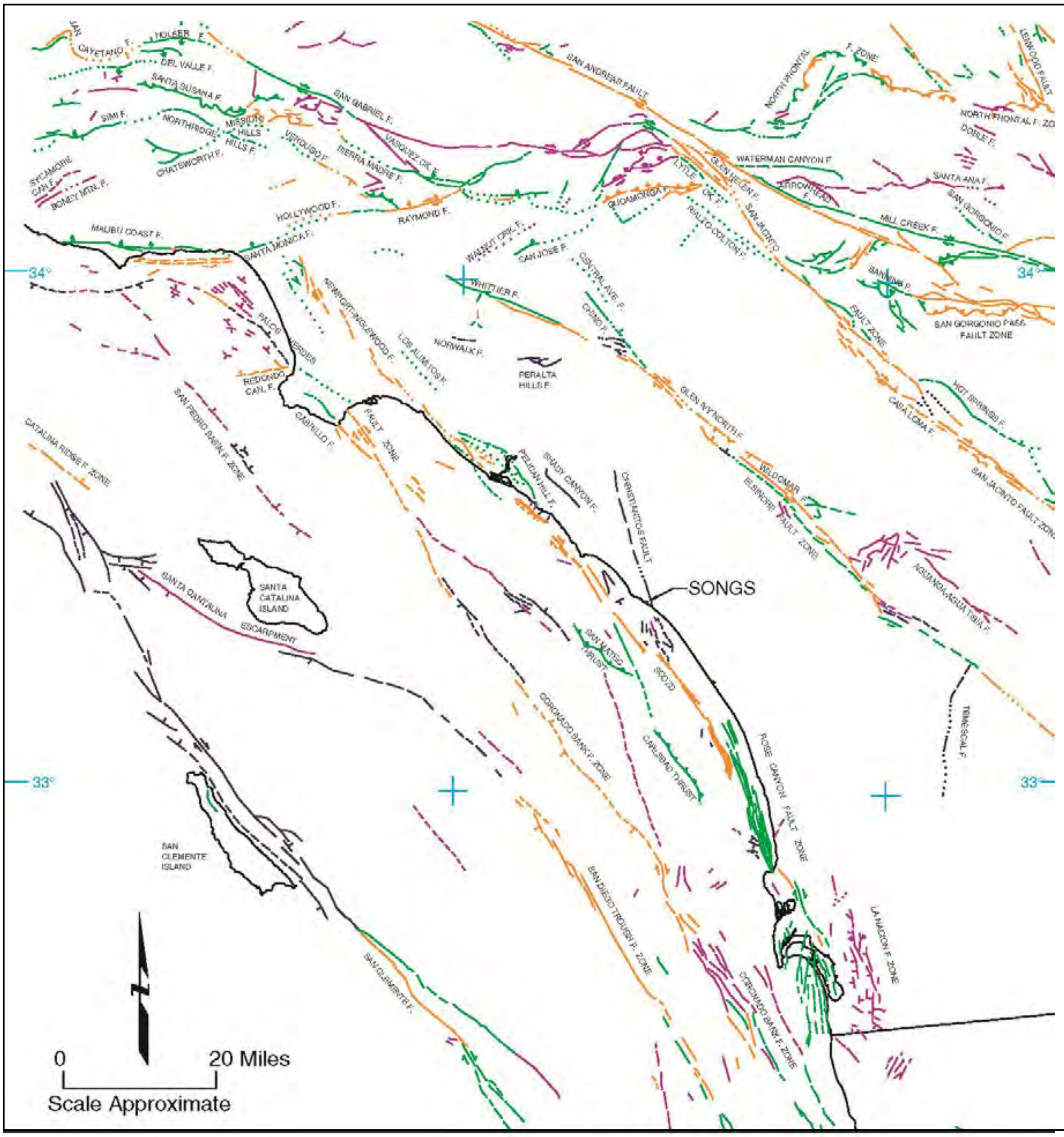

FAULT RECENCY CLASSIFICATION

- Faults that displace Holocene (~ 10 ka) or latest Pleistocene (~ 20 ka) deposits or geomorphic surfaces
- Faults that displace late Quaternary (~ 780 ka) deposits or geomorphic surfaces
- Quaternary faults (1.8 Ma)
- Faults that displace pre-Quaternary deposits. Receny of last displacement for offshore faults generally not known. Only selected faults from Jennings (1992) are shown

GeoPentech
Geotechnical & Geoscience Consultants

SCE (2001) QUATERNARY FAULT MAP

FIGURE A-1a

SAN ONOFRE NUCLEAR GENERATING STATION

SEISMIC HAZARD ASSESSMENT PROGRAM

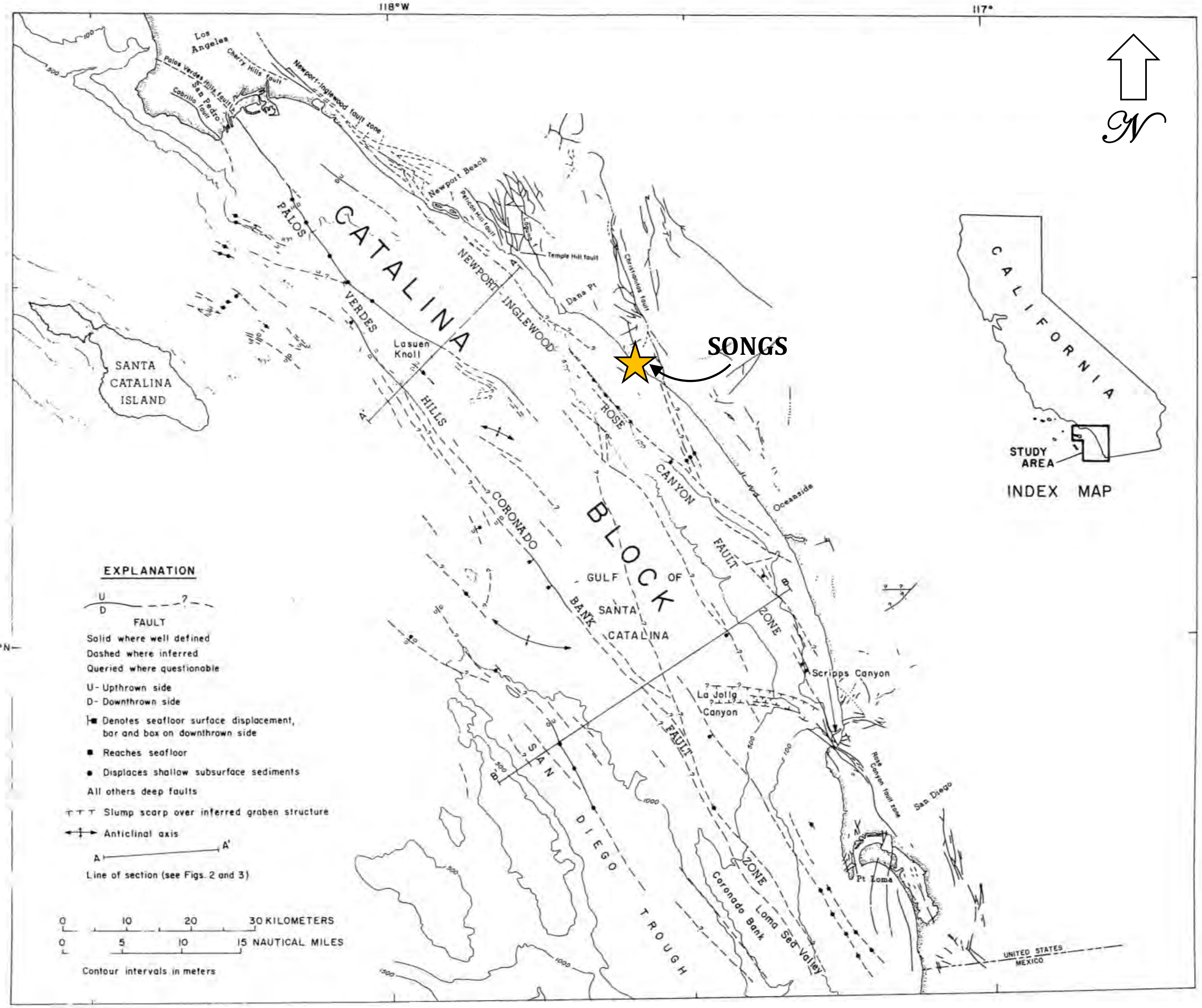

Modified from Greene et al. (1979)

GeoPentech Geotechnical & Geoscience Consultants	**SAN ONOFRE NUCLEAR GENERATING STATION** SEISMIC HAZARD ASSESSMENT PROGRAM	**CONTINENTAL BORDERLAND STRUCTURAL GEOLOGY MAP**	FIGURE A-1b

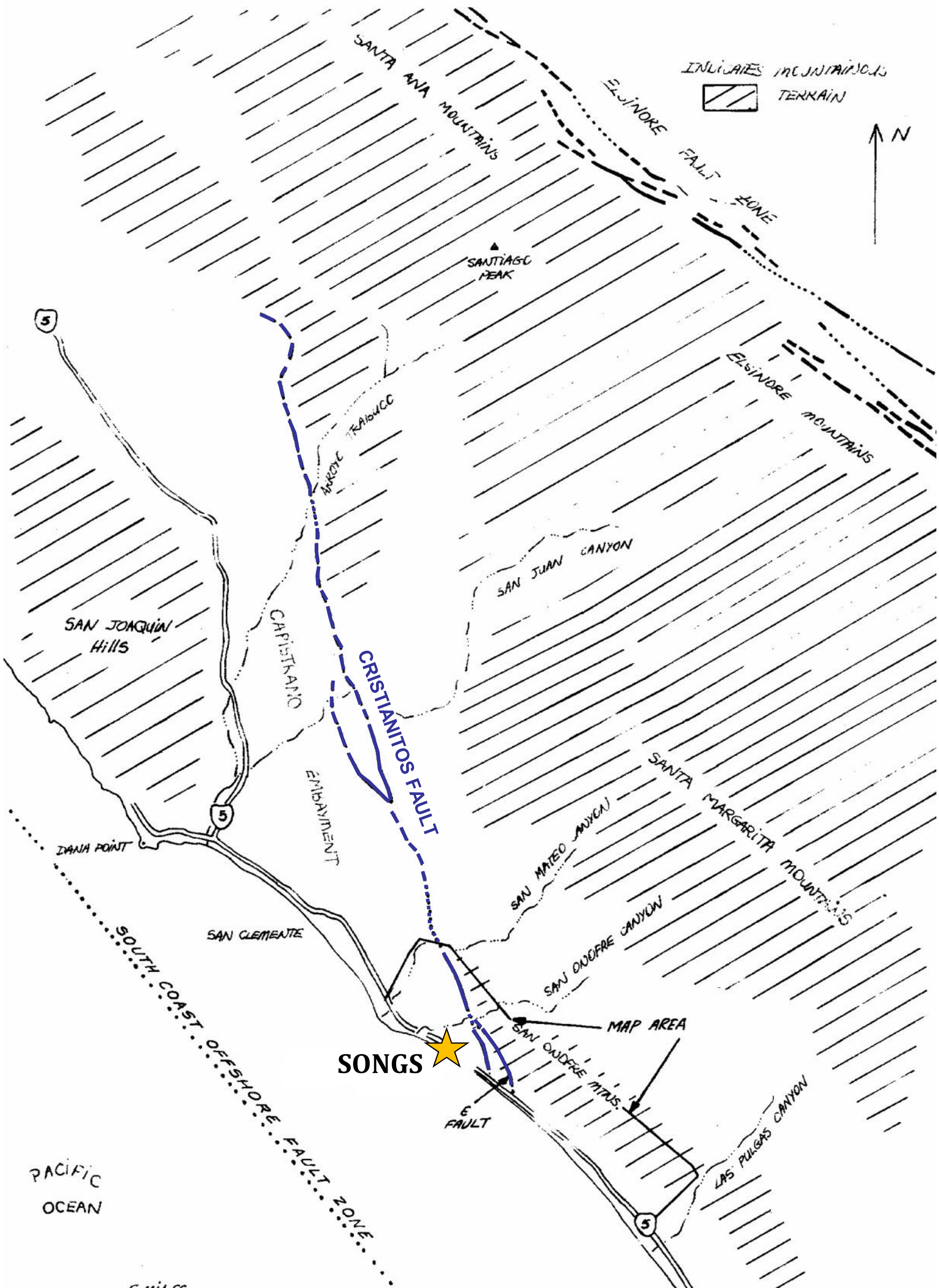

FIGURE 1

Modified from Ehlig (1977)

GeoPentech
Geotechnical & Geoscience Consultants

MAP OF CRISTIANITOS FAULT ZONE

FIGURE A-1c

SAN ONOFRE NUCLEAR GENERATING STATION

SEISMIC HAZARD ASSESSMENT PROGRAM

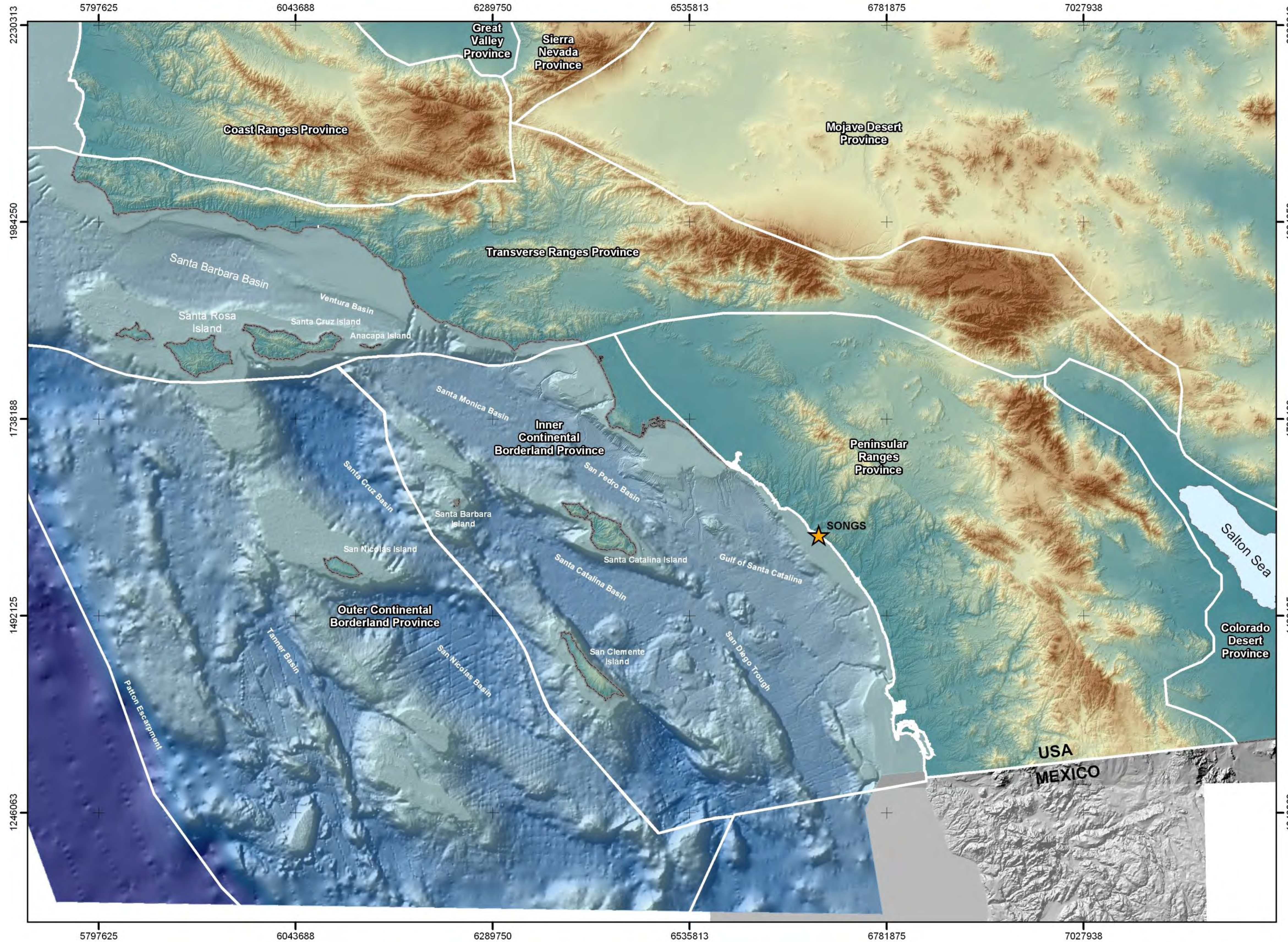

LEGEND

Approximate Geomorphic Province Boundary

Coordinate Grid: CA State Plane Zone 5, NAD83, Feet

Source: CGS (2002b) and Fisher et al. (2009a)

N

1:1,500,000

20 10 0 20 Miles

GeoPentech
Geotechnical & Geoscience Consultants

By Fugro West, Inc. (2010)

SAN ONOFRE NUCLEAR GENERATING STATION

SEISMIC HAZARD ASSESSMENT PROGRAM

GEOMORPHIC PROVINCES OF SOUTHERN CALIFORNIA

FIGURE
A-2a

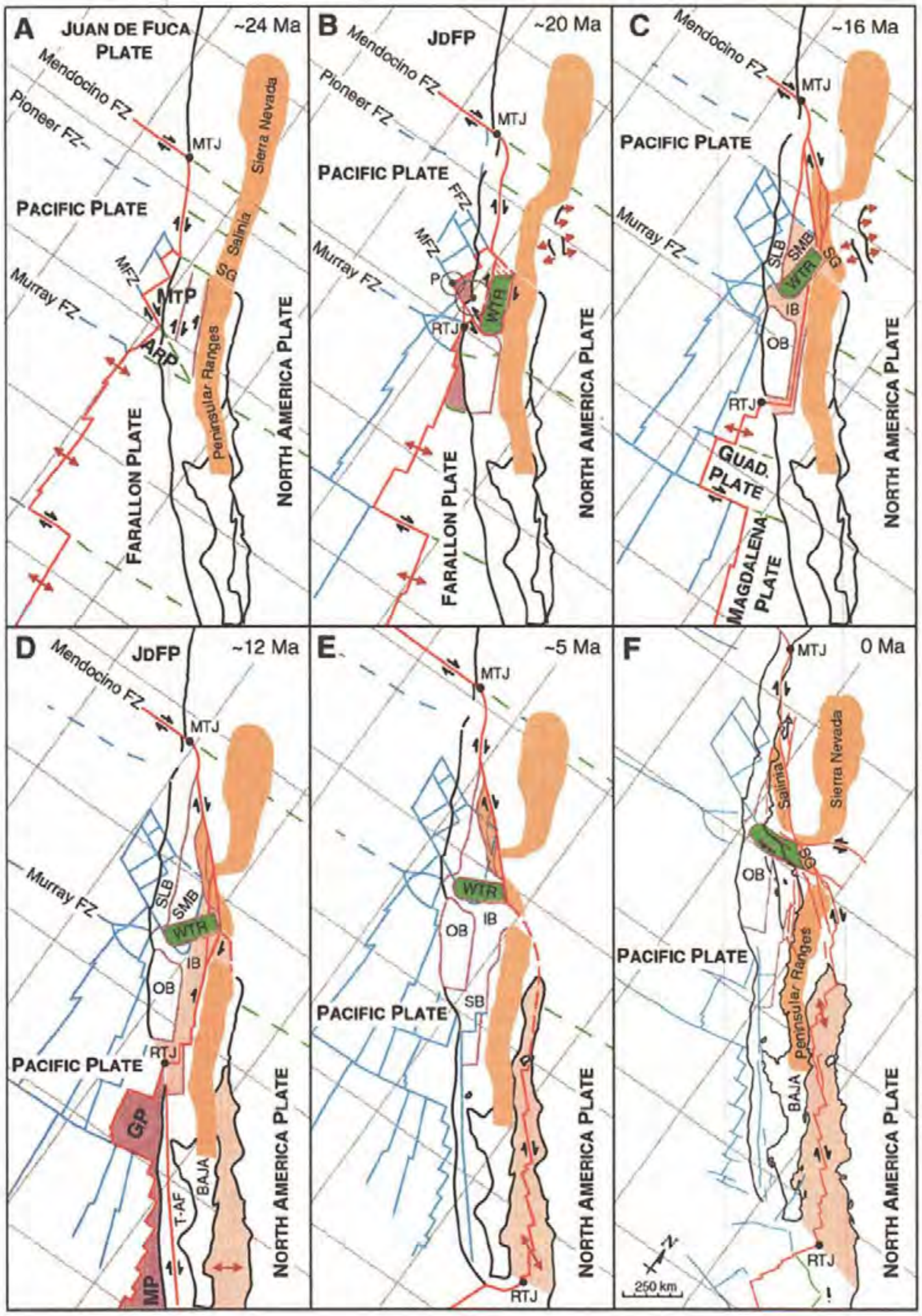

Simple tectonic model of Pacific–North America plate interactions since 24 Ma. Model assumes constant rate and direction of Pacific plate motion and constant rate of western Transverse Ranges (WTR) rotation. When partially subducted Monterey (20 Ma), Arguello (17.5 Ma), and Guadalupe and Magdalena (12 Ma) microplates are captured, part of North America upper plate is transferred to Pacific plate. Fine gray lines provide reference grid tied to fixed North America; error circles in B are estimated uncertainties in position P from this model and Stock and Molnar (1988). ArP—Arguello plate; GP—Guadalupe plate; MtP—Monterey plate; SG—San Gabriel block; JdFP—Juan de Fuca plate; SLB—Santa Lucia Bank; SMB—Santa Maria basin; IB, OB, SB—inner, outer, and southern borderland, respectively; T-AF—Tosco-Arbreojos fault; MP—Magdalena plate; red areas—regions of transtension; purple areas—captured or soon-to-be captured microplates. See Figure 2 for other abbreviations.

Source: Nicholson et al. (1994)

GeoPentech
Geotechnical & Geoscience Consultants

CENOZOIC EVOLUTION OF THE PACIFIC – NORTH AMERICA PLATE BOUNDARY

FIGURE A-2b

SAN ONOFRE NUCLEAR GENERATING STATION

SEISMIC HAZARD ASSESSMENT PROGRAM

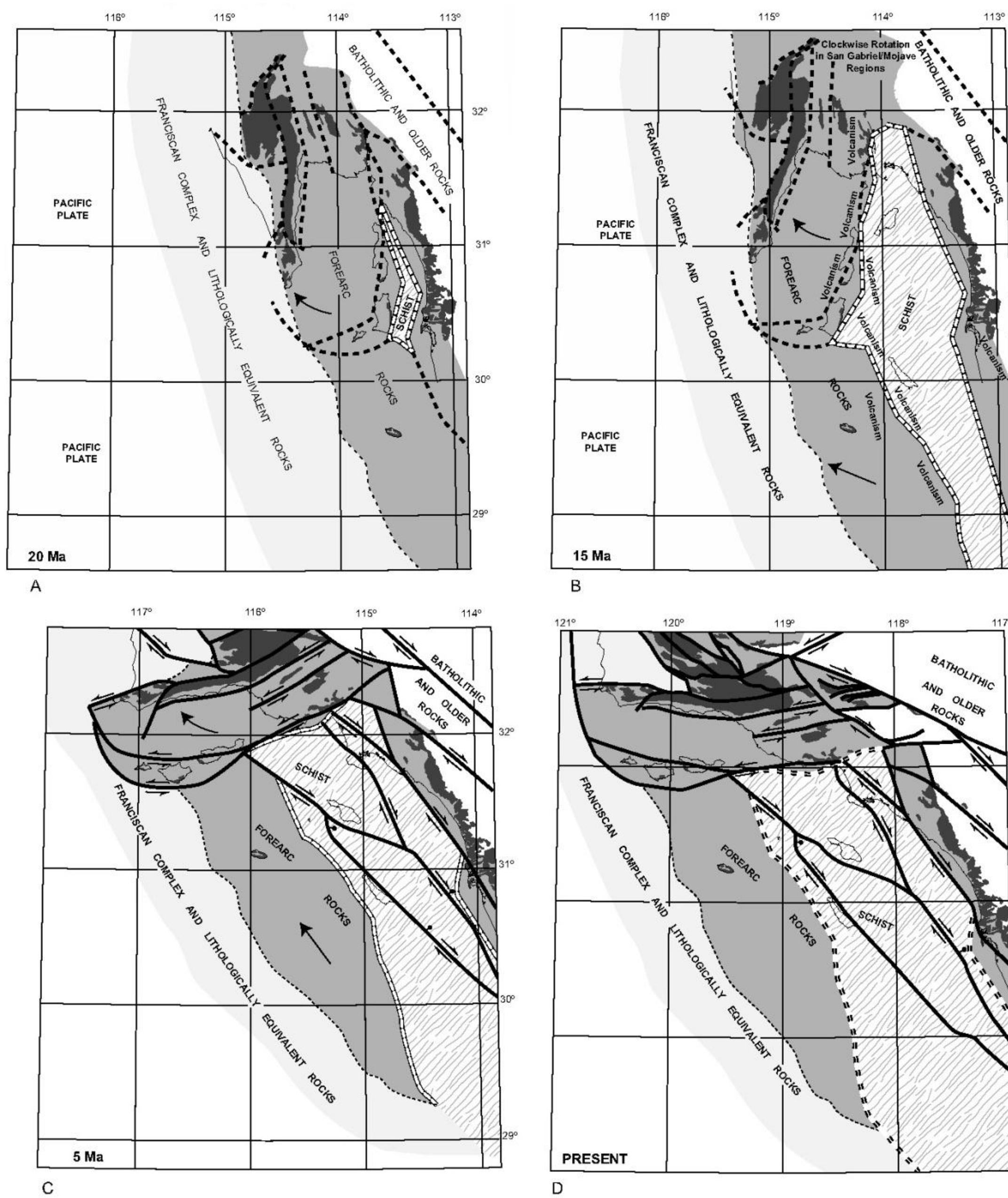

Palinspastic maps of California continental borderland and adjacent regions for past 20 m.y. Light gray areas are accretionary rocks of Franciscan Complex or belts that are lithologically similar to that complex. Medium gray areas are underlain by forearc strata. Dark gray areas are known outcrops of forearc strata. Area in wavy lined pattern is Catalina Schist belt. White areas are floored by batholithic basement rocks. Fine line is modern shoreline and island configuration, shown deformed and displaced for reference in earlier models. Heavy lines are major faults that are thought to be active during time represented. Dashed double line is fault-bounded margin of Catalina Schist belt. Dashed boxed line is active margin of extending region within Catalina Schist belt. Arrows show approximate trajectories of areas with respect to North America. (A) 20 Ma; time period prior to most of the deformation. (B) 15 Ma; time period in migrating-hinge phase of extension. (C) 5 Ma; time period in dispersed right-normal-slip phase of extension. (D) Present-day configuration.

Source: Bohannon and Geist (1998)

GeoPentech
Geotechnical & Geoscience Consultants

LATE CENOZOIC PALINSPASTIC RECONSTRUCTION MAPS OF THE CONTINENTAL BORDERLAND

FIGURE A-2c

SAN ONOFRE NUCLEAR GENERATING STATION

SEISMIC HAZARD ASSESSMENT PROGRAM

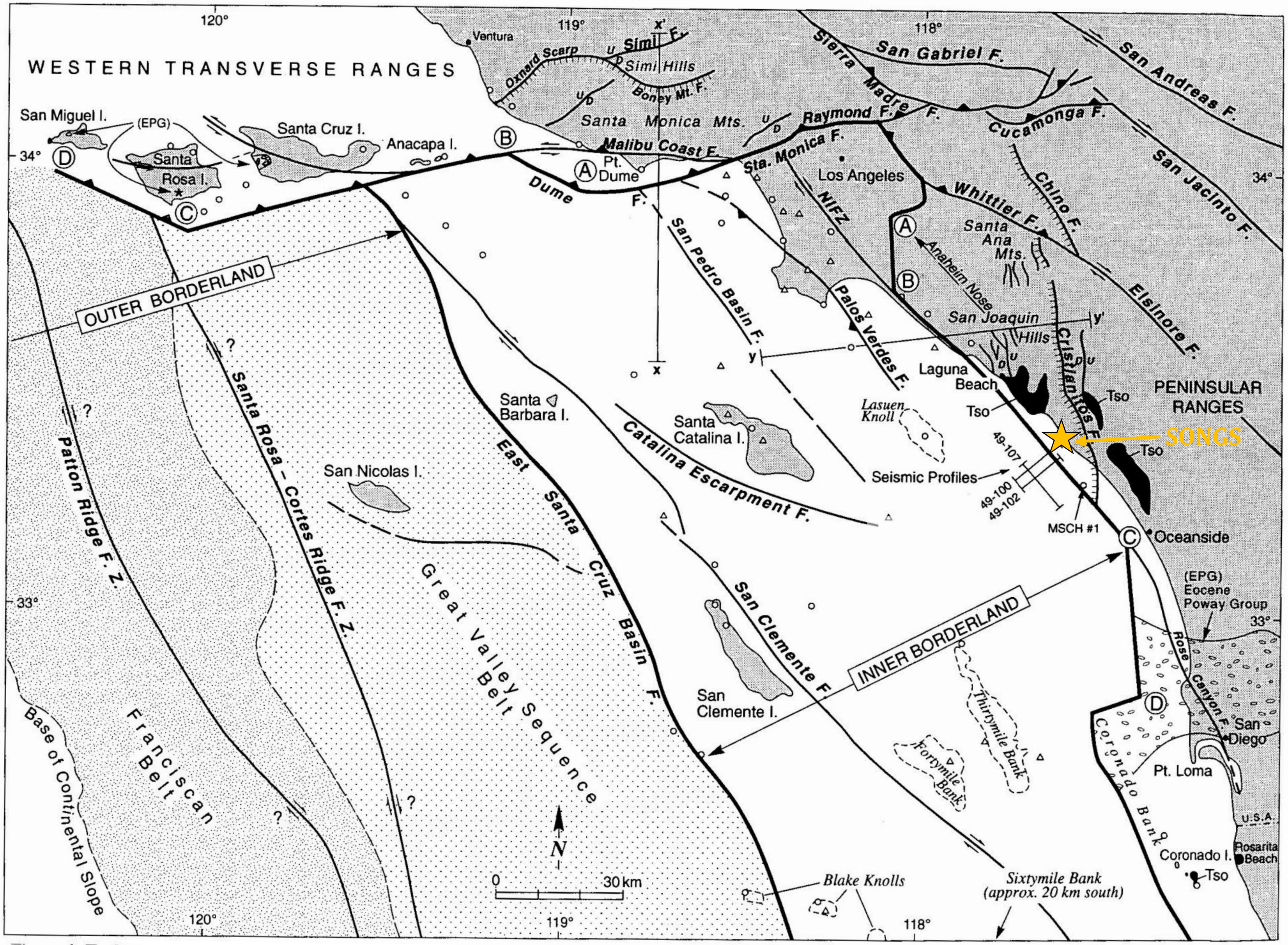

NOTES: (1) Modified from Crouch and Suppe (1993)
(2) Presented in SCE (2001)

GeoPentech Geotechnical & Geoscience Consultants	SAN ONOFRE NUCLEAR GENERATING STATION SEISMIC HAZARD ASSESSMENT PROGRAM	SIMPLIFIED MAP OF CALIFORNIA BORDERLAND PROVINCES WITH ONSHORE AND OFFSHORE FAULT TRACES	FIGURE A-2d

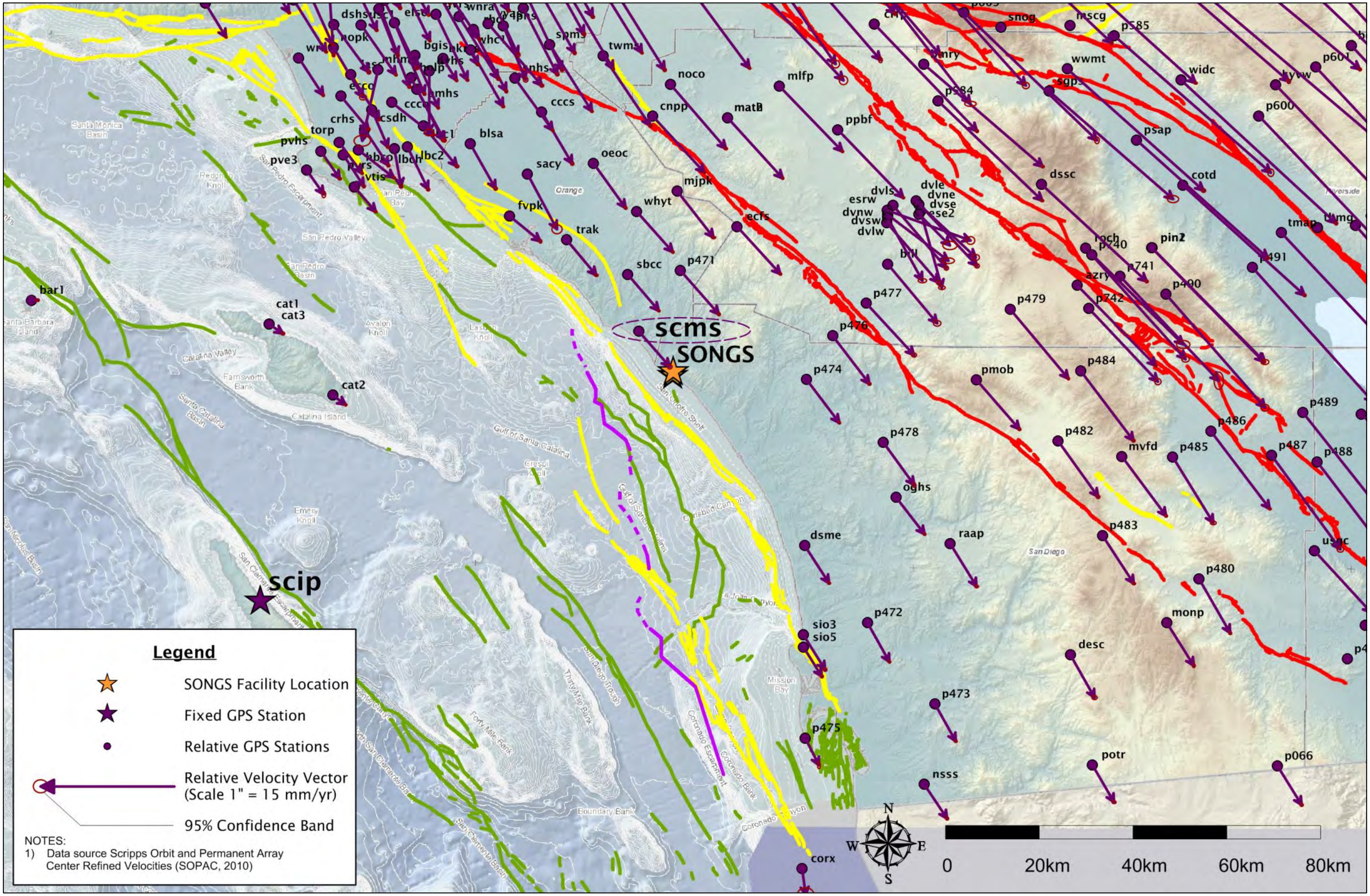

GeoPentech
Geotechnical & Geoscience Consultants

SAN ONOFRE NUCLEAR GENERATING STATION

SEISMIC HAZARD ASSESSMENT PROGRAM

GEODETIC DATA
VELOCITY RELATIVE TO SCIP

FIGURE
A-3

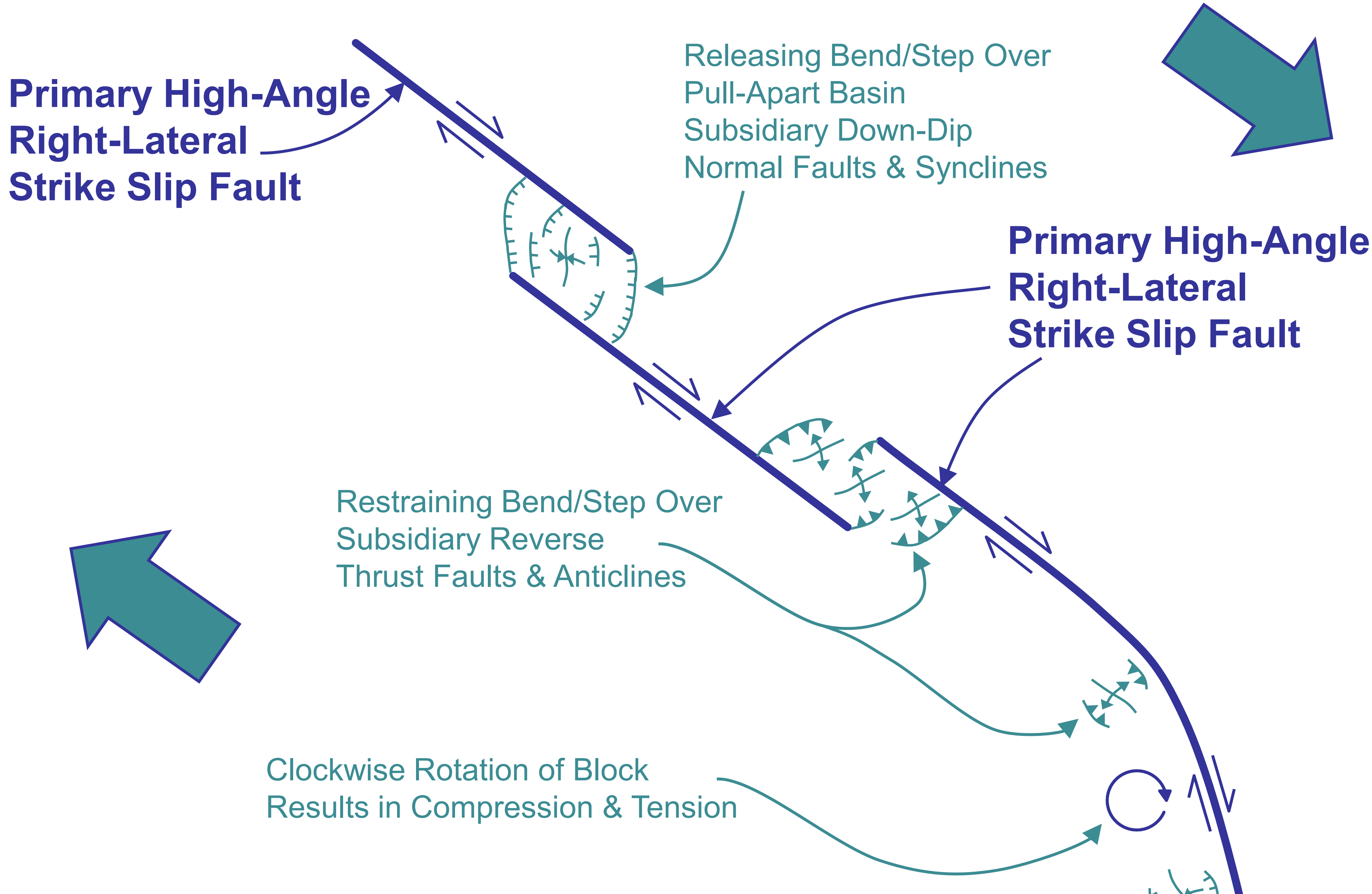

Modified from Moody and Hill (1956), Wilcox et al. (1973), and Harding (1973)

GeoPentech
Geotechnical & Geoscience Consultants

GeoPentech Geotechnical & Geoscience Consultants	**SAN ONOFRE NUCLEAR GENERATING STATION** SEISMIC HAZARD ASSESSMENT PROGRAM	**BASIC WRENCH FAULT TECTONICS**	FIGURE A-4a

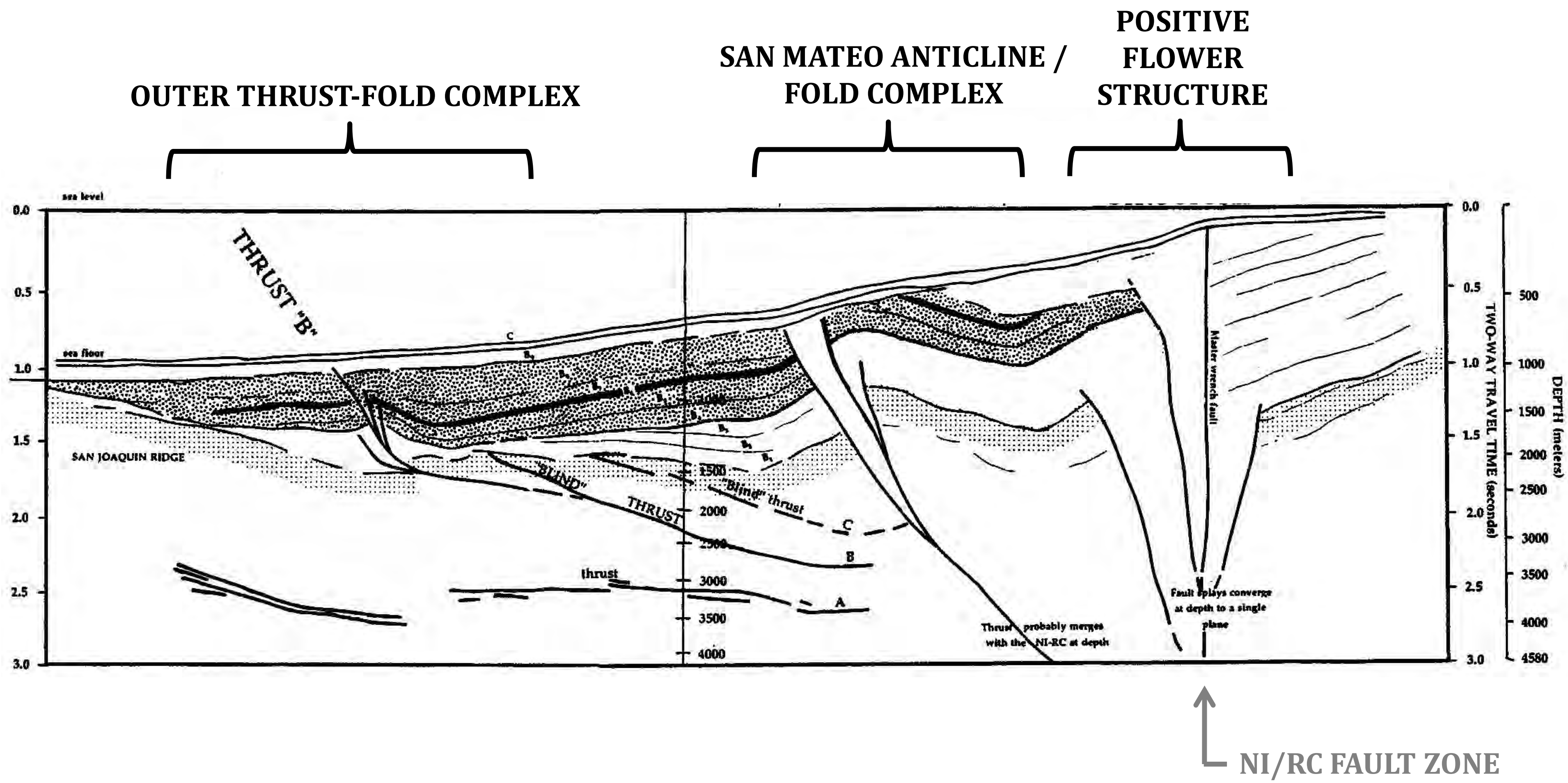

NOTES: (1) Modified from Fischer and Mills (1991)
(2) Presented in SCE (2001)

GeoPentech Geotechnical & Geoscience Consultants	**SAN ONOFRE NUCLEAR GENERATING STATION** SEISMIC HAZARD ASSESSMENT PROGRAM	**EXAMPLE OF A POSITIVE FLOWER STRUCTURE**	FIGURE A-4b

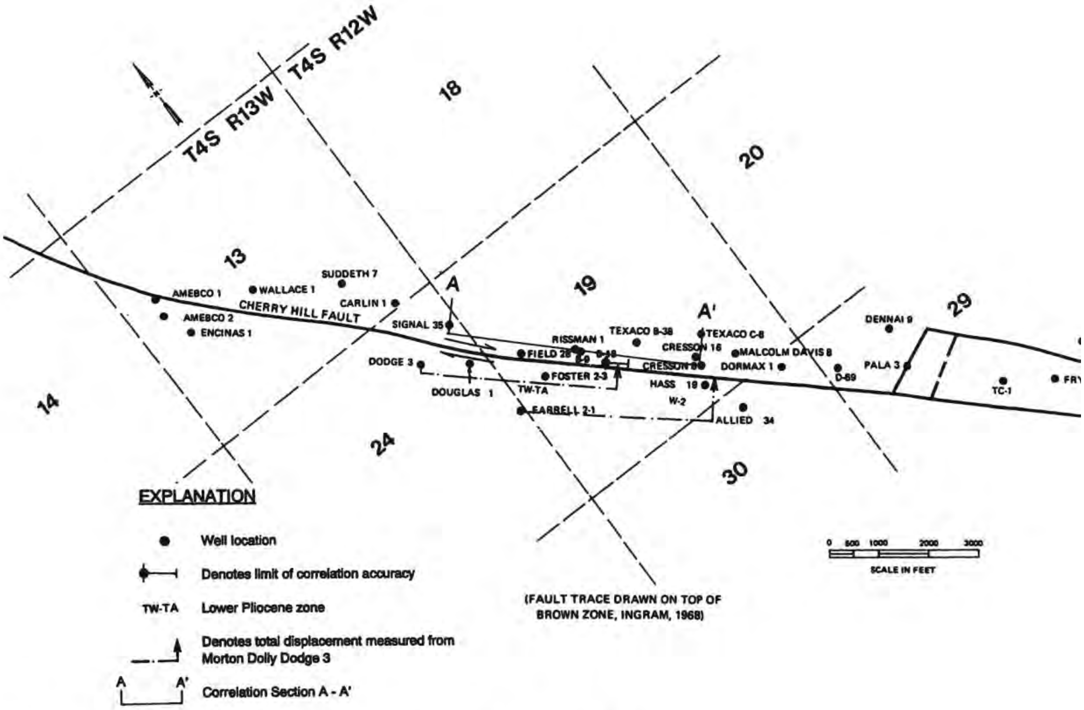

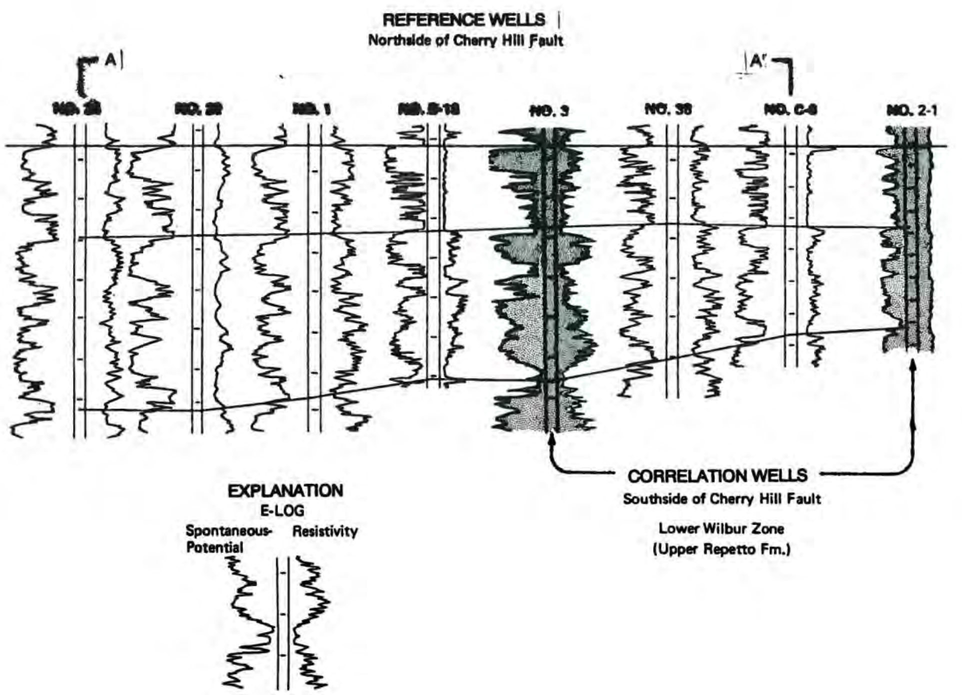

Source: Freeman et al. (1992)

GeoPentech Geotechnical & Geoscience Consultants	LONG BEACH OIL FIELD WELL MAPS AND LOGS	FIGURE A-5
	SAN ONOFRE NUCLEAR GENERATING STATION SEISMIC HAZARD ASSESSMENT PROGRAM	

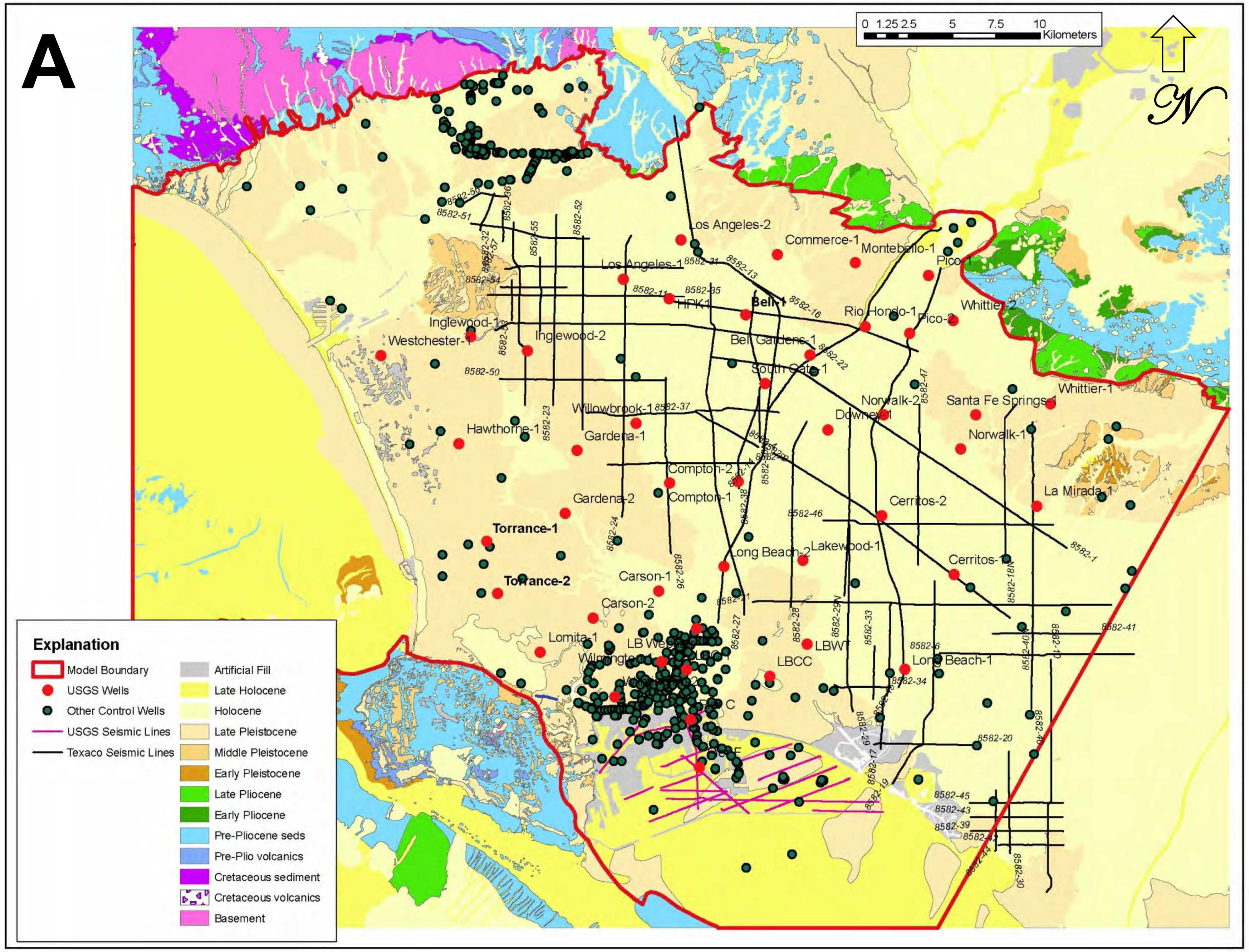

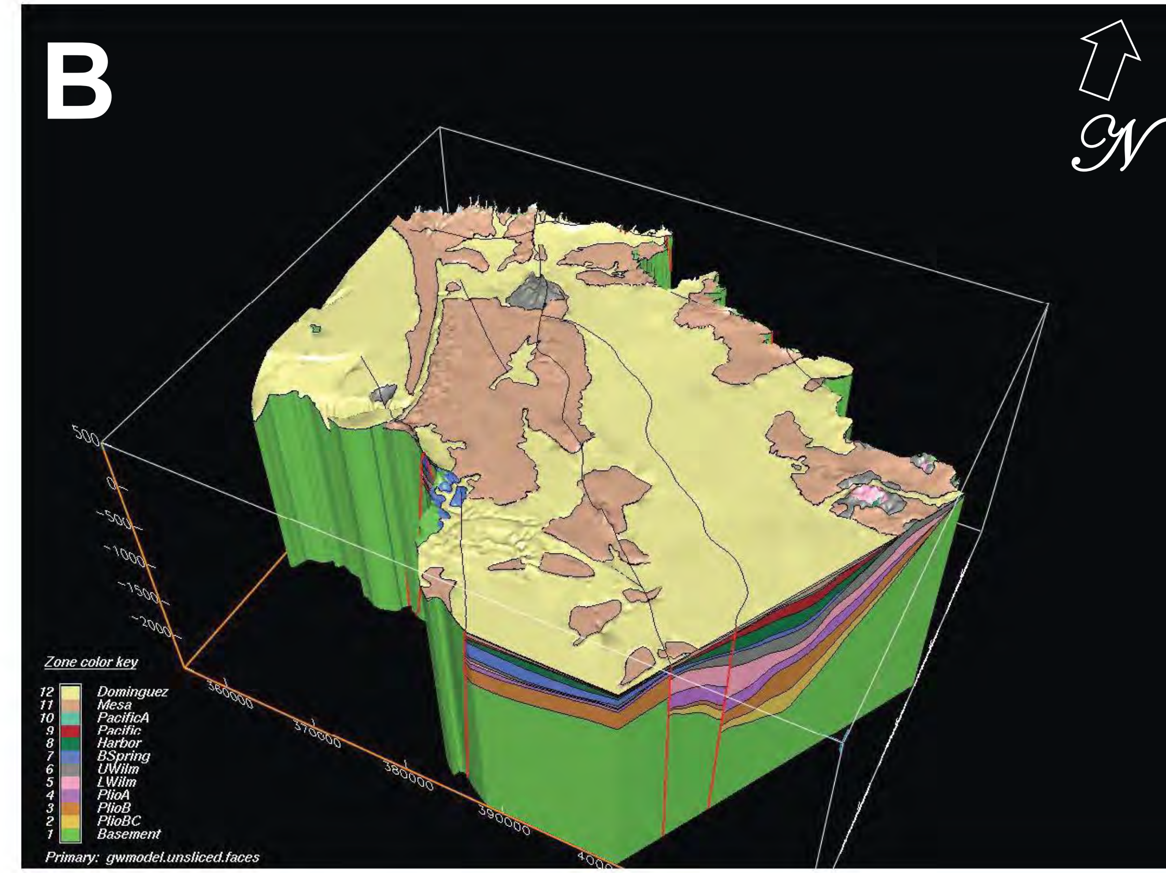

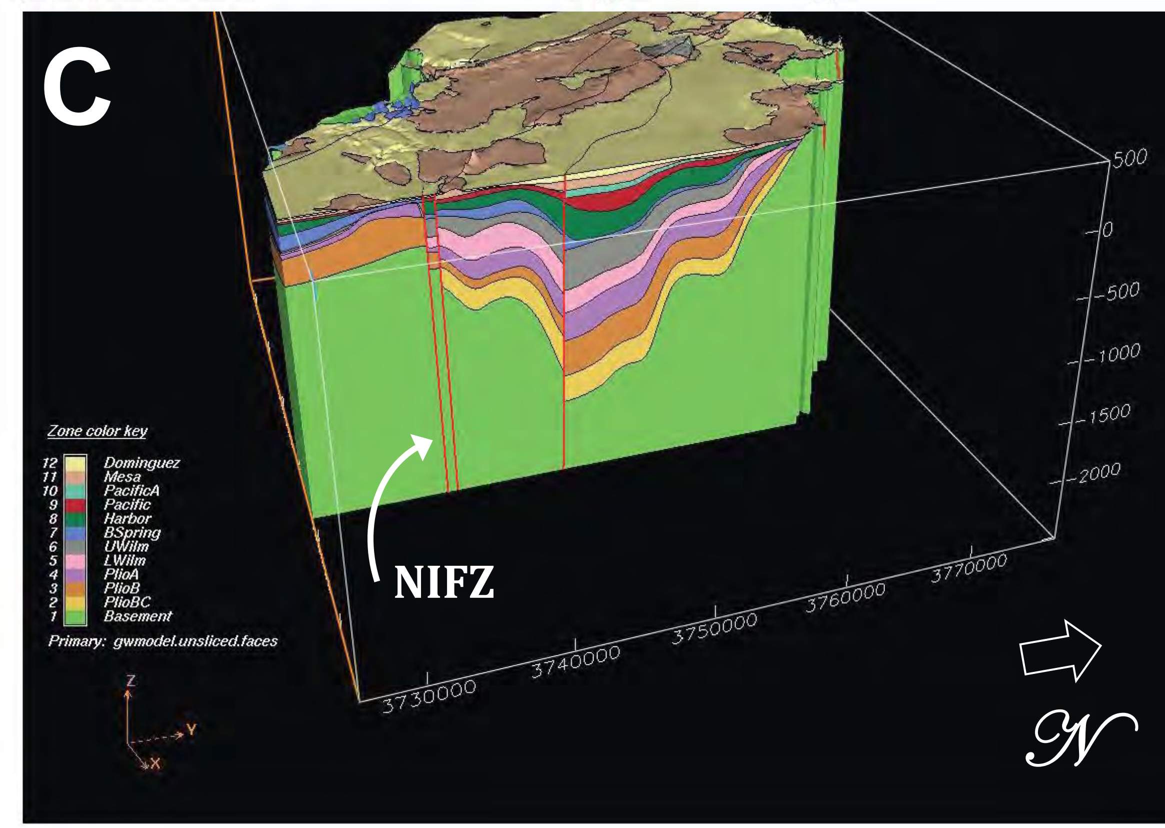

Modified from Ponti (2010)

GeoPentech

SAN ONOFRE NUCLEAR GENERATING STATION

SEISMIC HAZARD ASSESSMENT PROGRAM

MAP AND 3D STRUCTURAL MODEL OF THE LA BASIN

FIGURE A-6

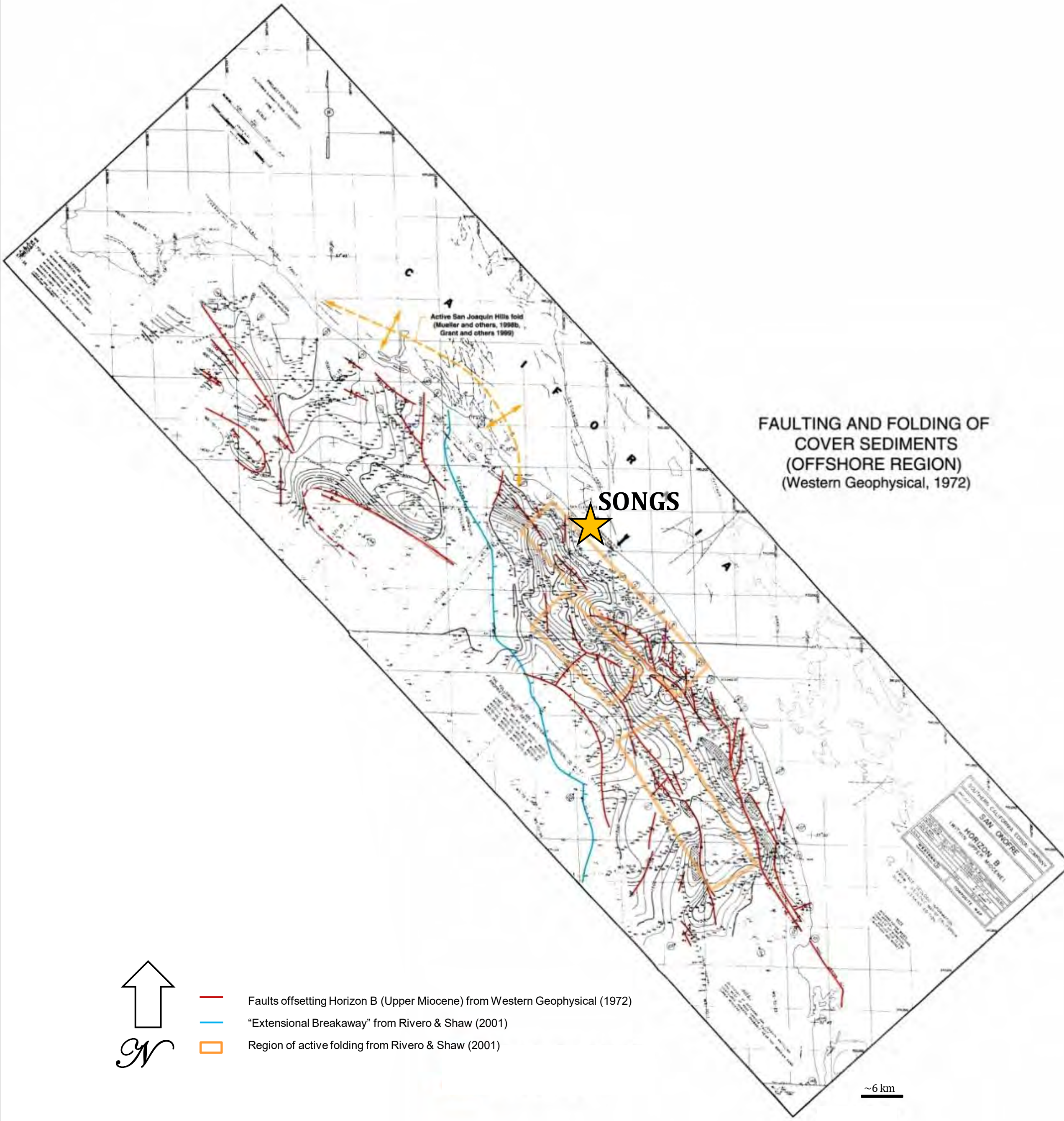

NOTES: (1) Modified from Western Geophysical (1972) and Rivero and Shaw (2001)
(2) Presented in SCE (2001)

GeoPentech Geotechnical & Geoscience Consultants	OFFSHORE FAULT AND FOLD MAP BY WESTERN GEOPHYSICAL (1972)	FIGURE A-7a
	SAN ONOFRE NUCLEAR GENERATING STATION SEISMIC HAZARD ASSESSMENT PROGRAM	

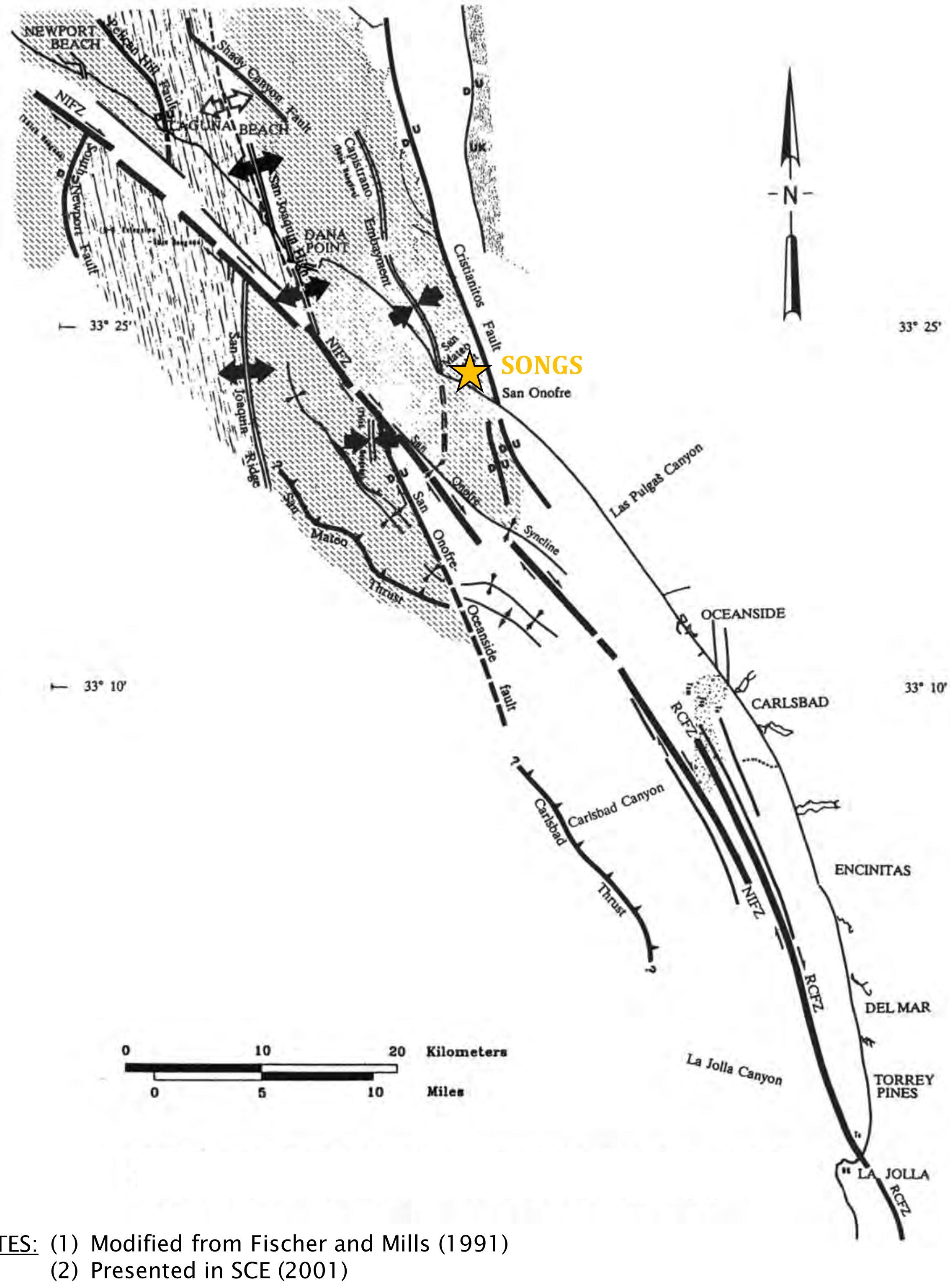

NOTES: (1) Modified from Fischer and Mills (1991)
(2) Presented in SCE (2001)

GeoPentech Geotechnical & Geoscience Consultants	FAULT AND FOLD MAP OF THE INNER CONINENTAL BORDERLAND AND COASTAL REGION	FIGURE A-7b
	SAN ONOFRE NUCLEAR GENERATING STATION SEISMIC HAZARD ASSESSMENT PROGRAM	

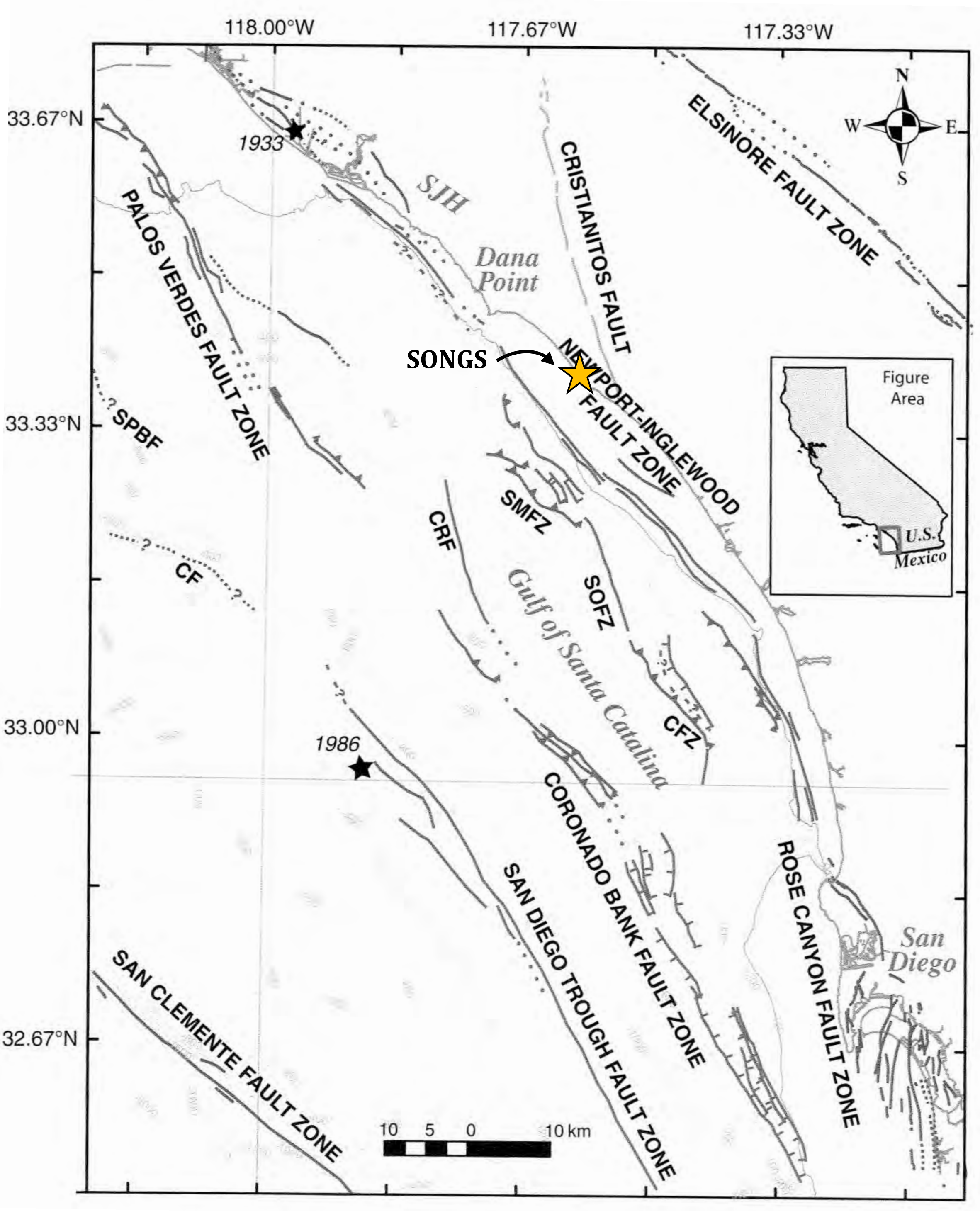

GeoPentech
Geotechnical & Geoscience Consultants

OFFSHORE FAULT MAP BY RYAN ET AL. (2009)

FIGURE A-7c

SAN ONOFRE NUCLEAR GENERATING STATION

SEISMIC HAZARD ASSESSMENT PROGRAM

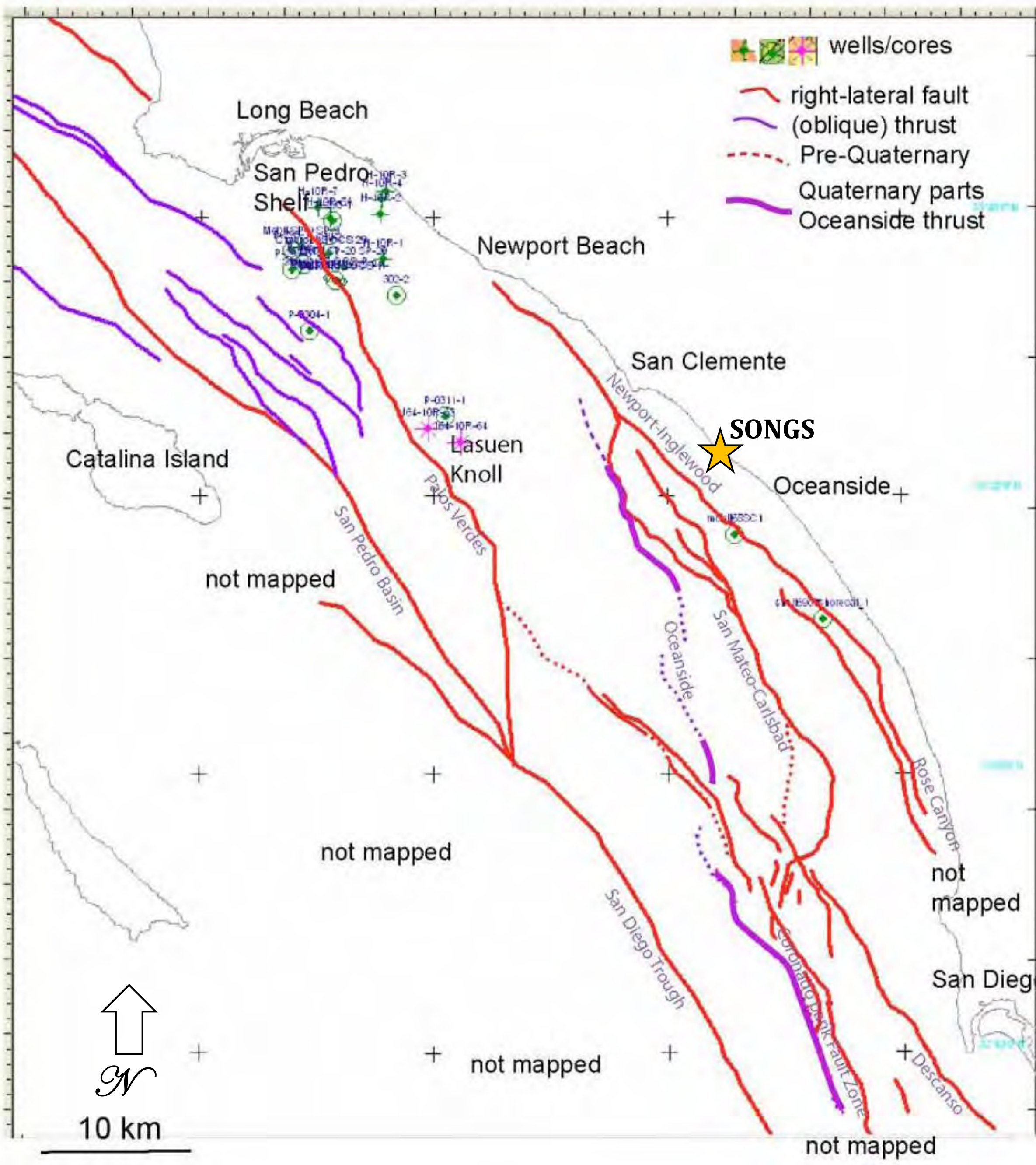

GeoPentech
Geotechnical & Geoscience Consultants

OFFSHORE FAULT MAP BY SORLIEN ET AL. (2009b)	FIGURE A-7d

SAN ONOFRE NUCLEAR GENERATING STATION

SEISMIC HAZARD ASSESSMENT PROGRAM

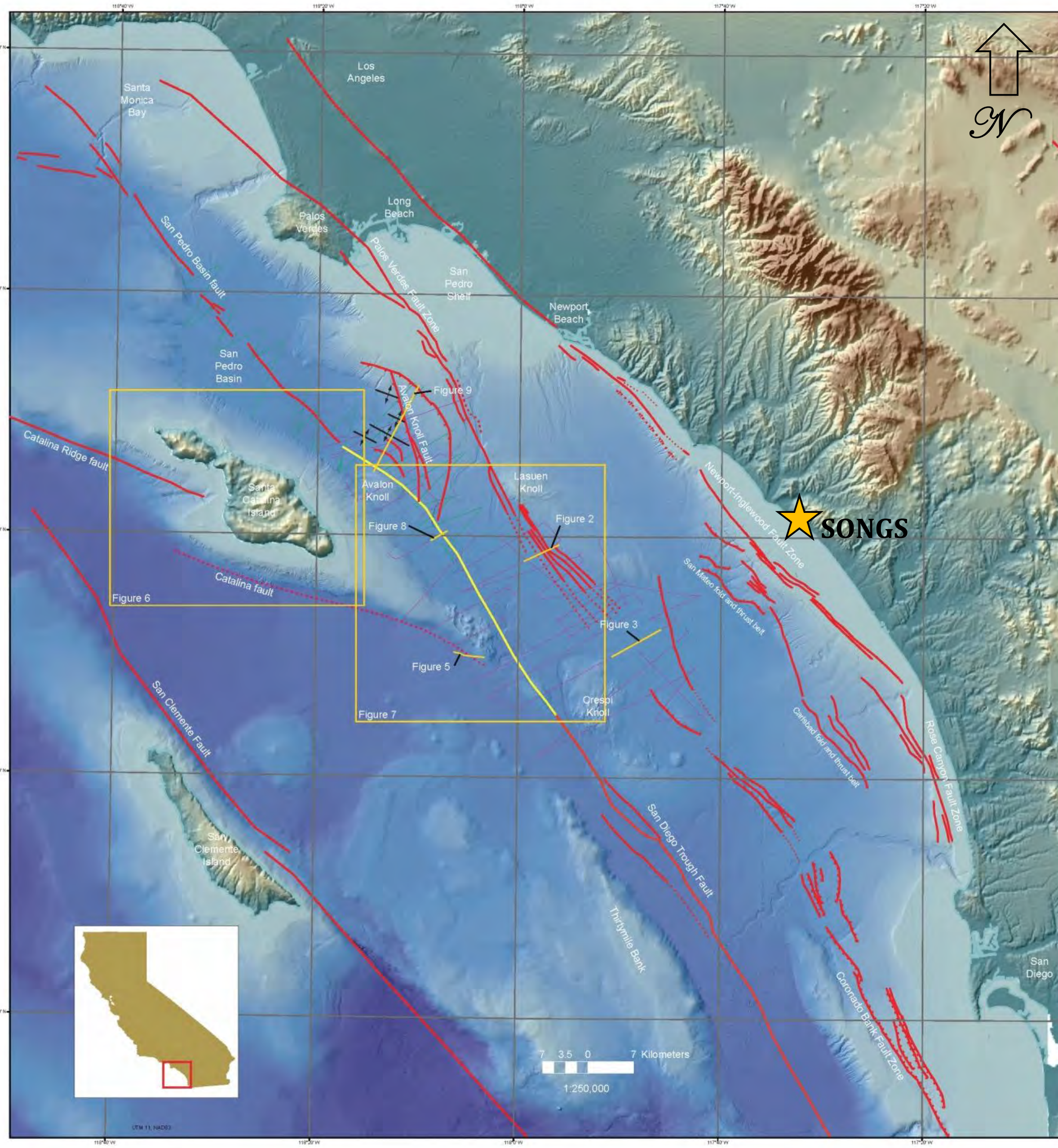

GeoPentech Geotechnical & Geoscience Consultants	OFFSHORE FAULT MAP BY CONRAD ET AL. (2010)	FIGURE A-7e
	SAN ONOFRE NUCLEAR GENERATING STATION SEISMIC HAZARD ASSESSMENT PROGRAM	

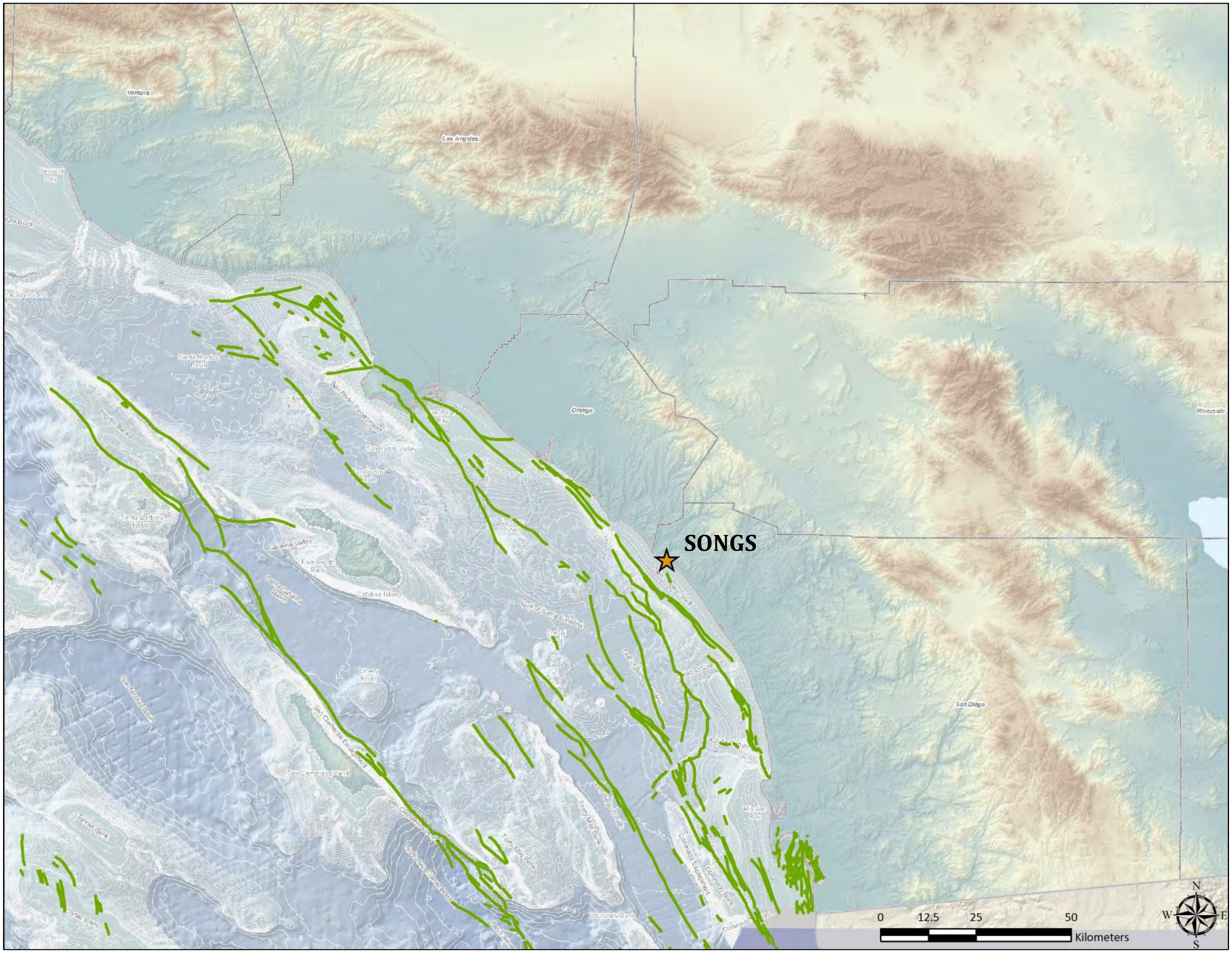

GeoPentech
Geotechnical & Geoscience Consultants

SAN ONOFRE NUCLEAR GENERATING STATION

SEISMIC HAZARD ASSESSMENT PROGRAM

QUATERNARY FAULT AND FOLD DATABASE OFFSHORE FAULT MAP FROM USGS (2009)

FIGURE A-7f

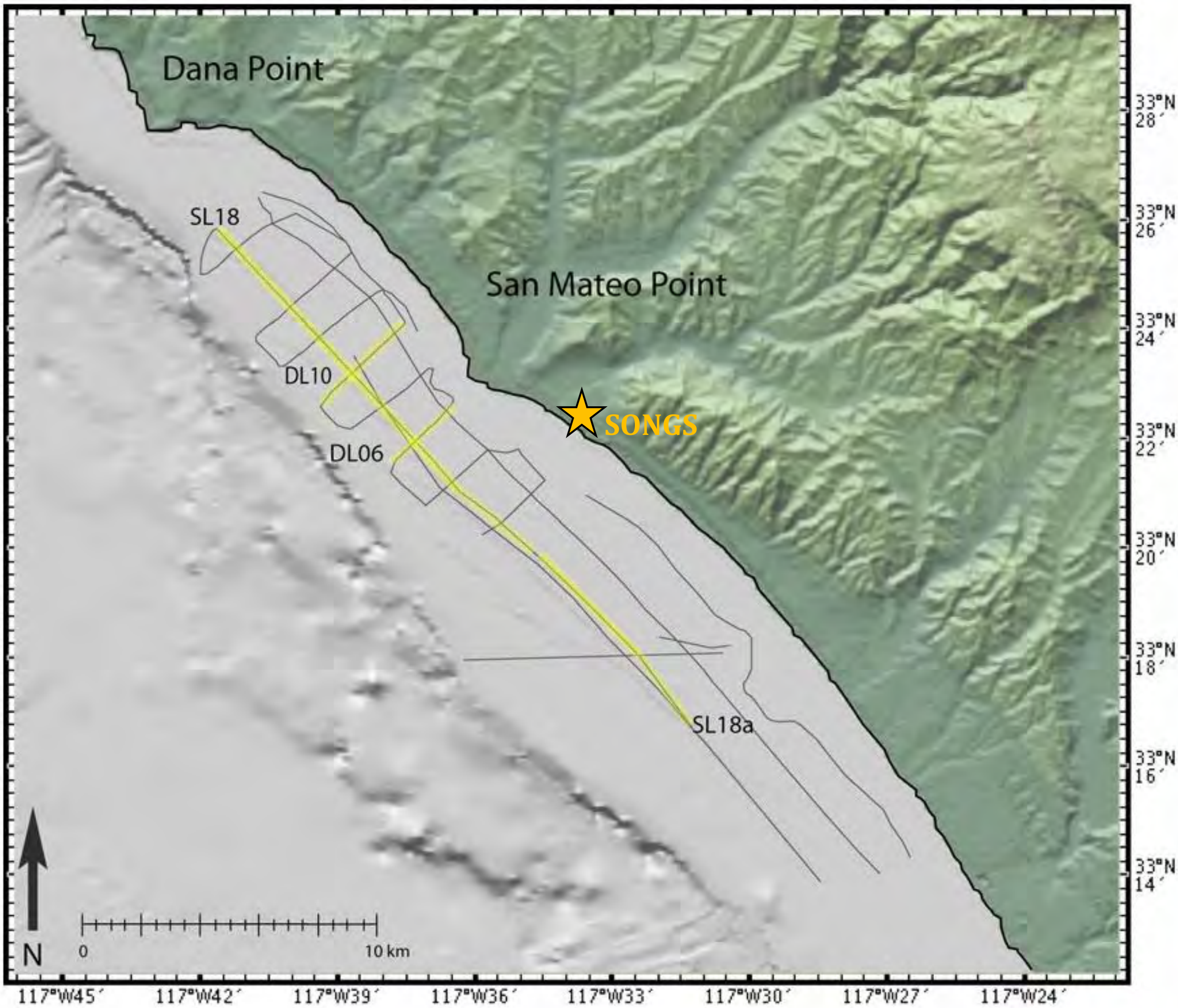

NOTE: Based on Rentz (2010)

GeoPentech
Geotechnical & Geoscience Consultants

SEISMIC LINE INTERPRETATIONS

FIGURE A-8a

SAN ONOFRE NUCLEAR GENERATING STATION

SEISMIC HAZARD ASSESSMENT PROGRAM

LINE DL10

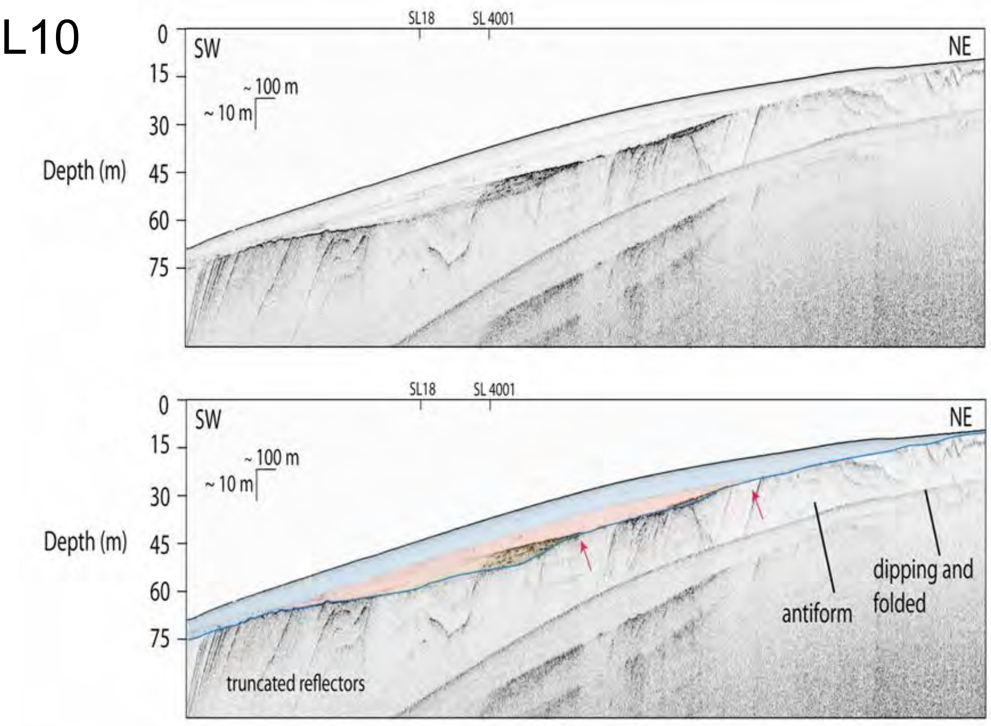

LINE DL06

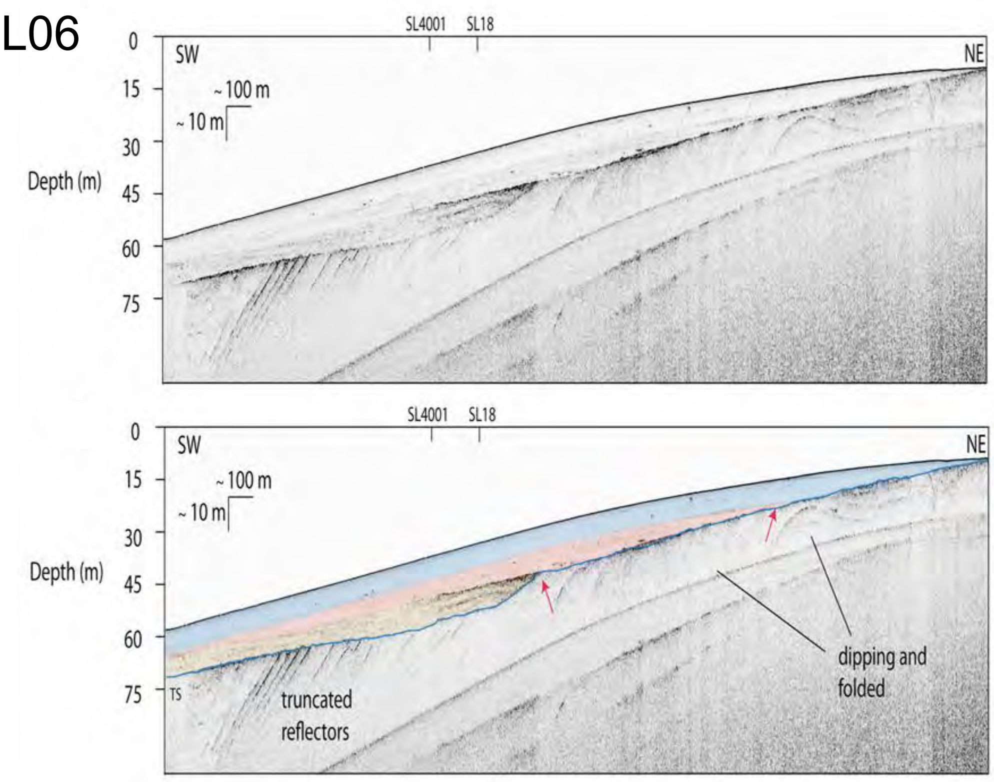

LINE SC18

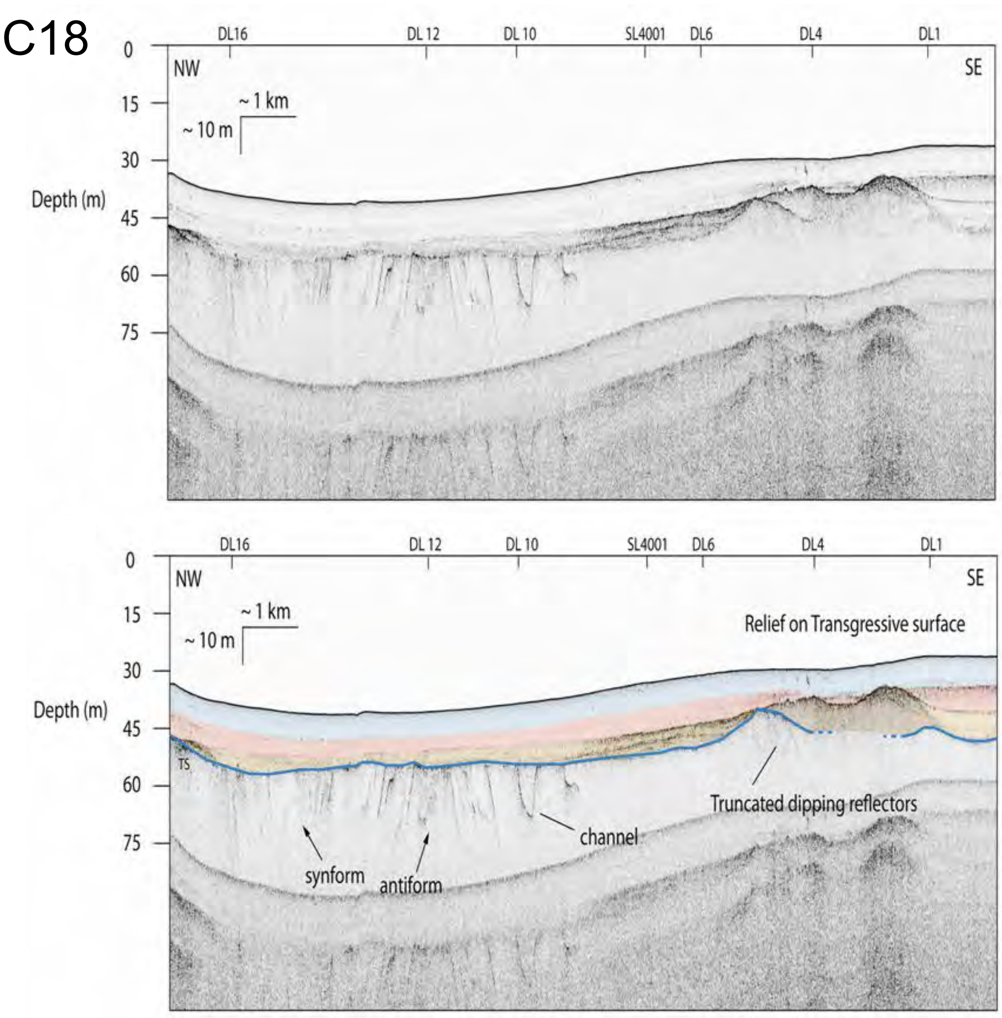

NOTES: (1) Based on Rentz (2010)
(2) Locations of seismic lines shown in Figure 8a

GeoPentech
Geotechnical & Geoscience Consultants

SEISMIC LINE INTERPRETATIONS

FIGURE
A-8b

SAN ONOFRE NUCLEAR GENERATING STATION

SEISMIC HAZARD ASSESSMENT PROGRAM

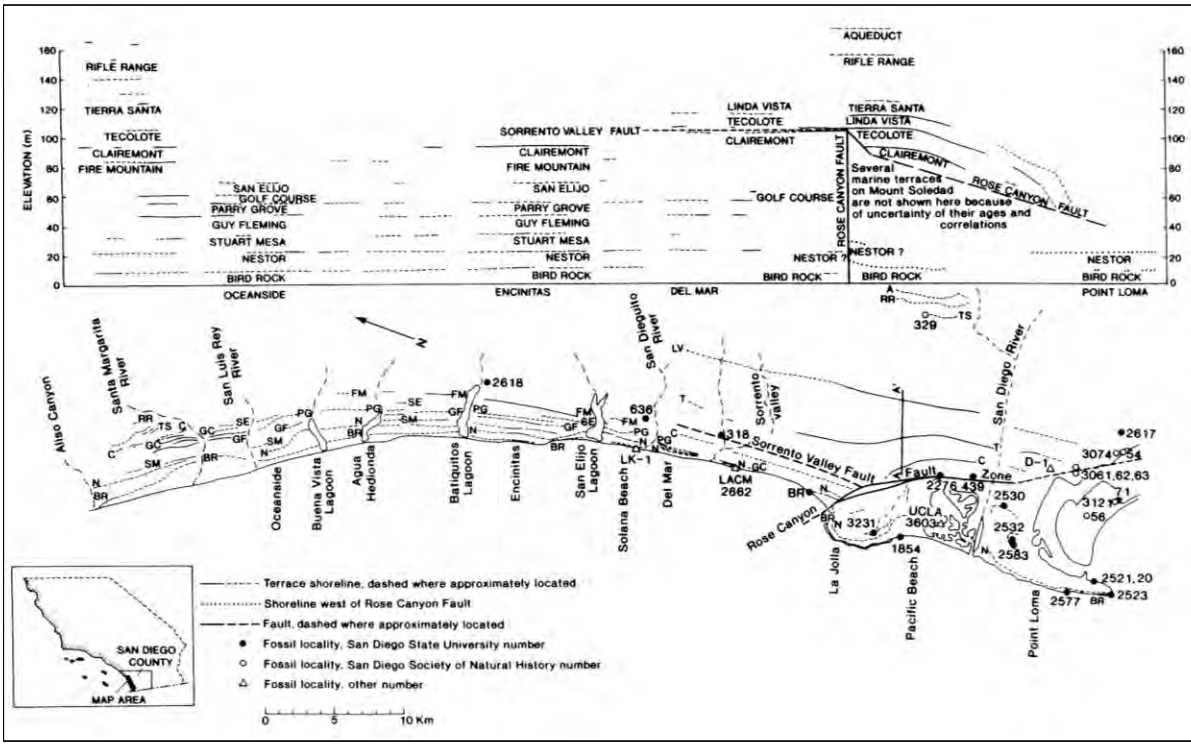

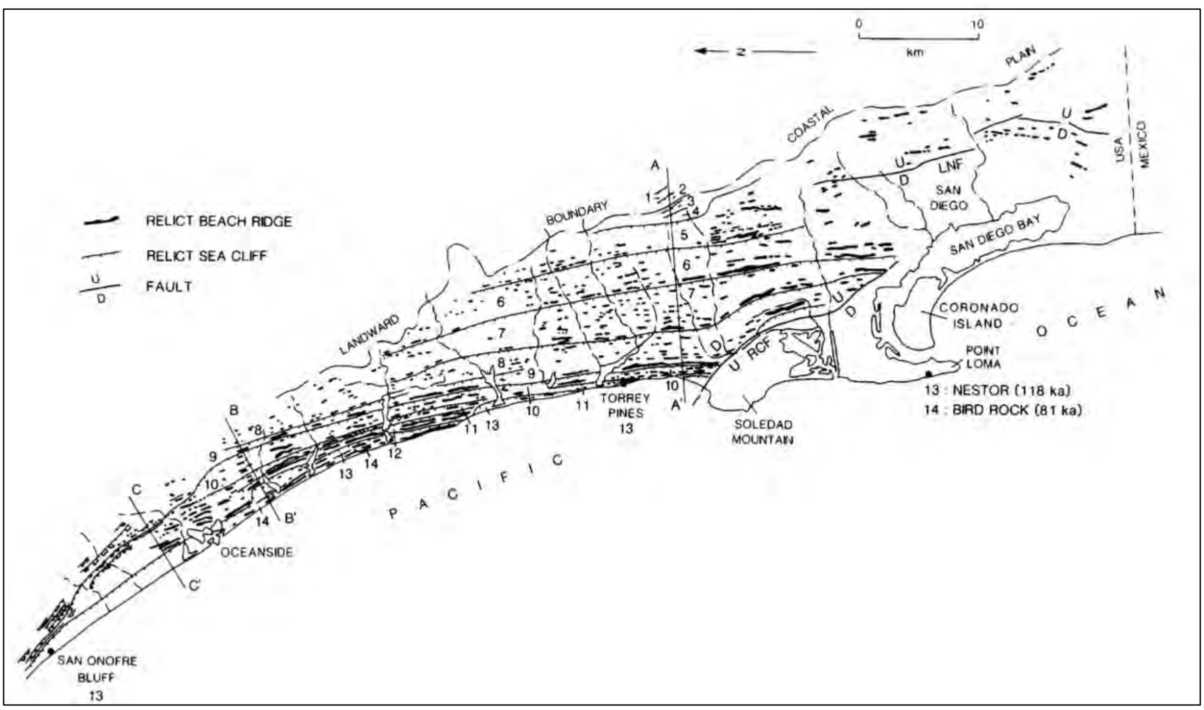

NOTES: (1) Top is from Kern & Rockwell (1992); Bottom is from Lajoie et al. (1992)
(2) Bottom presented in SCE (2001)

GeoPentech
Geotechnical & Geoscience Consultants

MAP OF MARINE TERRACES

FIGURE
A-9

SAN ONOFRE NUCLEAR GENERATING STATION

SEISMIC HAZARD ASSESSMENT PROGRAM

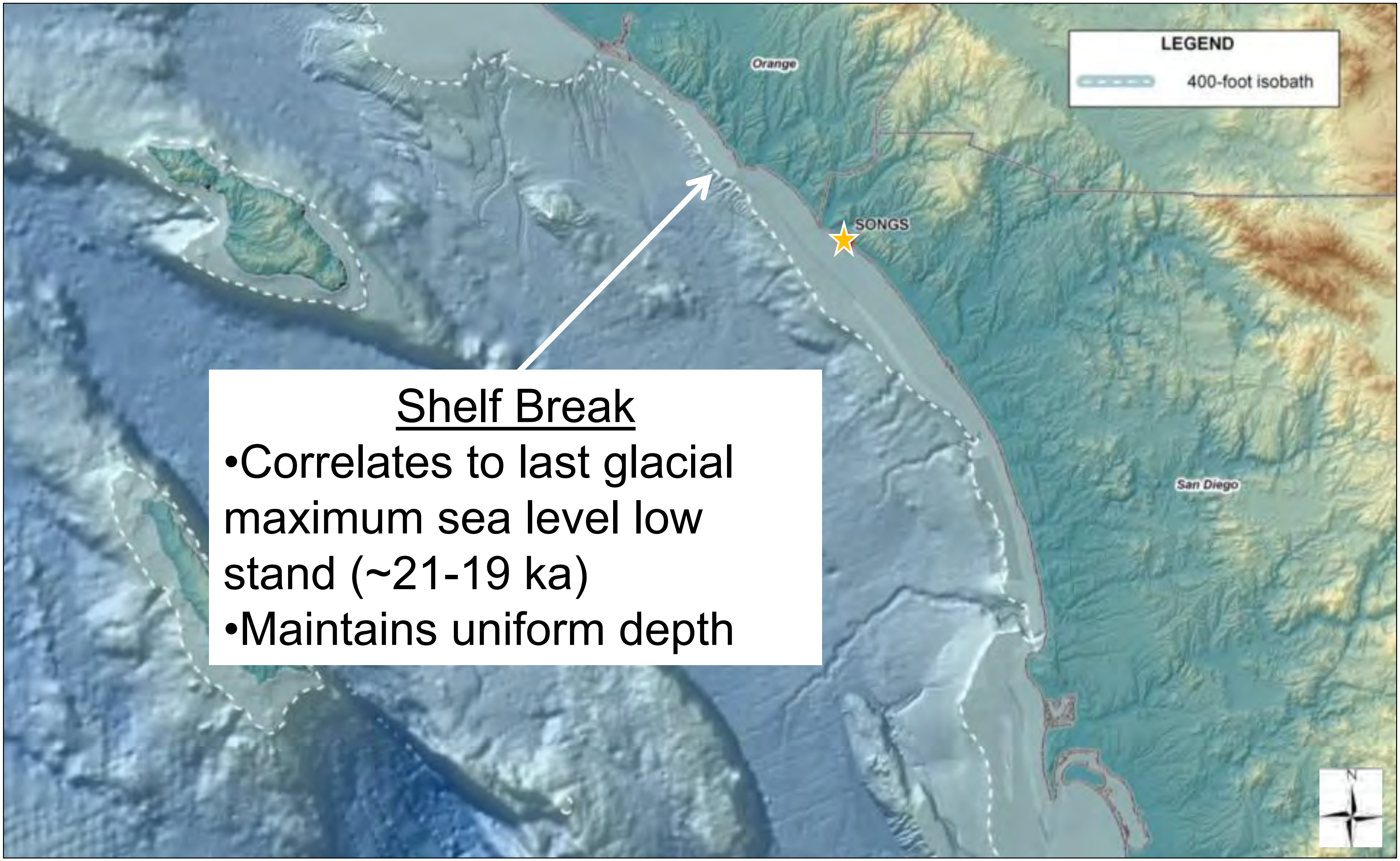

Modified from NOAA (2001, 2008), CSUMB (2010), and CaSIL (2006)

GeoPentech Geotechnical & Geoscience Consultants	**SAN ONOFRE NUCLEAR GENERATING STATION** SEISMIC HAZARD ASSESSMENT PROGRAM	**MAP OF SHELF BREAK**	FIGURE A-10

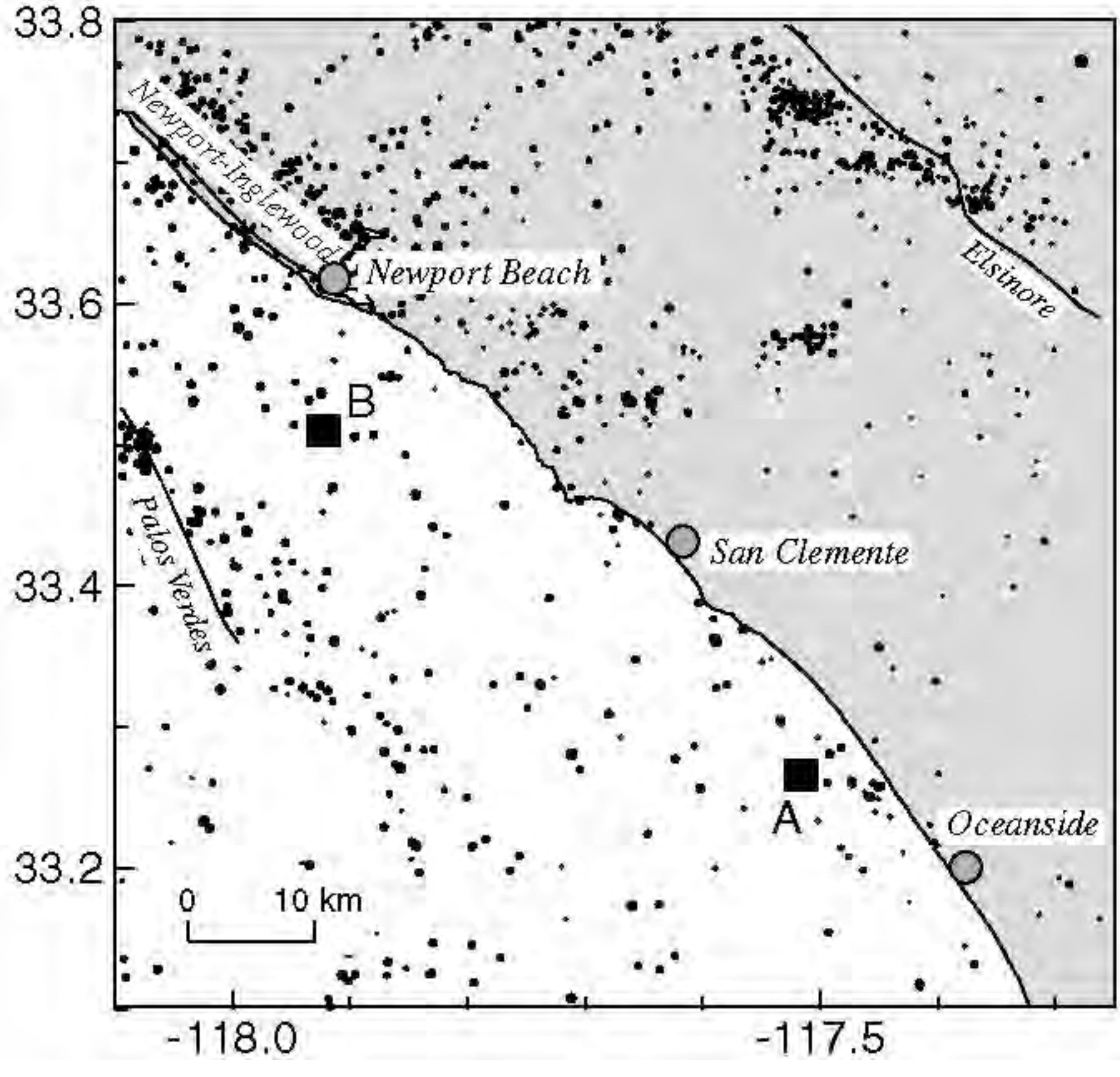

Source: Grant and Shearer (2004)

GeoPentech Geotechnical & Geoscience Consultants	**RELOCATED EPICENTERS FROM THE 1981 OCEANSIDE AND 2000 NEWPORT BEACH EARTHQUAKE CLUSTERS**	FIGURE A-11a
	SAN ONOFRE NUCLEAR GENERATING STATION SEISMIC HAZARD ASSESSMENT PROGRAM	

LOCATION A

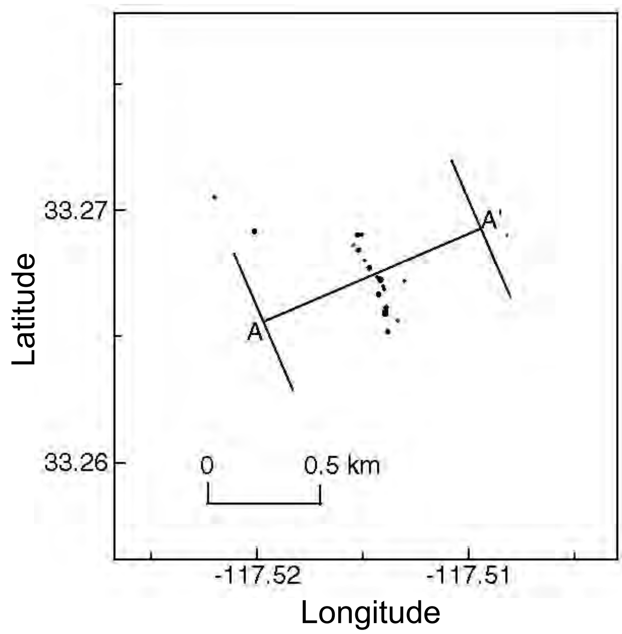

PLAN VIEW

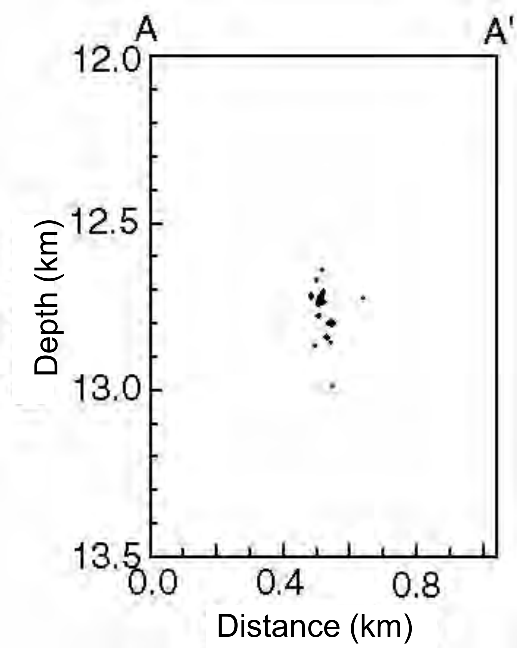

PROFILE VIEW

LOCATION B

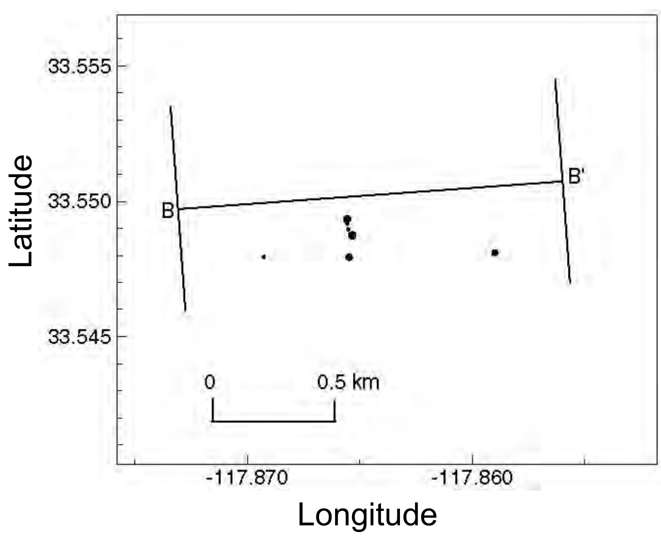

PLAN VIEW

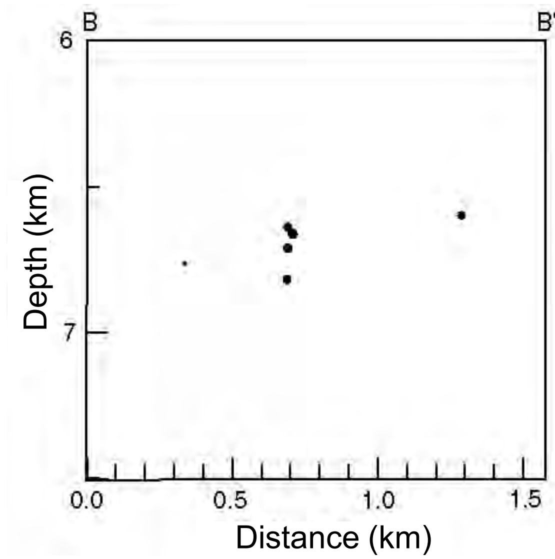

PROFILE VIEW

NOTES: (1) Modified from Grant and Shearer (2004)
(2) Locations of "A" and "B" shown in Figure A-11a

GeoPentech
Geotechnical & Geoscience Consultants

RELOCATED EPICENTERS FROM THE 1981 OCEANSIDE AND 2000 NEWPORT BEACH EARTHQUAKE CLUSTERS	FIGURE A-11b

SAN ONOFRE NUCLEAR GENERATING STATION

SEISMIC HAZARD ASSESSMENT PROGRAM

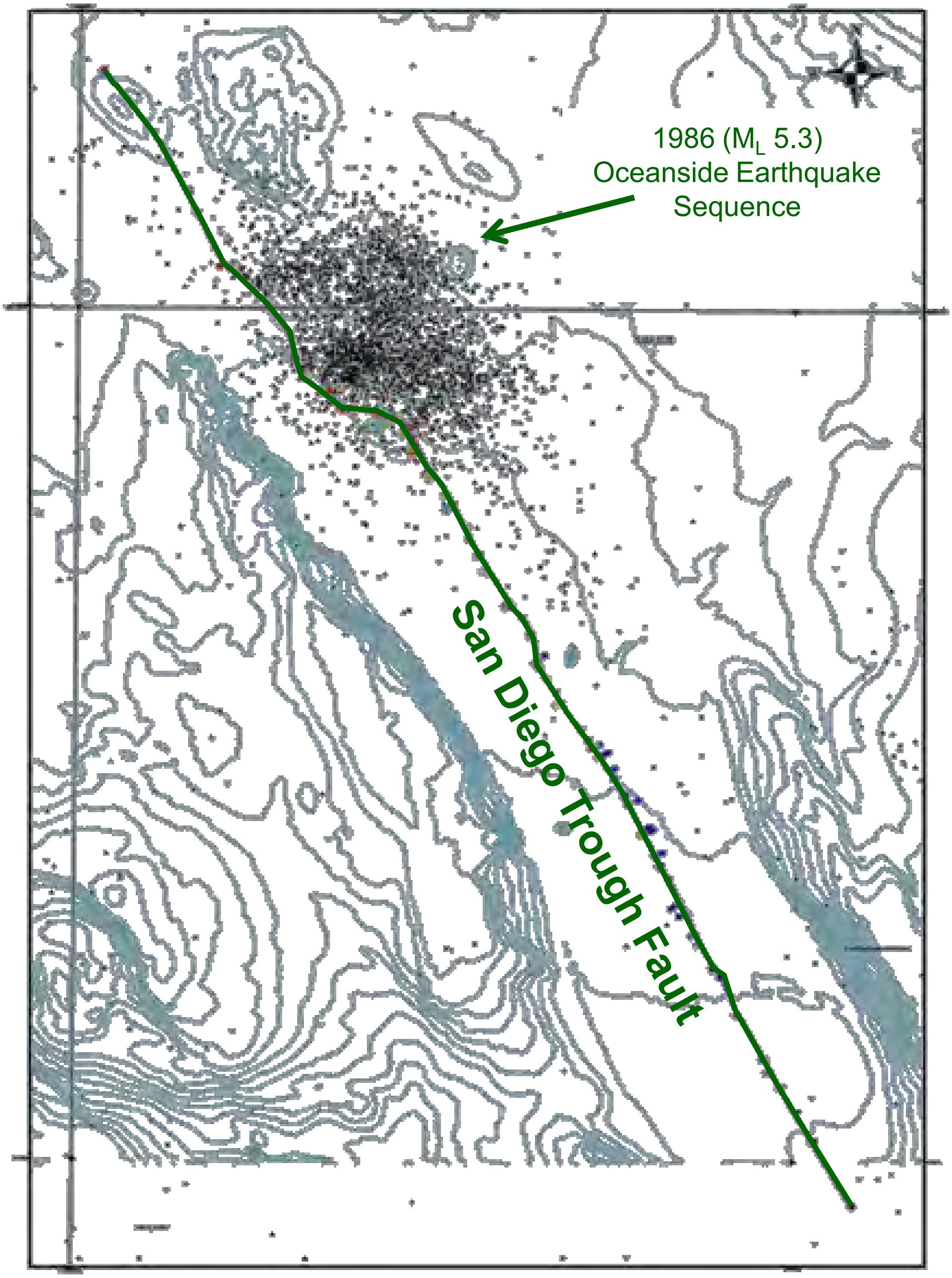

NOTE: Based on Ryan (2010, personal communication)

GeoPentech Geotechnical & Geoscience Consultants	RELOCATED EPICENTERS FROM THE 1986 OCEANSIDE EARTHQUAKE SEQUENCE	FIGURE A-12
	SAN ONOFRE NUCLEAR GENERATING STATION SEISMIC HAZARD ASSESSMENT PROGRAM	

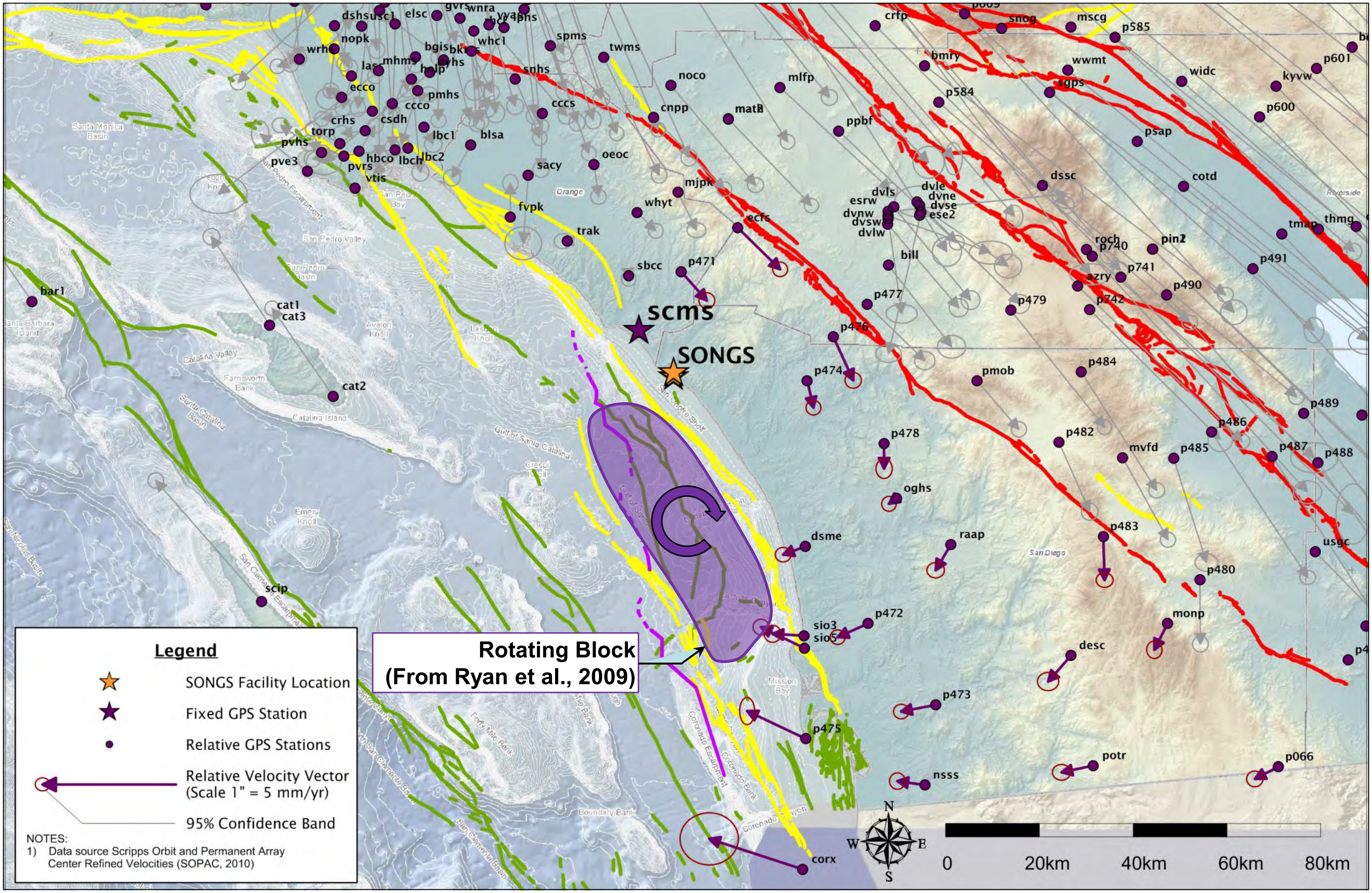

GeoPentech
Geotechnical & Geoscience Consultants

SAN ONOFRE NUCLEAR GENERATING STATION
SEISMIC HAZARD ASSESSMENT PROGRAM

GEODETIC DATA
VELOCITY RELATIVE TO SCMS

FIGURE
A-13

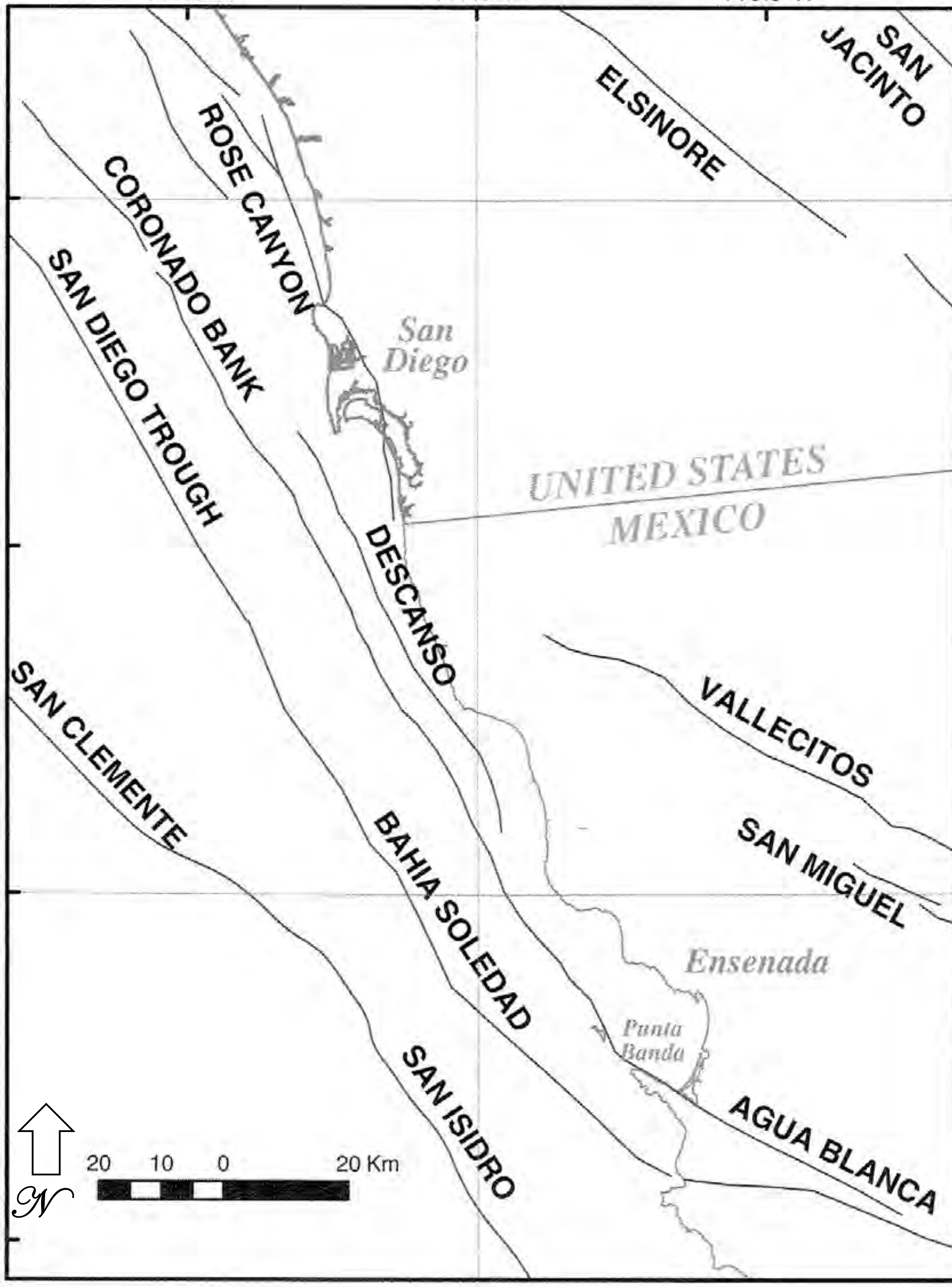

GeoPentech
Geotechnical & Geoscience Consultants

SIMPLIFIED FAULT MAP FOR BAJA CALIFORNIA, MEXICO REGION BY RYAN ET AL. (2009)

FIGURE A-14

SAN ONOFRE NUCLEAR GENERATING STATION

SEISMIC HAZARD ASSESSMENT PROGRAM

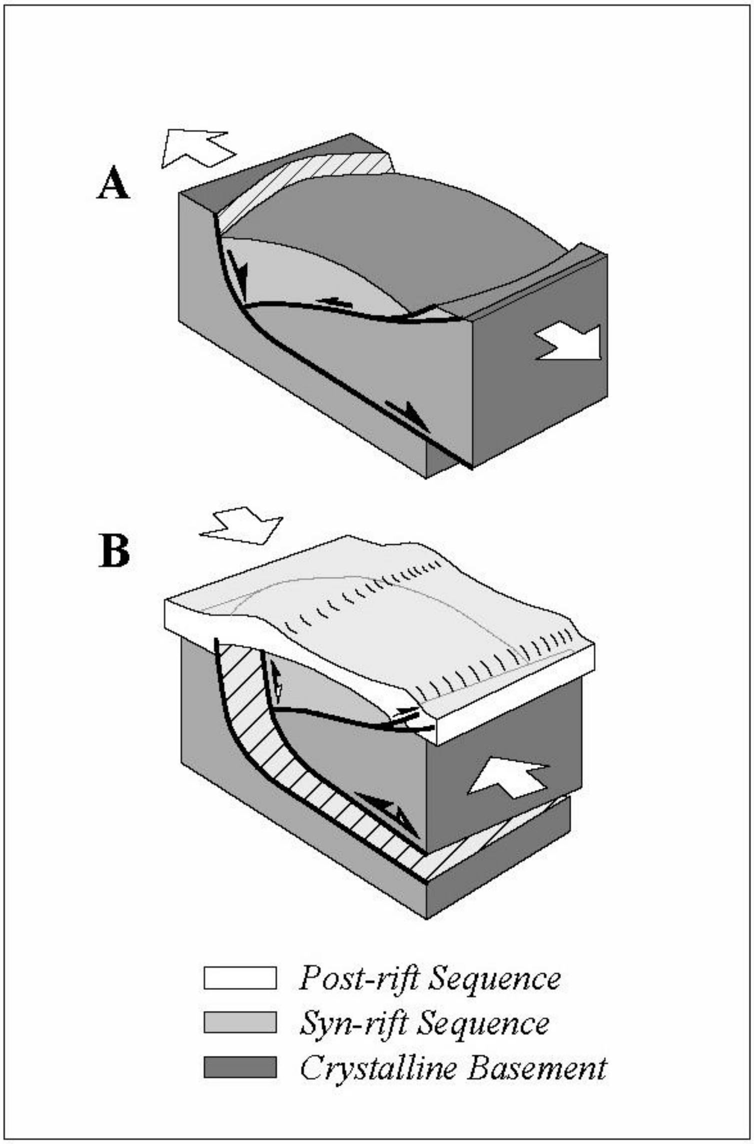

Conceptual model of basin inversion of a half–graben structure due to transpressional tectonics and wedging [modified after Bally, 1984]. **(A)** Development of the half–graben and associated roll-over structure by normal slip on an extensional detachment **(B)** Basin inversion phase characterized by development of a hanging–wall wedge and asymmetrical contractional folds due to the reactivation of the extensional detachment.

Source: Rivero (2004)

GeoPentech Geotechnical & Geoscience Consultants	SCHEMATIC DIAGRAM OF BASIN INVERSION PROCESS AND EVOLUTION	FIGURE A-15
	SAN ONOFRE NUCLEAR GENERATING STATION SEISMIC HAZARD ASSESSMENT PROGRAM	

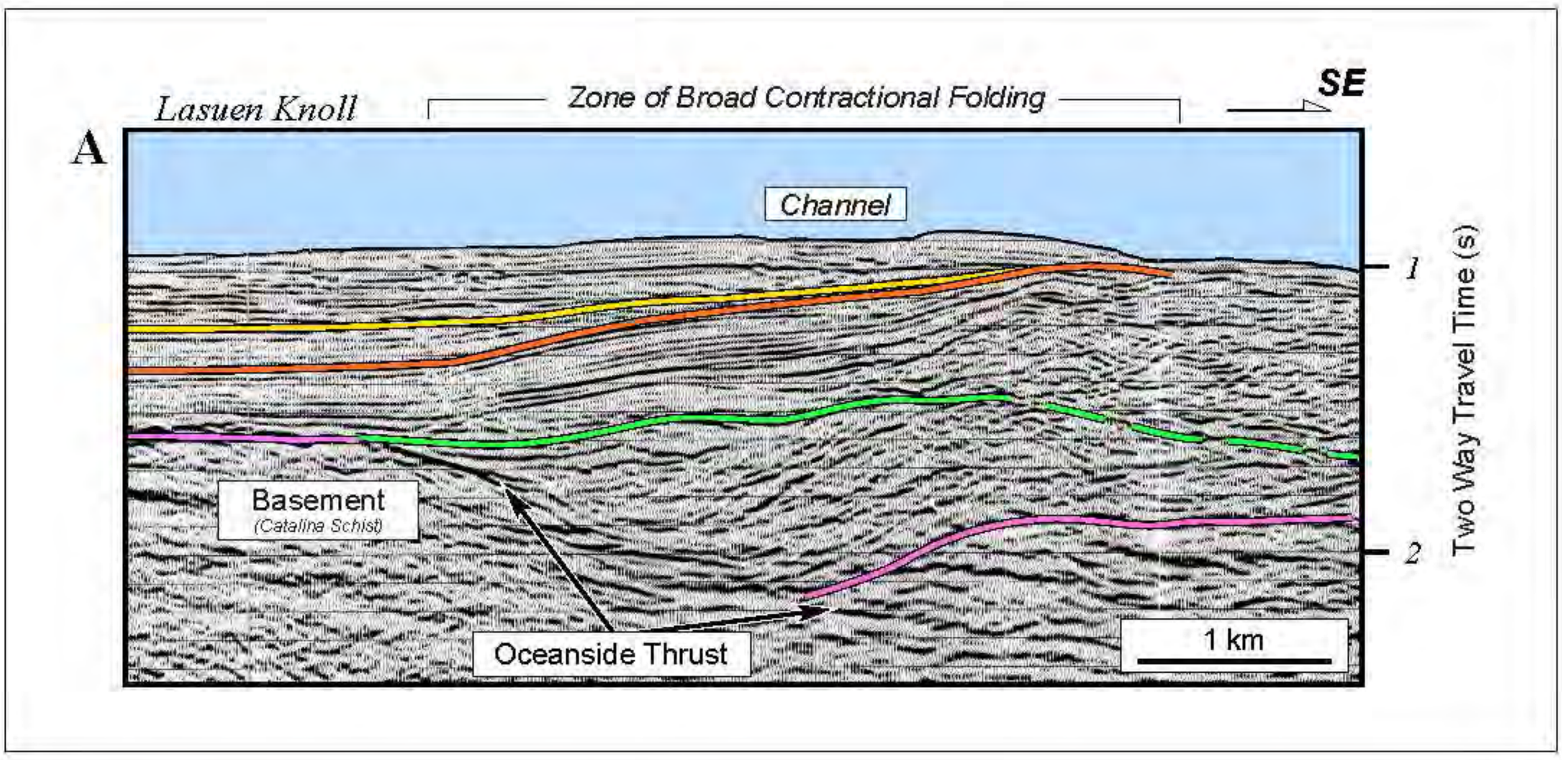

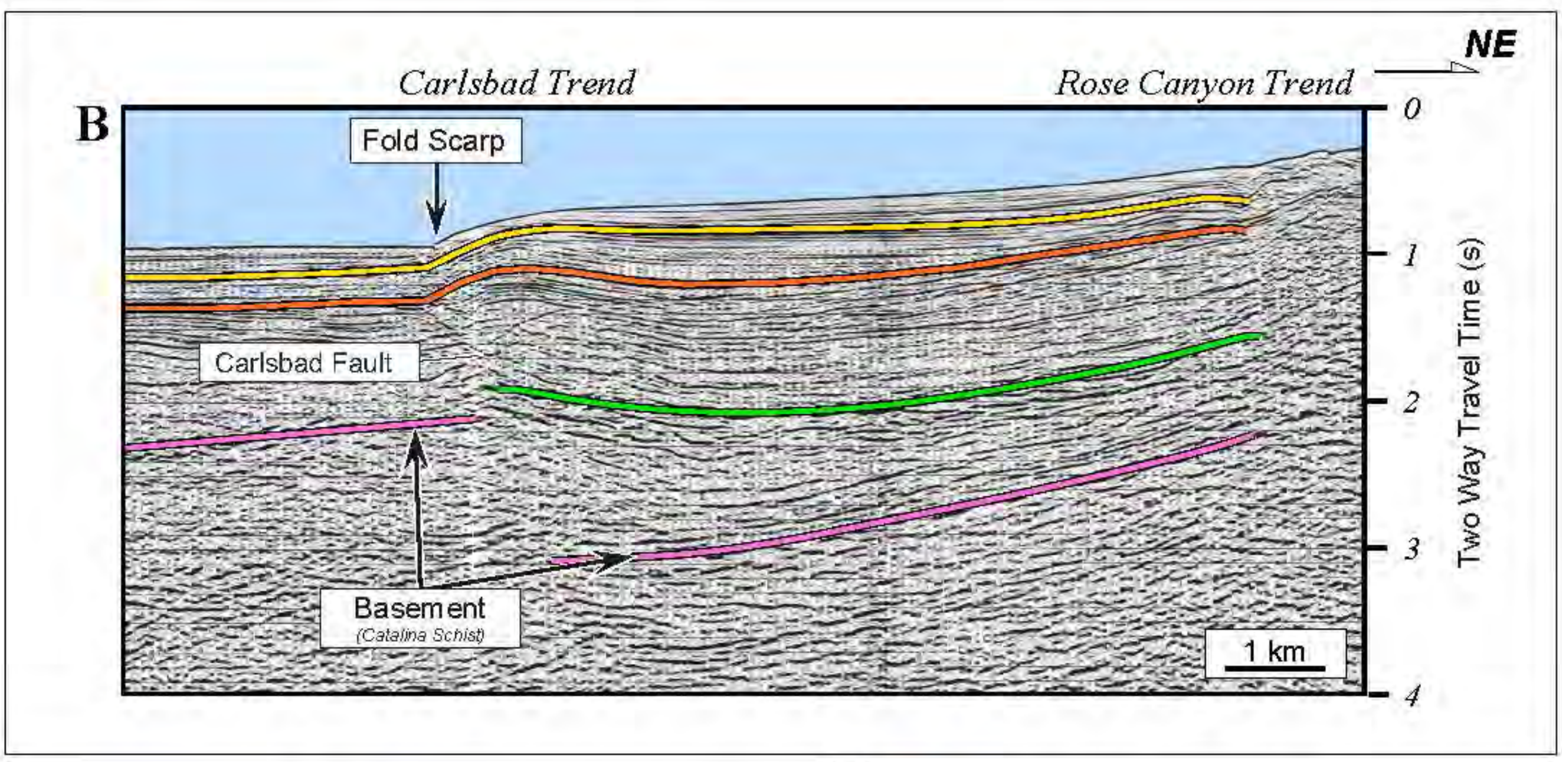

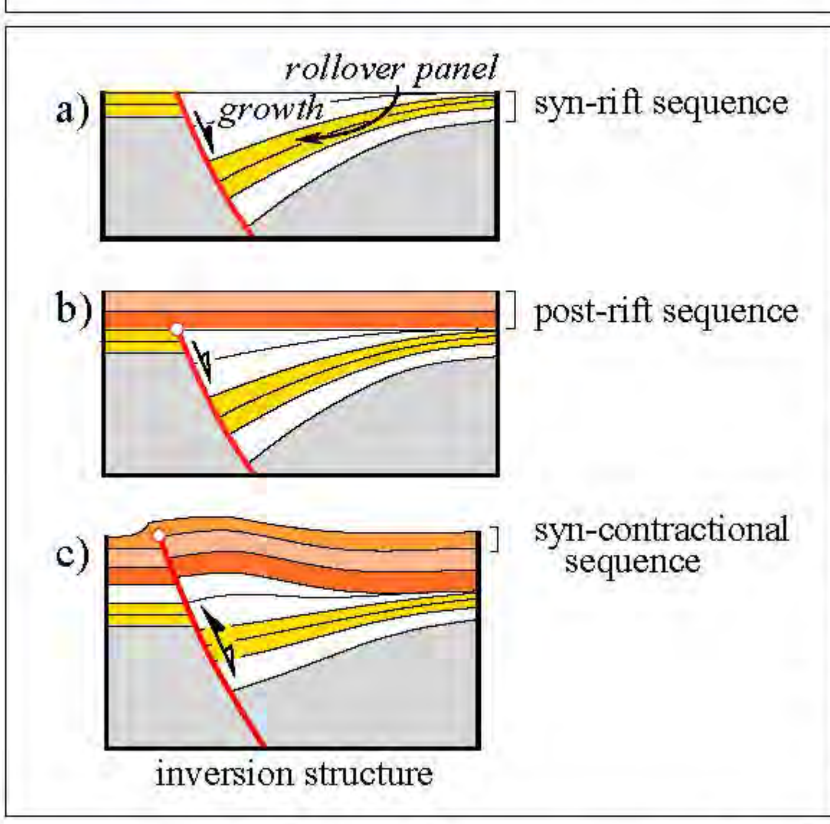

Seismic examples of basin inversion structures associated with activity of the Oceanside Thrust. **(A)** Half–graben reactivation along a lateral ramp of the Oceanside Thrust. **(B)** Tip–fold structure developed by contractional reactivation of the Carlsbad fault, which is located within the hanging wall block of the Oceanside Thrust. In both cases divergent termination of the seismic reflections within the Monterrey Fm. define the stratigraphic expansion of the syn–rift sequence. Similarly, the phase of basin inversion is well recorded by the contractional geometry, internal onlap terminations, and general thinning of the syn–contractional Pico Fm. on the crest of the anticlines. **Inset:** Conceptual model of basin inversion after Bally [1984] and Letouzey [1990]. **(a)** Development of the extensional half–graben and associated rollover structure, **(b)** Period of quiescence and sedimentation of the post–rift sediments, **(c)** Reactivation of the normal fault with development of asymmetrical contractional fold. The model highlights the stratigraphic relationships between the three main tectonosequences characteristics of basin inversion. Location of the seismic lines is shown in Figure 3.5.

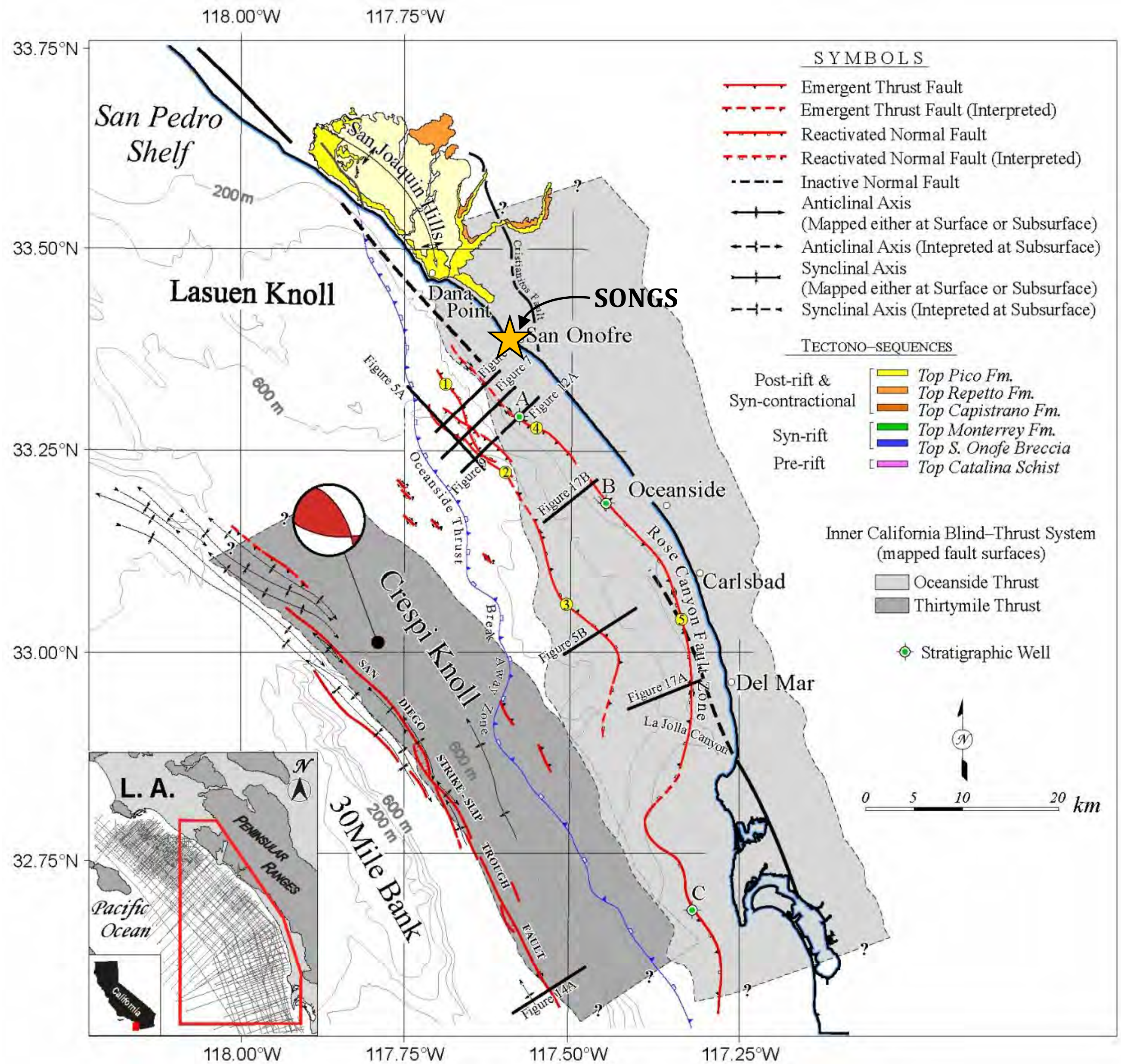

GeoPentech
Geotechnical & Geoscience Consultants

SAN ONOFRE NUCLEAR GENERATING STATION

SEISMIC HAZARD ASSESSMENT PROGRAM

FAULT MAP BY RIVERO AND SHAW (IN PRESS, 2010)

FIGURE A-17

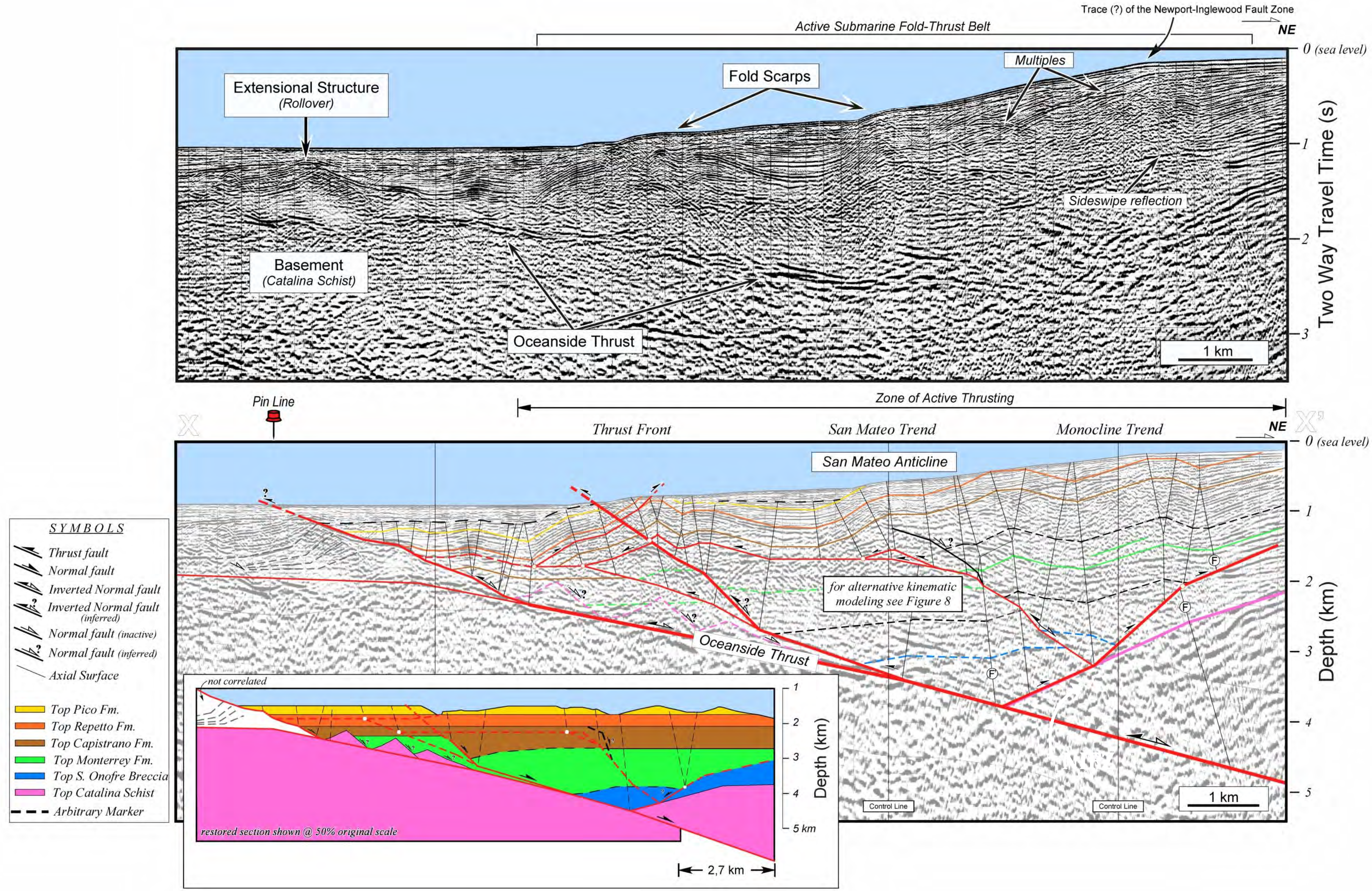

GeoPentech
Geotechnical & Geoscience Consultants

SAN ONOFRE NUCLEAR GENERATING STATION

SEISMIC HAZARD ASSESSMENT PROGRAM

SEISMIC REFLECTION PROFILE AND INTERPRETATION OF THE FOLD AND THRUST BELT SOUTH OF LASUEN KNOLL FROM RIVERO (2004)

FIGURE A-18

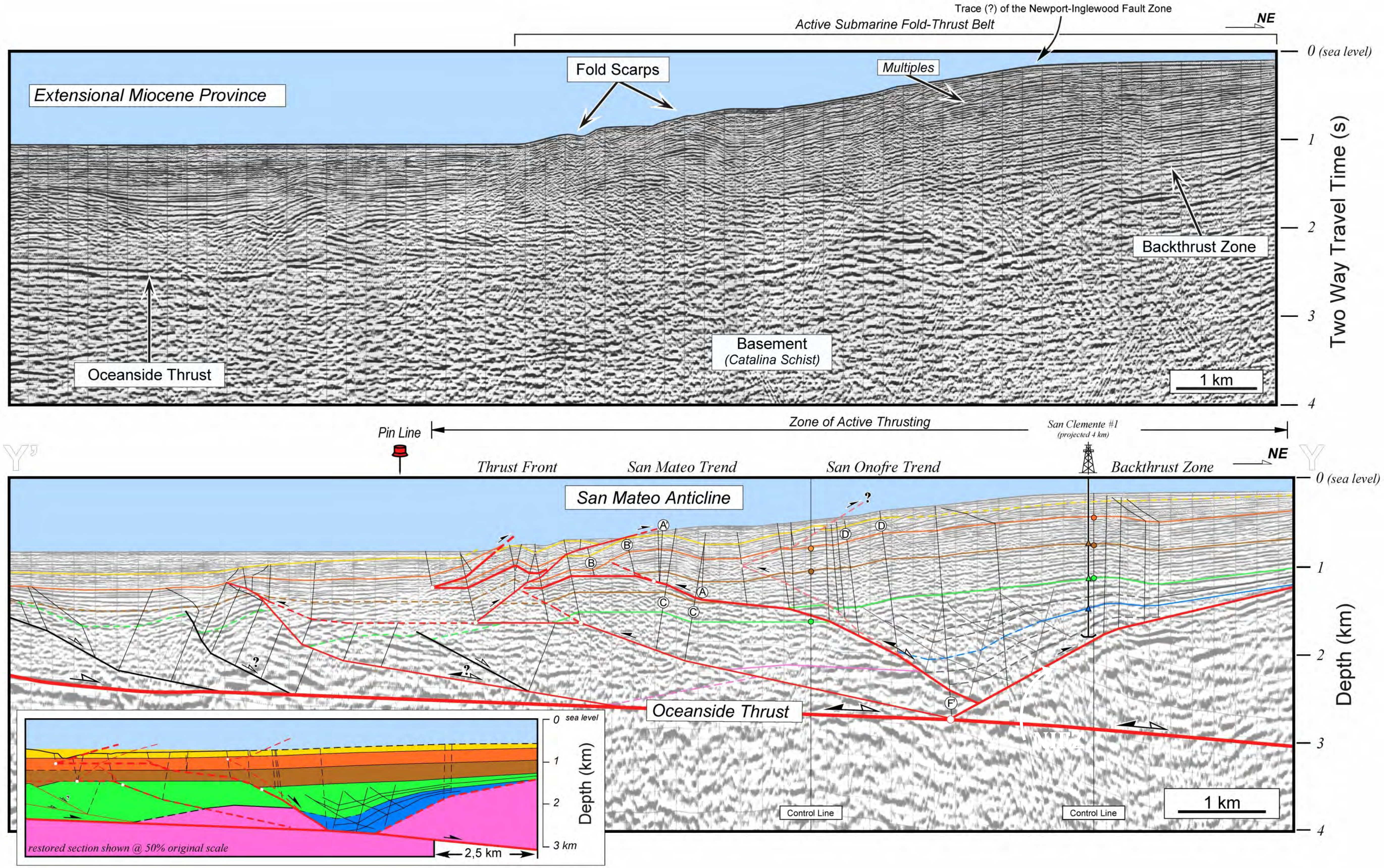

SAN ONOFRE NUCLEAR GENERATING STATION

SEISMIC HAZARD ASSESSMENT PROGRAM

SEISMIC REFLECTION PROFILE AND INTERPRETATION OF THE SAN MATEO TREND FROM RIVERO (2004)

FIGURE A-19

GeoPentech
Geotechnical & Geoscience Consultants

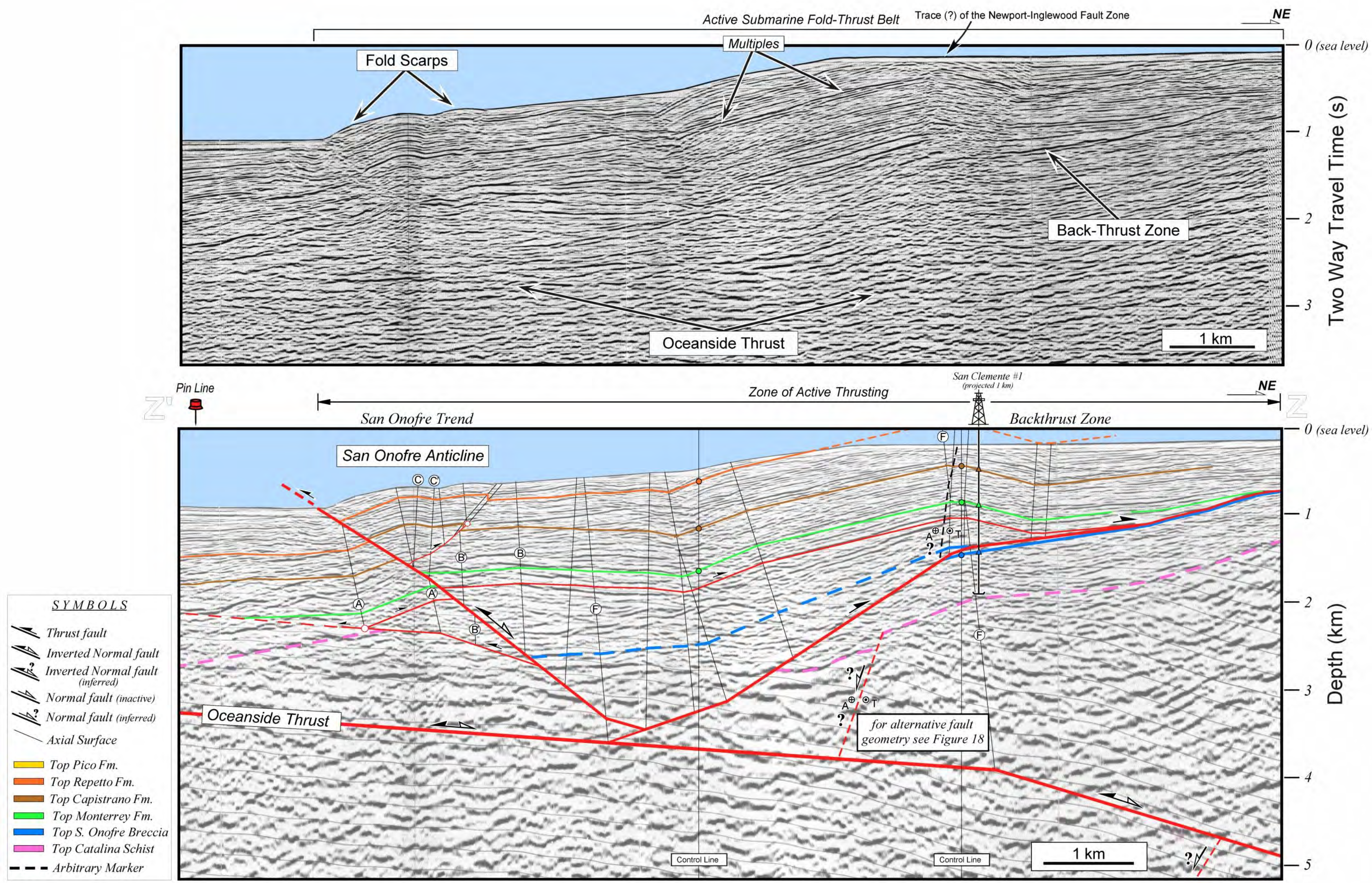

GeoPentech
Geotechnical & Geoscience Consultants

SAN ONOFRE NUCLEAR GENERATING STATION

SEISMIC HAZARD ASSESSMENT PROGRAM

SEISMIC REFLECTION PROFILE AND INTERPRETATION OF THE CARLSBAD TREND FROM RIVERO (2004)

FIGURE A-20

Diagramatic representation of the main structural elements and trends observed along transects X–X', Y–Y', and Z–Z'. The representation illustrates the lateral continuity of the offshore-dipping monocline, and the role of the Oceanside thrust as a regional basal detachment level. The diagram also highlights the complex arrangements of the modern contractional trends withint the active submarine fold–thrust belt, and the control induced by the Miocene normal fault system and the propagating structural wedge in their location. A common pitfall in structural interpretation is also evident, the most important fold structure in a profile do not necessarily correlates across the trends (i.e: observed the transicion of the San Mateo and San Onofre anticlines between profiles 2 and 3). Several basement riders located on top of the Oceanside thrust have been indetified based on local seismic expression. Some geometries have been simplified for clarity. The presence of the Newport–Inglewoodstrike–slip fault is inferred as restricted to the monocline location on Plate 3. Some modest amounts of dextral movement in the contractional trends is compatible with the interpretation and cannot be completely ruled out.

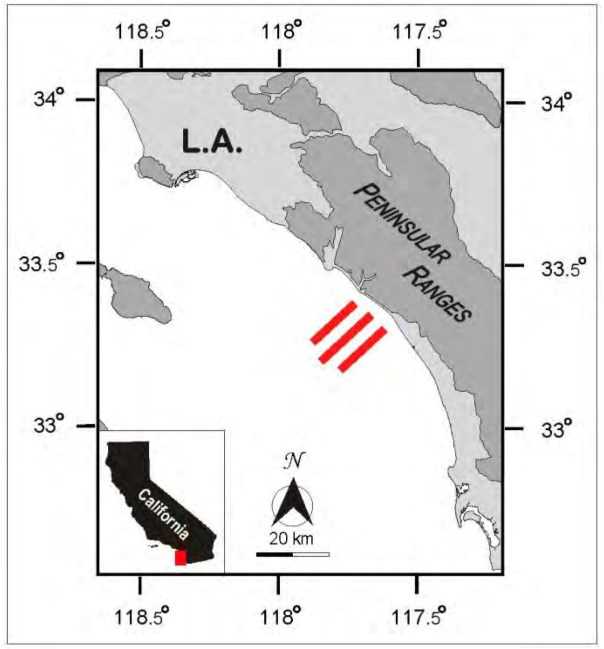

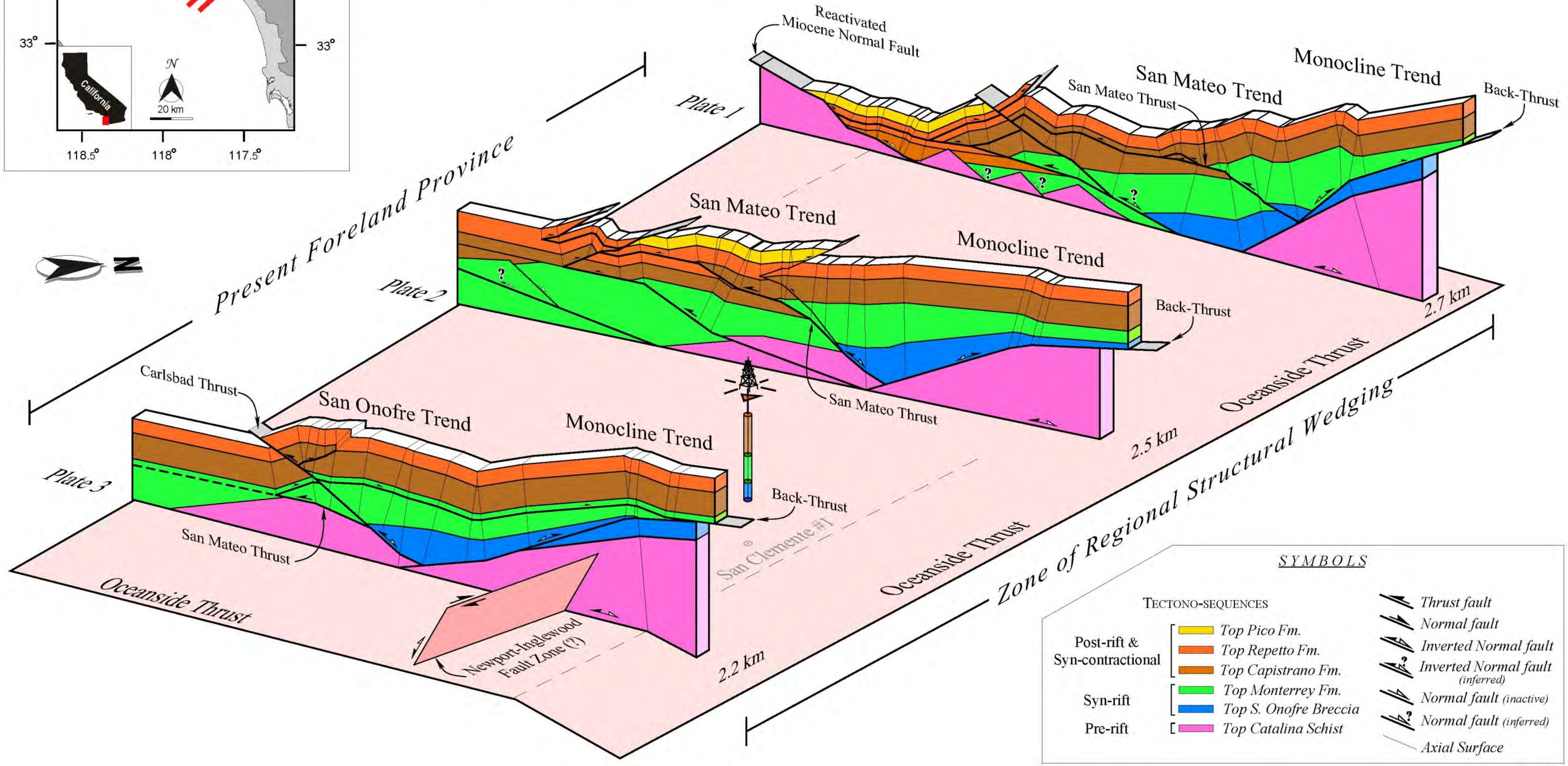

Modified from Rivero (2004)

GeoPentech Geotechnical & Geoscience Consultants	SAN ONOFRE NUCLEAR GENERATING STATION SEISMIC HAZARD ASSESSMENT PROGRAM	3D STRUCTURAL MAP OF FOLDING AND THRUSTING OFFSHORE SAN ONOFRE	FIGURE A-21

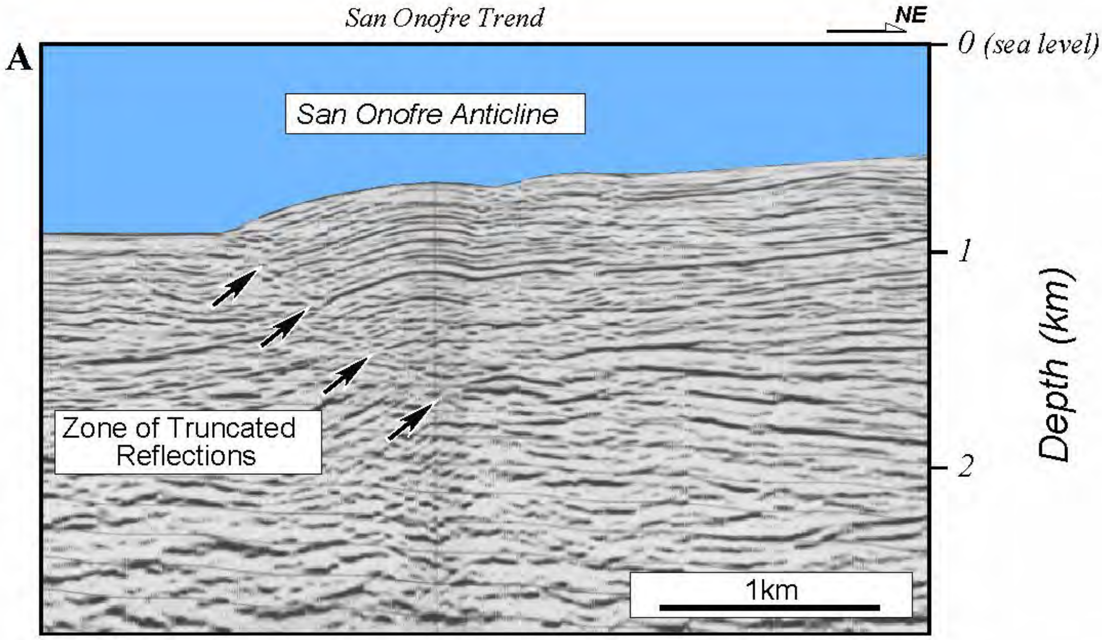

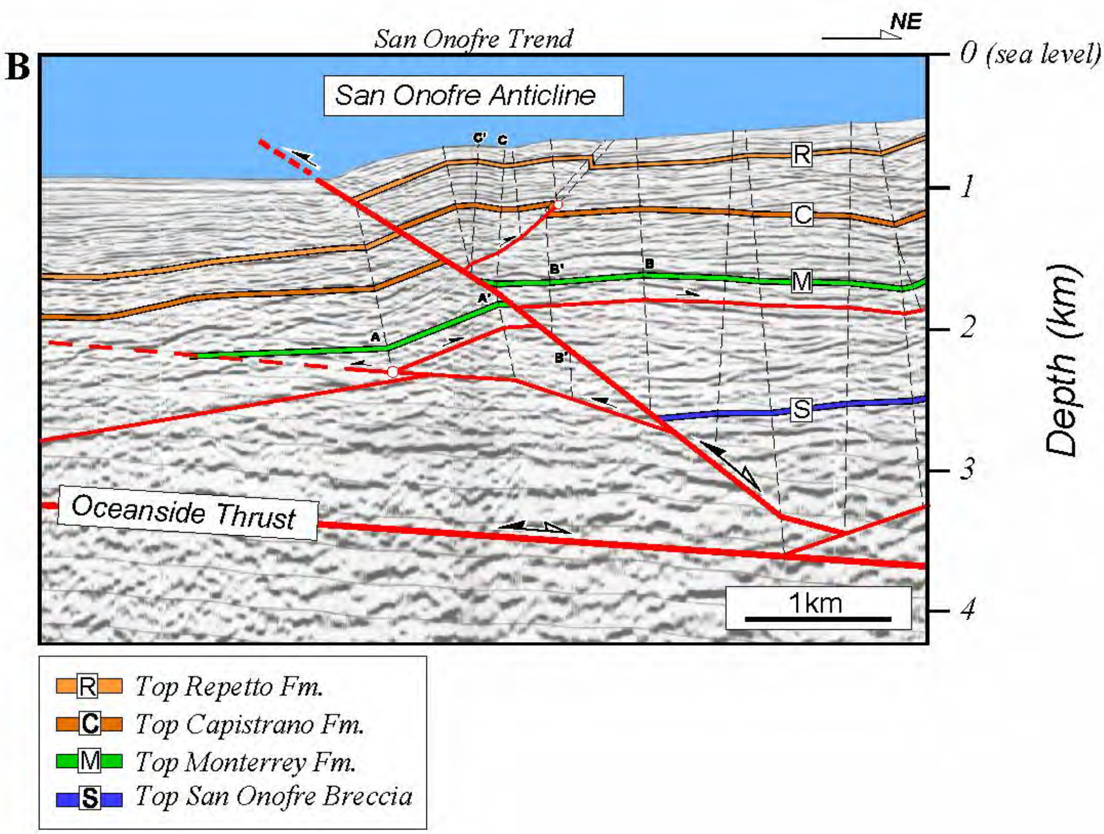

GeoPentech
Geotechnical & Geoscience Consultants

SEISMIC REFLECTION PROFILE AND INTERPRETATION OF THE SAN ONOFRE TREND FROM RIVERO (2004)

FIGURE A-22

SAN ONOFRE NUCLEAR GENERATING STATION

SEISMIC HAZARD ASSESSMENT PROGRAM

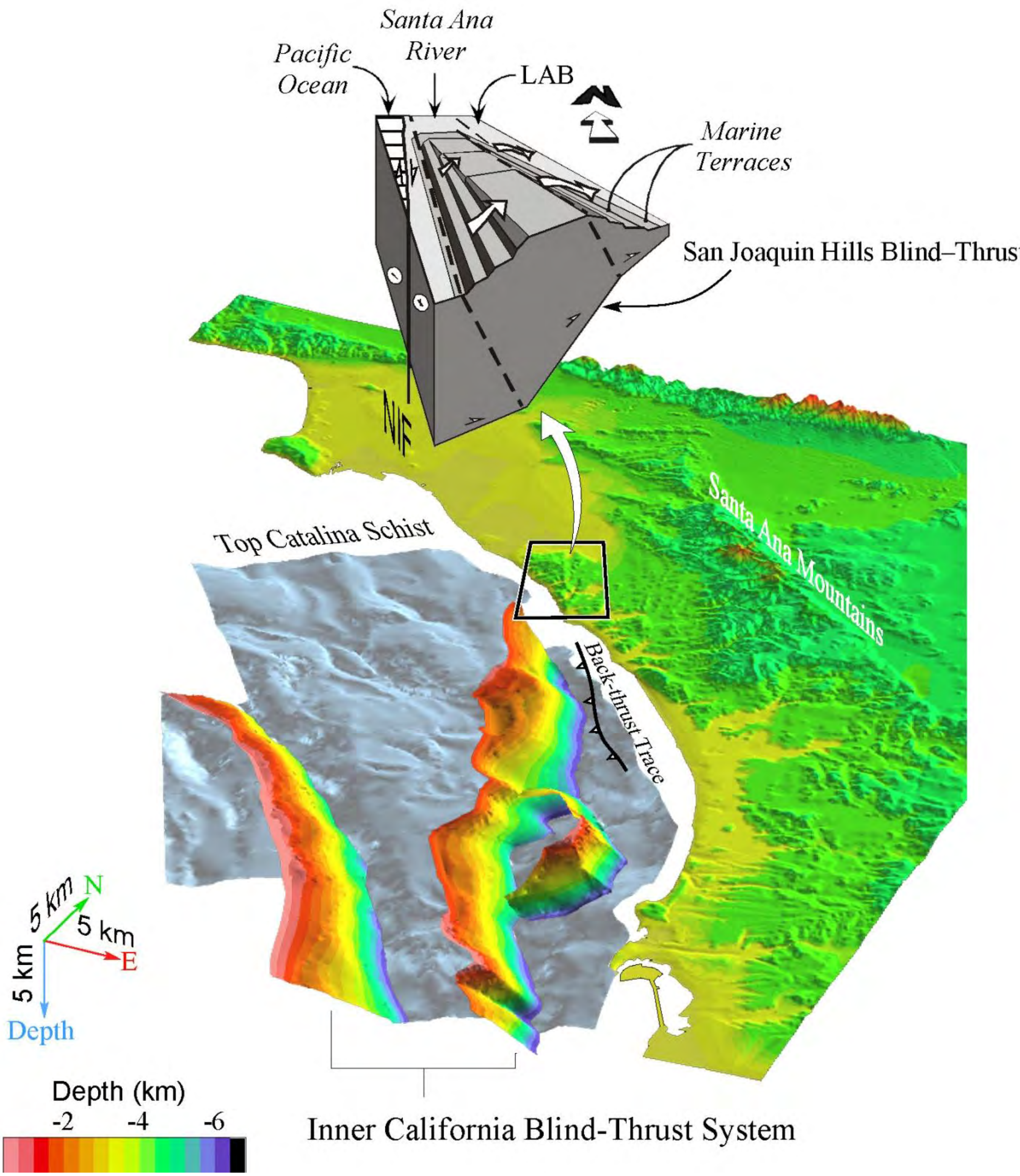

Source: Rivero (2004)

GeoPentech Geotechnical & Geoscience Consultants	SCHEMATIC DIAGRAM RELATING THE INNER CALIFORNIA BLIND THRUST SYSTEM TO THE SAN JOAQUIN HILLS	FIGURE A-23
	SAN ONOFRE NUCLEAR GENERATING STATION SEISMIC HAZARD ASSESSMENT PROGRAM	

Computed contractional slip on the Oceanside Thrust derived using the excess–area method discussed in Appendix B. Dashed lines represent maximum and minimum values yielded by the method, when accounting for uncertainties on the geometry of the Oceanside Thrust, and on the depth–conversion process. Fault slip measurements derived from balanced structural interpretations (Plates 1 to 3, and Figure 3.11) , and slip estimates derived from GPS analysis [Kier and Mueller, 1999] are also shown.

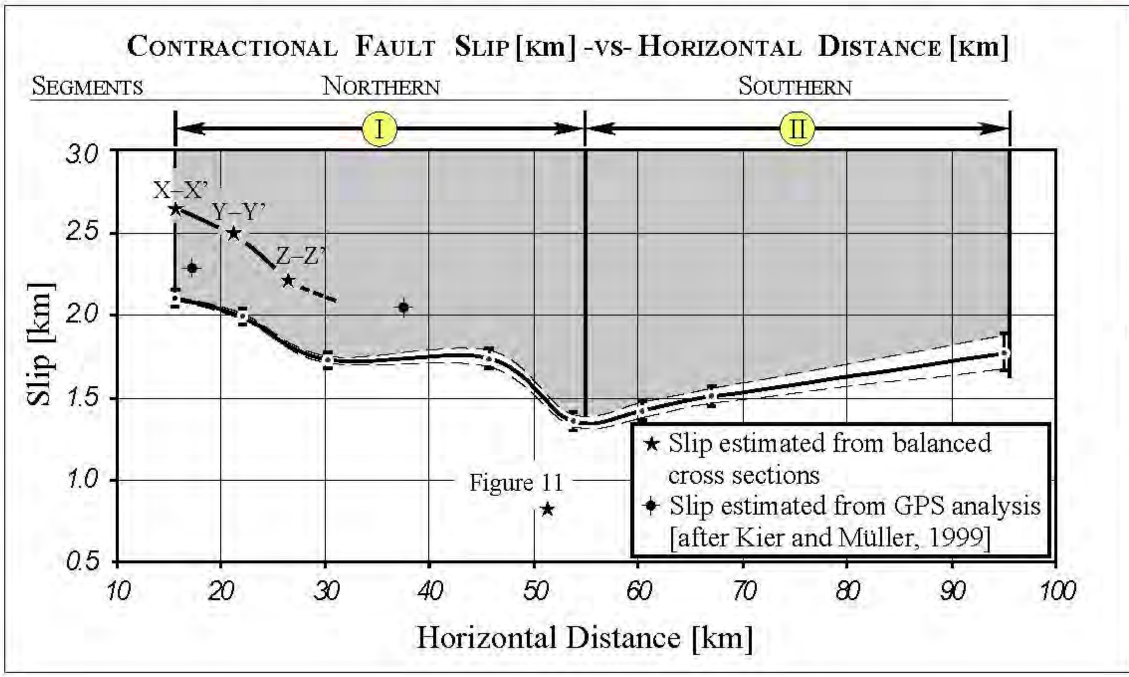

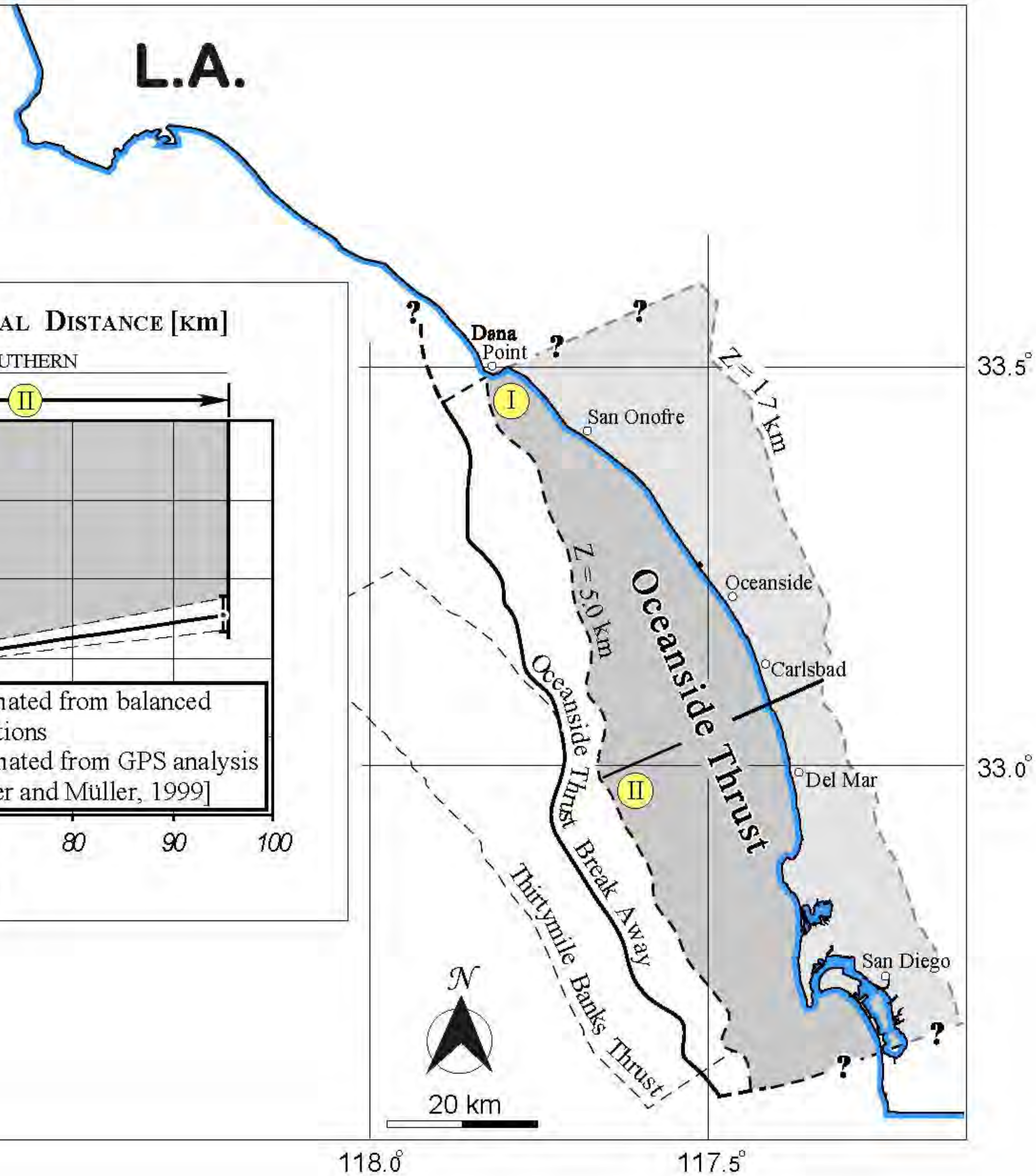

SEISMOGENIC AREAS

Segment I: 1,242.0 km^2

Segment II: 1,921.3 km^2

Total Area (Segment I + II): 3,163.5 km^2

GeoPentech
Geotechnical & Geoscience Consultants

SAN ONOFRE NUCLEAR GENERATING STATION

SEISMIC HAZARD ASSESSMENT PROGRAM

VARIABILITY OF CONTRACTIONAL SLIP ALONG THE OBT FAULT LENGTH FROM RIVERO (2004)

FIGURE A-24

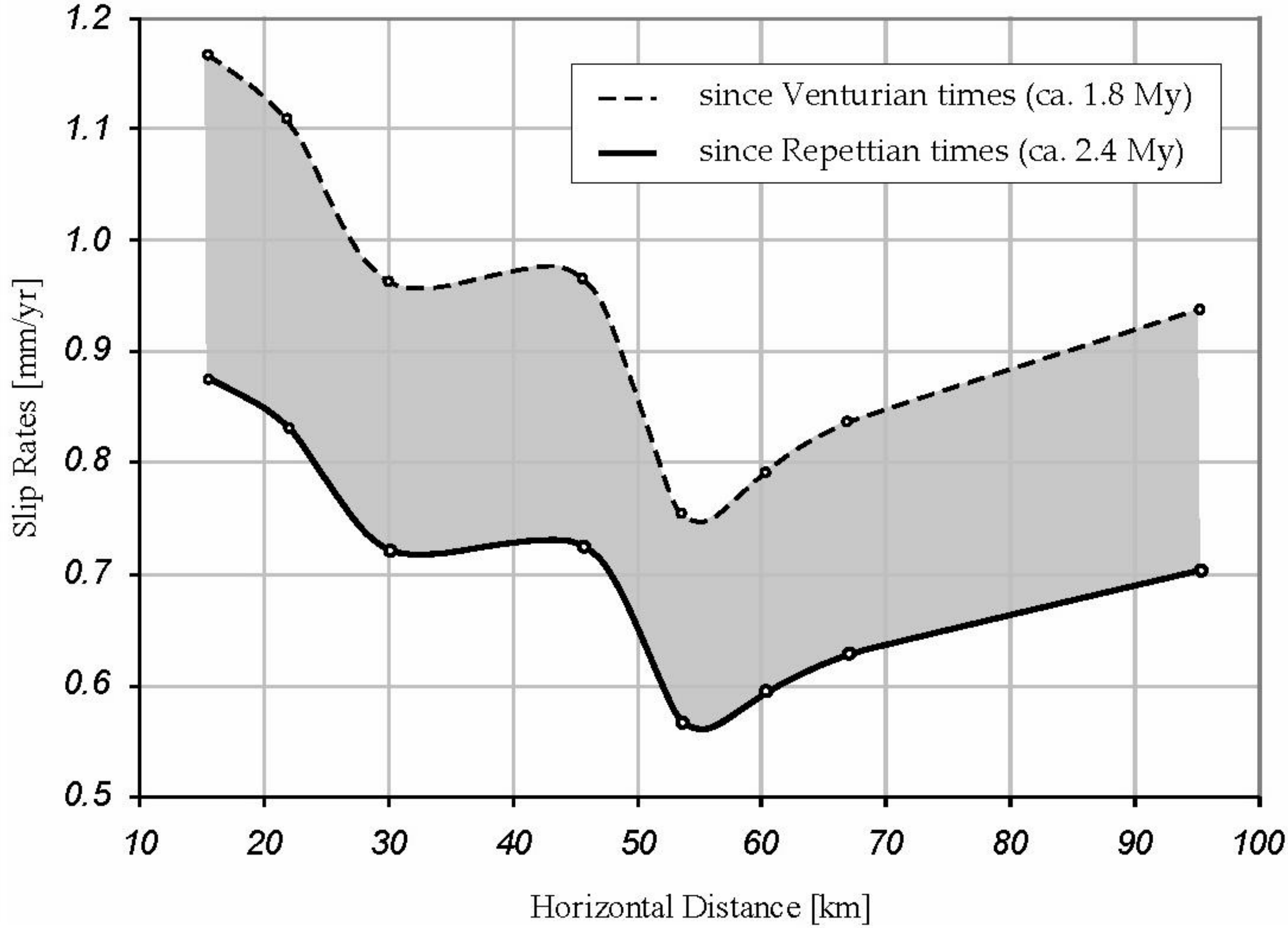

GeoPentech
Geotechnical & Geoscience Consultants

SAN ONOFRE NUCLEAR GENERATING STATION
SEISMIC HAZARD ASSESSMENT PROGRAM

PLOT OF MAXIMUM SLIP RATES FOR THE OBT FROM RIVERO (2004)

FIGURE A-25

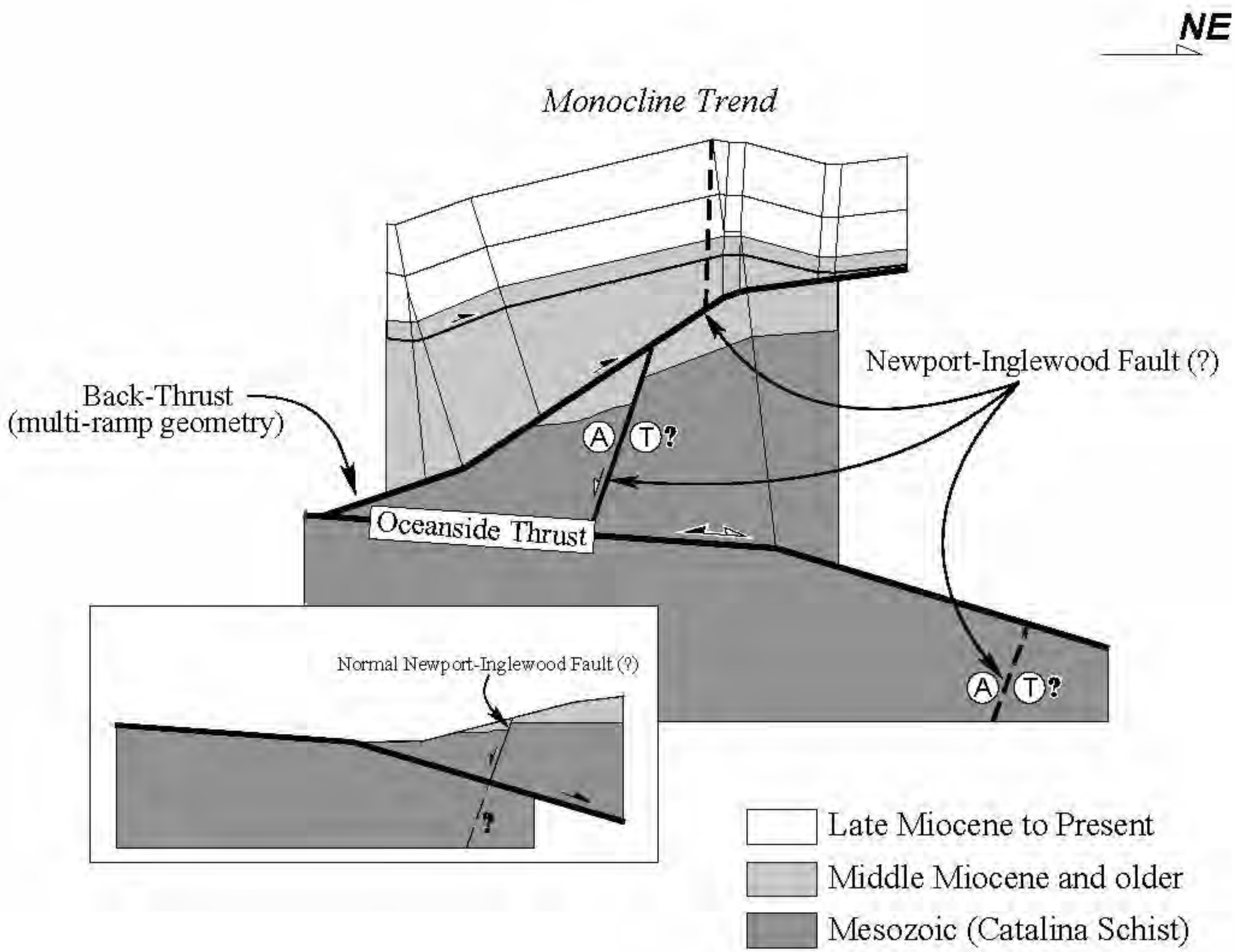

Source: Rivero (2004)

GeoPentech
Geotechnical & Geoscience Consultants

SAN ONOFRE NUCLEAR GENERATING STATION

SEISMIC HAZARD ASSESSMENT PROGRAM

SCHEMATIC DIAGRAM SHOWING POSSIBLE STRUCTURAL CONFIGURATION OF ACTIVE OBT AND ACTIVE NI/RC FAULTS

FIGURE A-26

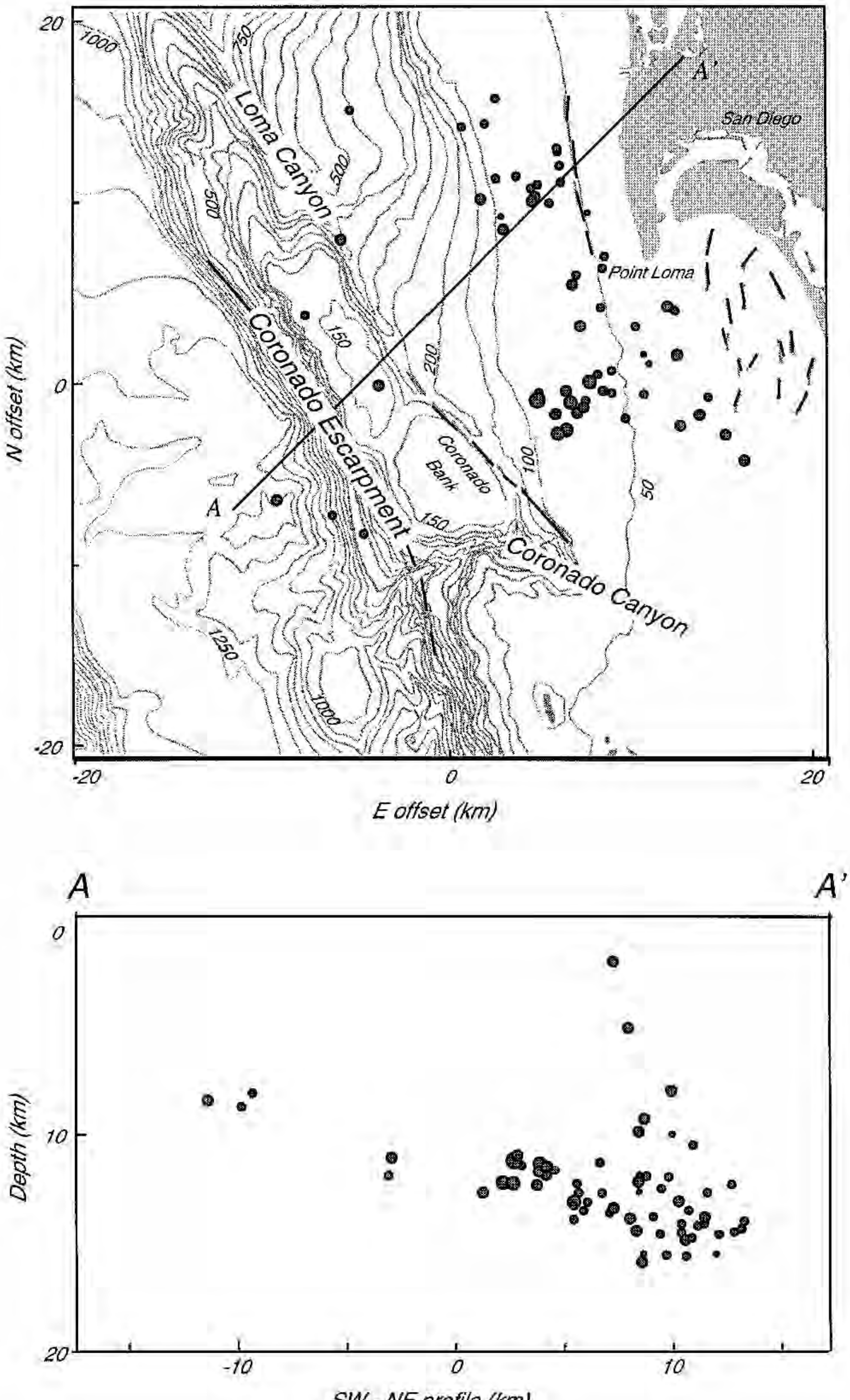

Source: Astiz and Shearer (2000)

RELOCATED CORONADO BANK EPICENTERS	FIGURE A-27
SAN ONOFRE NUCLEAR GENERATING STATION SEISMIC HAZARD ASSESSMENT PROGRAM	

APPENDIX A – ATTACHMENT A-1

ANNOTATED BIBLIOGRAPHIES

INTRODUCTION

The following references were considered in determining the weights for the end-member models discussed in Section 2.4. These references, in whole or in part, address the seismotectonic setting of southern California and the Continental Borderlands. Specifically, these authors offer information bearing on the structural, seismologic, paleoseismic, geomorphic, and/or geodetic character of the region. For convenience, the annotated bibliographies are subdivided into these same character categories.

ANNOTATED BIBLOGRAPHIES

Moore, G.W., 1972, Offshore extension of the Rose Canyon fault, San Diego, California: US Geological Survey Professional Paper 800-C, C113-C116.

STRUCTURAL

- First suggested possible offshore extension of Holocene active traces of the Rose Canyon Fault Zone based on “a net of subbottom acoustic profiles spaced about 5 km apart.” The survey completed by the USGS and Scripps Institution extending from La Jolla into Camp Pendleton (up to latitude 33º 20’).
- Pointed out that straight sections are relatively narrow (0.5 km wide) with wider reaches “as much as 2 km wide at curves.”
- Indicated that “...Cretaceous and Tertiary sedimentary rocks that are generally nearly flat lying but dip moderately to steeply within and near the fault zone...”
- “The greatest local uplift lies adjacent to an S-shaped bend in the Rose Canyon fault…”
- “This uplift is believed to have resulted from compression there as a consequence of right-lateral strike-slip movement along the fault.”
- Further stated that “Corey (1954) and the other previously cited investigations that extrapolated the Rose Canyon fault to the northwest connected it with the Newport-Inglewood fault zone, near which the 1933 Long Beach earthquake of magnitude 6.3 occurred. The offshore evidence of the present study agrees with such a projection, at least as far north as Camp Pendleton.”

Ehlig, P.L., 1977, Geologic report on the area adjacent to the San Onofre Nuclear Generating Station northwestern San Diego County, CA, for Southern California Edison Company, 31 September 1977, 32 pp.

STRUCTURAL

- Marine terraces near SONGS "do not appear to be deformed or tilted."

Hauksson, E., 1987, Seismotectonics of the Newport-Inglewood fault zone in the Los Angeles basin, southern California: Bulletin of the Seismological Society of America, v. 77, no. 2, p. 539-561.

SEISMOLOGY

- Shows focal mechanism solutions for 37 earthquakes along and near the onshore portion of the NI in Los Angeles and Orange Counties. Seventy-eight percent (78%) of these solutions are predominately strike-slip events; most of these are located along the main trace of the fault. The reverse or thrust events are mostly situated northeast or southwest of the main trace, most pronounced being along the Compton-Los Alamitos Fault to the northeast, but parallel to the trend of the of the NI.

Fischer, P.J. and Mills, G.I., 1991, The offshore Newport-Inglewood – Rose Canyon fault zone, California: structure, segmentation and tectonics *in* Abbott, P.L., and Elliott, W.J., eds., Environmental Perils San Diego Region: San Diego, San Diego Association of Geologists, p. 17-36.

STRUCTURAL

- “We used new (1989) digitally processed seismic reflection data with an average spacing of 1.5 km, in conjunction with older digital data and a grid of closely spaced, high resolution analog profiles, to map the geology of the inner margin.” Three major fault segments of the offshore NI/RC zone between Newport Beach and La Jolla and their geology are described
- Dana Point segment between Newport Beach and Las Pulgas Canyon is 43 km long, Oceanside segment between Las Pulgas Canyon and Encinitas is 32 km long, and Del Mar segment from Carlsbad to La Jolla is 34 km long.
- “Piercing points between Newport Beach and the correlative Cristianitos-San Onofre-Oceanside faults indicate that an average of 7 km of right-lateral displacement has occurred along the NIZ since early Pliocene time.”
- “Between San Mateo Point and Oceanside, multiple thrust faults and thrust generated folds or fault-propagation folds were mapped along the slope of the inner margin, west of the NI-RC fault zone…They may be separated into an inner thrust fault-fold complex that is probably a part of the flower structure of the NIFZ, and an outer thrust-fold complex. The inner thrust fault complex is located near mid-slope, about at the 500 m isobath while the outer thrust complex follows the base of the slope near the 700 m isobath.”
- The main thrust fault of the inner thrust-fold complex is between 3 and 4 km beyond the shelf-break and dips 20-30 degrees east.
- “The main thrust of the outer thrust-fold complex trends southeast along the base of the slope of the inner margin. It is southwest-vergent and dips about 9 degrees east shoreward of the thrust ramp.”
- “At this time, a most probable slip rate of 1 mm/yr for the NI-RC zone is suggested.”
- “At this time, it appears that the most probable horizontal slip rate for the NI-RC zone is between 1.3 mm/yr and 2.1 mm/yr. If the Quaternary slip rates are emphasized the most probable modern (?) slip rate is between 0.8 and 1.3 mm/yr, or about 1 mm/yr.”
- “The thrust faults along the inner margin are active, as is evidenced by their surficial topographic expression and the displacement of Quaternary reflectors.”

- "A potential seismic hazard, that has not been considered along the inner margin south of Dana Point, is posed by the thrust faults mapped off San Mateo Point-San Onofre to Oceanside and possible south to Encinitas."

SEISMOLOGY

- "The focal mechanisms are in general agreement with right-lateral, strike-slip faulting along the northwest trending NI-RC zone."

Hauksson, E., and Gross, S., 1991, Source parameters of the 1933 Long Beach earthquake: Bulletin of the Seismological Society of America, v. 81, no. 1, p. 81-98.

STRUCTURAL

- "The existence of a small normal component in the mechanism and in the geological cross sections suggests that the southwestern block of the Los Angeles basin is still subsiding."
- Recent data suggests that "most geological structures adjacent to the NIF are not secondary features resulting from wrench faulting (Wright, 1990 [sic]) but are rather primary structures resulting from north-south compression of the basin (Hauksson, 1990)."
- "[A]bsence of a thrust component is consistent with the slip partitioning model of the seismotectonics of the Los Angeles basin by Hauksson (1990)."
- In the slip partitioning model by Hauksson (1990), "strike-slip faulting on vertical faults and thrust faults on gently dipping faults replace a system of oblique faulting…[t]he almost pure strike-slip mechanism of the 1933 earthquake and the pure thrust mechanism for the 1987 (M_L=5.9) Whittier Narrows earthquake are consistent with this slip partitioning model."

SEISMOLOGY

- Relocated 1933 (M_W 6.4) mainshock "showed right-lateral motion along the NIF [Newport-Inglewood Fault] with a small normal component."
- The "centroidal depth [of the mainshock] was 10±2 km."
- The "best fitting focal mechanism shows right-lateral strike-slip motion with a minor normal component."
- "Both the focal mechanism of the 1933 main shock and the spatial distribution of aftershocks indicate that the earthquake occurred on the NIF."
- Woodward-Clyde (1979) determined a different focal mechanism for the main shock based on first motion polarities and suggested the earthquake was not on the Newport-Inglewood Fault; this study by Hauksson is more accurate because it is based on fitting the whole teleseismic waveforms.
- The "rupture initiated near the Huntington Beach–Newport Beach City boundary and extended unilaterally to the northwest to a distance of 13 to 16 km."
- "[N]o reliable surface rupture was reported."
- "The main shock caused 85–120 cm of slip at depth."

GEOPMORPHOLOGY

- "[P]rominent surface expression [of the Newport-Inglewood Fault] may be a manifestation of the basement boundary rather than being primarily caused by the right-lateral offset," (i.e., metamorphic basement on the west juxtaposed against metaseds and volcanic on the east).

Legg, M.R., 1991, Developments in understanding the tectonic evolution of the California Continental Borderland: Special Publication no. 46, Society for Sedimentary Geology, p. 291-312.

STRUCTURAL

- "[T]ranspressional structure along the offshore NI fault zone and prominent northwest-trending thrust faults at the base of the continental slope west of Newport and San Juan Capistrano suggest northeast-southwest convergence in this area."
- Post-Miocene north-south/northeast-southwest shortening in northern Borderland, extension or transtension on inner Borderland faults from latitude of San Diego southward.
- Palos Verdes Hills Fault is "recognized to have significant thrust or oblique-dextral reverse slip components."

SEISMOLOGY

- "[S]hortening in northeastern Borderland is manifested by the numerous earthquakes with reverse-faulting mechanisms."
- "[T]hrust-fault earthquake mechanisms have been observed as far south as the northern end of the San Diego trough."

Wright, T.L., 1991, Structural geology and tectonic evolution of the Los Angeles basin, California *in* Biddle, K.T., ed., Active margin basins: American Association of Petroleum Geologists Memoir 52, p. 35–134.

STRUCTURAL

- “The Newport-Inglewood fault zone (NIFZ) is the best known structural feature of the Los Angeles basin (Figure 7).”
- “The zone has long been considered a classical example of the development of en echelon folds and faults along a deep-seated-strike-slip fault….”
- Numerous examples are provided of the dominance of Pliocene and later strike slip displacements and the significant variations in their corresponding vertical displacements.
- “Harding concluded that the structures within the zone “may be taken as a unit and related dynamically to one type of deformation – wrenching.”
- “There are dissenting views to this interpretation. Yeats (1973) found it satisfactory for the late Pliocene and Quaternary history of the Newport-Inglewood zone, but too simple for the late Miocene and early Pliocene. It does not account for the fact that most of the more diversely oriented normal and reverse faults (except for Inglewood oil field) became inactive during the Pliocene whereas the en echelon right-lateral slip faults of the Newport-Inglewood zone continued to be active through the Pleistocene.”
- “Each of the Neogene episodes has probably involved regional right-lateral simple shear, but along the NIFZ itself, total right-lateral slip since the middle Miocene has not exceeded 3km (Yeats, 1973) or about 1-2 mi. Evidence of this from the subsurface is compatible with the

estimate of 0.5 mm/year during the past 5 m.y. (Guptill and Heath, 1981) and 0.4-0.8 mm/year (Bird and Rosenstock, 1984)."

- "Classic wrench-fault deformation, however, is not the primary cause of most of the anticlinal features along the NIFZ. In the preceding discussion we have seen that many of these structures do not conform to a pattern of en echelon folding, but are related to local basement geometry and perhaps to a wide zone of pervasive shear within the basement. Along the southern NIFZ, the Long Beach, Seal Beach, and Huntington Beach (onshore) structures are block-edged force folds (Harding and Tuminas, 1988) forced along the middle to late Miocene block boundary. Offshore Huntington Beach has been constricted against the Offshore Newport ridge. Dominguez is a part of the El Segundo-Lawndale-Alondra fold trend, complicated by offset on the NIFZ. Inglewood (and perhaps Potero) formed in concert with uplift of the Las Cienegas block that buckled the sedimentary wedge against shallow basement of the western shelf (Wright, 1987d)."
- Although Hazenbush and Allen 1958 implied a 0.5mm/yr to 1.0mm/yr slip rate since mid-Miocene on the NIFZ in Huntington Beach, "detailed subsurface mapping of oil fields along the NIFZ has revealed a variety of structural patterns and histories, and many of these cannot easily be reconciled with a pure strike-slip origin."
- "Faults within the San Andreas transform system may utilize relict zones of crustal weakness formed during earlier terrane accretion."
- "In analyzing Pasadenan deformation, the flake-tectonics model is more appropriate than the fold-and-thrust-belt model, although both models incorporate aseismic detachment at midcrustal depths. The flake-tectonics model is valid for all phases of Neogene deformation, both transtensional and transpressive, in the Los Angeles region."
- "The transition between the strong compressive shortening of the Transverse Ranges and the moderate right slip of the Peninsular Ranges blocks occurs systematically across the Los Angeles basin. Those relationships… show contrasting structural styles on the two sides of the basin. The northeast flank is dominated by blind thrusts of the Transverse Ranges system that flatten with depth. The southwest flank features right-oblique faults of the Peninsular Ranges system that steepen into near-vertical zones of active seismicity."; "Viewed south to north (GG' to AA'), these cross sections confirm the gradual change from extension at the southern end of the basin to compressive shortening at the northern end…."
- "Relative motion between crustal flakes may involve rifting and separation, transform movement, or collision and shortening, combinations of these, and superposition of several modes over time. Local structures are shaped not by regional stress fields embracing areas hundreds of miles across but by the interaction of adjacent tectonic flakes, creating basement blocks and sedimentary wedges that may differ significantly in their densities, ductilities, and thermal characteristics."; "In shaping local structure, the influence of these internal features of the shallow crust may be as important as the orientation of the stresses being applied."
- "In forming a structure, the shape of the mold counts for as much as how the hammer is swung."
- "All of those structures developed within a wide region of pervasive right slip associated with the evolving San Andreas transform zone. Nevertheless, strike-slip folding caused by displacement along an individual fault is not a dominant factor in the genesis of structures in the Los Angeles basin, though it may well have contributed to deformation along the

northern NIFZ (Figure 9) and perhaps the deformation along the Santa Monica fault (by left slip). That mechanism and other classic patterns of fold and fault development have been nullified by the effects of preexisting basement blocks and sedimentary wedges."

Kern, J.P., and Rockwell, T.K., 1992, Chronology and deformation of Quaternary marine shorelines, San Diego County, California *in* Kern, J.P., and Rockwell, T.K., eds., Quaternary Coasts of the United States: Marine and Lacustrine Systems, Special Publication no. 48, Society for Sedimentary Geology, 377-382.

STRUCTURAL

- Mapping of shorelines provides evidence for uniform uplift of the entire coastal zone in San Diego County (downtown San Diego to Oceanside) at a rate of 0.13 to 0.14 m/kyr during the Quaternary with exception of areas deformed locally by the Rose Canyon Fault Zone.
- Both higher and lower uplift rates are observed along the Rose Canyon Fault Zone, which is shown by its effects on shoreline configurations to have been active for at least the past million years.
- The average long-term uplift rate for the San Diego region is similar to those for other areas of coastal California that are dominated by strike-slip tectonics.

GEOPMORPHOLOGY

- Shoreline angle elevations are estimated for 16 shorelines estimated to range in age from 80 ka to perhaps as old as 1.29 Ma.
- Shoreline geometry is modified both by regional uplift and by extensive faulting in the right-slip wrench system of the Rose Canyon Fault Zone.

Rockwell, T.K., Lindvall, S.C., Haraden, C.C., Hirabayashi, C.K., and Baker, E., 1992, Minimum Holocene slip rate for the Rose Canyon fault in San Diego, California, *in* Heath, E.G., and Lewis, W.L., eds., The Regressive Pleistocene Shoreline Coastal Southern California: South Coast Geological Society, Inc., 1992 Annual field Trip Guide Book No. 20, p. 55-64.

STRUCTURAL

- "Rose Canyon fault appears to feed directly into the Newport-Inglewood fault zone to the northwest. Although the Coronado Bank fault may also feed slip into the Newport-Inglewood fault zone, the rate determined for the Rose Canyon fault in this study also provides a minimum slip rate for [the offshore NI/RC]."

PALEOSEISMOLOGY

- Rose Canyon Fault is Holocene active based on radiocarbon dates obtained from charcoal deposited stratigraphically below a tectonically offset channel.
- Authors demonstrate offset of channel is likely all or mostly tectonic with no or very minimal deflection.
- Minimum slip rate of the Rose Canyon Fault of ~1 mm/yr is afforded from the trenching, presuming 8.7 m of brittle slip in ~8150 years.

- The "actual rate could be substantially higher if the age of the [tectonically offset] channel is as much as 1000 years younger than the age of [the radiocarbon date obtained from the charcoal]."

GEOPMORPHOLOGY

- Rose Canyon Fault is late Pleistocene active based on a 17–28 ka terrace riser offset 33–35 m.
- Maximum slip rate of the Rose Canyon Fault of ~2 mm/yr is based on the maximum offset of the terrace riser (35 m) in the minimum amount of time (17 ka).

Crouch, J.K., and Suppe, J., 1993, Late Cenozoic tectonic evolution of the Los Angeles basin and Inner California Borderland: A model for core complex-like crustal extension: Geological Society of America Bulletin, v. 105, p. 1415-1434.

STRUCTURAL

- Propose large magnitude (>200 km) crustal extension formed LA Basin, Inner California Borderlands, and Southern California Borderlands in major late Cenozoic rifting.
- Several current right lateral strike slip structures originated as high-angle normal faults prior to Pliocene.
- "Faults such as the Newport-Inglewood and Whittier-Elsinore originated as high-angle, hanging-wall normal faults above detachments and hence, modern strike slip along these faults may end downward against the detachments."
- Image detachment fault over regional extent, from ~San Clemente to Oceanside.
- From San Clement to Oceanside, "30-km-long fold and thrust belt underlies the continental slope seaward of the Newport-Inglewood fault zone."
- "[The] detachment fault has become reactivated in places and now accommodates northeast-southwest-directed contraction that has formed the overlying fold and thrust belt."
- "Crustal shortening, which began in Pliocene time, appears to still be active."
- "Thrust faults within this belt appear to be rooted into the former detachment, and crustal shortening has structurally inverted (uplifted and folded) a former sediment-filled trough situated along the Newport-Inglewood fault zone."

Bohannon, R.G., and Geist, E., 1998, Upper crustal structure and Neogene tectonic development of the California Continental Borderland: Geological Society of America Bulletin, v. 110, n. 6, p. 779-800.

STRUCTURAL

- "The California continental borderland structural province offshore of the southwestern United States and northwestern Mexico is nearly as wide as the Basin and Range province, but it is less well known…."
- "[P]late interactions are generally thought to have caused the borderland deformation, but the specific history and style of tectonism has been debated."
- "Luyendyk et al. (1980) used paleomagnetic evidence to argue that the western Transverse Ranges had undergone 90°–105° of clockwise rotations, about vertical axes, mostly during middle to late Miocene time. Numerous way have been proposed to explain the clockwise

rotation and most of these link the rotation with large amounts of strike slip in the adjacent nonrotated regions to the north and south."

- "The linked rotation–strike-slip models do not explain the most pronounced lithotectonic abnormality—the regional occurrence of the Catalina Schist that forms the basement of the inner continental borderland and the western part of the Los Angeles basin."
- Other authors have suggested "that the Catalina Schist was exposed, from an undetermined depth, through a process of tectonic unroofing in a large inner continental borderland rift that developed behind the clockwise-rotating beam of the western Transverse Ranges."
- "The Peninsular Ranges and Catalina Schist boundary has commonly been drawn at the near-vertical Newport-Inglewood and Rose Canyon fault system (e.g., Vedder, 1987). However, Crouch and Suppe (1993) described the boundary as a detachment- fault surface that dips gently to the east in the subsurface north of Oceanside. They used industry seismic-reflection data to support their view. Our data corroborate the findings of Crouch and Suppe (1993) in that the Newport-Inglewood and Rose Canyon fault system is entirely within sedimentary rocks of the Peninsular Ranges belt on line 120 (Fig. 6), and we imaged a similar deeply buried, low-angle fault having an east dip at about the same depth and position as Crouch and Suppe's (1993) detachment fault. We think that the entire Peninsular Ranges–Catalina Schist boundary is along a low-angle detachment fault, which we call the Oceanside detachment fault."
- "The Oceanside detachment fault is defined in the seismic data by several aligned, high-amplitude reflections with gentle apparent east…. These project eastward to an indistinct east-dipping reflection beneath the shelf…and they project westward and upward, through a zone of discontinuous, short reflections, to a series of east-dipping reflections…beneath the western part of the gulf…. We locate the breakaway zone of the detachment fault at the inclined reflections beneath the western part of the gulf."
- "Numerous fault zones interrupt the coherency of the reflections that makes up the upper plate of the Oceanside detachment fault and some of these appear to disturb the sea floor."
- "The Newport-Inglewood zone is inclined steeply east and it penetrates the entire reflective sequence, including the sea floor. The fault may have a strong normal component of offset. Most of the lesser steep faults appear either to merge downward with the detachment or they truncate at it. This could also be true of the Newport-Inglewood fault zone, although clear documentation is lacking in our data."
- "Between the Gulf of Santa Catalina and the San Clemente Island region, there are several small fault-bounded and internally faulted basins….Much of the fill is probably syntectonic….It is not possible to determine the age of the basin fill."
- "The San Clemente Island–Cortes Bank region is within the Nicolas forearc belt….Overall deformation within the Nicolas forearc belt is slight and most of the belt remains intact. There are numerous small structural basins, filled with middle Miocene and younger strata, that are bounded by young faults with pronounced normal separations, and these indicate that the belt was deformed by an episode of extensional and possibly strike-slip tectonism."
- "The boundary between the Nicolas forearc and Catalina Schist belts is a prominent west-dipping fault…that has been called the East Santa Cruz basin fault."
- "It is not possible to determine the magnitude and sense of slip from the seismic data, but the East Santa Cruz basin fault is assumed to have a large amount of right slip…. It probably also has incurred a large, but unknown, amount of normal displacement….The fault appears to break through to the surface…."

- "The East Santa Cruz basin fault may splay into a group of west-dipping faults on north and west flanks of Sixtymile Bank…and between the East Cortes basin and the Blake Knolls."
- "The boundary between the Nicolas forearc and western Transverse Ranges belts is just south of the northern Channel Islands….[C]ontinuous reflectors…end abruptly at a steep fault that penetrates the seismic section to all depths. We call this the Channel Island fault zone."
- "The extensional basins, which serve to define the borderland structural province, formed during Miocene to Pliocene time."
- "Many of the largest basin-bounding faults…might still be active."
- "Most of the large northwest-oriented, basin-bounding faults exhibit characteristics that are consistent with a strong strike-slip component in addition to the large vertical separations that can be documented….They have long and straight fault traces and commonly have opposing down-thrown sides along the same fault trace…."
- "We think that the Oceanside detachment fault…is the primary structure upon which the schist basement was uplifted relative to the Peninsular Ranges batholithic basement along the east side of the Catalina Schist belt."
- "We propose a two-stage model of upper crustal extension. The inner borderland rift formed during the early stage, beginning in early Miocene time when the western Transverse Range belt was oriented more or less north-south. The Catalina Schist was uplifted from middle crustal levels and exposed in the rift as the western Transverse Ranges began to rotate and the Nicolas forearc belt began to be displaced to the west. Most of the modern borderland physiography formed in the later stage, which began at the end of middle Miocene time. The later stage occurred in conjunction with the bulk of the rotation of the western Transverse Ranges. The later stage is primarily one of right-normal faulting in the borderland. Some parts of the borderland may still be in a right-normal slip regime."
- "[T]here has been approximately 100 km of extension across the part of the borderland…About 60 km of that extension took place during the early stage as the result of a migrating hinge of localized uplift and extension. About 40 km of extension occurred during the later stage as the result of distributed faulting on right-normal faults having northwest orientations."
- "We speculate that, after 15 Ma, the pattern of borderland deformation changed from localized extension (migrating hinge-flexural uplift model) to more distributed shear on right0normal slip on faults with north-northwest trends."
- "The Channel Island fault zone and the Santa Cruz Island and related faults, which also probably have curved traces…are viewed as left-slip zones that compensate for differences between the southwest end of the rotating western Transverse Ranges…."

SEISMOLOGY

- "Patterns of seismicity (Legg, 1985) suggest that…the San Clemente, Coronado Bank, San Diego Trough, and Palos Verdes Hills faults, may be active."

Kier, G., and Mueller, K., 1999, Flexural modeling of the northern Gulf of California Rift: relating marine terrace uplift to the forebulge on a subsiding plate: Southern California Earthquake Center 1999 internship final report, 11 pp., [http://www.scec.org/education/college/internships/1999/99grant.pdf].

STRUCTURAL

- "Therefore, shortening must occur between 0.89 and 2.39 m/ka to achieve between 14±0.03 and 0.25±0.03 m/ka vertical uplift on a fault dipping 6-9 degrees. Using standard vector analysis we rotated the coordinate axes of the regional velocity field to calculate the component normal to the strike of the Oceanside fault as shown in figure 1 (SCEC Data Center, 1999). We then compare the regional surface velocity normal to the fault to the velocity required for current terrace uplift rates. This shows that the current surface shortening is within the range that would generate current uplift patterns but relies on the assumption that velocities at depth are consistent with surface velocities. The northern and southern terminations of the Oceanside fault are at approximately the San Joaquin Hills and the U.S. Mexican border respectively (John Shaw, work in progress)."
- "Of the three models tested in this project, uplift due to forebulging on a subsiding plate provides the best fit model for the observed uplift of marine terraces."

Grant, L.B., Mueller, K.J., Gath, E.M., Cheng, H., Edwards, R.L., Munro, R., and Kennedy, G., 1999, Late Quaternary uplift and earthquake potential of the San Joaquin Hills, southern Los Angeles basin, California: Geology, v. 27, p. 1031-1034.

STRUCTURAL

- "Indications of late Quaternary folding are present in the San Joaquin Hills at the southern margin of the Los Angeles basin."
- "The San Joaquin Hills are the topographic expression of a northwest-trending anticlines between San Juan Capistrano and Huntington Mesa."
- "Uplift of the San Joaquin Hills began in the early Pleistocene."
- "Analysis of emergent marine terraces in the San Joaquin Hills…and ^{230Th} dating of solitary corals from the lowest terraces reveal that the San Joaquin Hills have risen at a rate of 0.21–0.27 m/k.y. during the past 122 k.y."
- "The location and thickness of Holocene sediments in the San Joaquin Hills suggest that tectonic uplift continued during the middle to late Holocene."
- "[W]e do not have direct evidence for Holocene activity of the San Joaquin Hills thrust."
- "A fault-bend fold model with movement on a northwest-vergent thrust fault best explains the elevations of marine terraces…."
- "In [one] interpretation the San Joaquin Hills thrust is a backthrust that soles into the Oceanside detachment (Bohannon and Geist, 1998) as part of a wedge-thrust structure."
- "We prefer to interpret movement of the San Joaquin Hills blind thrust to be the product of partitioned strike slip and compressive shortening across the Newport-Inglewood fault zone."

Bender, E.E., 2000, Late Quaternary uplift and earthquake potential of the San Joaquin Hills, southern Los Angeles basin, California – COMMENT: Geology, v. 28, no. 4, p. 383.

STRUCTURAL

- "Grant and et al. (1999) [sic] rather unequivocally demonstrated that the San Joaquin Hills…have risen at a rate of 0.021–0.027 mm/yr over the past 122 k.y. Based largely on geomorphic evidence, they attribute this uplift as a fault-bend fold above a southwest-dipping blind thrust fault."
- Flower structures "have been shown to exist along the Newport-Inglewood fault zone (Harding, 1979; Wright, 1991), and the extensive, nearly vertical faulting observed in the San Joaquin Hills is suggestive of such a structure extending off of the fault zone."
- "It appears more likely, on geologic grounds, to suggest that the uplift within the San Joaquin Hills is generated by squeezing upward along the Newport-Inglewood fault zone in shortening deformation accompanying northwest-southeast horizontal shear or transpression."

Grant, L.B., Mueller, K.J., Gath, E.M., and Munro, R., 2000, Late Quaternary uplift and earthquake potential of the San Joaquin Hills, southern Los Angeles basin, California – REPLY: Geology, v. 28, no. 4, p. 384.

STRUCTURAL

- "Bender's conclusion that uplift within the San Joaquin Hills is generated by squeezing upward along the Newport-Inglewood fault zone by shortening that accompanies northwest-southeast horizontal shear (i.e., transpression) agrees with our statement that, 'We prefer to interpret movement of the San Joaquin Hills blind thrust to be the product of partitioned strike-slip and compressive shortening across the southern Newport-Inglewood fault zone,' (p. 1034, Grant et al., 1999)."
- "However, we disagree with Bender's assertion that the structure of the San Joaquin Hills and proximity to the Newport-Inglewood fault make a blind thrust model unattractive."
- The "San Andreas fault in central California [is described by Wilcox et al. (1973)] as an example of a wrench fault with a series of en echelon folds on the eastern side of the fault. These folds (anticlines) are now known to be underlain by seismogenic blind thrust faults (Stein and Yeats, 1989; Stein and Ekstrom, 1992) created by transpressive strain partitioned across western California (Lettis and Hanson, 1991). A similar structural relationship probably exists between the Newport-Inglewood fault zone and the San Joaquin Hills."
- "Our data do provide strong evidence that the San Joaquin Hills are rising in response to a potentially seismogenic, underlying blind fault, and we suggest that this potential earthquake source should be included in regional seismic hazard models."

Astiz, L., and Shearer, P.M., 2000, Earthquake locations in the Inner Continental Borderland, offshore Southern California: Bulletin of the Seismological Society of America, v. 90, no. 2, p. 425-449.

STRUCTURAL

- Evidence in article forms the basis of several arguments regarding the location, geometry, and style of faulting in the offshore structural models.

SEISMOLOGY

- "[F]ault geometries in this complex region [referring to offshore southern California] are often poorly constrained due to lack of surface observations and uncertainties in earthquake locations and focal mechanisms. To improve the accuracy of event locations in this area, we apply new location methods to 4312 offshore seismic events that occurred between 1981 and 1997 in seven different regions within the Borderland."
- "Obtaining accurate locations for these events is difficult, due to the lack of nearby stations, the limited azimuthal coverage, and uncertainties in the velocity structure for this area."
- "In general, our relocated events have small estimated relative location errors and the events are more clustered than the SCSN catalog locations"; "…under ideal conditions offshore events can be located to within 1 to 2 km of their true locations."
- "Our final locations for most clusters are well correlated with known local tectonic features."
- "We can relate the 1981 Santa Barbara Island (ML =5.3) earthquake with the Santa Cruz fault, the 13 July 1986 Oceanside (ML = 5.3) sequence with the San Diego Trough fault zone, and events near San Clemente Island with known trace of the San Clemente fault zone."
- "Our locations define a northeast-dipping fault plane for the Oceanside sequence, but in cross-section the events are scattered over a broad zone (about 4 km thick)….This could either be an expression of fault complexity or location errors due to unaccounted for variations in the velocity structure."
- "104 Events recorded between 1981 and 1997 that occur near Coronado Bank in the SCSN catalog, are relocated closer to the San Diego coast and suggest a shallow-angle, northeast-dipping fault plane at 10 to 15 km depth."
- "We plot 65 events, those with standard errors less than 1.5 km…. Locations for events near the Coronado Bank region…occur at 10 to 15 km depth along an apparent northeast dipping fault close to the San Diego Coast."
- "It is possible that these faults are shallow-angle thrust or detachment faults seen in seismic reflection data…to mark the boundary between the Peninsular Ranges to the east and the Catalina Schist best to the west"
- "If the Oceanside and/or Coronado events indeed occur on portions of a much larger system of offshore thrust faults, this would have important implications because it would establish that these faults are seismically active and a potential source of large future offshore events."

Rivero, C., Shaw, J.H., and Mueller, K., 2000, Oceanside and Thirtymile Bank blind thrusts: implications for earthquake hazards in coastal southern California: Geology, v. 28, no. 10, p. 891-894.

STRUCTURAL

- Oblique convergent slip at depth may be partitioned separately onto NI/RC and OBT (model "D").
- "San Joaquin Hills are formed by northeast-vergent anticline that uplifts and defines marine terraces...[offshore imaging confirms] it formed above a shallow blind thrust [dipping ~23° southwest that is] restricted to the hangingwall of the [OBT]; at depth, we interpret that this shallow fault soles into the [OBT]."

SEISMOLOGY

- From seismology (i.e. 1986 Oceanside earthquakes), interpretation suggests Thirtymile Bank Thrust is through-going and not cut by San Diego Trough; if logic is extrapolated to OBT, then OBT is through-going and not cut by NI/RC Fault.
- "[R]elocated mainshock and aftershocks of [1986] Oceanside earthquake [are] clustered at ~8 km depth and [define] a 25-30° east-dipping surface" consistent with slip on Thirtymile Bank Thrust fault plane and an epicenter ~14-17 km east of San Diego Trough Fault.

GEOPMORPHOLOGY

- Imaged thrusts are "commonly associated with pronounced seafloor fold scarps."

GEODETIC

- Geodetic observations from Kier & Mueller (1999) indicate "as much as 2 mm/yr of NE-SW convergence between Catalina Island and the coast."

Ponti, D.J., 2001, Changing deformation rates through time: insights from new Quaternary stratigraphic studies in the Los Angeles basin, California [abstract]: American Geophysical Union 2001 Fall Meeting, 10–14 December 2001, abstract #S12E-11.

STRUCTURAL

- Geologically-derived fault slip and fold deformation rates may only be applicable when rate of deformation is constant over time.
- “[S]tratigraphic analysis of Quaternary deposits in [the LA Basin] show [the rate of] fold growth has not been constant during the last ~1 Ma.”
- “[C]onstant deformation should not be broadly presumed without specific supporting evidence.”

Rivero, C., and Shaw, J.H., 2001, 3D geometry and seismogenic potential of the Inner California Borderland blind thrusts system [abstract]: Southern California Earthquake Center Proceedings and Abstracts, 23–26 September 2001, p. 105-106.

STRUCTURAL

- "Inner Continental Borderland blind-thrust system includes a pair of inverted Miocene extensional detachments…reactivated as low-angle thrust faults during the Pliocene."
- "Thrust motions on these detachments produced several trends of contractional fault-related folds (e.g., San Mateo and Carlsbad structures) that partition oblique convergence with regional strike-slip systems."

SEISMOLOGY

- "Earthquake hypocenters…suggest that the Inner California blind thrust system is active and seismogenic."

Sliter, R.W., Ryan, H.F., and Normark, W.R., 2001, Does recent deformation at the base of slope provide evidence of a connection between the Newport-Inglewood and the Rose Canyon fault zones offshore southern California? [abstract], American Geophysical Union 2001 Fall Meeting, 10–14 December 2001, abstract #S11A-0531.

STRUCTURAL

- Previous work by others suggests NIFZ and RCFZ connect along the continental shelf "with the main deformation occurring near the shelf edge."
- "[O]bserve sediments at the seafloor deformed near the base of the slope at water depths of about 700 m on [multichannel seismic reflection] data between Dana Point and Oceanside."
- Observe folding of seafloor between Oceanside and Carlsbad at 300 m depth.
- "[D]ata show recent faulting on the shelf (< 100 m water depth) associated with the Rose Canyon fault from Carlsbad to La Jolla."
- "[I]nterpret the base of the slope faulting to be related to a strand of the NIFZ…that may connect with the RCFZ by a left step near Carlsbad, as evidenced by recent folding of the seafloor."

Grant, L.B., and Rockwell, T.K., 2002, A northward propagating earthquake sequence in coastal southern California?: Seismological Research Letters, v. 73, no. 4, p. 461-469.

STRUCTURAL

- Faults within the Coastal Fault Zone (>300 km in length) "appear to be kinematical linked."
- "At a minimum, the Coastal Fault Zone extends from Beverly Hills, California (USA) southeast to the Punta Banda peninsula in Baja California (Mexico) and includes both [the] onshore and offshore…NIFZ (northern and southern segments), the offshore NIFZ, the Rose Canyon Fault, the Descanso strand of the offshore Coronado Bank Fault, and the Agua Blanca Fault."
- "The offshore NIFZ is a structurally complex zone of folds and faults."

- "Continuity of the offshore and southern NIFZ was debated. Several studies (e.g., Barrows, 1974; Fischer and Mills, 1991) have concluded that they are continuous or kinematically linked, and therefore the offshore NIFZ is assumed to be seismogenic."
- "An upper bound slip rate of 3.5 m/yr has been estimated (Fischer, 1992) based on total offset with an estimated age of 2 Ma (Crouch and Bachman, 1989), but the Holocene slip rate is probably lower."
- "Fischer and Mills (1991) report a seismically active positive flower structure and thrust complex approximately 240 km long."
- "Several high0angle faults in the [San Joaquin Hills (SJH)] may be strands of the ancestral NIFZ (Bender, 2000) and show evidence of Quaternary surface rupture (Grant et al., 2000). Based on measurements of late Quaternary and Holocene uplift, the SJH have been interpreted to be underlain by an active blind thrust fault (Grant et al., 1999, 2000, 2002). Movement of the SJH blind fault may be kinematically linked to the NIFZ (Grant et al., 1999, 2000), the offshore Oceanside Fault (Rivero et al., 2000), or both."

SEISMOLOGY

- "Scattered seismicity occurs along the [NIFZ], although events are difficult to locate accurately due to poor station coverage."
- "The date of most recent rupture of the offshore NIFZ is not known [sic], although seismic-reflection observations and microseismicty indicate that it was during the Holocene."
- "Toppozada et al. (1981) estimated a M≥6.5 [earthquake] and proposed a coastal or offshore location for the 1800 earthquake. If this interpretation is correct, the earthquake could have occurred on the offshore NIFZ."
- The onshore NIFZ northern and southern segments "have been seismically active during the historic period."
- "Despite relatively high historic levels of microseismicty, the northern NIFZ may be a seismic gap."
- "The recent seismicity suggest that the northern NIFZ might be in the latter stages of its seismic cycle."

PALEOSEISMOLOGY

- "[R]ecently published fault investigations in the northern Baja California peninsula (Mexico) and coastal southern California (USA) reveal evidence for geologically contemporaneous or sequential earthquakes along a >300-km-length, predominantly strike-slip seismic zone [which] includes structures previously mapped as the Agua Blanca, Rose Canyon, San Joaquin Hills, and southern Newport-Inglewood Fault zones."
- "The historic and paleoseismic records indicate that the Coastal Fault Zone has ruptures from the Agua Blanca to the southern NIFZ within the last few centuries, with the possible exception of the northern NIFZ and portions of the offshore NIFZ."
- "The date of the last surface rupture of the northern NIFZ is not known."
- "[T]he paleoseismic data and historic observations suggest that the northern NIFZ has not ruptured as recently as other sections of the Coastal Fault Zone."

GEODETIC

- "GPS measurements indicate that approximately 14% of the total Pacific-North America Plate motion occurs west of the Elsinore Fault, most likely distributed across the San

Clemente, Newport-Inglewood, Rose Canyon, and other coastal or offshore faults (Bennett et al., 1996).”

OTHER

- “Seismic hazard associated with [the Coastal Fault Zone] has been recognized for decades…but is still poorly quantified…due, in part, to the difficulty of integrating observations onshore and offshore.”
- “[T]he coastal faults have lower slip rates and longer recurrence intervals than many onshore faults and therefore are calculated to represent relatively low hazard…[h]owever, if we examine the entire zone, we find that it ruptured most recently in a temporal cluster or propagating sequence of large earthquakes. Therefore the hazard may be high if the sequence or cluster is still in progress.”
- “The southern California coastal fault zone [sic] might be in the later stages of [a] multicentury failure sequence.”

Grant, L.B., Ballenger, L.J., and Runnerstrom, E.E., 2002, Coastal uplift of the San Joaquin Hills, southern Los Angeles basin, California, by a large earthquake since A.D. 1635: Bulletin of the Seismological Society of America, v. 92, no. 2, p. 590-599.

STRUCTURAL

- “The San Joaquin Hills…are the surficial expression of a faulted anticline parallel to the active Newport-Inglewood fault zone….”
- “Grant et al. (1999, 2000) proposed that uplift was generated by movement on an underlying blind thrust fault due to partitioned strike-slip and compressive shortening across the southern Newport-Inglewood fault zone.”
- Study of marsh deposits in Newport Bay, “a late Pleistocene erosional gap between the northern San Joaquin Hills and Newport Mesa.”
- Prior work by Stevenson (1954) suggested “the marsh bench was created by emergence of late Holocene marshland and subsequent death of the elevated marsh community. Stevenson (1954) hypothesized that ‘the greater height of the ‘marsh bench’ in the central area is probably the result of movement during Recent time of a major anticline and fault system which cut through the Bay in a NW–SE direction.’”
- “The pattern of uplift reported by Stevenson (1954) is consistent with both the geomorphic expression of the San Joaquin Hills and the expected vertical displacement field that would be generated by coseismic growth of the San Joaquin Hills.”
- “Our data agree with Stevenson’s (1954) hypothesis that the marsh bench emerged due to tectonic uplift of the San Joaquin Hills.”
- “The spatial pattern of emergent shorelines and marsh deposits roughly mimics the topographic expression of the San Joaquin Hills and is consistent with a tectonic origin.”
- “The marsh bench and coastal benches could not have formed solely by erosion or deposition due to a sea level highstand because the elevations are different at different locations and the average elevations are different on each side of Newport Bay and along the open coast. Therefore, the most plausible mechanism for creating both the marsh bench and coastal platforms is emergence by tectonic uplift.”

- "The age of the marsh bench is constrained by radiocarbon dating…. Active marsh deposition and growth must have ceased on the marsh bench sometime after our samples were deposited."
- "Uplift of the San Joaquin Hills must have occurred after A.D. 1635, the earliest plausible age of the marsh bench."
- "Several fault models have been proposed to explain uplift and folding of the San Joaquin Hills. Grant et al. (1999) developed a model of a blind thrust fault dipping 30° to the southwest. Bender (2000) proposed that uplift is occurring in response to movement of the steeply dipping, strike-slip Newport–Inglewood fault system. Both types of faults may have contributed to uplift during the late Quaternary (Grant et al., 2000). A third model proposed by Rivero et al. (2000) attributes uplift to movement of a large regional thrust, the northeast-dipping Oceanside fault extending offshore of the San Joaquin Hills south to Oceanside and San Diego."
- "Several observations suggest that the San Joaquin Hills are underlain by a fault that is distinct from the NIFZ, although they may be linked kinematically."
- "Other topographically prominent anticlines, such as Signal Hill, are located within the structurally complex NIFZ and are associated with step-overs (Barrows, 1974). In contrast, the San Joaquin Hills anticline is east of the main NIFZ, and there is a releasing bend at the mouth of the Santa Ana River where the fault goes offshore (Morton and Miller, 1981) near the northern San Joaquin Hills."

SEISMOLOGY

- The 28 July 1769 historic earthquake is "a good candidate for the most recent earthquake that raised the San Joaquin Hills coastline."
- "Other candidates for the San Joaquin Hills earthquake occurred on 22 November 1800 and 10 July 1855."
- "There are no other documented earthquakes that could have generated more than 1 –m uplift of the San Joaquin Hills after 1855, so we conclude that uplift and the causative earthquake occurred between A.D. 1635 and 1855."
- "Based on out interpretations of the data, this region was more seismically active in the preinstrumental period."

GEOMORPHOLOGY

- "In the San Joaquin Hills, wave erosion and coastal processes have formed a suite of shore platforms extending from the modern shoreline up to an elevation of greater than 300 m above sea level, indicating late Quaternary tectonic uplift."
- "[T]here is common agreement that modern and ancient shorelines are geomorphic indicators of sea level relative to land."
- "Along the open coast of the San Joaquin Hills, the lower emergent platform and shoreline are a few meters above the lowest (modern) wave-cut platform and several meters below any previously mapped or dated shoreline…. Based on position between the modern shoreline and dated shorelines at higher elevation, the lower emergent shoreline should be younger than 83 ka (stage 5a sea level highstand)…. Therefore, the lowest emergent platform and shoreline…are most likely Holocene age (stage 1 sea level highstand)."
- "Most emergent Holocene shorelines in tectonically active areas are less than 6000 yr old and reflect coseismic uplift rather than sea level fluctuation or large storms."

- "Changes in pollen types, as well as sedimentation, reported from a core of San Joaquin Marsh (Davis, 1992) are consistent with an interpretation of latest Holocene tectonic uplift of the San Joaquin Hills. San Joaquin Marsh is currently a freshwater marsh located between the city of Irvine and upper Newport Bay…. Radiocarbon dates and analysis of pollen from core sediments show that San Joaquin marsh responded to changes in relative sea level during the Holocene (Davis, 1992). After approximately 4500 yr B.P., freshwater pollen types were replaced with salt marsh types as marsh flora responded to the Holocene sea level highstand (Davis, 1992). Freshwater conditions returned briefly circa 3800, 2800, 2300, and after 560 yr. B.P."
- A "possible explanation is that tectonic uplift of the San Joaquin Hills elevated San Joaquin Marsh above sea level, causing a return to freshwater conditions."

Grant, L.B., and Shearer, P.M., 2004, Activity of the offshore Newport-Inglewood Rose Canyon Fault Zone, coastal southern California, from relocated microseismicity: Bulletin of the Seismological Society of America, v. 94, no. 2, p. 747-752.

STRUCTURAL

- Structure of offshore NI/RC may be like onshore Newport-Inglewood Fault, with multiple strike-slip strands.

SEISMOLOGY

- Relocated two microearthquake clusters associated with offshore NI/RC: 1981 Oceanside cluster (19 events) and 2000 Newport Beach cluster (7 events).
- 1981 Oceanside cluster not associated with 1986 Oceanside earthquake sequence.
- The "events [in the 1981 Oceanside cluster] align along a north-northwest trend about 0.5 km long...[and] define a nearly vertical plane between 12.5 and 13.0 km depth" and are "approximately parallel to the fault zone."
- The "strike, dip, and location of a plane fit by these events are consistent with active strike-slip faulting" on the offshore NI/RC Fault Zone.
- Composite waveform polarities "are consistent with a right-lateral strike-slip focal mechanism," but "cannot eliminate other possible focal mechanisms."
- "[F]ive of seven events [in the 2000 Newport Beach cluster] are aligned in a pattern consistent with a shallow (7 km) north-northwest-striking, vertical or steeply dipping active fault," but polarities are too small for focal mechanism solutions.
- Overall, dataset too sparse to determine if there is (or is not) a through-going strike-slip fault zone.
- The "location and ~13 km depth of the Oceanside cluster suggests that the [OBT] is terminated by active strike-slip faults."

Rivero, C.A., 2004, Origin of active blind-thrust faults in the southern Inner California Borderlands, unpublished Ph.D. Dissertation: Harvard University, 146 pp.

STRUCTURAL

- "Several of [the] contractional and extensional structures [offshore Dana Point] were previously interpreted as wrench-related thrusts and folds, and as 'flower structures' produced by active offshore segments of the Newport-Inglewood."
- "[I]nterpret most of the contractional trends sole into, and do not cross, the [OBT]."
- Complex faulting in basin inversions may be "prone to be confused with flower structure."
- "Shallow slip partitioning is the most likely description of the structural relationship between the Thirtymile Bank and San Diego Trough faults."
- "In many cases, seismic reflection data indicate previously interpreted strike-slip fault splays correspond with active hinges of contractional anticlines produced by...motion on a deep structural wedge."
- OBT Segment I (Dana Point to south of Carlsbad) slip rate 0.88–1.17 mm/yr; M 7.1 → return interval (RI) = 1070–1430 yrs; M 7.3 → RI = 1480–1960 yrs.
- OBT Segment II (south of Carlsbad to south of San Diego) slip rate 0.70–0.94 mm/yr; M 7.3 → RI = 1840–2470 yrs.
- OBT full length, M 7.5 → RI = 2030–3390 yrs.

GEOPMORPHOLOGY

- "[L]ocal asymmetric anticlines with bathymetric expression, sitting on top of regional rollovers" are associated with mapped structures (proposed thrust systems).
- "Structural wedge system above the [OBT] shows a spatial correlation with the occurrence of Quaternary uplift in adjacent coastal areas," e.g. San Joaquin Hills, and marine terraces and strand lines along coastal Orange and San Diego Counties.

Rivero, C., and Shaw, J.H., 2005, Fault-related folding in reactivated offshore basins, California *in* Interpretations of Contractual Fault-Related Folds, An American Association of Petroleum Geologists Seismic Atlas, Studies in Geology, No. 53, Department of Earth and Planetary Sciences: Harvard University, Cambridge, MA, 3 pp.

STRUCTURAL

- “The San Mateo anticline developed by the upward propagation of reverse slip during the inversion of Miocene half-grabens.”
- Oceanside detachment “is not folded by the contractional structures; thus we interpret that the San Mateo Anticline is formed by thrusting ramping up from this detachment surface.”
- San Mateo ramp is also folded by a younger, deeper thrust.
- San Mateo thrust and underlying thrust “terminate in structural wedges…that propagate slip back to the hinterland…as no foreland structures that could account for the transfer of slip exist beyond the San Mateo anticline.”
- “[I]nterpret the San Mateo Anticline as an imbricated fault-bend fold produced by the upward propagation of contractional slip from an inverted normal fault into multiple detachment levels.”

- "The back-limb geometry…indicates the presence of a deeper structure [that] refolds the shallow thrust sheet of the San Mateo Anticline in a way consistent with a break-forward system."
- Estimated total shortening offshore the San Clemente region is 2.5 km.
- "The San Mateo anticline is an imbricated fault-bend fold originated by basin inversion processes" along a thrust that "reactivated a segment of a northeast-dipping Miocene normal fault."
- "The phase of basin inversion also reactivated a Miocene low-angle detachment as the [OBT]" and the OBT "transferred contractional slip to associated synthetic and antithetic normal structures, inverting a major graben-boundary fault, and generating a regional structural wedge [that] controls the location of a prominent monocline with bathymetric expression."

Legg, M.R., Goldfinger, C., Kamerling, M.J., Chaytor, J.D., and Einstein, D.E., 2007, Morphology, structure and evolution of California Continental Borderland restraining bends *in* Cunningham, W.D., and Mann, P., eds., Tectonics of Strike-Slip Restraining and Releasing Bends: Geological Society, London, Special Publications, 290, p. 143-168, doi: 10.1144/SP290.3.

STRUCTURAL

- A "restraining bend exists where the fault curves or steps to the left when following the fault trace. Crowding of crustal material by lateral movement into the fault bend produces uplift and crustal thickening…."
- "Right-slip on irregular fault traces in the California Continental Borderland "has produced numerous restraining bend pop-ups that exhibit distinctive seafloor morphology."
- "The submarine basins of the Borderland range in depth from a few hundred metres to more than 2000 m…erosion is greatly diminished in these deep basins compared with subaerial regions, so that pop-up morphology is well preserved on the seafloor."
- "The San Clemente fault zone includes a 60-km-long restraining bend that exhibits prominent seafloor uplift in the 1300-m deep Descanso Plain offshore of northwest Baja California…."
- San Clemente Fault bed region minimum uplift rate is 0.47 to 0.70 m/ka.
- "The Catalina Fault forms an 80-km-long restraining double bend (cf. Crowell 1974) between the Santa Cruz-Catalina Ridge and San Diego Trough fault zones. Uplift due to oblique convergence along this transpressional fault has produced Santa Catalina Island and the wide submerged shelf and slope surrounding the island."
- Model for restraining bend evolution:
    - "First, the strike of the principal displacement zone (PDZ) in the major restraining bends is parallel to the Miocene Pacific-North America (PAC-NOAM) relative motion vector(s)."
    - "Second, the major faults within the restraining bend pop-up have very steep to vertical dips."
    - "Third, the pop-up structures for the major restraining bends have structurally inverted Miocene basins."
    - "Fourth, there is an overall right-stepping en echelon character to the major right-slip fault pattern of the Borderland."

Campbell, B.A., Sorlien, C.C., Cormier, M., and Alward, W.S., 2009, Quaternary deformation related to 3D geometry of the Carlsbad fault, offshore San Clemente to San Diego [abstract], Southern California Earthquake Center Proceedings and Abstracts, 12–16 September 2009, v. 19, p. 263.

STRUCTURAL

- Parts of Carlsbad-Coronado fault system coincide with the SCEC CFM OBT.

Mueller, K., Kier, G., Rockwell, T., and Jones, C.H., 2009, Quaternary rift flank uplift of the Peninsular Ranges in Baja and southern California by removal of mantle lithosphere: Tectonics, v. 28, TC5003, doi:10.1029/2007TC002227.

STRUCTURAL

- Presents argument for the model that the elevated terraces along the Pacific coast of northern Baja California and southern California are the result of the distal effect of "flexture of the elastic lithosphere driven largely by heating and thinning of the upper mantle beneath the Gulf of California (and the Salton Trough) and eastern Peninsular Ranges."
- "Pliocene strata deposited at sea level along the Pacific coastline in southern California have not been uplifted significantly above Quaternary marine terrace deposits."

Ponti, D.J., and Ehman, K.D., 2009, A 3-D sequence-based structural model for the Quaternary Los Angeles basin, California [abstract]: Southern California Earthquake Center Proceedings and Abstracts, 12–16 September 2009, vol. 19, p. 262-263.

STRUCTURAL

- "A 3-D sequence-based structural/stratigraphic model for the Los Angeles Basin is being developed by the USGS for use in earthquake hazards and groundwater resources research."
- "The Quaternary section reaches a maximum thickness of more than 1280 m in the Lynwood area east of the Newport-Inglewood (N-I) fault zone. In the west basin, the Quaternary section reaches its greatest thickness (>410 m) in San Pedro Bay just east of the Palos Verdes fault. Of the inter-basin structures that impact the Quaternary section, the Compton-Alamitos fault (Wright, 1991) is the most prominent. Discreet faulting of mid-late Pleistocene deposits and structural relief of up to 300 m is suggested by the seismic data and by anomalous water levels near Los Alamitos. West of the N-I fault, two W-NW-trending inter-basin faults offset mid-late Pleistocene sediments and may serve to consume slip from the N-I. The M4.7 Hawthorne earthquake of May 18, 2009 was located near the northernmost of these structures and has a fault-plane solution consistent with the geometry and kinematics of this fault as evidenced in the geology."

Ryan, H.F., Legg, M.R., Conrad, J.E., and Sliter, R.W., 2009, Recent faulting in the Gulf of Santa Catalina: San Diego to Dana Point *in* Lee, H.J., and Normark, W.R., eds., Earth and Science in the Urban Ocean: The Southern California Continental Borderland: Geological Society of America Special Paper 454, p. 291-315, doi: 10.1130/2009.2454(4.5).

STRUCTURAL

- Where the Rose Canyon FZ "is imaged on industry MCS records, [it] forms a complex flower structure near the shelf break" (offshore Encinitas).
- "[M]ain strand of [offshore] Newport-Inglewood FZ forms a prominent positive flower structure" (offshore San Onofre).
- NI/RC bend/connection "is accommodated by reverse faulting...faulting dies off rapidly [away from bend/connection], however folding continues [from] Carlsbad Canyon [to] near the left step [in] Newport-Inglewood FZ."
- "[I]ndustry seismic reflection profiles suggest the [OBT] might not be continuous," and it is "uncertain [whether OBT] offsets San Onofre FZ south of San Mateo Point."
- "[lack sufficient data] to determine whether or not [OBT] intersects and offsets Newport-Inglewood FZ."
- "[S]outh of La Jolla Fan Valley...little evidence for shortening associated with [OBT]."
- Of the main, through-going offshore faults, the "more northerly...tend to be transtensional and the more westerly [tend to be] transpressional."
- Key issue of San Mateo FZ and Carlsbad FZ: are these reverse faults "indicative of broad scale contraction...related to the reactivation of the Oceanside detachment as a blind thrust...or related to more localized complexities associated with slip partitioning along Newport-Inglewood FZ."
- "[U]plift of marine terraces along much of the coastline between Newport Beach and La Jolla provides possible evidence for the large-scale reactivation of the entire Oceanside detachment surface as a blind thrust"..."however, uplift of terraces could also be explained by transpression along Newport-Inglewood FZ."
- "[A]lthough a low-angle detachment surface is imaged...throughout much of the offshore Gulf of Santa Catalina, there is not unequivocal evidence that it has been reactivated as an uninterrupted active thrust fault."

Sorlien, C.C., Campbell, B.A., Alward, W.S., Seeber, L., Legg, M.R., and Cormier, M., 2009a, Transpression along strike-slip restraining segments vs. regional thrusting in the Inner California Continental Borderland [abstract]: Southern California Earthquake Center Proceedings and Abstracts, 12–16 September 2009, v. 19, p. 264.

STRUCTURAL

- The OBT "has little effect on the ~2.5 Ma horizon above [it], and a regional anticline expected due to deeper blind thrust slip beneath the Gulf of Santa Catalina is lacking."
- "Significant Plio-Quaternary folding is only present where the [OBT] bends to merge with the Carlsbad fault."
- Carlsbad Fault is oblique-right reverse, "SW-verging thrust slip [on it] contributes to uplifting continental shelf...and San Joaquin Hills."

Sorlien, C.C., Campbell, B.A., and Seeber, L., 2009b, Geometry, kinematics, and activity of a young mainland-dipping fold and thrust belt: Newport Beach to San Clemente, California, USDI/USGS Award No. 08HQGR0103 Final Technical Report, 25 pp.

STRUCTURAL

- "[R]ight lateral NI fault [is] part of a larger 3D system of oblique-right reverse faults."
- The central OBT does not deform early Quaternary seds and has "normal separation near [the] base of [the] Pliocene horizon."
- Northwest OBT coincides with San Mateo/Carlsbad Fault; progressive tilting in hangingwall forelimb indicates subsidence; Newport Beach/Oceanside slope and shelf and San Joaquin Hills being uplifted on San Mateo/Carlsbad Fault.
- Southeast OBT coincides with Coronado Bank Fault, locally pure right lateral.

Conrad, J.E., Ryan, H.F., and Sliter, R.W., 2010, Tracing active faulting in the Inner Continental Borderland, Southern California, using new high-resolution seismic reflection and bathymetric data [abstract]: Seismological Society of America 2010 Annual Meeting, Seismological Research Letters, v.81, no. 2, p. 347.

STRUCTURAL

- Based on recent high resolution seismic and bathymetric surveys, the mapped traces of the Palos Verde, Coronado Bank, San Diego Trough, and San Pedro Faults have been significantly altered.
- Indicate that the Avalon Knoll Fault also shows evidence of recent offsets and “these faults are thought to accommodate about 5-8 mm/yr of slip …. but it is not clear how slip on these faults is distributed….”
- Re-defined the Catalina Fault as inactive and report the Catalina Island is subsiding rather than rising.
- Presented the USGS’s latest map of the NI/RC fault system, but do not discuss it specifically.
- The key value is the more accurate map of the San Diego Trough Fault and correlating this more location and mapped configuration with its associated step-overs and the 1986 Oceanside earthquake (See Ryan, 2010, personal communication).

Ponti, D., 2010, personal communication.

STRUCTURAL

- Amplifying on Ponti, D.J. and Ehman, K.D. (2009), “At present, faults are highly simplified in the model; we have not accounted for every known structure in the basin, but instead have focused on modeling faults that have an apparent impact on groundwater flow… Vertical terminations of the faults have also not yet been tightly constrained.”

SEISMOLOGY

- “The Charnock fault, originally proposed by Poland and others (1959) to explain groundwater anomalies within Pleistocene sediment, may in fact correspond with a more

NW-trending structure identified by Wright (1991) that appears associated with a trend of seismicity evident in recent relocations. The M4.7 Inglewood earthquake of May 18, 2009 was located near the southern end of this seismicity tren(d) and has a fault-plane solution consistent with the geometry and kinematics of this fault as evident in the geology."

Rivero, C., and Shaw, J.H., 2010, in press, Active folding and blind-thrust faulting induced by basin inversion processes, Inner California Borderlands: Tectonics, submitted for consideration of publication 2010, 45 pp.

STRUCTURAL

- "We evaluate several different styles of geometric and kinematic interactions between high-angle strike-slip faults and the low-angle detachments, and favor interpretations where deep oblique slip is partitioned at shallow crustal levels into thrusting and right-lateral strike-slip faulting. "
- "Restored and Balanced cross-sections provide a minimum SW-directed slip of 2.2-2.7 km on the Oceanside Thrust, and illustrate the role of this detachment in controlling the process of basin inversion and the development of the overlying fold-and-thrust belt."
- "Interpret observations to reflect a complex mixture of strike-slip and blind-thrust faulting in the Inner Borderlands that is similar to the style of deformation in the onshore LA basin."
- "Miocene low-angle normal (detachment) faults… that were reactivated by basin inversion processes initiated in the Late Pliocene, during the onset of the modern transpressional regime."
- "[N]ew geometric representations of the offshore Newport-Inglewood, Rose Canyon, and San Diego Trough fault zones…consistent with basin inversion processes and the presence of both active blind-thrust and strike-slip faults in the southern Inner California Borderlands."
- "[P]rovide insight into the subsurface geometries of complex zones where coeval active strike-slip and thrust faults interact. Both types of fault systems are deemed likely to be active, and should be considered in the context of regional earthquake hazards assessment."
- "[M]otion on the Oceanside Thrust generated four prominent contractional fold trends. Three of these are foreland-directed structures (San Mateo, San Onofre, and Carlsbad Trends) that produce prominent fold scarps at the seafloor…suggesting Quaternary activity. The fourth is a backthrust (hinterland-directed) system…manifested in a laterally continuous monocline that controls the relief and bathymetric expression of the shelf."
- "[C]ontractional and extensional structures represent local restraining and releasing bends along the offshore extension of the Rose Canyon strike-slip fault. At depth, the NI and RC strike-slip fault zones intersect with the Oceanside Thrust…at relatively shallow levels of~4km in the north and deeper ~10 km in the south. Data are insufficient to uniquely define the manner in which these two fault systems interact. Scenarios where the two fault systems interact at depth in a manner consistent with their coeval activity are favored."

SEISMOLOGY

- "The Inner Borderlands do not display the apparent spatial correlation between EQ activity and regional strike-slip fault zones that is observed around the onshore region of the Peninsular Ranges…Seismicity in this area is diffuse and scattered."

Rockwell, T., 2010, personal communication.

GEOPMORPHOLOGY

- 3-D trenching and "Paleoseismic work along the onshore Rose Canyon fault zone in the City of San Diego clearly demonstrates that the fault has sustained recurrent Holocene activity …"
- "Considering that the surface soil represents a long period of stability, it is not possible to simply space the timing of all six events equally for the past 9.3 ka. In fact, if the interpretation is correct that the surface soils represent at least 5 ka of development, then five of these events occurred as a cluster in the period between about 9.3 and 5 ka, with an average interval of recurrence of less than 1 ka."
- "If the fault principally behaves in a clustered seismicity mode, and if the five early Holocene events represent such a cluster, then one must consider the possibility that the recent earthquake of ca. AD 1650 represents a return to activity and is possibly the first in the next cluster of large earthquakes."

Rockwell, T.K., 2010, Appendix A, Attachment A-2, Seismic source characteristics of onshore Rose Canyon fault, for GeoPentech, Inc., 14 pp.

STRUCTURAL

- "Marine terraces on the southwest flank of the uplift (Kern, 1977; Kern and Rockwell, 1992), along with the presence of the Linda Vista Formation marine terrace alluvium capping Mount Soledad, attest to the higher rate of uplift of the restraining bend area (0.25 mm/yr) relative to the surrounding coastal plain (0.13 mm/yr) (Kern and Rockwell, 1992), with the background regional uplift attributed to rift-flank uplift from extension in the Gulf (Mueller et.al., 2009)."
- The combination of the releasing step plus a change in fault strike make the Oceanside step a likely (northern) termination zone for ruptures, although a through-going rupture cannot be precluded."
- "However, the San Joaquin Hills may represent uplift associated with a step from the northern termination of the Rose Canyon to the Newport-Inglewood fault zone."
- "If the Oceanside step-over is a barrier to rupture propagation, it would divide the Rose Canyon fault into two roughly similar-length sections: a 65 km segment from San Diego Bay to Oceanside, and a 55 km segment from Oceanside to the San Joaquin Hills…one cannot preclude rupture of the entire Rose Canyon fault for a distance of more than 100 km. However, I consider this model a lower likelihood than rupture of individual segments and weight it a 25%, versus 75%f for the more segmented rupture behavior."

PALEOSEISMOLOGY

- The "most recent earthquake occurred sometime between AD 1523 and 1769. These 3-D trenching data further suggest that about 3 m of right lateral, strike-slip displacement occurred during this event, with a 1:10 ratio of vertical to horizontal displacement."

- "In particular, the onshore data supports the argument that the high-angle, right-lateral, strike-slip as NI/RC Fault System is a primary seismic source fault whereas the nearby, shallow-dipping normal, oblique, and reverse faults are subsidiary."
- Paleoseismic data further suggest a termination zone near the San Joaquin Hills and "that the San Joaquin uplift is structurally tied to the coastal system of strike-slip faults."

GEOPMORPHOLOGY

- "The level of activity is indicated by both the relatively large lateral deflections of stream channels that are incised into low marine terraces (Figure A-4-4), and by the results of the three-dimensional trenching. These observations suggest a lateral slip rate of about 2 mm/yr during the late Quaternary (Rockwell, 2010a)."
- "For the southern termination, the right-step between the Rose Canyon and Descanso faults forms the depression occupied by San Diego Bay (Figure A-4-1, and is likely large enough (>5 km) to arrest dynamic slip."

OTHER

- "… I suggest using the maximum slip rate range of 1.1 to 2.5 mm/yr, with the best estimate of 1.5-2.5 mm/yr, with the following weights: 0.5 (0% weight), 1.0 (10% weight), 1.5 (30% weight), 2.0 (40% weight), 2.5 (20% weight), and 3.0 (0% weight)." In order to accommodate the possibility of clustering "I would suggest using the long-term rate (the above) with an 80% weight, and consider using an alternate weighting scheme for slip rate (in mm/yr) with a 20% overall weight as follows: 0.5 (0% weight), 1.0 (10% weight), 1.5 (30% weight), 2.0 (30% weight), 2.5 (20% weight), and 3.0 (10% weight)."

Ryan, H., 2010, personal communication.

STRUCTURAL

- Does not see OBT as single large structure, but rather small segments reactivated, possibly by block rotation and localized transpression in the San Diego Trough/Gulf of Santa Catalina region.
- San Diego Trough Fault connects in north with San Pedro Basin Fault, rather than Catalina Ridge.
- At the behest of the California Geological Survey, the extent of the OBT was mapped using industry MCS data available at the USGS NAMSS web site. The main OBT reflector is quite strong and well imaged off of San Mateo point (e.g., Crouch and Suppe, 1993). Following this prominent reflector on strike lines that extend along most of the Gulf of Catalina, it was not possible to tie the reflector to the OBT mapped south of the area around San Mateo Point. Hence, it is difficult to justify a pervasive areal extent of the OBT.
- High-resolution reflection profiles imaging folds within the hanging wall of the OBT show reflectors with increasing tilt with depth behind one of the prominent folds. Although this may indicate active folding/uplift, it is not possible to preclude the possibility that the progressively tilted beds are from sediment waves, which are pervasive in the area owing to the close proximity of the San Mateo channel and fan system.
- Notes no evidence for Holocene connection between Coronado Banks Fault and Palos Verdes Fault, contrary to what is depicted in UCERF 2 and the CFM.

- New USGS surveys planned for spring and summer of 2010.

SEISMOLOGY

- Comparison of the newly acquired map trace of the San Diego Trough Fault (as was currently being refined by Conrad, J.E.) with the Astiz and Shearer (2000) relocated epicenters of the 1986 Oceanside events indicates the earthquakes very clearly match a right step in the San Diego Trough Fault, which clearly explains the oblique thrust focal mechanisms in this earthquake sequence rather than the model presented in Rivero et al. (2000) and Rivero (2004).

Shaw, J.H., and Plesch, A., 2010, Appendix A, Attachment A-3, Seismic source characteristics of Inner California Borderland's blind thrust fault systems, for GeoPentech, Inc., 15 pp.

STRUCTURAL

- 1986 Oceanside thrust earthquake and "extensive research of hundreds of proprietary oil industry marine geophysical seismic reflection survey lines, lead us to infer the presence of two distinct, active thrust fault systems located offshore of southern Orange County and San Diego County."
- The "OBT extends at least from Laguna Beach to the Mexican border and may dip under the shoreline."
- "The slip rate was estimated for the OBT based on measures of fault offsets and uplift using the marine geophysical seismic reflection survey data and estimates of the ages of the deformed geologic formations."
- "We recognize that others believe that right-lateral strike slip faults (model 1) dominate the tectonics off-shore of Orange and San Diego Counties. However, based on the currently available data, we would assign a weight of '0' to rupture model 1 [as it] is not kinematically compatible with the large amount of displacement we document on the OBT."
- "[I]t is unclear whether the shallow dipping thrust faults (such as the OBT) are primary seismic source faults, with the steeply dipping, right-lateral, strike-slip faults, such as the NI or RC faults, being subsidiary, or whether the steep, strike-slip faults are the primary seismic sources, and the thrust faults are subsidiary."
- "Association of the OBT and the San Joaquin Hills thrust, combined with the patterns of uplifted coastal marine terraces, further support fault activity."
- "At the depths and locations where data is necessary to resolve the uncertainty…regarding the intersection between the NI/RC and the OBT, the faults are within the basement rocks and the velocity contrast/acoustic impedance of the basement rocks either side of where these faults are inferred to be interacting is not likely to be significant enough to produce adequate reflectors in the marine geophysical seismic reflection surveys."
- "[I]t is doubted whether high energy, deep penetrating 2-D or 3-D seismic surveys can retrieve the necessary data to be able to unequivocally resolve this particularly important uncertainty."

SEISMOLOGY

- "[R]everse/thrust focal mechanism solution tied to the offshore 1986 Oceanside (M_L 5.3) Earthquake demonstrated that active blind thrust faults also exist in Southern California's inner Continental Borderland."

GEODETIC

- Research and analysis considered "GPS data from the SCEC Crustal motion Map that Kier and Mueller (1999) used…our sense is that these geodetic data are poorly constrained….Thus, there is a large uncertainty with this rate deformation, but at present we simply lack another means to estimate this rate."

Wetmore, P.H., Malservisi, R., Fletcher, J., Alsleben, H., Callihan, S., Springer, A., and González-Yajimovich, O., 2010, in review, Transtension within a restraining bend domain of a transform plate boundary: the role of block rotations and the reactivation of preexisting crustal structures: Geological Society of America Lithosphere, submitted for consideration of publication 2010, 17 pp.

STRUCTURAL

- "Given its structural context the ABF should be characterized by a significant component of contractional dip-slip motion. However, the ABF is uniquely characterized by nearly pure strike-slip displacements along the east-west trending eastern portion and an increasing normal component of dip-slip motion along western segments where its trend becomes more northwesterly."
- "The net effect is to connect regions of high extension in the Gulf of California with those in the northern Continental Borderlands."
- "However, the kinematics and distribution of faults that accommodate the plate motion exhibit profound along-strike variations and the margin can be separated into three distinct tectonic domains."
- " The Gulf of California forms the southern segment of the plate margin where a system of en echelon transform and spreading centers accommodate integrated transtensional shearing across a relatively narrow deformation belt along the axis of the gulf."
- "In the northern plate-boundary segment, most of the shearing is accommodated by the San Andreas Fault system. Dextral strike-slip faults in this domain are kinematically coordinated with folds and thrust faults to produce strongly transpressional shearing."
- In the central domain of the plate margin, shearing is marked by the "Big Bend" of the San Andreas Fault, which "[l]inks plate-margin shearing along coastal California with that in the Gulf of California. In many ways the central domain is a transitional region between the two radically different domains to the north and south. However is also has unique pattern of faulting that is distinct from the other two domains. Although thrust faults and folds are present throughout the northern half of the central domain (Zoback and Zoback, 1980; Bartley et al., 1993) horizontal contraction is largely accommodated by conjugate strike-slip faults."
- Major late Miocene normal faults form an important kinematic component of deformation in the southern half of the central domain, but extreme crustal thinning is partially compensated by north-south shortening associated with detachment folds and conjugate strike-slip faults.

APPENDIX A – ATTACHMENT A-2

SEISMIC SOURCE CHARACTERISTICS OF ONSHORE ROSE CANYON FAULT

By
Dr. Thomas Rockwell
San Diego State University

INTRODUCTION

The following document has been prepared at the request of Southern California Edison (SCE) in consultation with technical members of their Seismic Hazard Assessment Program (SHAP).

The onshore traces of the Rose Canyon (RC) Fault Zone, as currently mapped through San Diego, are shown on Figure A2-1 (Rockwell, 2010a). The onshore evidence for the presence and recent activity of the Rose Canyon Fault Zone is abundant, with tectonic geomorphic expression of the active traces clearly evident in early aerial photography (Treiman, 1993; Lindvall and Rockwell, 1995, Rockwell, 2010a). As presented in Rockwell (2010a), 3-D trench data suggest that the most recent earthquake on the fault that resulted in surface rupture occurred sometime between AD 1523 and 1769. These 3- D trenching data further suggest that about 3 m of right-lateral, strike-slip surface displacement occurred during this event, with a 1:10 ratio of vertical to horizontal displacement.

Although the evidence for onshore rupture of the RC fault is not specific to the fault traces offshore of SONGS, these onshore data are some of the only available to address the size and frequency of earthquakes that may be expected from the Newport-Inglewood-Rose Canyon (NI/RC) Fault System, and therefore supports its seismic source characteristics. In particular, the onshore data supports the argument that the high-angle, right-lateral, strike-slip NI/RC Fault System is a primary seismic source fault whereas the nearby, shallow- dipping normal, oblique, and reverse faults are subsidiary.

The following sections of this appendix provide more information regarding:

1. How the onshore RC data supports the conclusion that the high-angle, right- lateral, strike-slip NI/RC Fault System is the primary seismic source fault, as was concluded during the 1980s licensing of the plant, and as was recently incorporated into the preparation of the current version of the National Seismic Hazard Map (USGS, 2009);

2. Why these data are appropriate to use to define the current model of the NI/RC Fault System for incorporation into the update of the plant's Probabilistic Seismic Hazard Assessment, and the update of its deterministic tsunami assessment with a Probabilistic Tsunami Hazard Assessment; and

3. The identification of recommended future research that will further strengthen our understanding of the potential hazards associated with the NI/RC Fault System.

PRESENCE AND LEVEL OF ACTIVITY

The active surface trace of the RC fault can clearly be mapped southward from the La Jolla coastline, up over Mount Soledad, down through Rose Canyon, across the San Diego River Valley, through Old Town San Diego and downtown San Diego, and across Coronado Island based on analysis of early aerial photography (Treiman, 1993, Lindvall and Rockwell, 1995, Rockwell, 2010a). The location of the fault is marked by the presence of scarps, deflected drainages, a sag and several pressure ridges, all of which attest to its recent activity (Figure A2-2). Most of these features also demonstrate that the fault has been repeatedly active throughout the late Quaternary with essentially the same kinematic motion. The traces beneath San Diego Bay have been imaged by shallow seismic techniques, where several strands of the fault clearly cut Holocene marine sediments (Kennedy and Clarke, 1996), also indicating that the Rose Canyon fault is young and active. Surprisingly, an early (Glover, 1876) artists rendition of Newtown (present day downtown San Diego) shows the trace of the fault as a scarp and several deflected drainages precisely where recent trenching has determined to be the main traces of the fault (see Figure A2-3), and supports the recency of displacement that has been demonstrated in the trenching studies (Lindvall and Rockwell, 1995; Rockwell, 2010a).

The linearity of the fault trace across hilly topography argues that the fault maintains a steep dip through much of San Diego, except in the Mount Soledad area, where the fault appears to dip to the southwest beneath the uplift. The fault strike in this area is also more westerly, consistent with a restraining bend geometry that has resulted in the uplift of the mount. Marine terraces on the southwest flank of the uplift (Kern, 1977; Kern and Rockwell, 1992), along with the presence of the Linda Vista Formation marine terrace alluvium capping Mount Soledad, attest to the higher rate of uplift of the restraining bend area (0.25 mm/yr) relative to the surrounding coastal plain (0.13 mm/yr) (Kern and Rockwell, 1992), with the background regional uplift attributed to rift-flank uplift from extension in the Gulf (Mueller et al., 2009).

The level of late Quaternary fault activity is indicated by both the relatively large lateral deflections of stream channels that are incised into low marine terraces (Figure A2-4), and by the results of the three-dimensional trenching. These observations suggest a lateral slip rate of about 2 mm/yr during the late Quaternary (Rockwell, 2010a).

SEISMIC CHARACTERISTICS

The expected length of a future rupture on the Rose Canyon fault may be limited by structural controls, such as steps, bends, and changes in strike that may be large enough to terminate dynamic rupture. For the southern termination, the right-step between the Rose Canyon and Descanso faults forms the depression occupied by San Diego Bay (Figure A2-1), and is likely large enough to arrest dynamic slip. This step exceeds 5 km in step-over width (Figure A2-5), which is more than the largest releasing step that has been ruptured through in historical, well-documented strike-slip earthquakes (Wesnousky, 2008). Based on this, the southern termination of future large earthquakes on the Rose Canyon fault is expected to be in San Diego Bay.

For the northern termination, there are several structural features that may play a role, but none are as large as the step across San Diego Bay. The left bend in the Rose Canyon fault that facilitated the uplift of Mt. Soledad is only on the order of a couple kilometers in cross-fault dimension (Figure A2-5) and many historical earthquakes have ruptured through bends and steps of such dimensions (Wesnousky, 2008) (cf. the 1968 Mw6.4 Borrego Mountain earthquake ruptured across the 1.5-2 km wide Ocotillo Badlands with less than a half meter of displacement, Clark, 1972). Thus, the Mt. Soledad bend and uplift is not likely to be large enough to define a rupture segment boundary, especially if the Rose Canyon fault has 3 m of displacement in Rose Creek. Furthermore, it is a continuous surface fault through the region of this bend based on the geomorphology and extensive local trenching (Lindvall and Rockwell, 1995; Rockwell and Murbach, 1999).

Farther north, the Rose Canyon fault steps to the right (releasing step) near Oceanside, but the dimensions of the step are only on the order of 2-3 km or so (Figure A2-5). This can be a significant barrier to rupture in moderate earthquakes, but is less likely to stop a large dynamic displacement. More significantly, however, the Rose Canyon fault has a more westerly strike to the northwest of this step, and the change in azimuth is on the order of 15 degrees from the average strike of the fault between Oceanside and San Diego Bay. The combination of the releasing step plus a change in fault strike make the Oceanside step a likely termination zone for ruptures, although a through-going rupture cannot be precluded.

The SONGS sits along the coast between Oceanside and the San Joaquin Hills uplift, and there are no major, obvious structural complexities that can be used to segment the Rose Canyon fault along this stretch. However, the San Joaquin Hills may represent uplift associated with a step from the northern termination of the Rose Canyon to the Newport- Inglewood fault zone. Grant et al. (2002) consider the uplift as the consequence of slip on a blind thrust, but likely structurally linked to the Newport-Inglewood fault zone (Grant et al., 1999, 2000). A closely related model is that the Rose Canyon fault bends northward and steps left across the hills to the Newport Inglewood fault, producing uplift by slip on the low-angle accommodation fault. An alternative model is that the San Joaquin uplift is related to a blind thrust system, the Oceanside thrust, that accommodates shortening in the Borderland (Rivero et al., 2000). In any case, the San Joaquin uplift is a structural complexity and may serve to segment the offshore zone of faulting.

An approach to shedding light on this problem, and to better constrain the likely sizes and termination zones for future earthquakes associated with the Rose Canyon and Newport-Inglewood faults, is to assess the current paleoseismic data in terms of whether they support co-seismic rupture of these faults together in the past. Grant and Rockwell (2002) documented the occurrence of a sequence of large earthquakes that ruptured the coastal zone of faults in the past few hundred years, but was pre-historical in age. This sequence involved the onshore Agua Blanca fault in northern Baja California, as well as the onshore Rose Canyon fault in San Diego and the San Joaquin Hills fault beneath Newport Bay, and was succeeded by the 1933 rupture of the Newport- Inglewood fault in Los Angeles Basin (Figure A2-6). Based on radiocarbon dating of the most recent earthquakes on these three faults, this sequence appears to have propagated northward, because rupture of the Agua Blanca fault is apparently the oldest of the events. In actuality, the dates of these three events all overlap to some degree, but there is the appearance that events to the north are younger than those to the south. Furthermore, it is unlikely that an earthquake ruptured both the Agua Blanca- Descanso and Rose Canyon faults simultaneously because of the large step-over at San Diego Bay. Combined with the occurrence of the 1933 event, which is clearly the youngest, the interpretation presented by Grant and Rockwell (2002) seems reasonable. Alternatively, as the most recent event on the Rose Canyon fault overlaps with the interpreted uplift of Newport Bay, it is possible that the entire Rose Canyon fault ruptured in a large earthquake just prior to the Mission period, and that the Newport Bay uplift is a consequence of this event. Because of the inherent problems in precise radiocarbon dating in this time period, this question may be difficult to resolve. Nevertheless, the occurrence of the sequence (or single event) supports the idea that the San Joaquin uplift is structurally tied to the coastal system of strike-slip faults.

There is a clearer difference in timing between Rose Canyon and onshore Newport- Inglewood fault ruptures (Figure A2-6; compiled from Grant et al., 1997; Grant and Rockwell, 2002; Leon, et al., 2009), which argues against the likelihood of a very long rupture. Although the timing is similar, Grant and Rockwell argue that the pre-Mission sequence of ruptures represent multiple events, and likely propagated northward, culminating in the relative small M6.4 1933 Long Beach earthquake. It is noteworthy that the 1933 earthquake is not known to have ruptured the surface, and there were plenty of people around who should have noticed a significant rupture. Grant et al. (1997) use this observation to argue that the Holocene events identified for the Newport-Inglewood fault at Bolsa Chica likely represent larger earthquakes than that which occurred in 1933.

The pre-historic Newport-Inglewood and Compton-Los Alamitos events are nearly indistinguishable in timing (Figure A2-6), considering their large uncertainties. Nevertheless, they both have a similar return period for large earthquakes – those that can be identified by CPT and core correlation techniques, which implies that they are larger than 1933. One could argue that the Compton Los Alamitos and Newport- Inglewood faults ruptured together in the largest earthquakes, suggesting that they are kinematically linked. This may support Wright's (1991) interpretation of the Compton fault as a high angle oblique splay of the Newport-Inglewood fault. In any case, it is clear that the 1933 earthquake is smaller, and it was not associated with a large event on the Compton structure. Barrows (1974) does, however, document that the area between the Los Alamitos and Newport-Inglewood faults was uplifted in the 1933 earthquake (Figure A2-7), again indicating a structural tie between these structures.

Rose Canyon fault has a very different paleoseismic record of past earthquakes than those faults to the north. The Rose Canyon fault experienced a cluster of events in the early Holocene, followed by a hiatus of several thousand years (Figures A2-6)(Rockwell, 2010a). Although one could argue that the mid-Holocene event documented at Bolsa Chica on the Newport-Inglewood fault could correlate to one of the mid-Holocene Rose Canyon events, it is clear that the others do not, as there are no other recognized events during this cluster at Bolsa Chica. Unfortunately, the San Joaquin Hills record is too short (one event) to assess whether there is a correlation between Rose Canyon events and uplift at Newport Bay. Nevertheless, it appears that the Rose Canyon earthquake history is generally dissimilar to that of the Newport-Inglewood fault, which likely means that these faults do not typically rupture together.

In summary, the Rose Canyon fault is interpreted as a distinct seismic source that does not likely rupture with the Newport-Inglewood fault to the north, nor the Agua Blanca-Descanso fault to the south. If the Oceanside step-over is a barrier to rupture propagation, it would divide the Rose Canyon fault into two roughly similar-length sections: a 65 km segment from San Diego Bay to Oceanside, and a 55 km segment from Oceanside to the San Joaquin Hills. From the short paleoseismic record at Newport Bay, it is not possible to test long-term patterns of recurrence between these two segments. Further, due to the overlap in ages between the most recent ruptures inferred for these two segments (assuming the Newport Bay uplift is associated with a northern Rose Canyon rupture that involved the San Joaquin Hills), one cannot preclude rupture of the entire Rose Canyon fault for a distance of more than 100 km. However, I consider this model a lower likelihood than rupture of individual segments and weight it at 25%, versus 75% for the more segmented rupture behavior.

For PSHA and PTHA seismic source characterization model, I suggest using the maximum slip rate range of 1.1 to 2.5 mm/yr, with the best estimate of 1.5-2.5 mm/yr, with the following weights:

0.5 (0% weight)

1.0 (10% weight)

1.5 (30% weight)

2.0 (40% weight)

2.5 (20% weight)

3.0 (0% weight)

For calculations that involve lapse time since the most recent event (time-based probabilities), you may want to consider that the Rose Canyon fault apparently behaves in a clustered mode, where the time between events within a cluster is shorter than the average long-term recurrence interval. This can be viewed, in effect, as variations in short term slip rate, with the period between about 10-5 ka having a higher rate than the long term average (Figure A2-8), the rate from 5-0.5 ka being essentially zero, and the current rate somewhat uncertain. Considering that the fault experienced a recent large earthquake after several thousand years of quiecence, and if it is reasonable to assume that we have entered another cluster which reflects a short-term increase in slip rate, then it follows that the time to the next event will be shorter than that inferred from the long-term average. Rockwell (2010a) inferred the intra-cluster recurrence interval to be less than 1 ka, with five events between 9.3 and 5 ka. This yields a recurrence interval of about 900 years within that cluster. If each event was as large as the most recent event, about 3 m, this would suggest a slip rate of more than 3 mm/yr for this interval. Considering that short and long-term fault behavior of faults is somewhat enigmatic and a current topic of debate within the scientific community (see Rockwell, 2010b), I would suggest using the long-term rate with an 80% weight, and consider using an alternative weighting scheme for slip rate (in mm/yr) with a 20% overall weight as follows:

0.5 (0% weight)

1.0 (10% weight)

1.5 (30% weight)

2.0 (30% weight)

2.5 (20% weight)

3.0 (10% weight)

KEY REMAINING UNCERTAINTIES

There are two key uncertainties that need to be resolved. For understanding the short and long-term pattern of earthquakes on the Rose Canyon fault, and their implications for future activity, it is critical to test the cluster model of Rockwell (2010a) by resolving whether there were any surface ruptures between about 5 and 0.5 ka. There was no deposition at the Rose Creek site during this period, and the inference of no ruptures is based on the strength of a soil that is developed across the earlier Holocene fault strands (Rockwell, 2010a), so it is possible that an event was missed or not well-recorded. Paleoseismic investigations in mid-late Holocene sediments across the Rose Canyon fault could resolve whether other events may have occurred, as well as potentially determine their amount of displacement. This may affect our perception of recurrence and earthquake magnitude along the Rose Canyon Fault.

The other remaining major question relates to the nature of the inferred shortening deformation suggested by Rivero et al. (2000) in the offshore region, and its relationship to the Rose Canyon fault. Geodetic observations clearly see significant right-lateral shear between San Clemente Island and Monument Peak, but there is no observable shortening or extension (figure A2-9). In fact, the right-lateral nature of the Agua Blanca fault in Baja California, along with its westerly strike, could be interpreted that there should be a small amount of continuing extension in the Borderland region (Wetmore et al., 2010 in review). Therefore, the cause of the apparent folding in the offshore Inner Borderland Region (Rivero et al., 2000) remains open to interpretation.

There are other areas where similar patterns of deformation have been observed, and it may prove valuable to assess these areas in terms of their overall structural style and seismic potential. One area that appears to have slip partitioned between strike-slip and convergence is in central California. In this area, the San Andreas fault (at 35 mm/yr) is the undisputed dominant seismic source, both in terms of magnitude and frequency. Nevertheless, a small component of shortening, estimated at no more than 3 mm/yr from geodetic data, is partly expressed as a series of folds and blind thrust faults to the east of the San Andreas fault (Coalinga anticline, Kettleman Hills, etc.: Yerkes, 1990, Wentworth, 1990). In this case, these secondary seismic sources are clearly seismically active, having produced several earthquakes in the M5.5- M6.5 range during the instrumental period, but are subordinate to the San Andreas fault. However, in comparison to the Inner Borderland, the central California example is clearly different because 1) there are clearly-defined folds that overlie blind thrusts; 2) these folds have significant structural relief and fold Holocene terraces; 3) there is a clear geodetic signal to the shortening; 4) there are earthquakes with thrust mechanisms clearly associated with these structures.

In the Inner Borderland Region, the association is not nearly as clear. There is a Miocene detachment surface, above which there has apparently been some folding (Rivero et al., 2000). However, there is no recognizable geodetic signal of shortening, nor is the seismicity clearly associated with this inferred detachment surface. An analogous situation is present in the western Salton Trough along the southern San Jacinto fault zone.

The West Salton Detachment-San Jacinto Example: The West Salton Detachment underlies much of the western Salton Trough east of the Peninsular Ranges from Borrego Valley and to the south to the Mexican Border (Axen and Fletcher, 1998). In this area, the high-angle, right-lateral San Jacinto fault cuts and offsets the West Salton Detachment and is clearly the dominant structure. Of note is the ubiquitous presence of extensive folding in the Borrego Badlands, San Filipe Hills, and Fish Creek Badlands, all of it post-detachment in age and all of it related to the continuing development of the southern San Jacinto fault zone (Dorsey and Janecke, 2002; Lutz et al., 2006).

There are many similarities between the western Salton Trough and the Inner Borderland Region. First, there is young folding above the Miocene-Pliocene detachment system, with the folding in the western Salton Trough being of substantially greater magnitude and significance than the folding in the offshore region. Furthermore, the folding is not only associated with bends in the strike-slip faults, but rather, appears to be more regionally scaled and related to secondary space accommodation above the detachment surface driven by the dominant strike-slip faulting. Second, neither region shows a geodetic signal of convergence, but rather, GPS and InSAR show virtually pure strike slip at the regional scale for the southern San Jacinto fault zone (see Fialko, 2006). Third, at least one fold grew during the 1987 Superstition Hills earthquake sequence in the western Salton Trough (Klinger and Rockwell, 1989), so there is a demonstrable association between strike-slip faulting and fold growth in this area. These and other similarities warrant a thorough examination and comparison between these two structural domains, in part because the western Salton Trough is well-studied and easily accessible.

RECOMMENDATIONS TOWARD RESOLVING REMAINING UNCERTAINTIES

For the Rose Canyon Fault itself, there are potential paleoseismic study sites to resolve whether the fault sustained displacement between about 5 and 0.5 ka. The sediments within and adjacent to the San Diego River are of the appropriate age, as river aggradation probably ceased about the time sea level rose to its present level at about 5-6 ka, and after that, sedimentation on the flood plain has locally preserved alluvium of various ages in the 0.5 to 5 ka timeframe. One area that may preserve such a record is in Old Town, where the landscape is only minimally altered. One potential site is in a golf course that essentially preserved the original topography; the fault is still expressed as a linear depression. The golf course property is owned by the City of San Diego, although it is currently under lease. Another potential site is close to the Lindvall and Rockwell (1995) trench site where a closed depression (sag) is observed in the 1928 and 1941 aerial photography. This is on private land, so access will likely be an issue. A third general site is in the flood plain of the San Diego River in Mission Valley. The fault is expressed in the 1928 aerial photographs, so the fault location can be determined with some work. The fault location may be better determined with CPT or geophysical means, once it is approximately located by interpretation of the old aerial photography. It may be possible to trench along a street, once the fault is well located.

To assess and understand the significance of the folding above the detachment surface in the offshore region, I also recommend that we thoroughly document the structural styles, rates of folding and faulting, etc. for the analogous Western Salton Trough and compare to that of those observed for the Inner Borderland Region. We need to better understand the relationship between the strike-slip faulting and the folding in the Borderland, and the western Salton Trough is far more open to study and analysis because it is sub-aerial and easily accessible. In the southern San Jacinto fault zone, we can better understand how, and when, the folding occurred, and how it relates to the dominant strike-slip faulting, perhaps even to individual events. We should also reanalyze the geodetic signals of these two areas for a component of convergence and test whether a small shortening component can be precluded or accepted.

REFERENCES

Axen, G. J., and Fletcher, J. M. 1998. Late Miocene-Pleistocene extensional faulting, northern Gulf of California, Mexico and Salton Trough, California. Int. Geol. Rev. 40:217–244.

Barrows, A.G., 1974, A review of the geology and earthquake history of the Newport- Inglewood structural zone, southern California: California Division of Mines and Geology Special Report 114, 115 p.

Clark, M.M., 1972, Surface Rupture Along the Coyote Creek Fault, USGS Professional Papers, 787, 55-86.

Dorsey, R. J., and Janecke, S. U. 2002. Late Miocene to Pleistocene West Salton detachment fault and basin evolution, southern California: new insights. Geol. Soc. Am. Abstr. Program 34:248.

Fialko, Y., 2006, Interseismic strain accumulation and the earthquake potential on the southern San Andreas fault system, Nature v. 441, 968- 971.10.1038/nature04797.

Glover, E.S., 1876, Bird’s Eye View of San Diego, California. Map published by Schneider and Kueppers, San Diego.

Grant, L.B., Waggoner, J.T., Rockwell, T.K., and von Stein, C., 1997, Paleoseismicity of the north branch of the Newport-Inglewood fault in Huntington Beach, California: *Bulletin of the Seismological Society of America*, v. 87, pp. 277-293.

Grant, L. B., K. J. Mueller, E. M. Gath, H. Cheng, R. L. Edwards, R. Munro and G. L. Kennedy, Late Quaternary Uplift and Earthquake Potential of the San Joaquin Hills, southern Los Angeles Basin, California, Geology, v. 27, no. 11, p. 1031-1034, 1999.

Grant, L. B. L. J. Ballenger, and E. E. Runnerstrom. Coastal uplift of the San Joaquin Hills, Southern Los Angeles basin, California, by a large earthquake since 1635 A.D. Bulletin Seismological Society of America, v. 92, no. 2, p.590-599, 2002.

Grant L. B. and Rockwell, T. K., 2002, A northward propagating earthquake sequence in coastal southern California?: *Seismological Research Letters*, v. 73, no. 4, p. 461-469.

Kennedy, M. P. and Clarke, S.H., 1996, Analysis of late Quaternary faulting in San Diego Bay and hazard to the Coronado Bridge, prepared for Caltrans.

Kern, J.P., 1977, Origin and history of upper Pleistocene marine terraces, San Diego, California, Geological Society of America Bulletin, v. 88, p. 1553-1566.

Kern, J.P. and Rockwell, T.K., 1992, Chronology and deformation of Quaternary marine shorelines, San Diego County, California: in Quaternary Coasts of the United States: Marine and Lacustrine Systems: Society of Economic Paleotologists and Mineralogists Special Publication.No. 48, p. 377-382.

Klinger, R.E. and Rockwell, T.K., 1989, Flexural-slip folding along the eastern Elmore Ranch fault in the Superstition Hills earthquake sequence of November 1987: Bulletin of the Seismological Society of America, v. 79, no. 2, p. 297-303.

Leon, L.A., Dolan, J.F., Shaw, J.H., and Pratt, T.L., 2009, Evidence for large Holocene earthquakes on the Compton-Los Alamitos fault, Los Angeles, California. Journal of Geophysical Research, v. 114, B12305, doi:10.1029/2008JB006129.

Lindvall, S. and Rockwell, T.K., 1995, Holocene activity of the Rose Canyon fault, San Diego, California: Journal of Geophysical Research, v. 100, no. B12, p. 24121- 24132.

Lutz, A. T.; Dorsey, R. J.; Housen, B. A.; and Janecke, S.U. 2006. Stratigraphic record of Pleistocene faulting and basin evolution in the Borrego Badlands, San Jacinto fault zone, southern California. Geol. Soc. Am. Bull. 118:1377–1397.

Mueller, K., Kier, G., Rockwell, T. and Jones, C. 2009, Quaternary Rift-Flank Uplift of the Peninsular Ranges in Baja and Southern California by Removal of Mantle Lithosphere. Tectonics, v. 28, 17 p. doi:10.1029/207TC002227.

Rivero, C., Shaw, J.H., and Mueller, K.J., 2000, Oceanside and Thirty Mile Bank blind thrusts: Implications for earthquake hazards in coastal southern California. Geology, v 28, p. 891-894.

Rockwell, T., 2010a, The Rose Canyon Fault Zone in San Diego; Proceeding of Fifth International Conference on Recent Advances in Geotechnical Earthquake Engineering and Soil Dynamics and Symposium in Honor of Professor I.M. Idriss; Paper No. EQ 5, 9pgs.

Rockwell, T., 2010b, The non-regularity of earthquake recurrence in California: Lessons from long paleoseismic records from the San Andreas and San Jacinto faults in southern California, and the north Anatolian fault in turkey, Proceeding of Fifth International Conference on Recent Advances in Geotechnical Earthquake Engineering and Soil Dynamics and Symposium in Honor of Professor I.M. Idriss; Paper No. EQ 5, 9pgs.

Rockwell, T.K. and Murbach, M., 1999, Holocene earthquake history of the Rose Canyon fault zone. USGS Final Technical Report for Grant No. 1434-95-G-2613, 36 p + App.

Treiman, J., 1993, The Rose Canyon fault zone, southern California, California Div. of Mines and Geology, Open File Report 93-02, 45 p.

USGS, 2009, Personal Communication.

Wentworth, C.M., 1990, Structure of the Coalinga region and thrust origin of the earthquake, in The Coalinga, California earthquake of May 2, 1983. U.S. Geological Survey Professional Paper 1487, p. 41-68.

Wetmore et al., 2010 in review, The Agua Blanca Fault in Baja California, submitted to Tectonics.

Wesnousky, S.G., 2008, Displacement and geometrical characteristics of earthquake surface ruptures: Issues and implications for seismic-hazard analysis and the process of earthquake rupture. Bull. Seismological Society of America, v. 98, p. 1609-1632.

Wright, T.L.,1991, Structural geology and tectonic evolution of the Los Angeles basin, California. In Am. Assoc. Petroleum Geologists Memoir 52, p. 35-134.

Yerkes, R.F., 1990, Tectonic setting, in The Coalinga, California earthquake of May 2, 1983. U.S. Geological Survey Professional Paper 1487, p. 13-22.

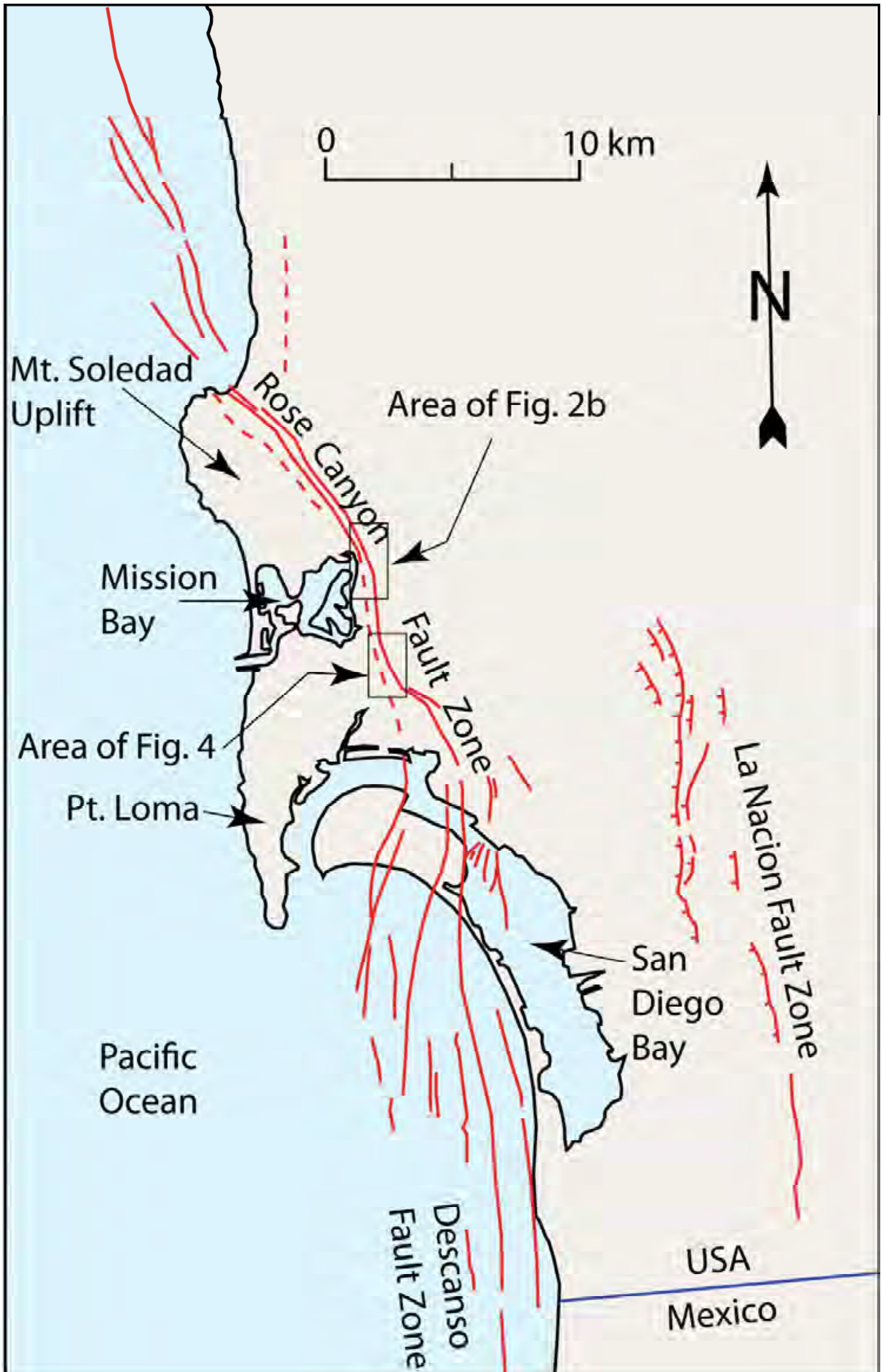

By Rockwell (2010)

MAP OF THE MAIN ELEMENTS OF THE ROSE CANYON FAULT IN SAN DIEGO	FIGURE A2-1
SAN ONOFRE NUCLEAR GENERATING STATION SEISMIC HAZARD ASSESSMENT PROGRAM	

GeoPentech
Geotechnical & Geoscience Consultants

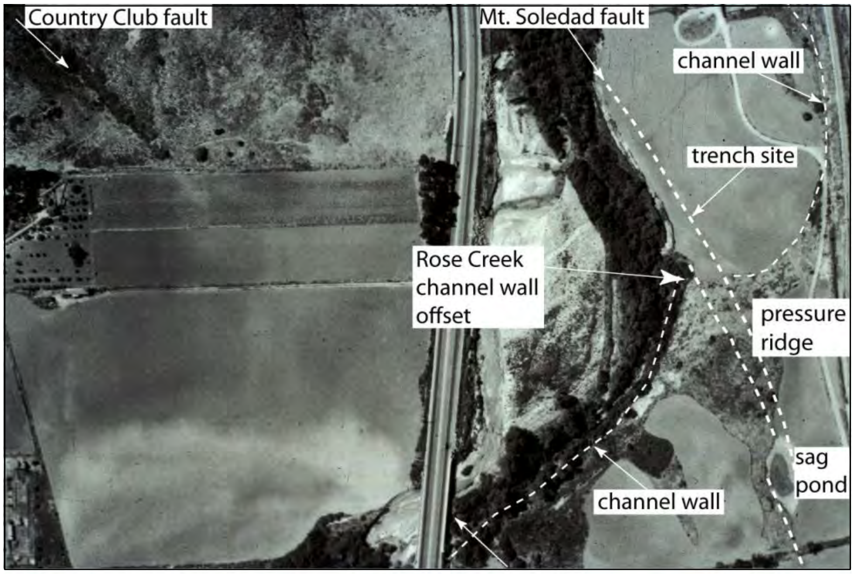

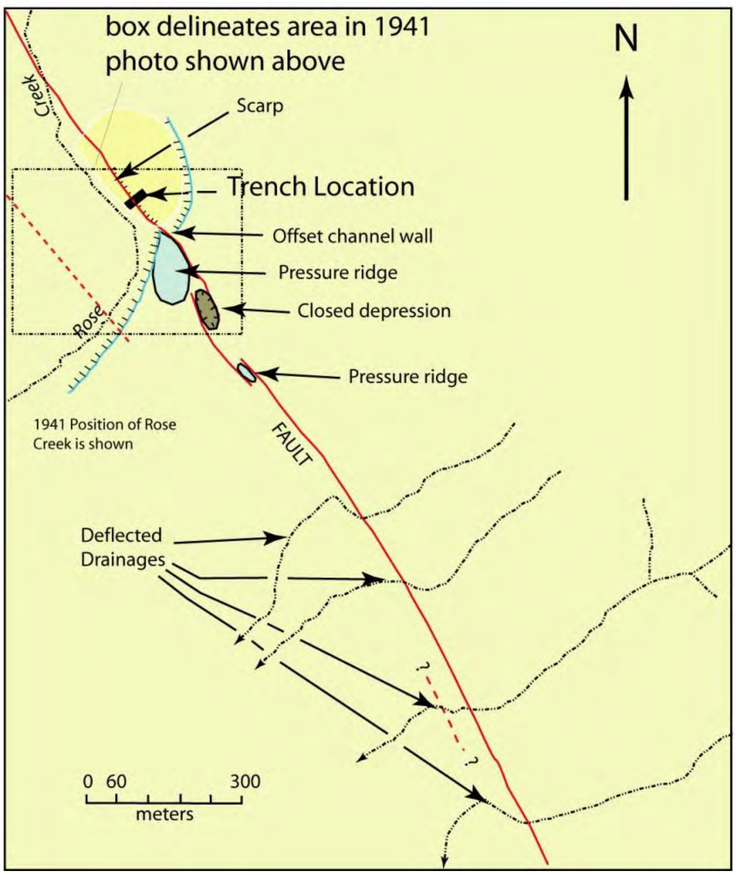

NOTE: Annotated air photo (upper) shows detail of area in the box in the lower diagram (from Lindvall and Rockwell, 1995, Rockwell, 2010).

GeoPentech Geotechnical & Geoscience Consultants By Rockwell (2010)	**INTERPRETIVE MAP OF TECTONIC GEOMORPHIC FEATURES IN THE ROSE CREEK AREA**	FIGURE A2-2
	SAN ONOFRE NUCLEAR GENERATING STATION SEISMIC HAZARD ASSESSMENT PROGRAM	

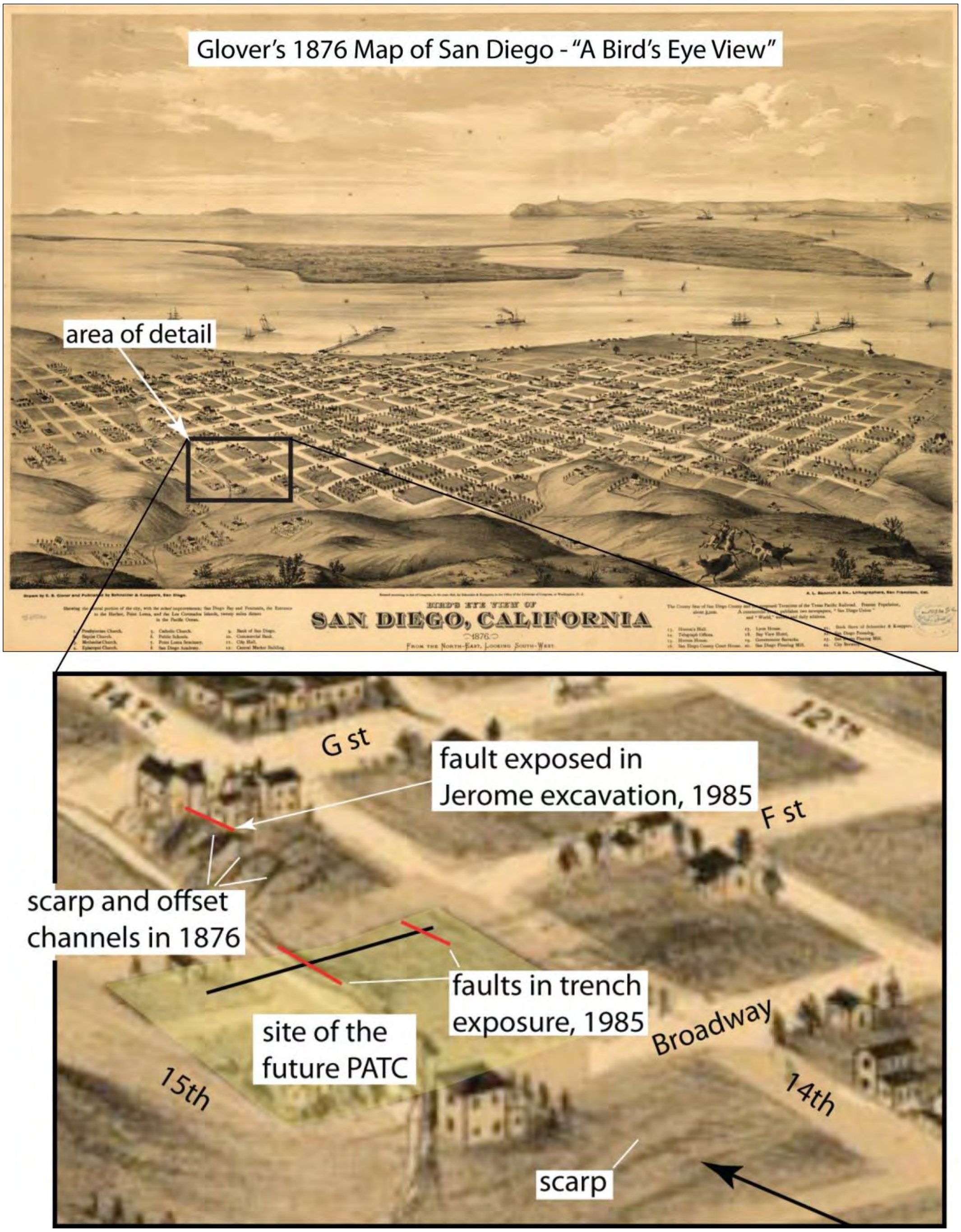

NOTE: Remarkably, the artist's eye picked out and drew scarps and deflected drainages along the Rose Canyon fault: the location of the fault in this area was determined by excavations in 1985 for the new Police headquarters building (PATC) and for a foundation excavation for a Jerome's warehouse.

GeoPentech Geotechnical & Geoscience Consultants By Rockwell (2010)	**ANNOTATED ARTIST'S RENDITION OF DOWNTOWN SAN DIEGO IN 1876**	FIGURE A2-3
	SAN ONOFRE NUCLEAR GENERATING STATION SEISMIC HAZARD ASSESSMENT PROGRAM	

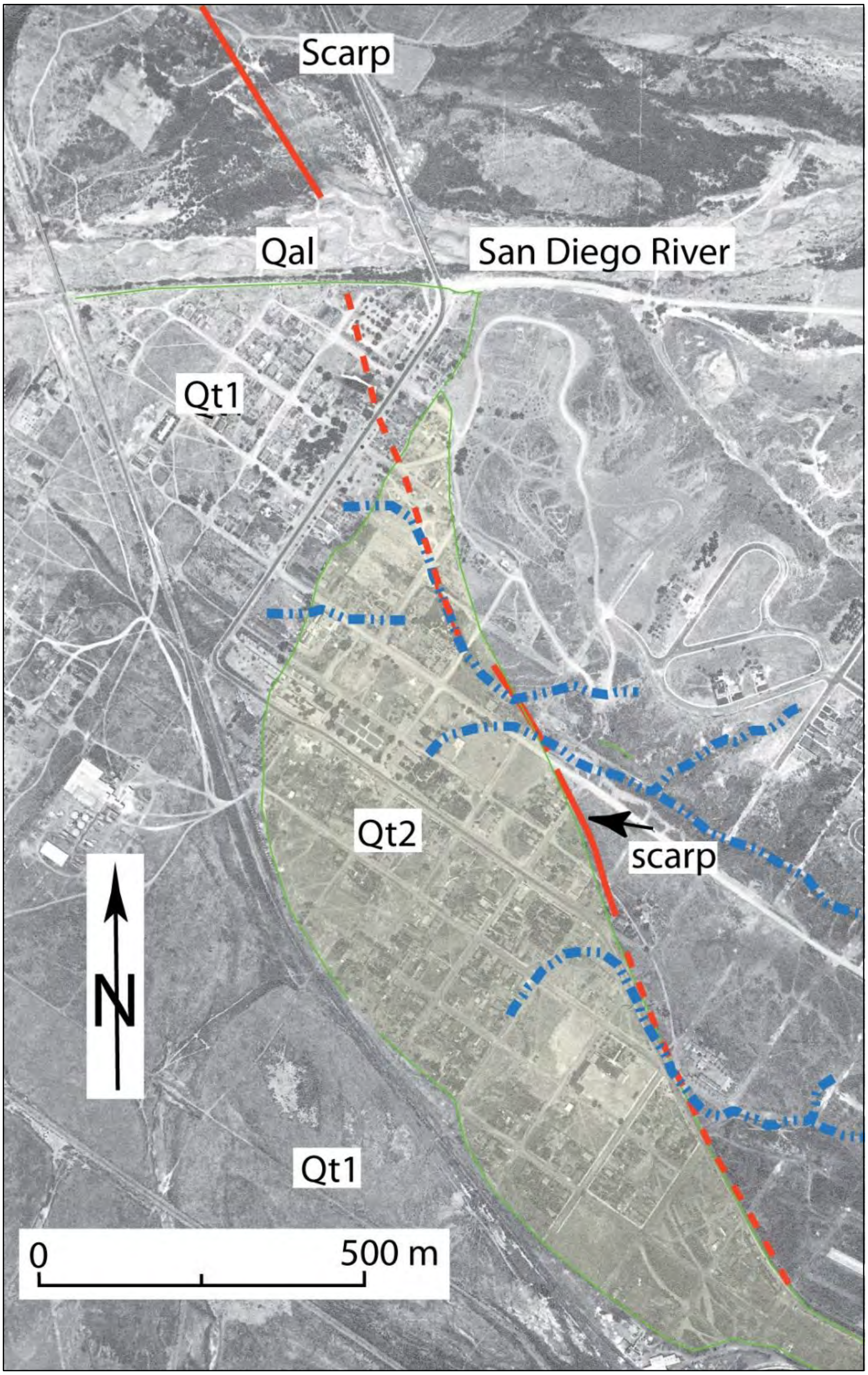

NOTE: Note the deflected channels incised into the Qt2 surface, which is interpreted to be last the interglacial terrace based on its elevation (from Rockwell, 2010).

GeoPentech Geotechnical & Geoscience Consultants By Rockwell (2010)	**INTERPRETED 1941 AERIAL PHOTOGRAPHY OF THE OLD TOWN AREA OF SAN DIEGO**	FIGURE A2-4
	SAN ONOFRE NUCLEAR GENERATING STATION SEISMIC HAZARD ASSESSMENT PROGRAM	

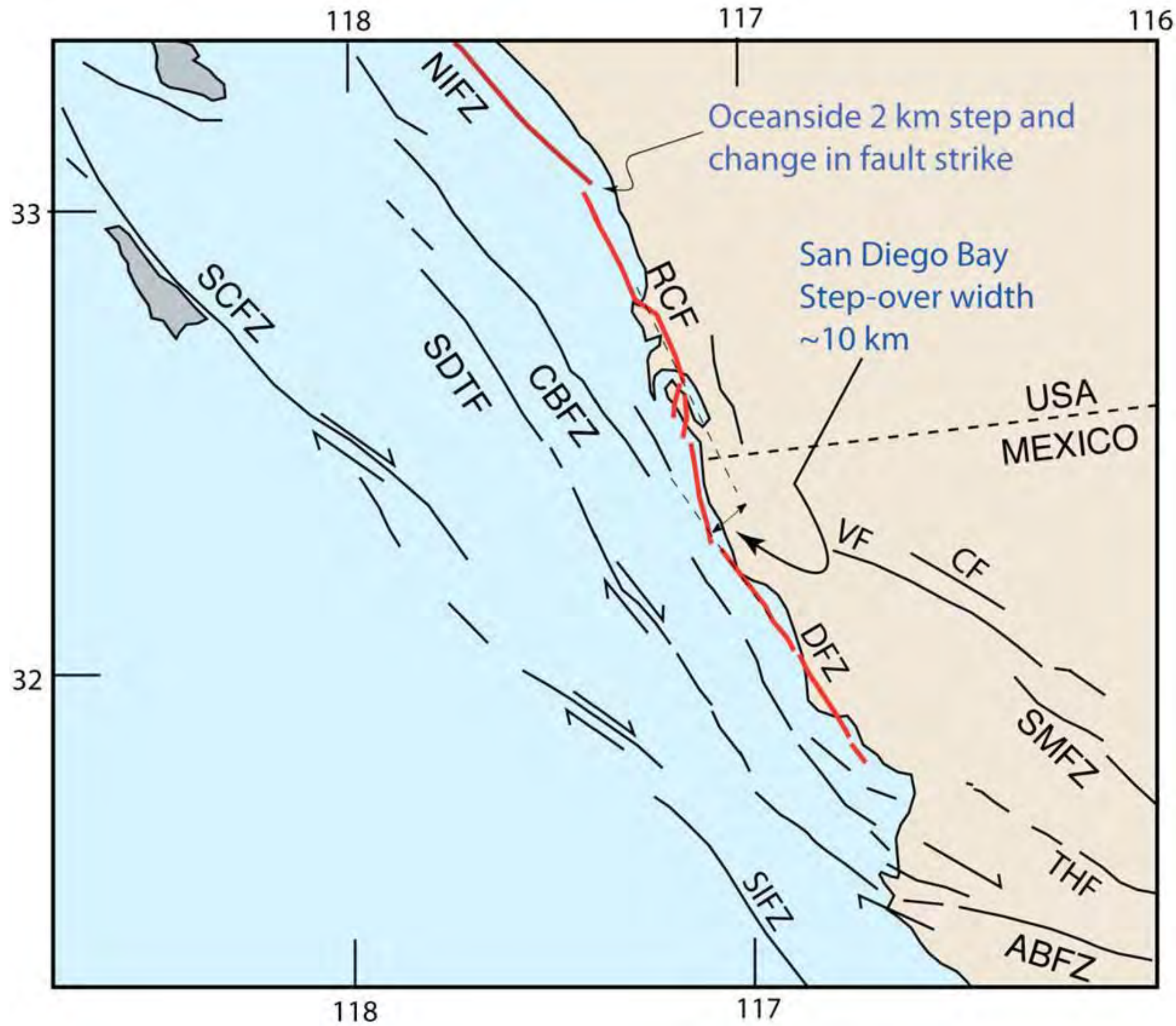

NOTE: Also shown is the smaller step at Oceanside with the change in fault strike. SAFZ - San Andreas fault zone; SJFZ - San Jacinto fault zone; IF - Imperial fault; CPF - Cerro Prieto fault; LSF - Laguna Salada fault; NIFZ - Newport- Inglewood fault zone; RCF - Rose Canyon fault; CF - Calabasas fault; VF - Vallecitos fault; SMFZ - San Miguel fault zone; THF - Tres Hermanes fault; ABFZ - Agua Blanca fault zone; CBFZ - Coronado Bank fault zone; DFZ - Descanso fault zone; SDTF - San Diego Trough fault; SCFZ - San Clemente fault zone; SIFZ - San Isidro fault zone.

GeoPentech
Geotechnical & Geoscience Consultants

By Rockwell (2010)

MAP SHOWING HOW STEP-OVER WIDTH WAS MEASURED FOR THE SAN DIGEO BAY STEP

FIGURE A2-5

SAN ONOFRE NUCLEAR GENERATING STATION

SEISMIC HAZARD ASSESSMENT PROGRAM

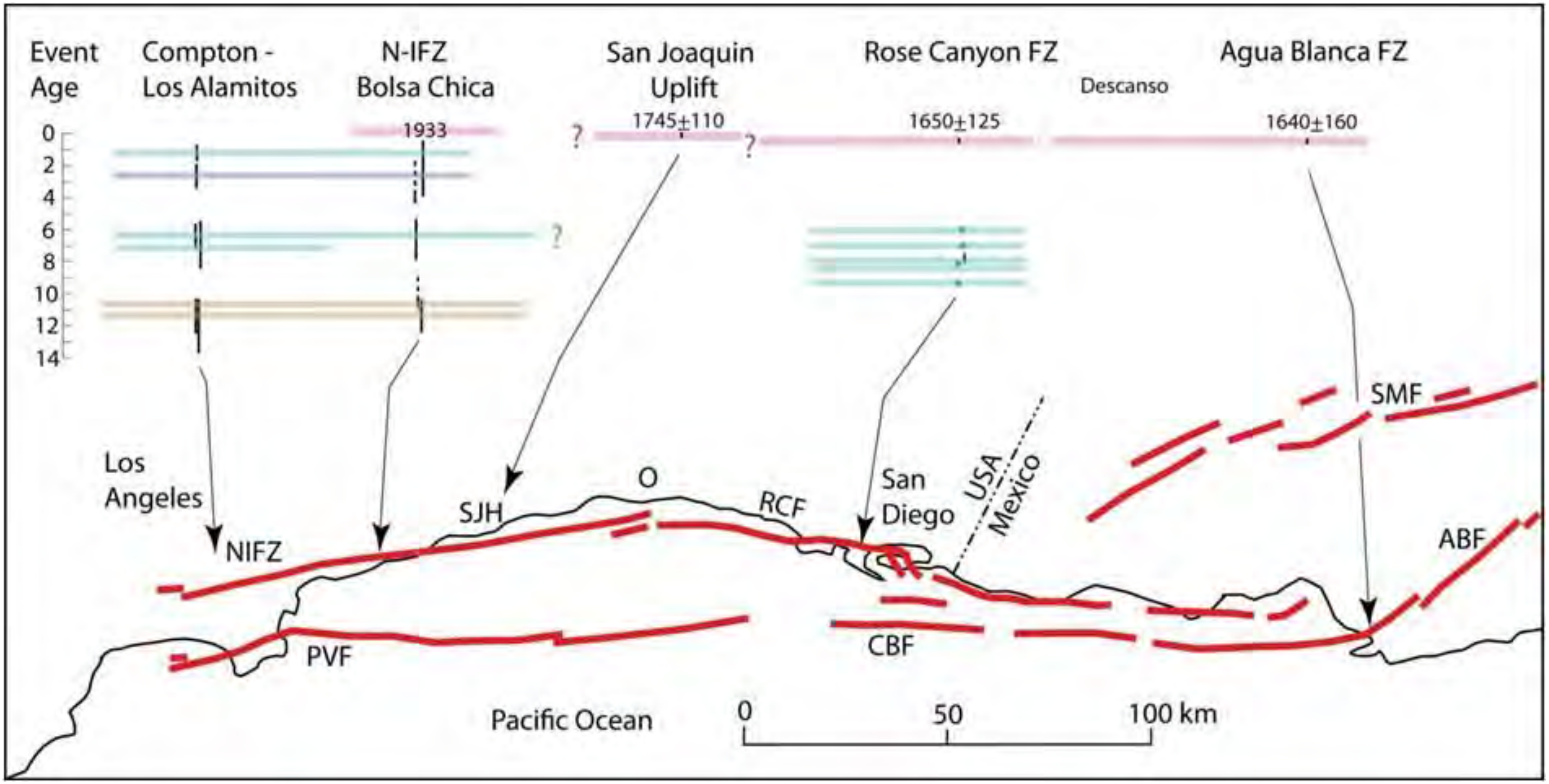

NOTE: Results from paleoseismic studies for the Agua Blanca, Rose Canyon, San Joaquin Hills, Newport-Inglewood, and Compton faults (from Grant and Rockwell, 2002; Grant et al., 1997, Leon et al., 2009).

GeoPentech Geotechnical & Geoscience Consultants By Rockwell (2010)	SAN ONOFRE NUCLEAR GENERATING STATION SEISMIC HAZARD ASSESSMENT PROGRAM	PALEOSEISMICITY FOR NI/RC FAULT ZONE	FIGURE A2-6

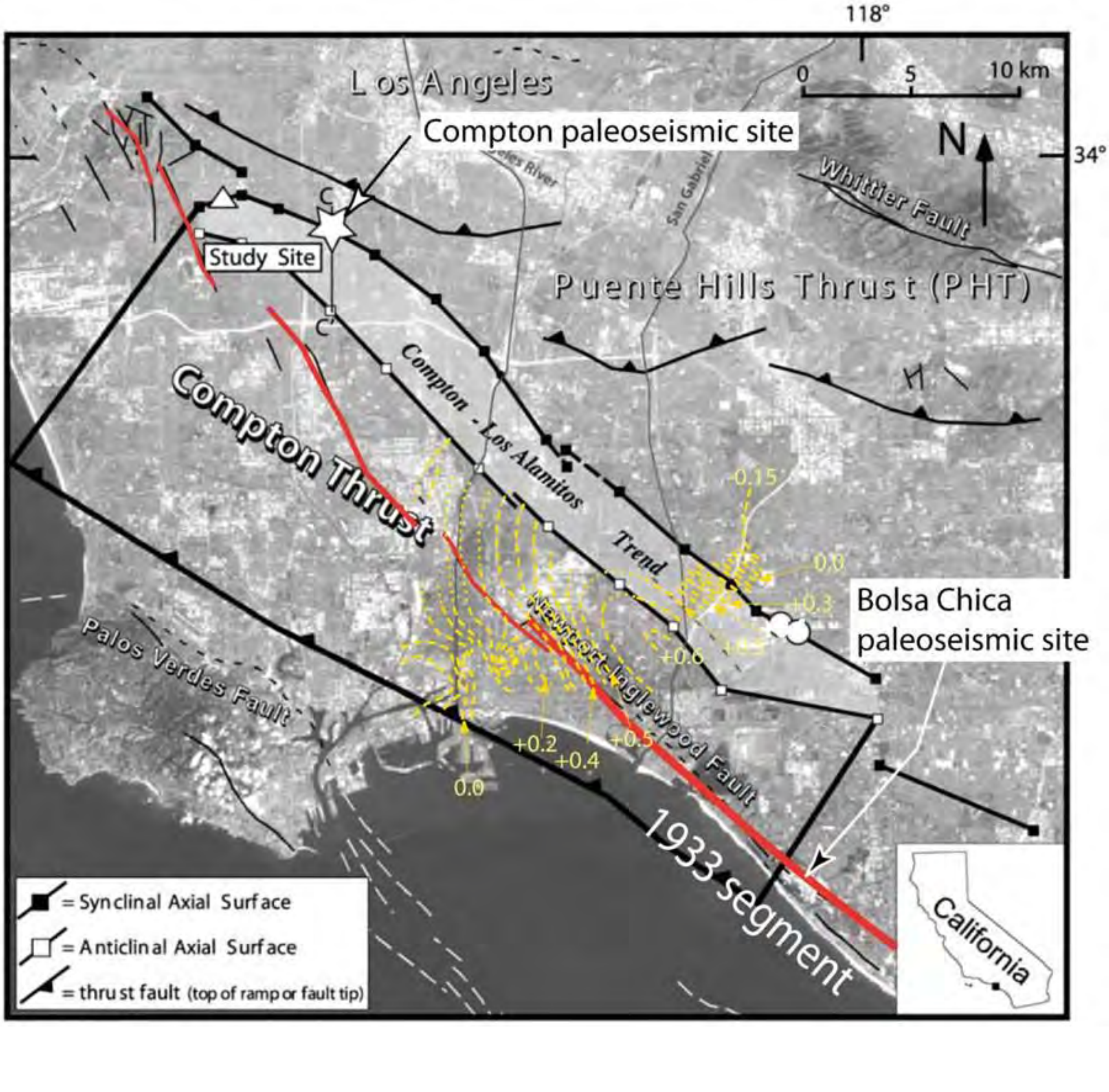

NOTE: Location figure from Leon et al. (2009), showing their Compton paleoseismic site. The bolded red line is the inferred segment that ruptured in 1933 (Barrows, 1974), along with the area that sustained uplift in the 1933 earthquake, based on leveling data (Barrows, 1974). Maximum uplift was documented as more than 60 cm, with the locus between the Newport-Inglewood and Los Alamitos structures, supporting Wright's (1991) interpretation that the Compton-Los Alamitos trend is deformation associated with an oblique, high-angle fault.

GeoPentech Geotechnical & Geoscience Consultants By Rockwell (2010)	LOCATION FIGURE FROM LEON ET AL. (2009)	FIGURE A2-7
	SAN ONOFRE NUCLEAR GENERATING STATION SEISMIC HAZARD ASSESSMENT PROGRAM	

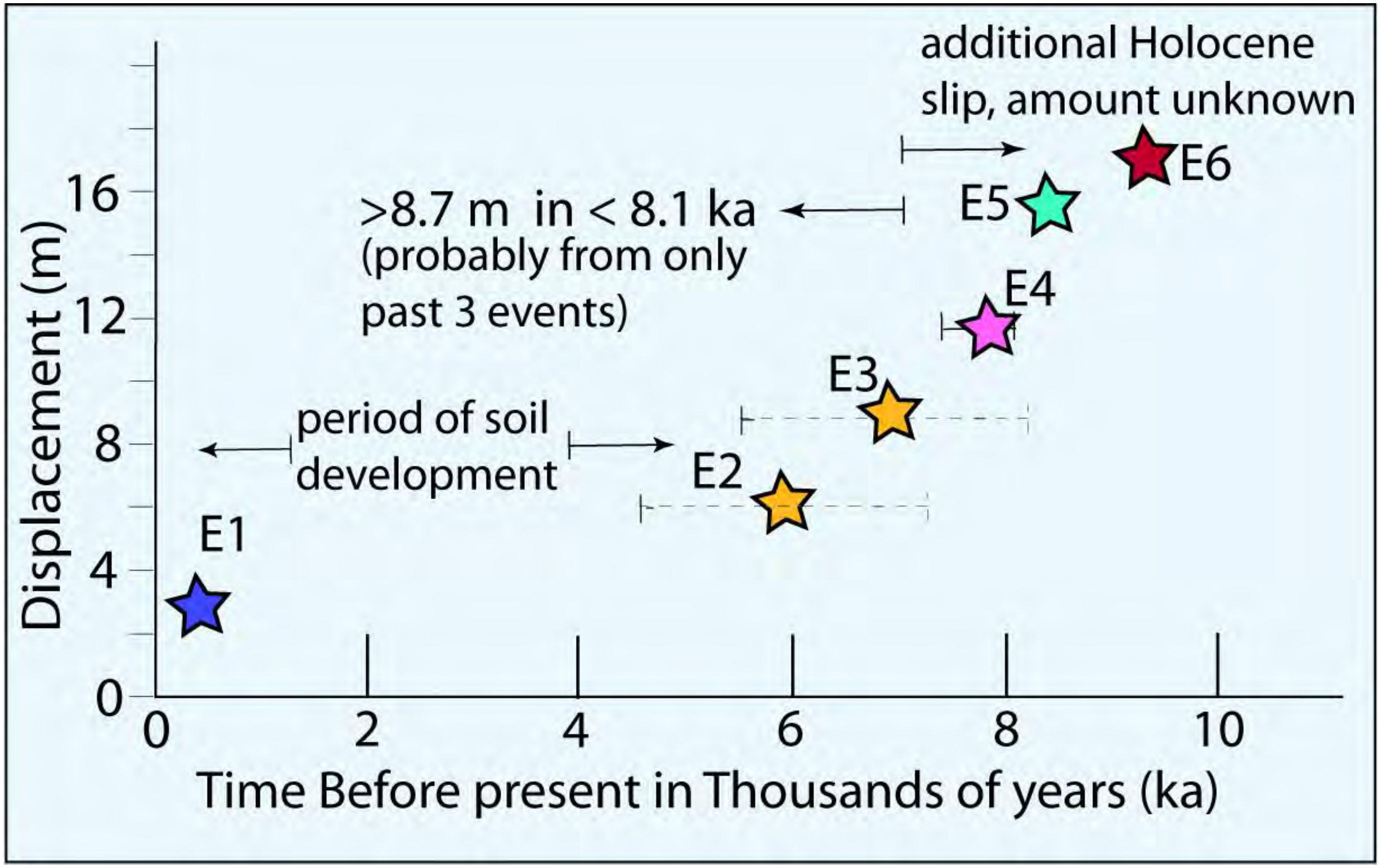

NOTE: Timing of surface ruptures at Rose Creek, assuming that the strong soil development across the early Holocene fault splays accurately represents a lack of activity for several thousand years (from Rockwell, 2010a).

GeoPentech
Geotechnical & Geoscience Consultants

By Rockwell (2010)

SAN ONOFRE NUCLEAR GENERATING STATION
SEISMIC HAZARD ASSESSMENT PROGRAM

TIMING OF SURFACE RUPTURES AT ROSE CREEK

FIGURE A2-8

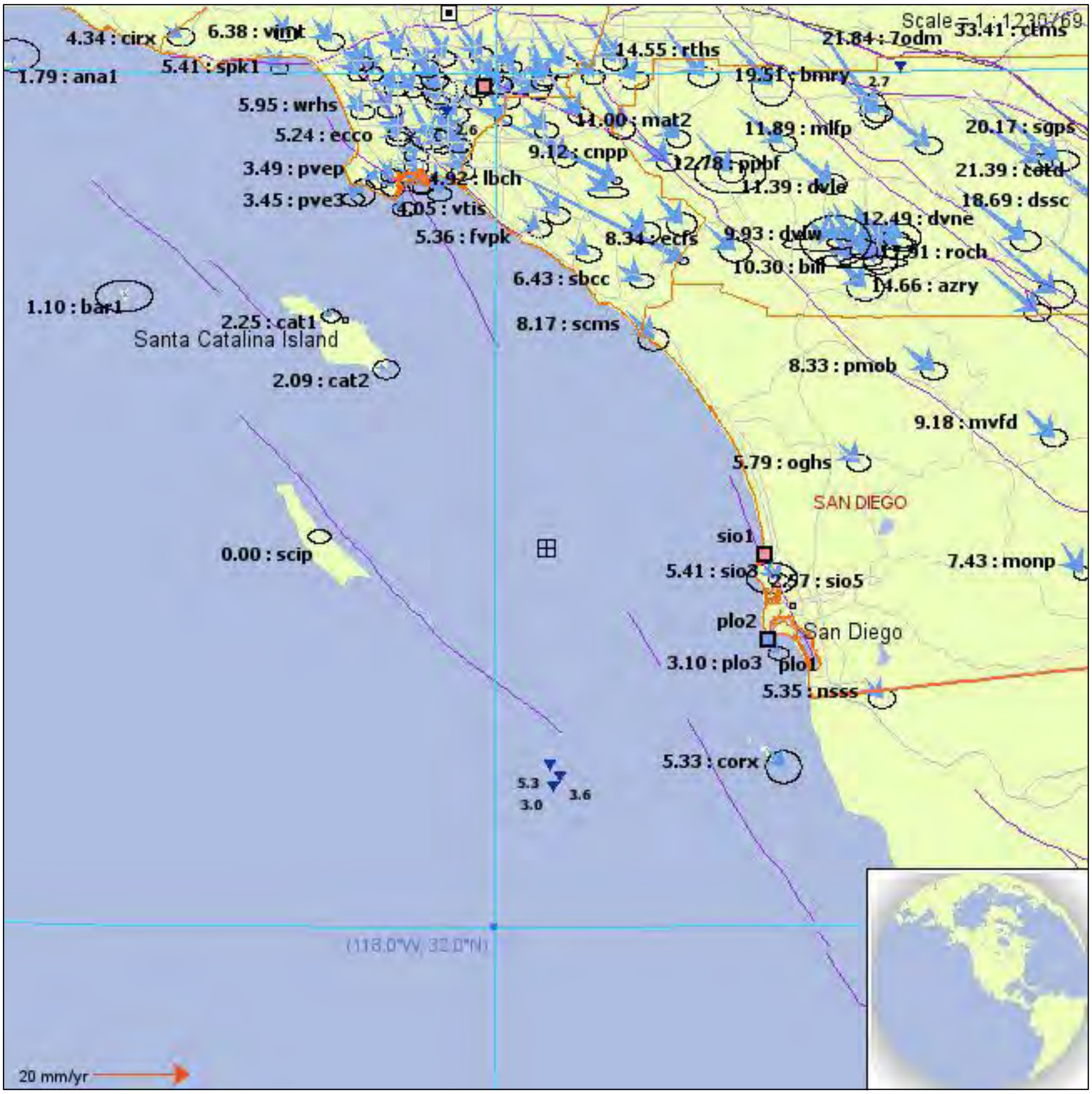

NOTE: GPS velocity field of the southern California Borderland, plotted with San Clemente Island as the reference frame (plotted in 2005 from the SCIGN web page).

GeoPentech Geotechnical & Geoscience Consultants By Rockwell (2010)	GPS VELOCITY FIELD OF THE SOUTHERN CALIFORNIA BORDERLAND	FIGURE A2-9
	SAN ONOFRE NUCLEAR GENERATING STATION SEISMIC HAZARD ASSESSMENT PROGRAM	

APPENDIX A – ATTACHMENT A-3

SEISMIC SOURCE CHARACTERISTICS OF INNER CALIFORNIA BORDERLAND'S BLIND THRUST FAULT SYSTEMS

By
Dr. John Shaw and Dr. Andreas Plesch
Department of Earth and Planetary Sciences Harvard University, Cambridge, MA

INTRODUCTION

The following document has been prepared at the request of Southern California Edison (SCE) in consultation with technical members of their Seismic Hazard Assessment Program (SHAP).

Active thrust faults have long been known to exist in southern California, particularly in the Transverse Range Province. Awareness of the seismic risk associated with these thrust faults was heightened by the 1971 San Fernando (M_W 6.6) Earthquake, which resulted from slip on the San Fernando segment of the Sierra Madre Thrust Fault System; slip that ruptured the ground surface. Later, the 1987 Whittier Narrows (M_L 5.9) and the 1994 Northridge (M_W 6.7) earthquakes demonstrated the seismic hazards posed by these 'blind' thrust faults; slip that does not rupture the ground surface. The lack of surface ruptures on 'blind' thrust faults hinders our ability to locate them and assess their level of seismic activity.

The reverse/thrust focal mechanism solution tied to the offshore 1986 Oceanside (M_L 5.3) Earthquake demonstrated that active blind thrust faults also exist in southern California's Inner Continental Borderland. This offshore earthquake, combined with our extensive research of hundreds of proprietary oil industry marine geophysical seismic reflection survey lines, lead us to infer the presence of two distinct, active thrust fault systems located offshore of southern Orange County and San Diego County (Rivero et.al., 2000). As shown on Figure A3-1, the Oceanside Blind Thrust (OBT) extends at least from Laguna Beach to the Mexican border and may dip under the shoreline. The smaller Thirty-mile Bank Blind Thrust (TMBT) lies to the west, farther offshore.

Following is a brief discussion of our current understanding of the seismic source characteristic of the OBT and the TMBT developed since Rivero et.al. (2000). This briefing also summaries our current understanding of the relationship between the OBT and the TMBT with other thrust, reverse, normal, and strike-slip faults in southern California's Inner Continental Borderland. Most of what is presented herein is derived from what has been described in Rivero (2004) and Rivero and Shaw (in press).

Specifically, in this briefing we summarize:

1) Constraints on the location of the OBT and TMBT and our assessment of their level of seismic activity;
2) Our current understanding and weightings of the seismic characteristics of these two fault systems;

3) The logic tree developed to facilitate incorporating, particularly the OBT fault systems into SCE's Probabilistic Seismic Hazard Assessment (PSHA) and Probabilistic Tsunami Hazard Assessment (PTHA) updates for the San Onofre Nuclear Generating Station (SONGS);
4) The key remaining uncertainties regarding each fault's seismic source characteristics; and
5) Our recommendations for future efforts to resolve these key remaining uncertainties. A list of the references flagged herein is included at the end of this briefing document.

PRESENCE AND LEVEL OF ACTIVITY

In Rivero (2004) and Rivero and Shaw (in press) we supplemented the information provided in Rivero et.al., (2000) with more details on the various data supporting the presence and activity of the OBT and TMBT and their connections with the offshore high-angle, strike slip faults; the latter including the Newport-Inglewood (NI), Rose Canyon (RC), and San Diego Trough (SDT) faults.

These data include:

a) High-resolution seismic reflection data that image the OBT and TMBT. These faults are defined by deep, shallow dipping, seismic reflections off the coast of southern California underlying folded and faulted sediments. The youngest of these sediments are inferred to be at least Plio-Pleistocene in age (some apparently displacing the sea floor).
b) Balanced and restored cross sections that document significant contraction or shortening on these structures since the Pliocene (such as the ~2.2 to 2.7 km across the OBT within the last ~1.8 – 2.4 million years).
c) Earthquake epicenter/hypocenter/focal mechanisms, particularly the Oceanside 1986 M_L 5.3 event, which occurred between San Clemente Island and Oceanside, CA and ruptured the TMBT. In addition, the 1986 Coronado Bank earthquake events, max M_L 3.7, which occurred offshore of Point Loma in August 1986 (Astiz and Shearer, 2000), were incorporated in our analysis;
d) Elevated marine terraces along the Orange/San Diego County's shoreline; and
e) GPS data from the SCEC Crustal Motion Map that Kier and Mueller (1999) used to calculate the components of motion perpendicular to the offshore thrust fault traces. Rivero 2005 used the maximum of these station values, minus the slip rate derived for the OBT, to bracket the slip rate on the Thirty-mile Bank fault. Our sense is that these geodetic data are poorly constrained, largely due to the lack of offshore data coverage. Thus, there is a large uncertainty associated with this rate determination, but at present we simply lack another means to estimate this rate.

SEISMIC CHARACTERISTICS

Figure A3-1 provides a map of the OBT and TMBT and their associated hanging wall and footwall subsidiary faults, as modified from Rivero (2004). Also modified from Rivero (2004), Figure A3-2 summarizes the various rupture models considered for these faults. Figure A3-3 provides a more simplified version of the fault map presented on Figure A3-1. This more simplified map was used to obtain the representative three dimensional coordinates for the OBT, TMBT and their associated splay faults relative to the location of the SONGS for input into the PSHA program (Abrahamson, 2010).

The table presented in Figure A3-4 provides a complete listing of our current estimates of the OBT's and TMBT's seismic source characteristics. In addition, we provide seismic source characteristics of other thrust, reverse, normal, and strike-slip faults in the region that may rupture in conjunction with the OBT and TMBT Fault Systems. Each row of the table represents different individual or multi-segment combinations of plausible rupture scenarios, keyed to the schematic drawings of the four alternative rupture models presented in Figure A3-2.

The rupture area (km^2) for each plausible rupture scenario listed in Figures A3-3 and A3-4 was estimated based on the 3-D mapping of the fault in the SCEC Community Fault Model that we have developed (Plesch et al., 2007), assuming a seismogenic depth > 5 km and <17 km. The resulting maximum magnitude earthquake was then calculated using the rupture area versus magnitude relationships developed by Wells and Coppersmith (1994).

The slip rate was estimated for the OBT based on measures of fault offsets and uplift using the marine geophysical seismic reflection survey data and estimates of the ages of the deformed geologic formations. Using the estimated slip rates we then calculated recurrence intervals of the maximum magnitude earthquake for each particular rupture scenario using Wells & Coppersmith (1994) and Shaw and Suppe (1996).

The slip rate for the TMBT was estimated from limited GPS data, as discussed above. We have no constrains on the slip rate of the SDT fault, although it appears to be active based on offsets of near seafloor horizons.

The slip rate on the Carlsbad Fault was estimated by Rivero (2004) based on a range of dip-slip values (0.4 to 0.6 km) using two alternative structural models. The rates are derived using maximum and minimum ages (2.4 and 1.8 mya, respectively) for the initiation of faulting and folding, as defined by patterns of syntectonic (growth) sediments.

Slip rate estimates for the offshore extensions of the NI and RC right-lateral strike-slip faults were based on slip rates assigned to the on-shore traces of these faults from CGS (2002).

LOGIC TREE FOR PSHA/PTHA

Our sense is that these alternative rupture models represent a range of possible scenarios. In reality, however, some may not occur. If more than 1 of these alternatives does occur (which seems plausible), it implies that various fault segment rupture in different types of earthquakes. Thus, the alternatives attempt to capture both epistemic and aleatory uncertainty.

The first step in utilizing the above seismic source characterization of the OBT, TMBT and related subsidiary faults in the SONGS PSHA involved the preparation of the logic tree presented on Figure A3-5. This logic tree was used to accommodate both the epistemic and aleatory uncertainty in the seismic source characteristics (SSC) of the various alternative rupture models. A digital file of this logic tree is also provided in the attached CD.

In terms of our confidence in the reality of the various branches of the logic tree presented on Figure A3-5, we feel it is acceptable to apply equal weights to accommodate the epistemic uncertainty in both model 3 and 4, and a reduced weight for model 2. Although this is a subjective assessment, we would suggest that model 2 should be weighted substantially lower than model 3 or 4 (by a factor 4 or more).

Our reasoning for this weighting is that no viable structural model has been presented to explain the observed slip on the Oceanside thrust is driven by motion on the strike-slip faults. Therefore on a percentage basis, in terms of our best guess, something like 45% for model 3, 45% for model 4, and 10% for model 2, would be a reasonable fit.

We recognize that others believe that right-lateral strike slip faults (model 1) dominate the tectonics off-shore of Orange and San Diego Counties. However, based on the currently available data, we would assign a weight of '0' to rupture model 1 on Figure A3-5. As we stated above, rupture model 1 is not kinematically compatible with the large amount of displacement we document on the OBT Fault. Thus, we believe that the seismogenic potential of the strike-slip faults is represented most effectively in models 2, 3, or 4.

Our percentage weightings applied to the alternative linkage hypotheses for both single and complex strike-slip and thrust earthquake sources in rupture models 3 and 4, are also shown on Figure A3-5. These best guess percentages also reflect on the current epistemic uncertainty of the existing data regarding the connection of the various possible rupture linkages within a seismogenic depth > 5 km and <17 km.

Based on the available data and interpretations there are 67 combinations of fault rupture segments as shown on Figure A3-5. Those branches of the logic tree that reflect the "either/or" epistemic uncertainty of the data are highlight with blue colored lines. The "sometime this way/ sometimes that way" aleatory uncertainty in the data is highlighted in the logic tree by orange line boxes.

Model 1 (0% weighting) focuses the remaining portion of this Appendix on the remaining three OBT models. The possibility of Model 1 as a likely seismic source is discussed in more detail in the other subsections of Appendix A.

Model 2 (10% weighting) reflects two separate alternative seismic sources, i.e., the high angle, strike-slip NI and RC faults. Either these two sources is reflected as 'sometimes' rupturing only on a single segment and 'sometimes' rupturing on multisegments, both onshore and offshore. Model 2 also accommodates the aleatory possibility that the OBT will rupture as a southwest vergent subsidiary fault off of either the NI or the RC faults' rupture. Using the magnitude and slip rate calculations listed in Figure A3-4, the resulting earthquake recurrence was calculated using the Wells and Coppersmith, (1994) Maximum Magnitude recurrence models.

Model 3 (45% weighting) reflects three separate alternative seismic sources, i.e., the onshore/near shore segments of the NI and RC strike-slip faults and the OBT. The OBT has two epistemic branches reflecting the uncertainty as to its extent on-shore to the north of Dana Point and under the San Joaquin Hills. This uncertainty impacts the source area/maximum magnitude calculation, but otherwise the make-up of the logic tree is the same for the branch "North of Dana Point" as is for the branch "South of Dana Point". Using the "South of Dana Point" branch as an example for Model 3, the 4 "linkage" options, i.e., 3a, $3b_1$, $3b_2$, and 3c and their corresponding epistemic weightings are considered. Then under each of these four linkage alternatives, the single and multiple thrust fault/hanging and footwall subsidiary fault aleatory randomness is accommodated. Then, as was explained in the Model 2 discussion, for each of these rupture models the corresponding slip rates and recurrence calculations are provided.

Model 4 (45% weighting) reflects a similar logic three as Model 3, but with fewer branches to reflect the lack of a footwall faults in Model 4 in comparison with Model 3. However, two differences exist between Model 3 and Model 4 rupture scenarios. The first of these differences is reflected by "linkage 4b" were no seismogenic links exist between the high-angle strike-slip fault in the hanging wall above the OBT because of its depth below the seismic zone (> 17 km). In this situation the hanging wall, high angle, strike-slip fault ruptures as an independent source in addition to the thrust fault source. The second Model 4 versus Model 3 variation was to accommodate the presence of the Carlsbad Thrust Fault in the hanging wall above the OBT. The Carlsbad fault rupture scenario was not part of Model 3 because it presence only in the hanging wall was clearly supported by the marine seismic reflection data, thus only fitting Model 4.

KEY REMAINING UNCERTAINTIES

The key uncertainties associated with representing these potential seismic sources in the SONGS's PSHA result from the lack of good constraints on the fault slip rates and the inability to distinguish between the several single and multi-segment rupture scenarios that are considered. Specifically, it is unclear whether the shallow dipping thrust faults (such as the OBT) are the primary seismic source faults, with the steeply dipping, right-lateral, strike-slip faults, such as the NI or the RC faults, being subsidiary, or whether the steep, strike-slip faults are the primary seismic sources, and the thrust faults are subsidiary.

Unfortunately this uncertainty continues to exist. The TMBT fault is locally imaged in the seismic reflection to the east of its intersection of the San Diego Trough strike-slip fault. This, combined with the location and focal mechanism of the 1986 Oceanside earthquake, imply that the TMBT is a continuous, active structure. This favors models 3 and 4. None of the seismic reflection profiles we examined, however, clearly imaged subsurface conditions at the depths and locations necessary to resolve the critical interactions of the OBT and NI-RC system. The OBT is not imaged in these locations because it juxtaposes basement on top of basement rocks. Thus, no significant impedance boundary exists, and the fault cannot be imaged by the seismic data.

Regarding fault activity and slip rates, the TMBT is clearly active based on the 1986 Oceanside earthquake. However, its recent (Holocene) slip rate is largely unconstrained, as is the slip rate for the San Diego Trough strike-slip fault. We simply lack the ability to measure direct fault offsets and/or to have constraints on the ages of offset horizons given the lack of well data in this area. The evidences for activity of the OBT are more indirect. Perhaps the best constrains on recent activity of the OBT come from folded and offset horizons at or near the seafloor. However, lacking direct age control for these young sediments limits our ability to constrain how recently the fault has rupture and its slip rate. Association of the OBT and the San Joaquin Hills thrust, combined with the patterns of uplifted coastal marine terraces, further support fault activity.

RECOMMENDATIONS TOWARDS RESOLVING REMAINING UNCERTAINTIES

At the depths and locations where data is necessary to resolve the uncertainty discussed above regarding the intersection between the NI/RC and the OBT, the faults are within the basement rocks and the velocity contrast/acoustic impedance of the basement rocks either side of where these faults are inferred to be interfacing is not likely to be significant enough to produce adequate reflectors in the marine geophysical seismic reflection surveys. As such, even if environmental hurdles to future deep seismic surveys are overcome, it is doubted whether high energy, deep penetrating 2-D or 3-D seismic surveys can retrieve the necessary data to be able to unequivocally resolve this particularly important uncertainty.

In lieu of this data, the following is recommended to better define the extent of the OBT and the TMBT and to more precisely estimate their late Pleistocene and Holocene activity.

- High-resolution side-scan sonar and seismic reflection imaging of seafloor deformation combined with sediment sampling and dating, would likely provide better constraints on activity and slip rates for the OBT, TMBT, and San Diego Trough strike-slip fault (highest priority). Regarding recommended sites of future studies, Figure A3-6 highlights three possible study regions. Clearly, we would need to do a more thorough evaluation of current data to confirm the appropriateness of each site, and the particular types of data (side-scan sonar, high-res seismic) that would be most useful. Nevertheless, region 1 would target improving our understanding of the along strike continuity of the Oceanside and San Joaquin Hills structures, as well as the offshore Newport-Inglewood fault. Region 2 would target defining a slip rate on the Carlsbad fault based on the discrete near-surface fold, as well as perhaps a slip rate on the offshore Rose Canyon fault system. Region 3 would target the San Diego Trough fault in a releasing bend, thereby constraining the fault slip rate.
- Precise relocation of offshore seismicity using newly available 3D velocity models for the region and advanced relocation methods. Better earthquake locations will improve our ability to establish which fault segments are active, and to define better their subsurface geometries.
- Evaluation of current geodetic observations to improve constraints on shortening and strike-slip rates.

REFERENCES

Abrahamson, Norm A. (personal communication, 2010)

Astiz, Luciana, and Shearer, Peter (2000). Earthquake Locations in the Inner Continental Borderland, Offshore Southern California, *Bulletin of the Seismological Society of America, v. 90, no. 2. 425-449*.

California Geological Survey (2002). California fault parameters-Interactive fault parameter map of California, http://www.consrv.ca.gov/cgs/rghm/psha/fault_parameters/htm/Pages/index.aspx.

Kier, Grant, and Mueller, Karl (1999). Flexural modeling of the northern Gulf of California Rift: Relating marine terrace uplift to the forebulge on a subsiding plate, *Southern California Earthquake Center 1999 internship final report, 11p*.

Plesch, Andreas, et. al. (2007). Community Fault Model (CFM) for Southern California, *Bulleting of the Seismological Society of America, v. 97, no. 6, 1793-1802.*

Rivero, Carlos, et. al. (2000). Oceanside and Thirty-mile Bank blind thrusts: Implications for earthquake hazards in coastal southern California, *Geology, v. 28, no. 10, 891-894.*

Rivero-Ramirez, Carlos Alberto (2004). Origin of Active Blind-Thrust Faults in the southern Inner California Borderlands, thesis, *Department of Earth and Planetary Sciences, Harvard University, Cambridge, Massachusetts, 176 p.*

Rivero, Carlos, and Shaw, John H. (2005). Fault related folding in reactivated offshore basins, California, *Interpretation of Contractional Fault-Related Folds, An AAPG Seismic Atlas, Studies in Geology, no. 53, 3 p.*

Rivero, Carlos, and Shaw, John H. (in press). Active Folding and Blind-thrust Fault Induced by Basin Inversion Processes, Inner California Borderlands, *AAPG*.

Shaw, John H. and Suppe, John (1996). Earthquake Hazards of Active Blind–thrust Faults Under the Central Los Angeles Basin, California: *Journal of Geophysical Research 101, B4, p. 8623–8642.*

Wells, D.L., and Coppersmith, K. J., (1994). New empirical relationships among the Magnitude, Rupture Length, Rupture Width, Rupture Area, and Surface Displacement: *Bulletin of the Seismological Society of America*, v. 84, p. 974-1002.

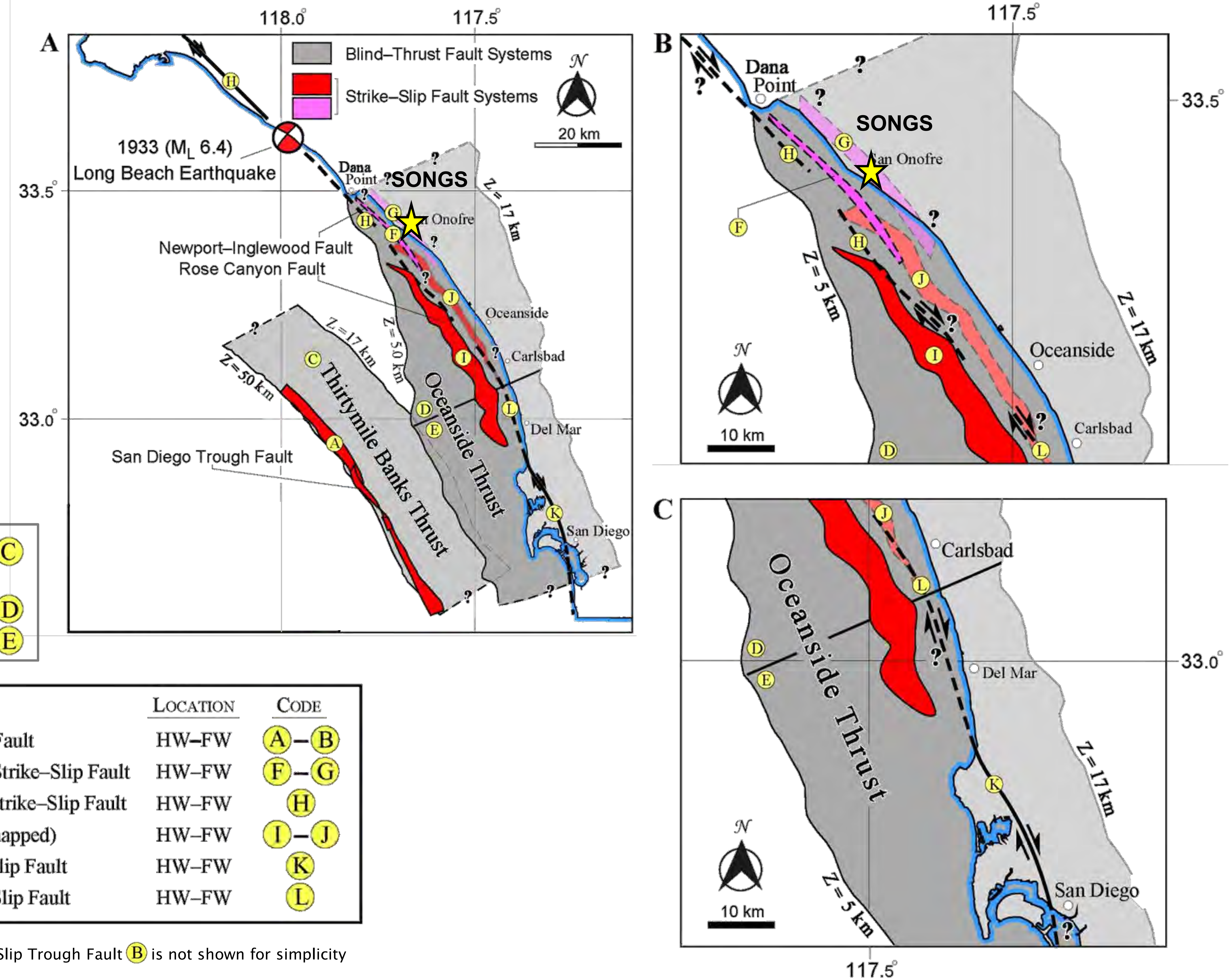

Thirtymile Banks Thrust		C
Oceanside Thrust:		
North Segment	HW	D
South Segment	FW	E

FAULT SEGMENTS	LOCATION	CODE
San Diego Trough Strike–Slip Fault	HW–FW	A – B
Offshore Newport–Inglewood Strike–Slip Fault	HW–FW	F – G
Onshore Newport–Inglewood Strike–Slip Fault	HW–FW	H
Offshore Rose Canyon Fault (mapped)	HW–FW	I – J
Onshore Rose Canyon Strike–Slip Fault	HW–FW	K
Offshore Rose Canyon Strike–Slip Fault	HW–FW	L

Notes: (1) Modified from Rivero (2004)
(2) Footwall segment of the San Diego Strike-Slip Trough Fault B is not shown for simplicity
(3) Latitude and longitude approximate

GeoPentech
By Shaw and Plesch (2010)

SAN ONOFRE NUCLEAR GENERATING STATION
SEISMIC HAZARD ASSESSMENT PROGRAM

INNER SOUTHERN CALIFORNIA CONTINENTAL BORDERLANDS
BLIND THRUST FAULT SYSTEMS

FIGURE
A3-1

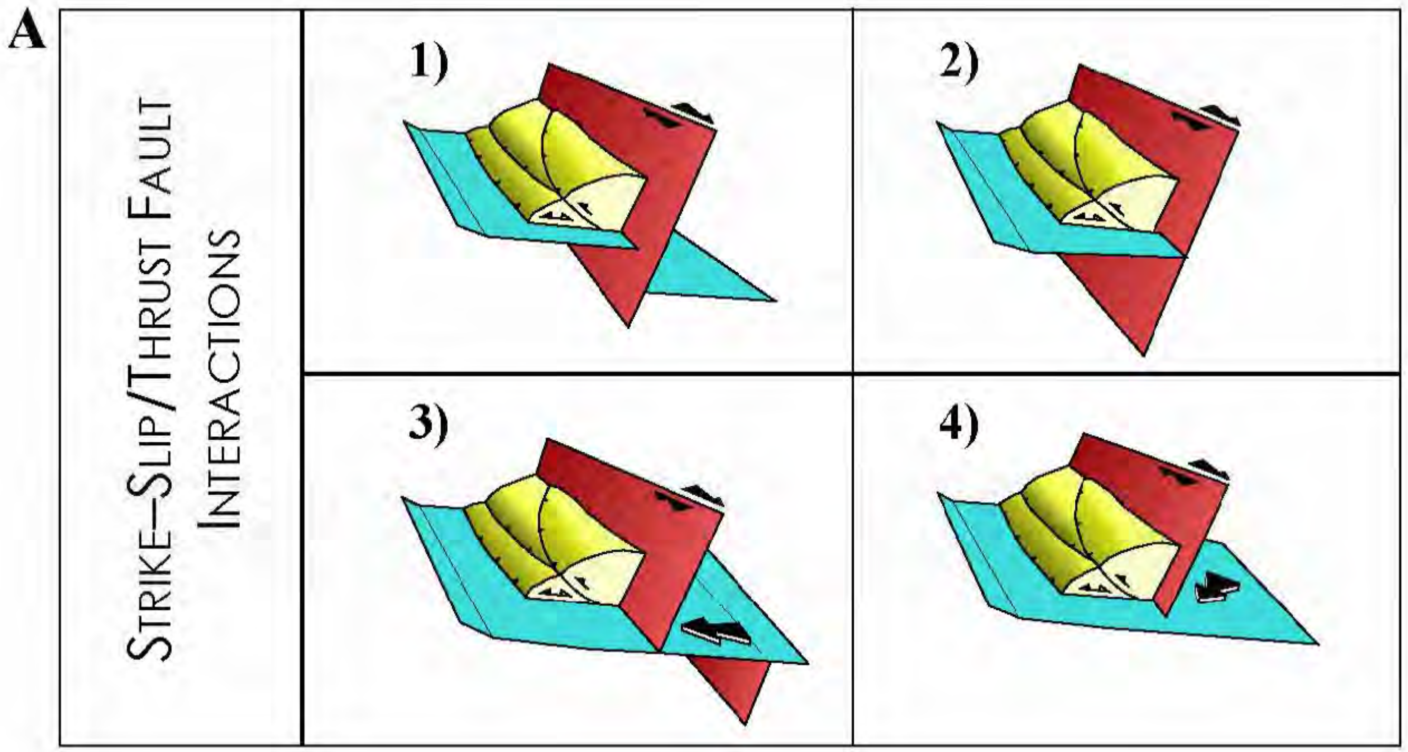

3a) Non–Seismogenic linkages with 1 earthquake source
3b) Hybrid Seismogenic linkages with 2 earthquake sources
3c) Seismogenic linkages with 3 earthquake sources
4a) Non–Seismogenic linkage with 1 earthquake source
4b) Non–Seismogenic linkage with 2 earthquake sources
4c) Seismogenic linkage with 2 earthquake sources

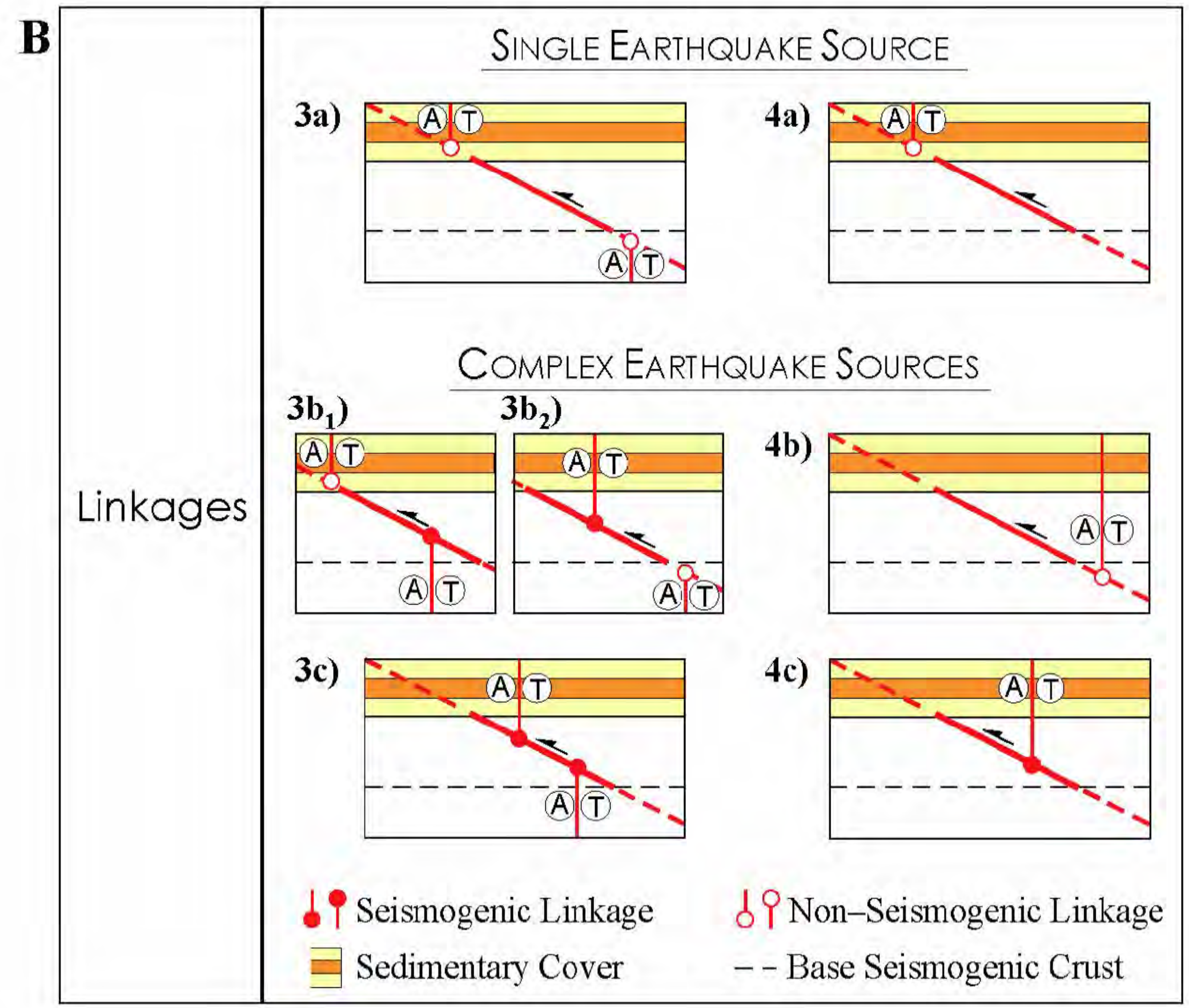

(A) Schematic representation of different structural scenarios considered in this study for strike–slip and blind–thrust fault interactions [modified from Rivero *et al.*, 2000].**(B)** Geometric linkages between strike–slip and blind–thrust faults defined for preferred structural scenarios 3.25A3 and 3.25A4. The type of geometric linkage and their position relative to the depth of the sediments and the seismogenic crust determine the seismogenic potential of the faults and the type of earthquake source.

Notes: Modified from Rivero (2004)

GeoPentech Geotechnical & Geoscience Consultants By Shaw and Plesch (2010)	SAN ONOFRE NUCLEAR GENERATING STATION SEISMIC HAZARD ASSESSMENT PROGRAM	ALTERNATIVE RUPTURE MODELS AND LINKAGES BETWEEN BLIND THRUST AND RIGHT LATERAL STRIKE-SLIP SYSTEMS	FIGURE A3-2

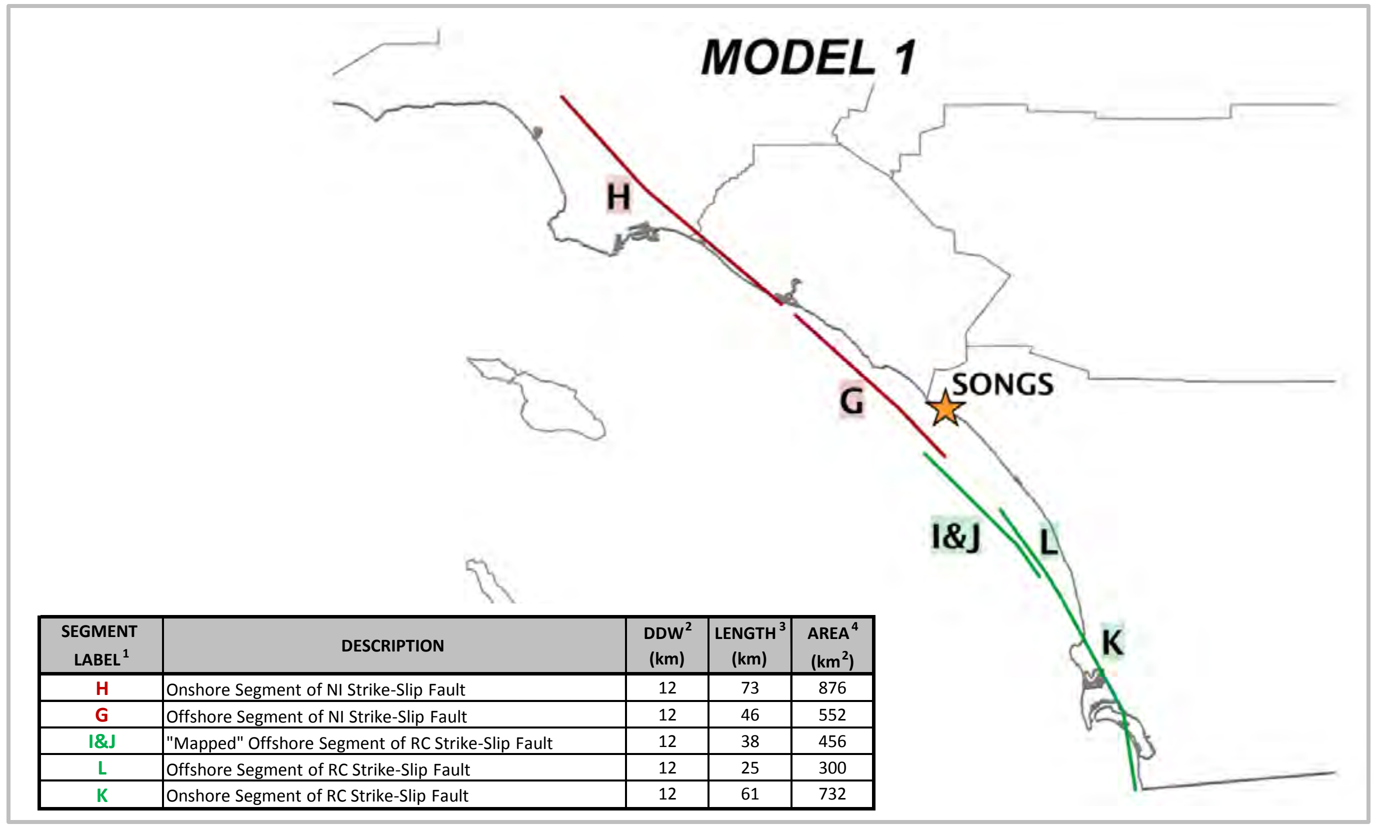

SEGMENT LABEL[1]	DESCRIPTION	DDW[2] (km)	LENGTH[3] (km)	AREA[4] (km^2)
H	Onshore Segment of NI Strike-Slip Fault	12	73	876
G	Offshore Segment of NI Strike-Slip Fault	12	46	552
I&J	"Mapped" Offshore Segment of RC Strike-Slip Fault	12	38	456
L	Offshore Segment of RC Strike-Slip Fault	12	25	300
K	Onshore Segment of RC Strike-Slip Fault	12	61	732

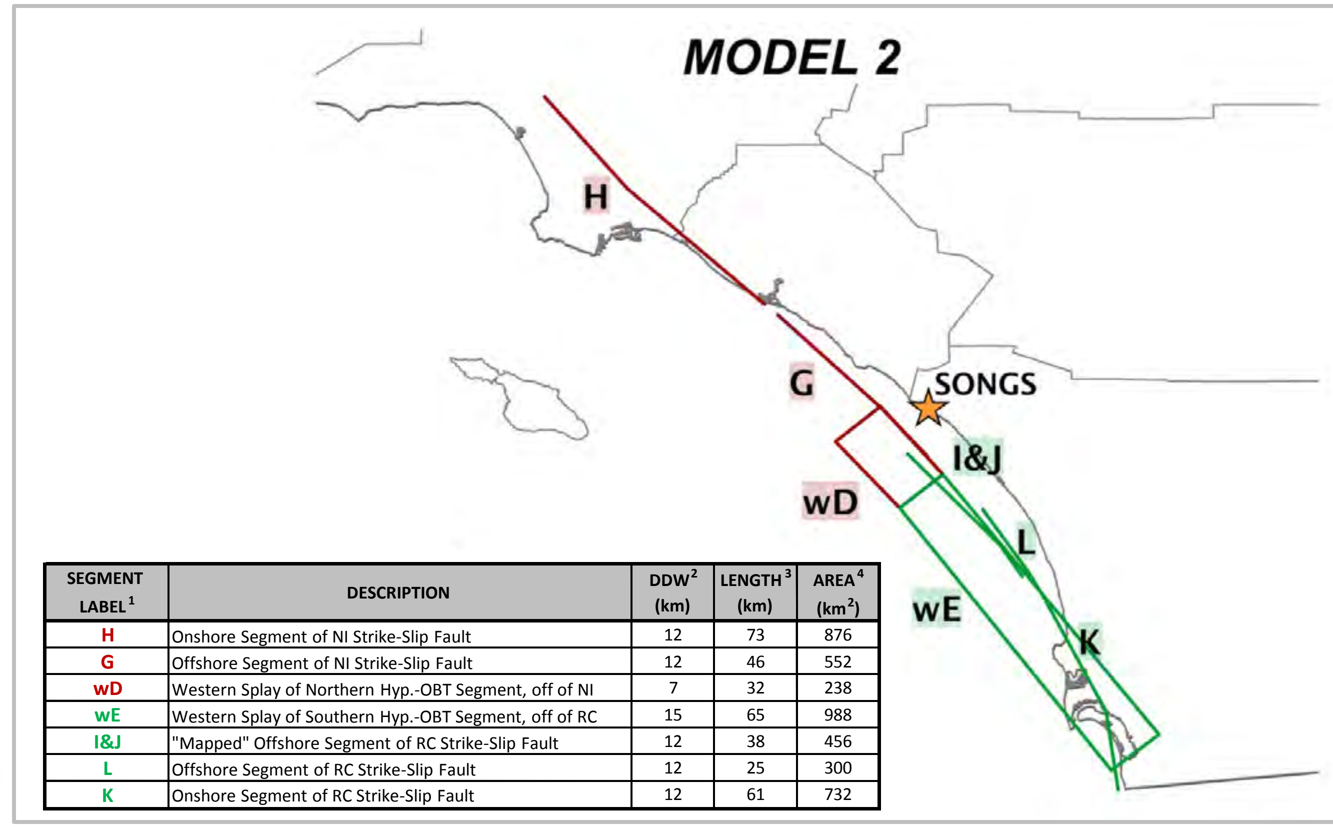

SEGMENT LABEL[1]	DESCRIPTION	DDW[2] (km)	LENGTH[3] (km)	AREA[4] (km^2)
H	Onshore Segment of NI Strike-Slip Fault	12	73	876
G	Offshore Segment of NI Strike-Slip Fault	12	46	552
wD	Western Splay of Northern Hyp.-OBT Segment, off of NI	7	32	238
wE	Western Splay of Southern Hyp.-OBT Segment, off of RC	15	65	988
I&J	"Mapped" Offshore Segment of RC Strike-Slip Fault	12	38	456
L	Offshore Segment of RC Strike-Slip Fault	12	25	300
K	Onshore Segment of RC Strike-Slip Fault	12	61	732

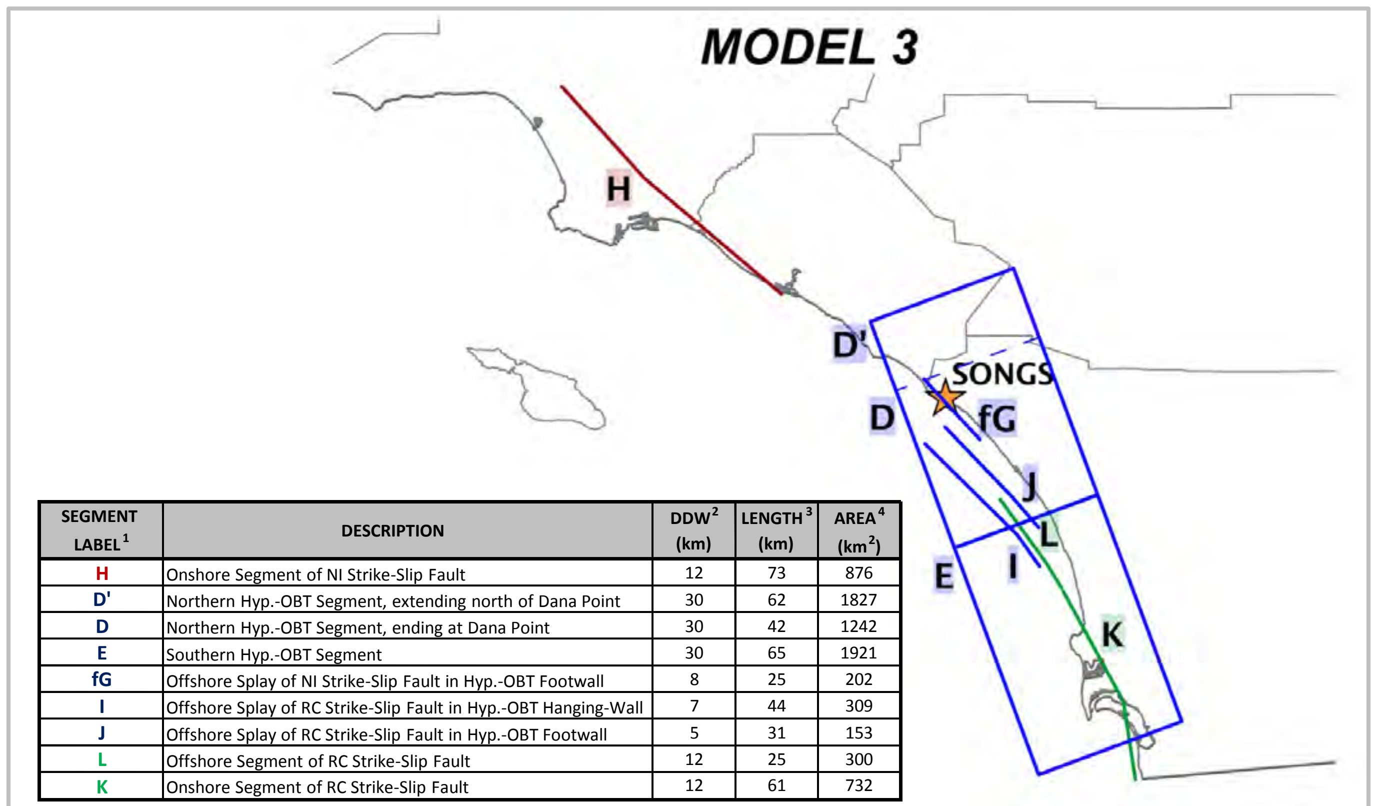

SEGMENT LABEL[1]	DESCRIPTION	DDW[2] (km)	LENGTH[3] (km)	AREA[4] (km^2)
H	Onshore Segment of NI Strike-Slip Fault	12	73	876
D'	Northern Hyp.-OBT Segment, extending north of Dana Point	30	62	1827
D	Northern Hyp.-OBT Segment, ending at Dana Point	30	42	1242
E	Southern Hyp.-OBT Segment	30	65	1921
fG	Offshore Splay of NI Strike-Slip Fault in Hyp.-OBT Footwall	8	25	202
I	Offshore Splay of RC Strike-Slip Fault in Hyp.-OBT Hanging-Wall	7	44	309
J	Offshore Splay of RC Strike-Slip Fault in Hyp.-OBT Footwall	5	31	153
L	Offshore Segment of RC Strike-Slip Fault	12	25	300
K	Onshore Segment of RC Strike-Slip Fault	12	61	732

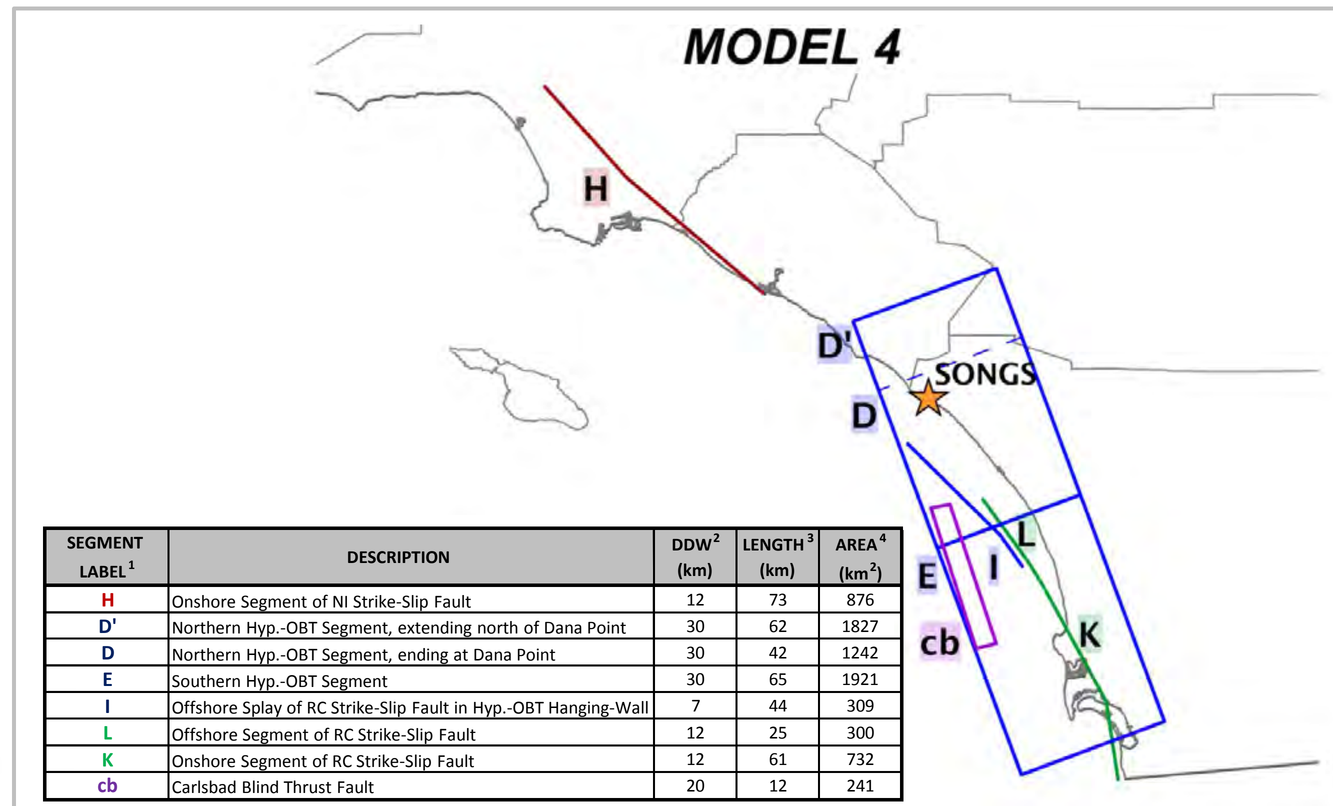

SEGMENT LABEL[1]	DESCRIPTION	DDW[2] (km)	LENGTH[3] (km)	AREA[4] (km^2)
H	Onshore Segment of NI Strike-Slip Fault	12	73	876
D'	Northern Hyp.-OBT Segment, extending north of Dana Point	30	62	1827
D	Northern Hyp.-OBT Segment, ending at Dana Point	30	42	1242
E	Southern Hyp.-OBT Segment	30	65	1921
I	Offshore Splay of RC Strike-Slip Fault in Hyp.-OBT Hanging-Wall	7	44	309
L	Offshore Segment of RC Strike-Slip Fault	12	25	300
K	Onshore Segment of RC Strike-Slip Fault	12	61	732
cb	Carlsbad Blind Thrust Fault	20	12	241

Notes:

[1] Labels modified from Figure A-2-1

[2] Assuming 5km to 17km Seismogenic Depth

[3] Based on Rivero (2004)

[4] Calculated based on DDW and Length

GeoPentech
Geotechnical & Geoscience Consultants
By Shaw and Plesch (2010)

SAN ONOFRE NUCLEAR GENERATING STATION

SEISMIC HAZARD ASSESSMENT PROGRAM

SIMPLIFIED GEOMETRY AND SEGMENTATION FOR BLIND THRUST AND RIGHT LATERAL STRIKE-SLIP SYSTEMS

FIGURE A3-3

KINEMATIC MODEL	SEISMIC SOURCE	OBT LIMIT	LINKAGE	SINGLE SEGMENT					MULTI SEGMENT				
				SEGMENTS	RUPTURE AREA (KM^2)	MAX MAG[1] (M)	SLIP RATE[2] (mm/yr)	RECURRANCE[3] (yr)	SEGMENTS	RUPTURE AREA (KM^2)	MAX MAG[1] (M)	SLIP RATE[2] (mm/yr)	RECURRANCE[3] (yr)
1) 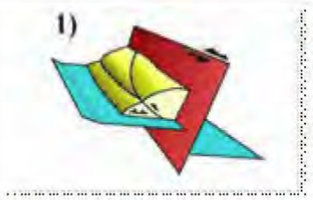	NI Strike-Slip			G	552	6.8	1.5+/-0.5	390 - 780	G + H	1428	7.2	1+/-0.5	980 - 2940
				H	876	7.0	1+/-0.5	710 - 2140					
	RC Strike-Slip			I&J	456	6.7	1.07+/-0.03	600 - 640	I&J + K	1188	7.1	1.07+/-0.03	1140 - 1210
				K	732	6.9	1.07+/-0.03	830 - 880	K + L	1032	7.0	1.07+/-0.03	970 - 1030
				L	300	6.5	1.07+/-0.03	440 - 470	L + I&J	756	6.9	1.07+/-0.03	830 - 880
				-	-	-	-	-	I&J + K + L	1488	7.2	1.07+/-0.03	1340 - 1420
2) 	NI Strike-Slip			G&wD	790	6.9	1.02+/-0.14	790 - 1040	G&wD + H	1666	7.2	1.02+/-0.14	1270 - 1670
				H	876	7.0	1+/-0.5	710 - 2140					
	RC Strike-Slip			I&J&wE	1444	7.2	0.82+/-0.12	1570 - 2100	I&J&wE + K	2176	7.3	0.82+/-0.12	1840 - 2470
				K	732	6.9	1.07+/-0.03	830 - 880	K + L	1032	7.0	1.07+/-0.03	970 - 1030
				L	300	6.5	1.07+/-0.03	440 - 470	L + I&J&wE	1744	7.2	0.82+/-0.12	1570 - 2100
				-	-	-	-	-	I&J&wE + K + L	2476	7.4	0.82+/-0.12	2150 - 2890
3) 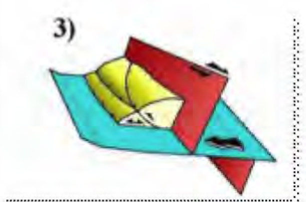	NI Strike-Slip			H	876	7.0	1+/-0.5	710 - 2140	-	-	-	-	-
	RC Strike-Slip			K	732	6.9	1.07+/-0.03	830 - 880	K + L	1032	7.0	1.07+/-0.03	970 - 1030
				L	300	6.5	1.07+/-0.03	440 - 470					
	Oceanside Thrust	Ends at Dana Point (D)	3a	D	1242	7.1	1.02+/-0.14	1080 - 1430	D + E	3163	7.5	1.02+/-0.14	2040 - 2690
				E	1921	7.3	0.82+/-0.12	1840 - 2470					
			3b1	D&fG	1444	7.2	1.02+/-0.14	1270 - 1670	D&fG + E&J	3518	7.6	1.74+/-0.2	1430 - 1810
				E&J	2074	7.3	0.82+/-0.12	1840 - 2470					
			3b2	D	1242	7.1	1.02+/-0.14	1080 - 1430	D + E&I	3472	7.5	1.74+/-0.2	1220 - 1540
				E&I	2230	7.4	0.82+/-0.12	2150 - 2890					
			3c	D&fG	1444	7.2	1.02+/-0.14	1270 - 1670	D&fG + E&I&J	3827	7.6	1.74+/-0.2	1430 - 1810
				E&I&J	2383	7.4	0.82+/-0.12	2150 - 2890					
		Extends North of Dana Point (D')	3a	D'	1827	7.3	1.02+/-0.14	1490 - 1960	D' + E	3748	7.6	1.02+/-0.14	2400 - 3160
				E	1921	7.3	0.82+/-0.12	1840 - 2470					
			3b1	D'&fG	2029	7.3	1.02+/-0.14	1490 - 1960	D'&fG + E&J	4103	7.6	1.74+/-0.2	1430 - 1810
				E&J	2074	7.3	0.82+/-0.12	1840 - 2470					
			3b2	D'	1827	7.3	1.02+/-0.14	1490 - 1960	D' + E&I	4057	7.6	1.74+/-0.2	1430 - 1810
				E&I	2230	7.4	0.82+/-0.12	2150 - 2890					
			3c	D'&fG	1444	7.2	1.02+/-0.14	1270 - 1670	D'&fG + E&I&J	4412	7.6	1.74+/-0.2	1430 - 1810
				E&I&J	2383	7.4	0.82+/-0.12	2150 - 2890					
4) 	NI Strike-Slip			H	876	7.0	1+/-0.5	710 - 2140	-	-	-	-	-
	RC Strike-Slip			K	732	6.9	1.07+/-0.03	830 - 880	K + L	1032	7.0	1.07+/-0.03	970 - 1030
				L	300	6.5	1.07+/-0.03	440 - 470					
	Oceanside Thrust	Ends at Dana Point (D)	4b	D	1242	7.1	1.02+/-0.14	1080 - 1430	D + E	3163	7.5	1.02+/-0.14	2040 - 2690
				E	1921	7.3	0.82+/-0.12	1840 - 2470					
				I	309	6.5	1.07+/-0.03	440 - 470					
			4c	D	1242	7.1	1.02+/-0.14	1080 - 1430	D + E&I	3472	7.5	1.74+/-0.2	1220 - 1540
				E&I	2230	7.4	0.82+/-0.12	2150 - 2890					
		Extends North of Dana Point (D')	4b	D'	1827	7.3	1.02+/-0.14	1490 - 1960	D' + E	3748	7.6	1.02+/-0.14	2400 - 3160
				E	1921	7.3	0.82+/-0.12	1840 - 2470					
				I	309	6.5	1.07+/-0.03	440 - 470					
			4c	D'	1827	7.3	1.02+/-0.14	1490 - 1960	D' + E&I	4057	7.6	1.74+/-0.2	1430 - 1810
				E&I	2230	7.4	0.82+/-0.12	2150 - 2890					
	Carlsbad Thrust			cb	241	6.4	0.25+/-0.08	1250 - 2430	-	-	-	-	-

Notes:

[1]Maximum Magnitude based on Wells & Coppersmith (1994)

[2]Value estimated by Rivero (2004) or Shaw & Plesch (2010)

[3]Recurrence Interval based on Shaw & Suppe (1996)

GeoPentech
Geotechnical & Geoscience Consultants
By Shaw and Plesch (2010)

SAN ONOFRE NUCLEAR GENERATING STATION

SEISMIC HAZARD ASSESSMENT PROGRAM

POTENTIAL RUPTURE SCENARIOS FOR BLIND THRUST AND RIGHT LATERAL STRIKE-SLIP SYSTEMS

FIGURE A3-4

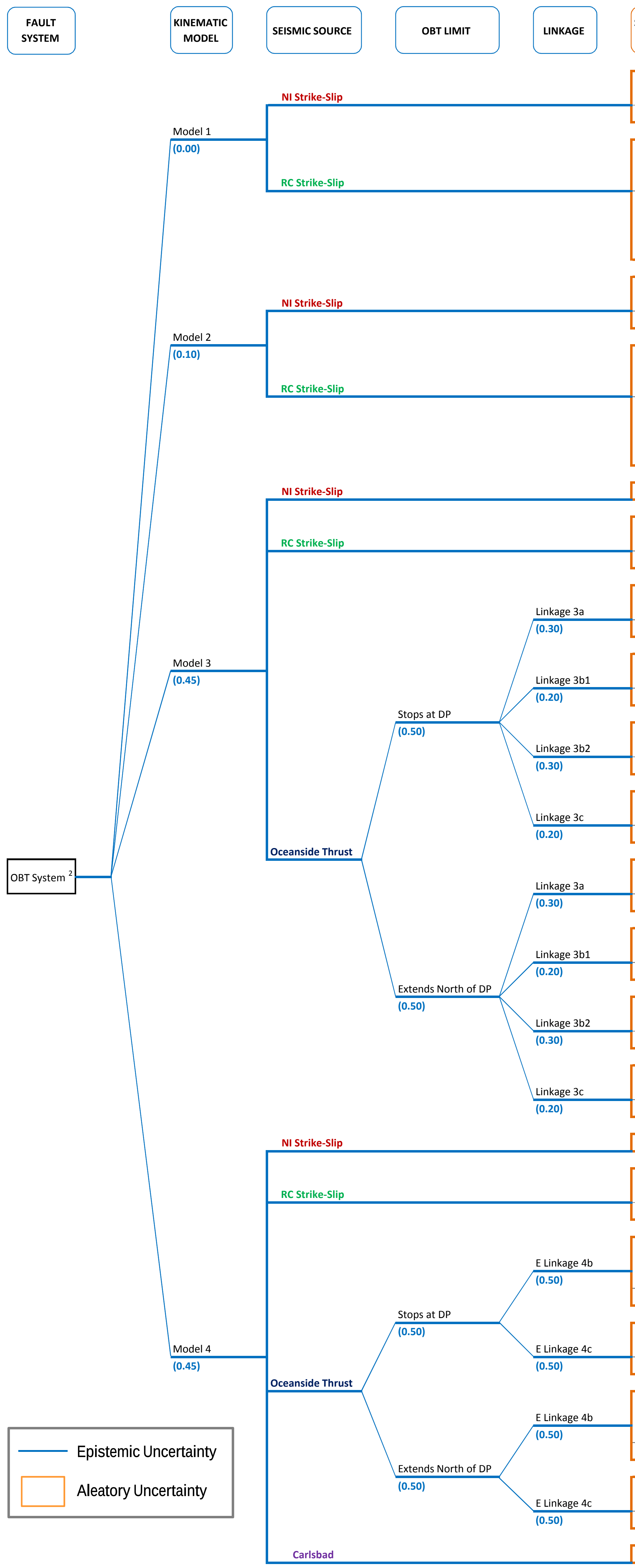

SEGMENTATION	FAULT SEGMENT COMBINATION	DISTRIBUTION OF SEGMENT RUPTURE	LONG-TERM SLIP RATE (mm/yr)	RECURRENCE MODEL [1]	
Single	G	25%	1.5+/-0.5	Characteristic	Trunc G-R
	H	50%	1.0+/-0.5	Characteristic	Trunc G-R
Multi	G + H	25%	1.0+/-0.5	Characteristic	Trunc G-R
Single	I&J	10%	1.07+/-0.03	Characteristic	Trunc G-R
	K	20%	1.07+/-0.03	Characteristic	Trunc G-R
	L	20%	1.07+/-0.03	Characteristic	Trunc G-R
Multi	I&J + K	10%	1.07+/-0.03	Characteristic	Trunc G-R
	K + L	20%	1.07+/-0.03	Characteristic	Trunc G-R
	I&J + L	10%	1.07+/-0.03	Characteristic	Trunc G-R
	I&J + K + L	10%	1.07+/-0.03	Characteristic	Trunc G-R
Single	G&wD	25%	1.02+/-0.14	Characteristic	Trunc G-R
	H	50%	1.0+/-0.5	Characteristic	Trunc G-R
Multi	G&wD + H	25%	1.02+/-0.14	Characteristic	Trunc G-R
Single	I&J&wE	10%	0.82+/-0.12	Characteristic	Trunc G-R
	K	20%	1.07+/-0.03	Characteristic	Trunc G-R
	L	20%	1.07+/-0.03	Characteristic	Trunc G-R
Multi	I&J&wE + K	10%	0.82+/-0.12	Characteristic	Trunc G-R
	K + L	20%	1.07+/-0.03	Characteristic	Trunc G-R
	I&J&wE + L	10%	0.82+/-0.12	Characteristic	Trunc G-R
	I&J&wE + K + L	10%	0.82+/-0.12	Characteristic	Trunc G-R
Single	H	100%	1.0+/-0.5	Characteristic	Trunc G-R
Single	K	33%	1.07+/-0.03	Characteristic	Trunc G-R
	L	33%	1.07+/-0.03	Characteristic	Trunc G-R
Multi	K + L	33%	1.07+/-0.03	Characteristic	Trunc G-R
Single	D	33%	1.02+/-0.14	Characteristic	Trunc G-R
	E	33%	0.82+/-0.12	Characteristic	Trunc G-R
Multi	D + E	33%	1.02+/-0.14	Characteristic	Trunc G-R
Single	D&fG	33%	1.02+/-0.14	Characteristic	Trunc G-R
	E&J	33%	0.82+/-0.12	Characteristic	Trunc G-R
Multi	D&fG + E&J	33%	1.74+/-0.2	Characteristic	Trunc G-R
Single	D	33%	1.02+/-0.14	Characteristic	Trunc G-R
	E&I	33%	0.82+/-0.12	Characteristic	Trunc G-R
Multi	D + E&I	33%	1.74+/-0.2	Characteristic	Trunc G-R
Single	D&fG	33%	1.02+/-0.14	Characteristic	Trunc G-R
	E&I&J	33%	0.82+/-0.12	Characteristic	Trunc G-R
Multi	D&fG + E&I&J	33%	1.74+/-0.2	Characteristic	Trunc G-R
Single	D'	33%	1.02+/-0.14	Characteristic	Trunc G-R
	E	33%	0.82+/-0.12	Characteristic	Trunc G-R
Multi	D' + E	33%	1.02+/-0.14	Characteristic	Trunc G-R
Single	D'&fG	33%	1.02+/-0.14	Characteristic	Trunc G-R
	E&J	33%	0.82+/-0.12	Characteristic	Trunc G-R
Multi	D'&fG + E&J	33%	1.74+/-0.2	Characteristic	Trunc G-R
Single	D'	33%	1.02+/-0.14	Characteristic	Trunc G-R
	E&I	33%	0.82+/-0.12	Characteristic	Trunc G-R
Multi	D' + E&I	33%	1.74+/-0.2	Characteristic	Trunc G-R
Single	D'&fG	33%	1.02+/-0.14	Characteristic	Trunc G-R
	E&I&J	33%	0.82+/-0.12	Characteristic	Trunc G-R
Multi	D'&fG + E&I&J	33%	1.74+/-0.2	Characteristic	Trunc G-R
Single	H	100%	1.0+/-0.5	Characteristic	Trunc G-R
Single	K	33%	1.07+/-0.03	Characteristic	Trunc G-R
	L	33%	1.07+/-0.03	Characteristic	Trunc G-R
Multi	K + L	33%	1.07+/-0.03	Characteristic	Trunc G-R
Single	D	25%	1.02+/-0.14	Characteristic	Trunc G-R
	E	25%	0.82+/-0.12	Characteristic	Trunc G-R
	I	25%	1.07+/-0.03	Characteristic	Trunc G-R
Multi	D + E	25%	1.02+/-0.14	Characteristic	Trunc G-R
Single	D	33%	1.02+/-0.14	Characteristic	Trunc G-R
	E&I	33%	0.82+/-0.12	Characteristic	Trunc G-R
Multi	D + E&I	33%	1.74+/-0.2	Characteristic	Trunc G-R
Single	D'	25%	1.02+/-0.14	Characteristic	Trunc G-R
	E	25%	0.82+/-0.12	Characteristic	Trunc G-R
	I	25%	1.07+/-0.03	Characteristic	Trunc G-R
Multi	D' + E	25%	1.02+/-0.14	Characteristic	Trunc G-R
Single	D'	33%	1.02+/-0.14	Characteristic	Trunc G-R
	E&I	33%	0.82+/-0.12	Characteristic	Trunc G-R
Multi	D' + E&I	33%	1.74+/-0.2	Characteristic	Trunc G-R
Single	cb	100%	0.25+/-0.08	Characteristic	Trunc G-R

Notes:
[1] Recurrence based on 2/3 Characteristic Model and 1/3 Truncated Gutenberg-Richter Distribution
[2] See Appendix A, Attachment A-3 for details

GeoPentech
Geotechnical & Geoscience Consultants

BLIND THRUST AND RIGHT LATERAL STRIKE-SLIP FAULT SYSTEM LOGIC TREE

FIGURE A3-5

SAN ONOFRE NUCLEAR GENERATING STATION

SEISMIC HAZARD ASSESSMENT PROGRAM

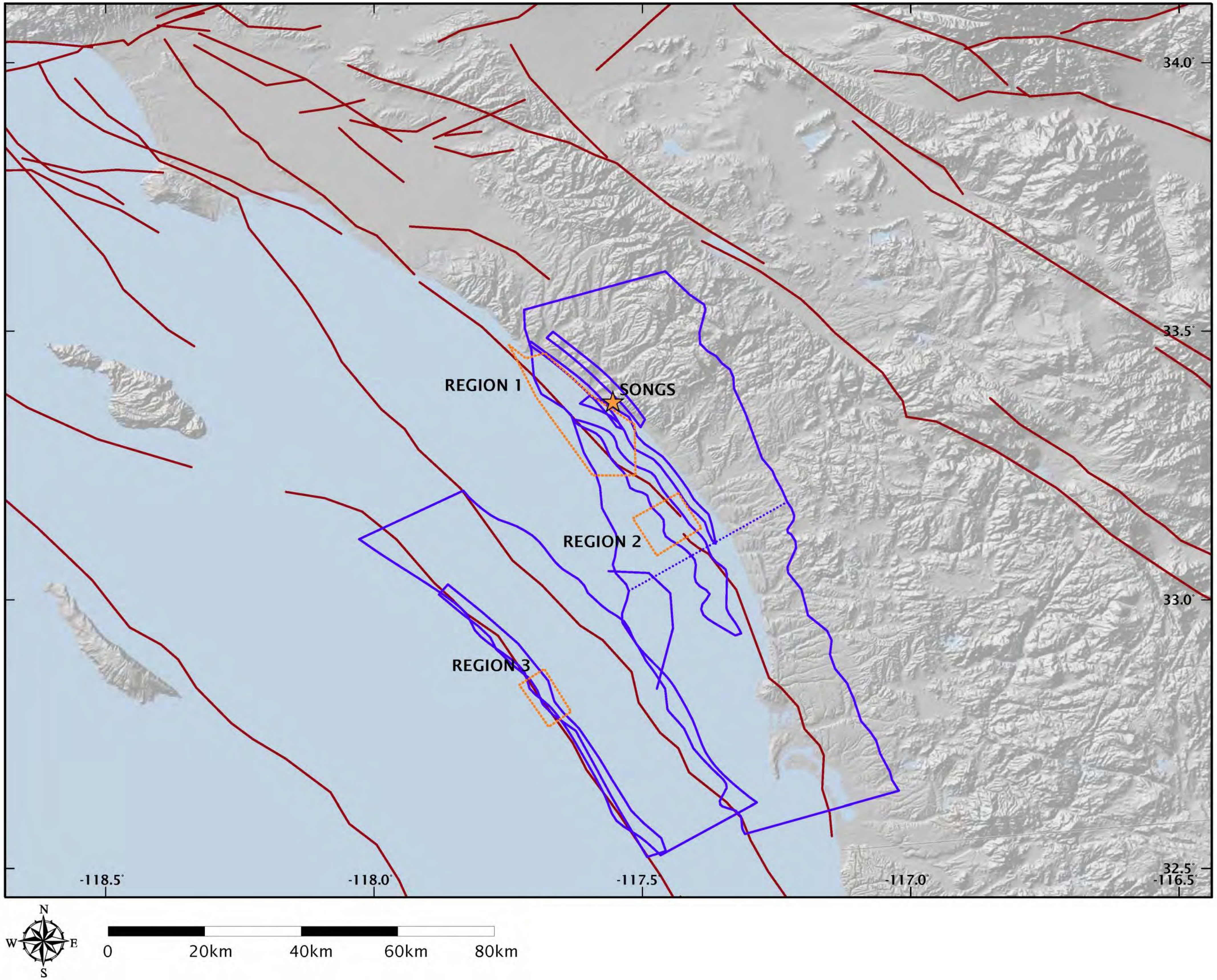

Legend

- SONGS Facility Location
- Fault Systems from Rivero (2004)
- Fault Traces from USGS (2009)
- Areas Recommended for Future Study

Region	Approx. Area
Region 1	250 km^2
Region 2	90 km^2
Region 3	50 km^2

Notes:

Base map is shaded relief of southern California based on SRTM model prepared by ESRI, 2009.

GeoPentech
Geotechnical & Geoscience Consultants
By Shaw and Plesch (2010)

SAN ONOFRE NUCLEAR GENERATING STATION
SEISMIC HAZARD ASSESSMENT PROGRAM

LOCATIONS FOR RECOMMENDED FUTURE STUDIES

FIGURE
A3-6

APPENDIX B
2010 PSHA GROUND MOTION CHARACTERIZATION

APPENDIX B OUTLINE

APPENDIX B
2010 PSHA GROUND MOTION CHARACTERIZATION

B1.0 INTRODUCTION

This Appendix provides further discussions on selected PSHA-related issues addressed in the main report. The selected issues consist of QA/QC work done on the PSHA computer program HAZ4.2 (Abrahamson, 2010); characterization of the site shear wave velocity parameters used in the attenuation relationships; epistemic uncertainty associated with the attenuation relationships used; and recurrence relationships for the hypothesized OBT source.

B2.0 QA/QC OF HAZ4.2 PSHA COMPUTER PROGRAM

The PSHA computer program HAZ4.2, developed by Dr. Norman Abrahamson (2010) as the newest version of his PSHA program, was selected for use in the 2010 PSHA. This latest version enabled SHAP to implement the NSHM 2009 (USGS, 2009, PC) seismic source model and adopt the UCERF 2 (WGCEP, 2008) time independent model for conducting PSHA. However, because HAZ4.2 had not yet gone through a QA/QC process, SHAP, guided by Dr. Norman Abrahamson, followed the PSHA Validation Project methodology described in Thomas et al. (2010) to initiate this QA/QC process. The process was completed for the elements of HAZ4.2 pertinent to this study, but not others. The resulting QA/QC'd portion of the HAZ4.2 computer program will be considered an interim version of HAZ4.2 on the 2010 PSHA. The actual process in completing the QA/QC'd portion of HAZ4.2 involved interactions of SHAP with Dr. Nicholas Gregor who works with Dr. Norman Abrahamson in developing the program. SHAP and Dr. Nicholas Gregor completed a series of computer runs followed by identifications and modification resolutions on various aspects of the computer program.

The purpose of the PSHA Validation Project (Thomas et al., 2010) was to develop a consistent method for testing several aspects of the PSHA calculation process for various, widely-used PSHA computer programs in the engineering community. The validation process consisted of test cases using strike-slip, reverse, and areal sources along with various site locations as illustrated on Figure B-1. Figure B-1 also shows the sites used in the validation. The test cases were designed to address calculation of site distance, rate, ground motion attenuation, hanging wall effects, earthquake recurrence, ground motion variability, and rupture area variability against hand-calculations whenever available. The test case results for each computer program were validated by comparing them to Pacific Earthquake Engineering Research (PEER) reported results by Thomas et al. (2010) for each test case.

SHAP compared the HAZ4.2 results for all test cases against the PEER reported results from Thomas et al. (2010). Figures B-2 and B-3 compare the HAZ4.2 results with the PEER reported results for two different cases as example results. As shown on Figures B-2 and B-3, the HAZ4.2 results match with the PEER reported results from Thomas et al. (2010). The comparisons of results shown on Figures B-2 and B-3 are representative of the remaining 104 cases considered. The final results for all test cases of the QA/QC process, when eventually completed, will be presented in a report titled "QA/QC of HAZ4.2 PSHA Computer Program."

B3.0 SHEAR WAVE VELOCITY PARAMETERS USED IN NGA RELATIONSHIPS

Table B-1 shows the attenuation relationships from the NGA models used in the PSHA. These attenuation relationships are called the NGA relationships herein and consist of the following:

- Abrahamson and Silva (2008)
- Boore and Atkinson (2008)
- Campbell and Bozorgnia (2008)
- Chiou and Youngs (2008)
- Idriss (2008)

Table B-1 also summarizes the estimated shear-wave velocity parameters for SONGS used in the NGA relationships, including 1) the average shear-wave velocity from the ground surface to a depth of 30 m (V_{S30}), 2) the approximate depth to 1 km/s shear-wave velocity material ($Z_{1.0}$), and 3) the approximate depth to 2.5 km/s shear-wave velocity material ($Z_{2..5}$). These shear wave velocity parameters, not all of them used by all five relationships listed above, were based on relevant data compiled from past reports documenting previous site investigations. Figures B-4 and B-5 present compilations of the site seismic velocity data from the ground surface to a depth of 30 m and 4,000 m, respectively. These figures show both shear- and pressure-wave data that was either directly measured in the site vicinity (colored solid lines) or was estimated based on other data (colored dashed lines). Also, a generalized stratigraphic column showing the geologic units is presented between the shear- and pressure-wave graphs on Figures B-4 and B-5. This geologic interpretation is based on data presented in Dames & Moore (1970) and SCE (2001).

As shown on Figures B-4 and B-5, the pressure-wave velocities at the site were directly measured from 1) a surface seismic velocity survey by Dames & Moore (1970), 2) an acoustic velocity survey of borehole B-1 by Dames & Moore (1970), 3) a downhole seismic velocity survey by Weston Geophysical (1971), 4) an offshore seismic reflection survey by Western Geophysical (1972), and 5) geophysical data compiled by Dames & Moore (1970) to the base of the San Onofre Breccia (Tso) or to a depth of approximately 1,525 m (5,000 ft). Below the base of the San Onofre Breccia, the pressure-wave data was estimated by Dames & Moore (1970) based on measurements performed within the deeper rock units in the region by others.

As shown on Figures B-4 and B-5, the shear-wave velocities at the site were directly measured from 1) a surface seismic velocity survey by Dames & Moore (1970), 2) a downhole seismic velocity survey by Weston Geophysical (1971), 3) Rayleigh wave tests by Woodward-McNeill (1974), and 4) geophysical data compiled by Dames & Moore (1970) to the base of the Monterey Formation Tm (see Figure B-5) or to a depth of approximately 760 m (2,500 ft).

Shear-wave velocities at the site were also estimated based on pressure-wave velocities, Poisson's ratio, and shear modulus relationships. As shown on Figures B-4 and B-5, shear-wave velocities below the base of the Monterey Formation were computed by Dames & Moore (1970) from pressure-wave velocities and estimates of the Poisson's ratio measured in similar materials. Estimates of the shear-wave velocity were also calculated from the acoustic velocity log within B1 shown on Figures B-4 and B-5 (Dames & Moore, 1970) and the offshore seismic pressure-wave data (Western Geophysical, 1972) using the

Poisson's ratio values presented in Dames & Moore (1970). Lastly, shear-wave velocities estimates were calculated based on shear modulus relationships presented in Woodward-McNeill (1972). These estimates were calculated for the San Mateo Formation to a depth of 285 m (935 ft).

The San Mateo Formation sandstone comprises the first 30 m of geologic material beneath SONGS. As shown on Figure B-4, the shear-wave velocities measured or estimated within the first 30 m below the site are relatively similar to each other with the widest spread in values in the near-surface between approximately 0 and 12 m. The V_{s30} values based on Dames & Moore (1970) data (solid yellow and red lines on Figure B-4) and estimated based on offshore data by Western Geophysical (1972) (dashed green line on Figure B-4) are approximately 670 m/s and 730 m/s, respectively. These V_{s30} values were based on widely spaced survey data and pressure-wave velocity measurements that resulted in poor resolution of the near-surface shear-wave velocity values. Investigations resulting in a higher resolution of near-surface shear-wave velocities were performed by Weston (1971) (solid magenta line on Figure B-4) and Woodward-McNeill (1974) (solid purple line on Figure B-4). The V_{s30} based on the Weston (1971) data is approximately 500 m/s. The V_{s30} value was also calculated by combining the Woodward-McNeill (1974) data (solid purple line), which had a maximum exploration depth of about 4.5 m, with the shear-wave velocity estimated based on the San Mateo Formation's shear modulus relationship developed by Woodward-McNeill (1972) (dashed cyan line on Figure B-4). As shown on Figure B-4, this combined V_{s30} is about 500 m/s, which is the same as the V_{s30} based on the Weston (1971) data. Since the Weston and Woodward-McNeill data provided the best resolution of shear-wave velocities within the first 30 m of the San Mateo Formation, the V_{s30} within the San Mateo Formation at the site is estimated to be 500 m/s for the NGA relationships in Table B-1.

As shown on Figure B-5, the estimated $Z_{1.0}$ varies depending on the source of the shear-wave velocity data. The upper bound of $Z_{1.0}$ is approximately 135 m and is based on the San Mateo Formation shear modulus relationship developed by Woodward-McNeill (1972) (dashed cyan line on Figure B-5). The $Z_{1.0}$ based on the Dames and Moore (1970) data (solid red line on Figure B-5) and Western Geophysical (1972) data (dashed green line on Figure B-5) is approximately 610 m and 305 m, respectively. This puts the $Z_{1.0}$ at the top of the Monterey Formation, which varies between the two sources. It is noted that the top of the Monterey Formation at the site, as shown on the geology log on Figure B-5, is based on the Western Geophysical (1972) offshore seismic data presented in SCE (2001), and includes the latest geologic interpretation. This latest geologic interpretation together with the idea that the $Z_{1.0}$ depth occurs at the top of the Monterey Formation leads to a $Z_{1.0}$ depth of approximately 305 m, which was used in the NGA relationships in Table B-1. This value is similar to the average of all $Z_{1.0}$ sources, which is approximately 350 m.

Dames and Moore (1970) provides the only site-specific shear-wave data below the base of the Monterey Formation (dashed red lines on Figure B-5). As shown on Figure B-5, the $Z_{2.5}$ is estimated to occur at approximately 3,350 m, which corresponds to the approximate top of the crystalline basement igneous and metamorphic rocks.

B4.0 GROUND MOTION PREDICTION EQUATION EPISTEMIC UNCERTAINTY

The attenuation relationships associated with the NGA work are often referred to as the GMPE. In using attenuation relationships, their epistemic uncertainty should be considered. In the past, this epistemic uncertainty was often accommodated by using multiple attenuation relationships. However, given the coordinated process used to develop the NGA relationships, it should not be adequate to address this epistemic uncertainty by just using multiple NGA relationships. An epistemic GMPE uncertainty in addition to the use of five NGA relationships was reflected in the PSHA herein as described below.

The additional epistemic uncertainty follows USGS (2008) as summarized below:

The USGS applies the epistemic uncertainty dgnd symmetrically (USGS, 2008) so that the weights for (ln(gnd)+dgnd) and (ln(gnd)-dgnd) are the same at 0.185 and the unmodified ln(gnd) has a weight of 0.63. Here, ln(gnd) stands for the natural logarithm of the median peak or spectral acceleration, "gnd", for a given attenuation relationship. The term "dgnd" stands for the median or spectral acceleration uncertainty for any given attenuation relationship.

Due to the limitations of the data (particularly for large earthquakes) used in developing the NGA relationships and the considerable interactions that took place among the NGA modelers (USGS, 2008), NGA modelers suggested that the NGA relationships should also incorporate epistemic uncertainty (beyond using multiple relationships). Following the NGA modelers' suggestion, the USGS partitioned the source space into nine (9) bins determined by three partitions in the distance space (0 to 10 km, 10 to 30 km, and larger than 30 km) and three partitions in the magnitude space (5 to 6, 6 to 7, and larger than 7) as shown in Table B-2. However, of all the attenuation relationships considered by the USGS, only Campbell and Bozorgnia (2008) and Chiou and Youngs (2008) provided sufficient information to estimate the epistemic uncertainty within the nine bins considered. Based on an average epistemic uncertainty, Table B-2 shows the resulting epistemic uncertainty within each of the 9 bins considered by the USGS (2008).

As in the USGS evaluation, the space was divided into 9 bins (3 ranges in the magnitude space and 3 ranges in the distance space). Within each bin, an average value of the range was used to compute the peak or spectral accelerations for all 5 attenuation relationships considered. For example, in the case of the magnitude range 6 to 7, and distance the range 0 to 10 km, an average magnitude value of 6.5 and an average rupture distance of 5 km was used to compute the spectral ordinates from all 5 attenuation relationships. Figures B-6 and B-7 show the computed spectral ordinates for strike-slip and reverse faulting mechanism, respectively. Next, the ratio of the maximum to minimum calculated spectral accelerations was computed for each frequency. Figure B-8 shows the resulting ratios for each of the two styles of faulting mechanism considered, as well as their average values within the range of frequencies of interest. In general, the average ratio for the reverse faulting mechanism tends to be larger than that of the strike-slip faulting mechanism. In the present evaluation, average ratios obtained from the reverse faulting mechanism were used.

The epistemic uncertainty from the attenuation relationships can be compared to the epistemic uncertainty values provided by the USGS by noting that the minimum and maximum spectral accelerations are provided by (ln(gnd)-dgnd) and (ln(gnd)+dgnd), respectively. Therefore, in the USGS case, the ratio of maximum ("max") to minimum ("min") response spectra is provided by:

$Sa_{Max,USGS}/Sa_{Min,USGS} = \exp[\ln(gnd) + dgnd] / \exp[\ln(gnd) – dgnd]$

$Sa_{Max,USGS}/Sa_{Min,USGS} = \exp(2 \times dgnd)$

where $Sa_{Max,USGS}/Sa_{Min,USGS}$ is the ratio of the maximum and minimum USGS spectral acceleration. Conversely, for a given average ratio value, the corresponding epistemic dgnd term can also be computed as follows:

$$dgnd = \ln(Sa_{Max,USGS}/Sa_{Min,USGS})/2$$

In the example case cited above, the comparison of the USGS epistemic uncertainty ratio and the attenuation relationship epistemic uncertainty is shown on Figure B-9. The computed dgnd term obtained from the attenuation relationship epistemic uncertainty is provided in Table B-3.

A comparison of the dgnd terms provided by the USGS listed in Table B-2 and the attenuation relationship epistemic uncertainty listed in Table B-3 is also shown in graphical form on Figure B-10.

The results from the use of the five attenuation relationships already reflect some epistemic uncertainty from the attenuation relationships. In order to account for the "full" GMPE epistemic uncertainty due to the lack of data, the difference between the two dgnd values for each of the nine bins above needs to be considered. The final epistemic uncertainty included in the current study is provided in Table B-4.

In this study, the events controlling the shaking condition at the site were mainly magnitude 6 to 7 events with a distance range of less than 10 km. Therefore, the epistemic uncertainty for this magnitude range and distance range is the only one that was used for all five attenuation relationships considered in the PSHA evaluation.

B5.0 RECURRENCE RELATIONSHIPS

The recurrence relationships used for the NI/RC Fault Zone source were based on the time-independent part of the UCERF 2 and followed the UCERF 2 methodology (WGCEP, 2008). Following this methodology, a characteristic recurrence relationship (Youngs and Coppersmith, 1985) was assigned a weight of 2/3, and a truncated exponential relationship (Youngs and Coppersmith, 1985) was assigned a weight of 1/3. For the hypothesized OBT source, which was not based on the UCERF 2, appropriate recurrence relationships to be used were guided in part by available historic seismicity data.

Figure B-11 shows 1) the limited observed historic main shock seismicity evaluated for completeness in the area of SONGS and 2) a region generally within 10 km of the hypothesized OBT used in the evaluation of historic seismicity data for the hypothesized OBT source. The historic seismicity catalog and general methodologies used to process this catalog are from UCERF2 (WGCEP, 2008). Figure B-12 shows the hypothesized OBT earthquake recurrence based on the observed historic earthquakes within the hypothesized OBT region (five total, as shown on Figure B-11). The historic seismicity model shown on Figure B-12 includes: 1) the cumulative annual frequency of occurrence of various magnitude or greater observed earthquakes (shown as open circles) and 2) the upper and lower standard deviation recurrence bounds based on Weichert (1980) (shown as vertical bars). Figure B-12 also shows the earthquake recurrence relationship developed using the seismic source parameters for the hypothesized OBT source (Section 2.0 and Appendix B) and assuming only the characteristic recurrence model by Youngs and Coppersmith (1985). As shown on Figure B-12, the use of only the characteristic recurrence relationship to represent the hypothesized OBT source results in the recurrence relationship that is reasonably consistent with the historic seismicity in the hypothesized OBT region. On the basis of the results shown on Figure B-12, only the characteristic recurrence relationship was used to represent the hypothesized OBT source.

TABLE B-1
NGA Relationships and Shear-wave Velocity Parameters

NGA	Epistemic Weight	Shear-Wave Velocity Parameters†		
		V_{s30}*	$Z_{1.0}$**	$Z_{2.5}$***
Abrahamson and Silva (2008)	0.20	500-m/s	0.31-km	3.35-km
Boore and Atkinson (2008)	0.20			
Campbell and Bozorgnia (2008)	0.20			
Chiou and Youngs (2008)	0.20			
Idriss (2008)	0.20			

†Used as needed in each NGA relationship
*V_{s30} = the average shear wave velocity from the ground surface to a depth of 30-m
**$Z_{1.0}$ = the approximate depth to 1.0 km/s shear wave velocity material
***$Z_{2.5}$ = the approximate depth to 2.5 km/s shear wave velocity material

TABLE B-2
Epistemic Uncertainty in the GMPE (natural log term)

Magnitude Range	Rupture Distance Range	Average *dgnd* Term
5 to 6	0 to 10km	$\pm$0.375
	10 to 30km	0.21
	$\geq$30km	0.245
6 to 7	0 to 10km	0.23
	10 to 30km	0.225
	$\geq$30km	0.23
$\geq$7	0 to 10km	0.40
	10 to 30km	0.36
	$\geq$30km	0.31

TABLE B-3
Epistemic Uncertainty in the Attenuation Relationships (natural log term)

Magnitude Range	Rupture Distance Range	Average *dgnd* Term
5 to 6	0 to 10km	±0.285
	10 to 30km	0.252
	≥30km	0.293
6 to 7	0 to 10km	0.157
	10 to 30km	0.15
	≥30km	0.208
≥7	0 to 10km	0.17
	10 to 30km	0.154
	≥30km	0.147

TABLE B-4
Epistemic Uncertainty (natural log term) Used in the Current Study

Magnitude Range	Rupture Distance Range	Average *dgnd* Term
5 to 6	0 to 10km	±0.090
	10 to 30km	0.0*
	≥30km	0.0*
6 to 7	0 to 10km	0.073
	10 to 30km	0.075
	≥30km	0.022
≥7	0 to 10km	0.230
	10 to 30km	0.206
	≥30km	0.163

* signifies that when the dgnd value from the attenuation relationships exceeds the USGS dgnd value, an epistemic uncertainty value of 0.0 was conservatively used.

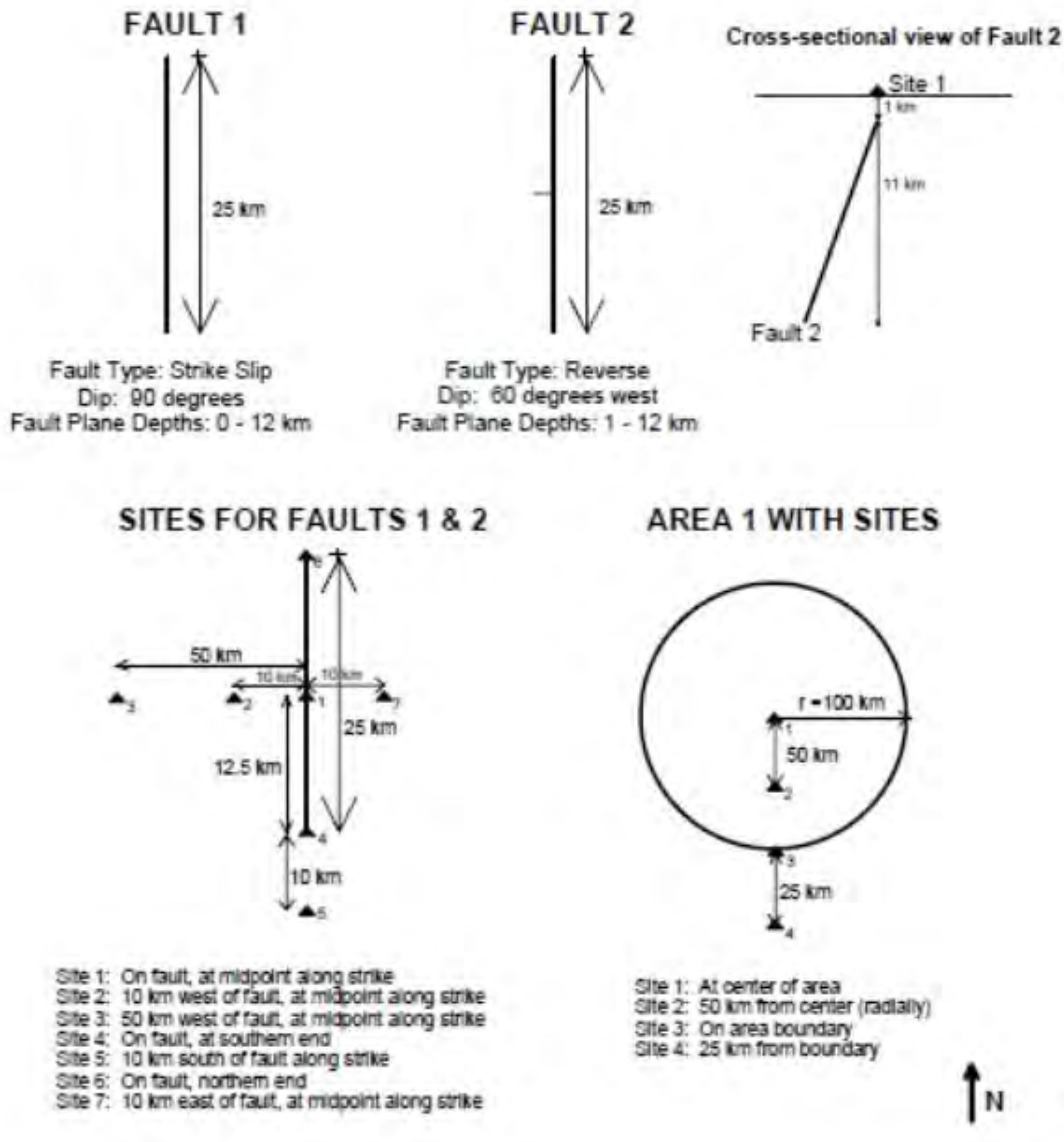

GeoPentech
Geotechnical & Geoscience Consultants

QA/QC OF HAZ4.2 –
FAULT AND SITE GEOMETRY FOR TEST CASES

FIGURE
B-1

SAN ONOFRE NUCLEAR GENERATING STATION

SEISMIC HAZARD ASSESSMENT PROGRAM

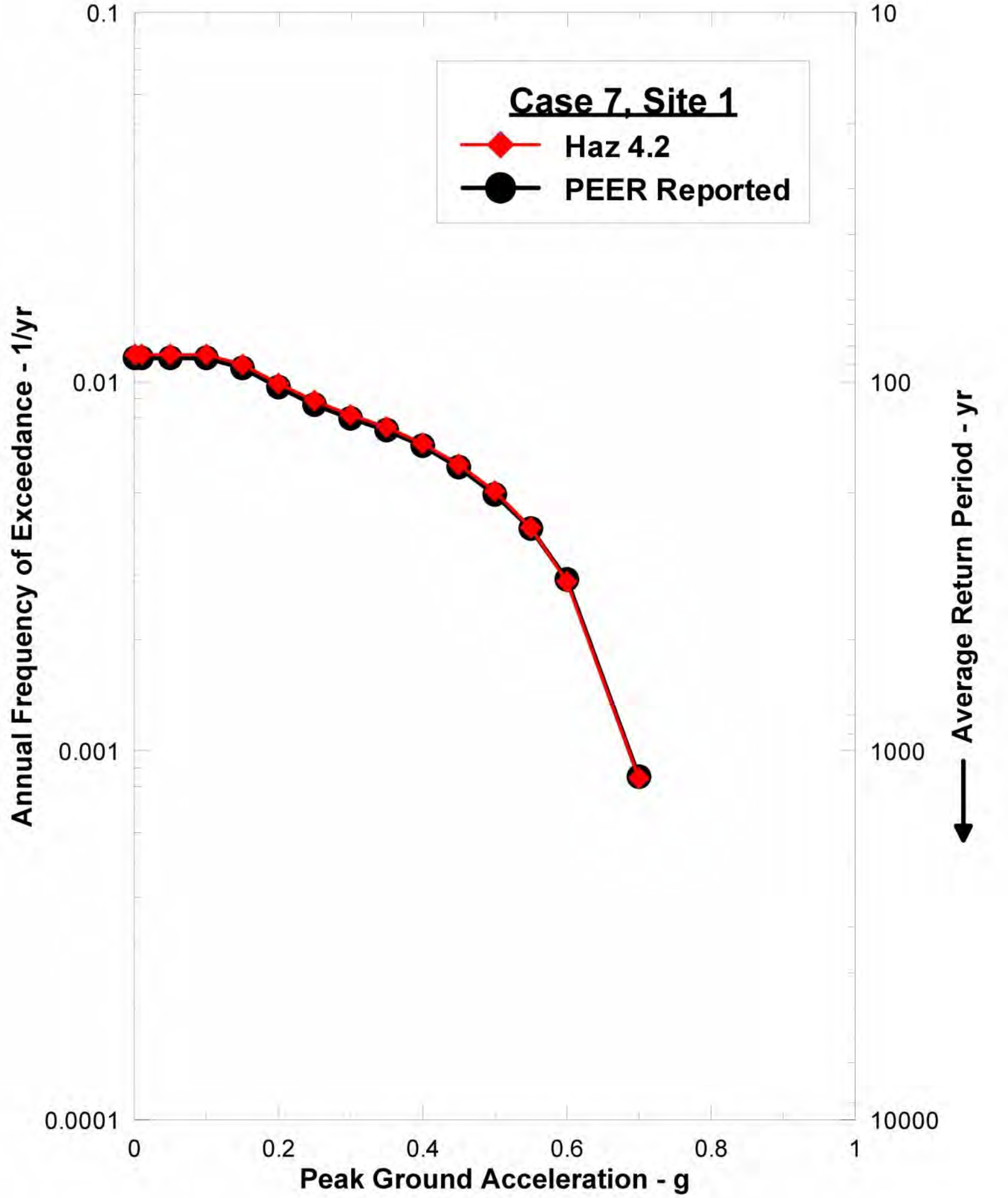

GeoPentech Geotechnical & Geoscience Consultants	QA/QC OF HAZ4.2 – TEST CASE 7, SITE 1	FIGURE B-2
	SAN ONOFRE NUCLEAR GENERATING STATION SEISMIC HAZARD ASSESSMENT PROGRAM	

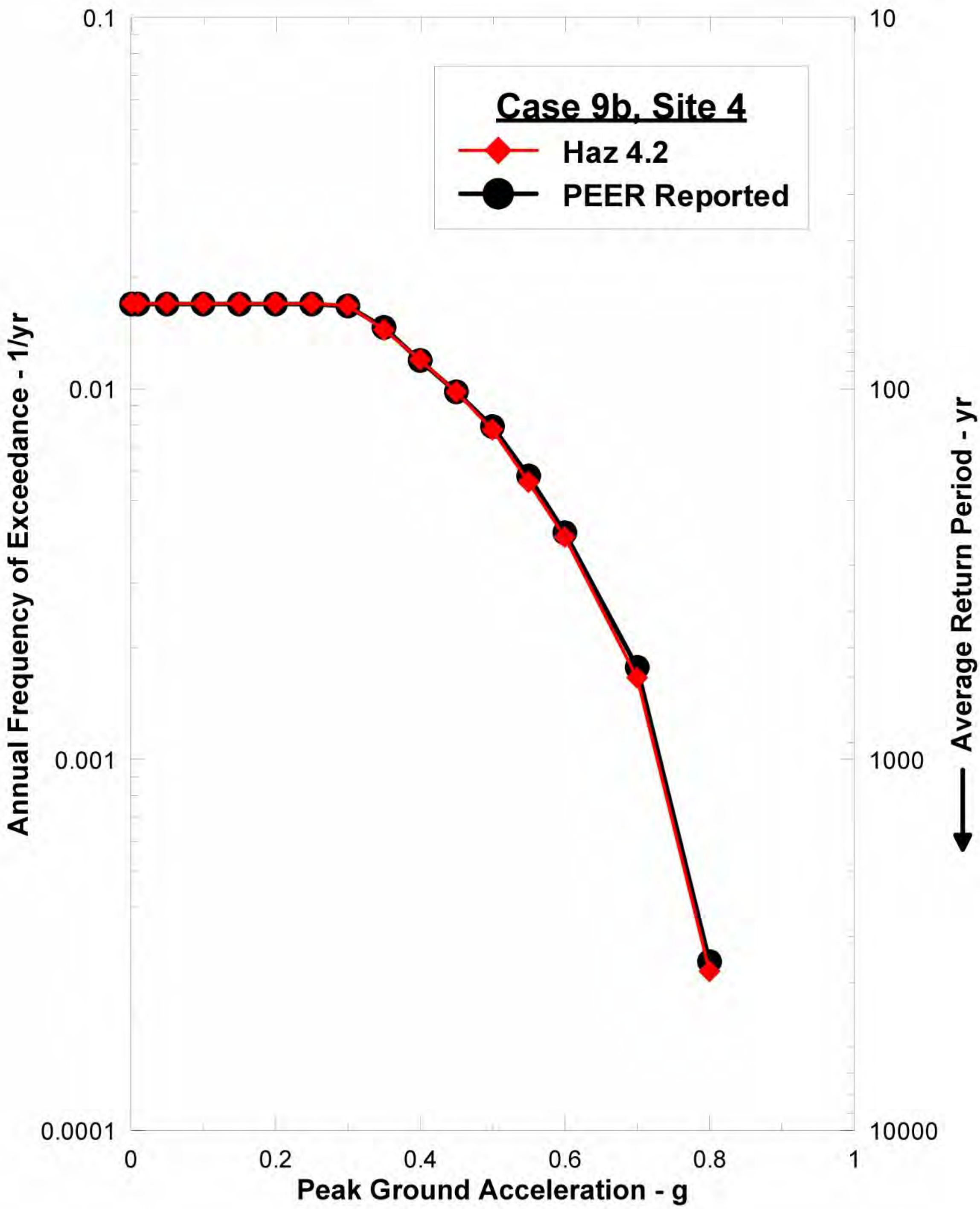

GeoPentech
Geotechnical & Geoscience Consultants

QA/QC OF HAZ4.2 –
TEST CASE 9b, SITE 4

FIGURE
B-3

SAN ONOFRE NUCLEAR GENERATING STATION

SEISMIC HAZARD ASSESSMENT PROGRAM

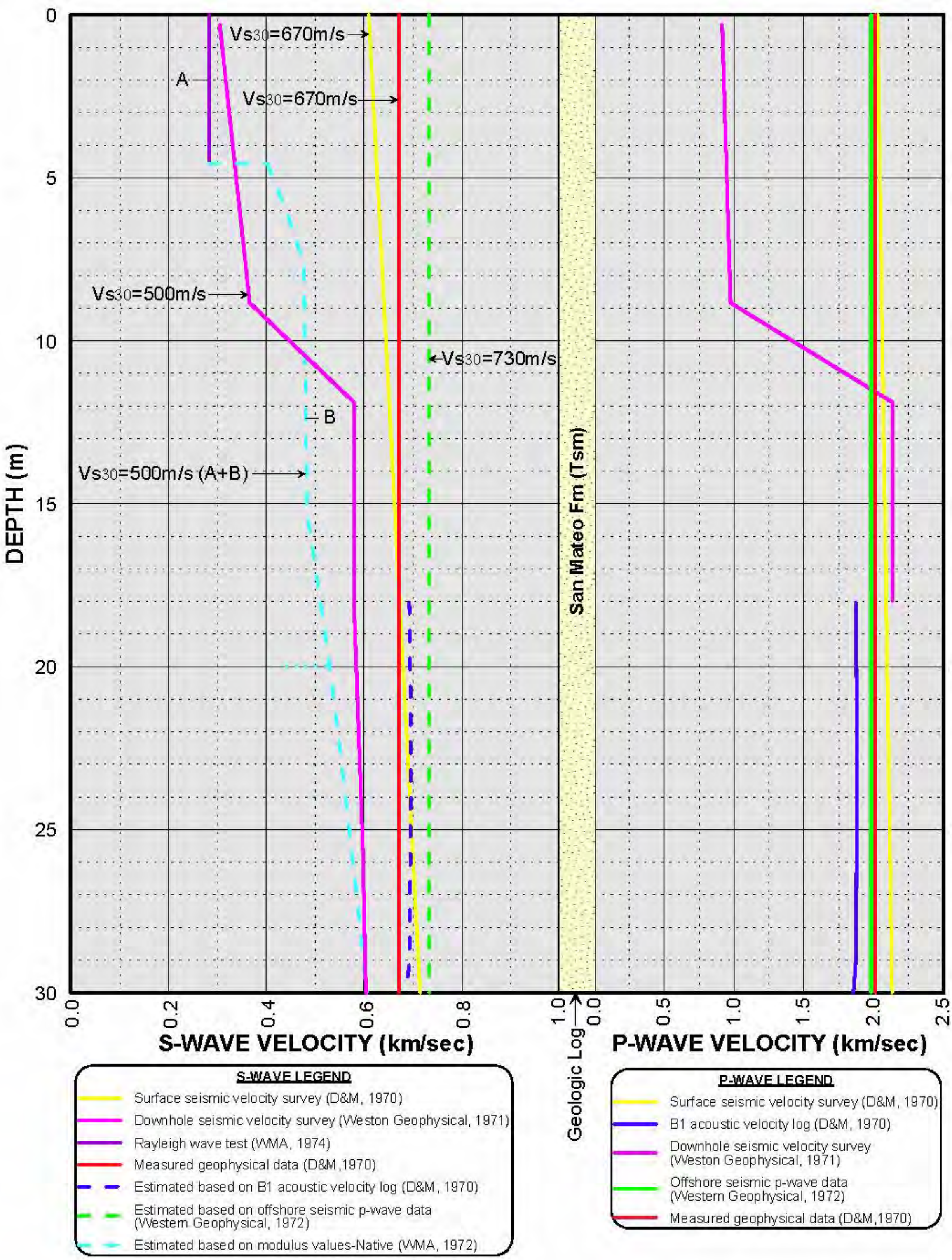

GeoPentech
Geotechnical & Geoscience Consultants

SHEAR- WAVE AND PRESSURE- WAVE VELOCITY SUMMARY (0 to 30 m)

FIGURE B-4

SAN ONOFRE NUCLEAR GENERATING STATION

SEISMIC HAZARD ASSESSMENT PROGRAM

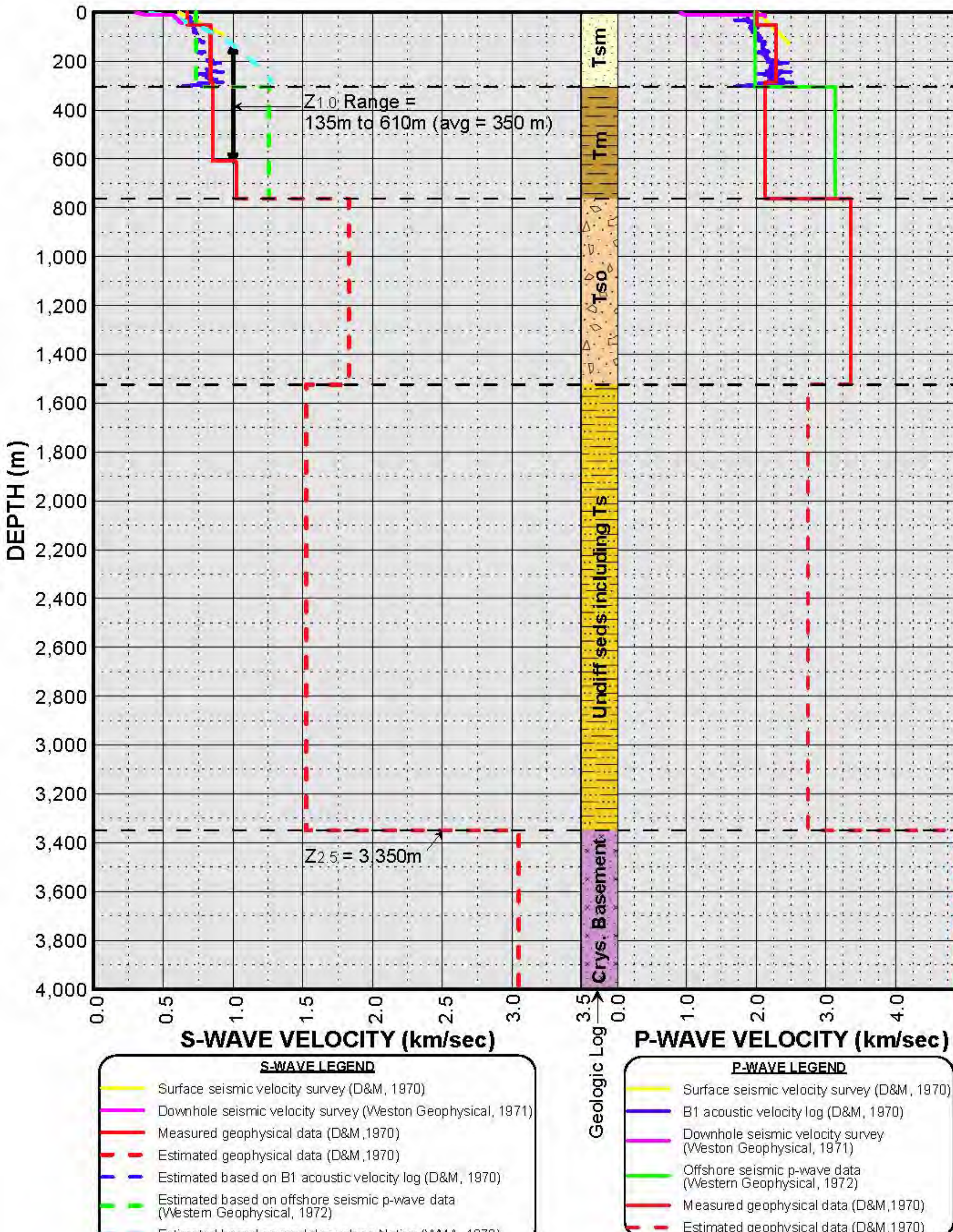

NOTE: Geology based on D&M (1970) and SCE (2001).
Tsm= San Mateo Fm.; Tso=San Onofre Breccia; Ts=Santiago Fm.

GeoPentech
Geotechnical & Geoscience Consultants

SHEAR- WAVE AND PRESSURE- WAVE VELOCITY SUMMARY (0 to 4,000 m)

FIGURE B-5

SAN ONOFRE NUCLEAR GENERATING STATION

SEISMIC HAZARD ASSESSMENT PROGRAM

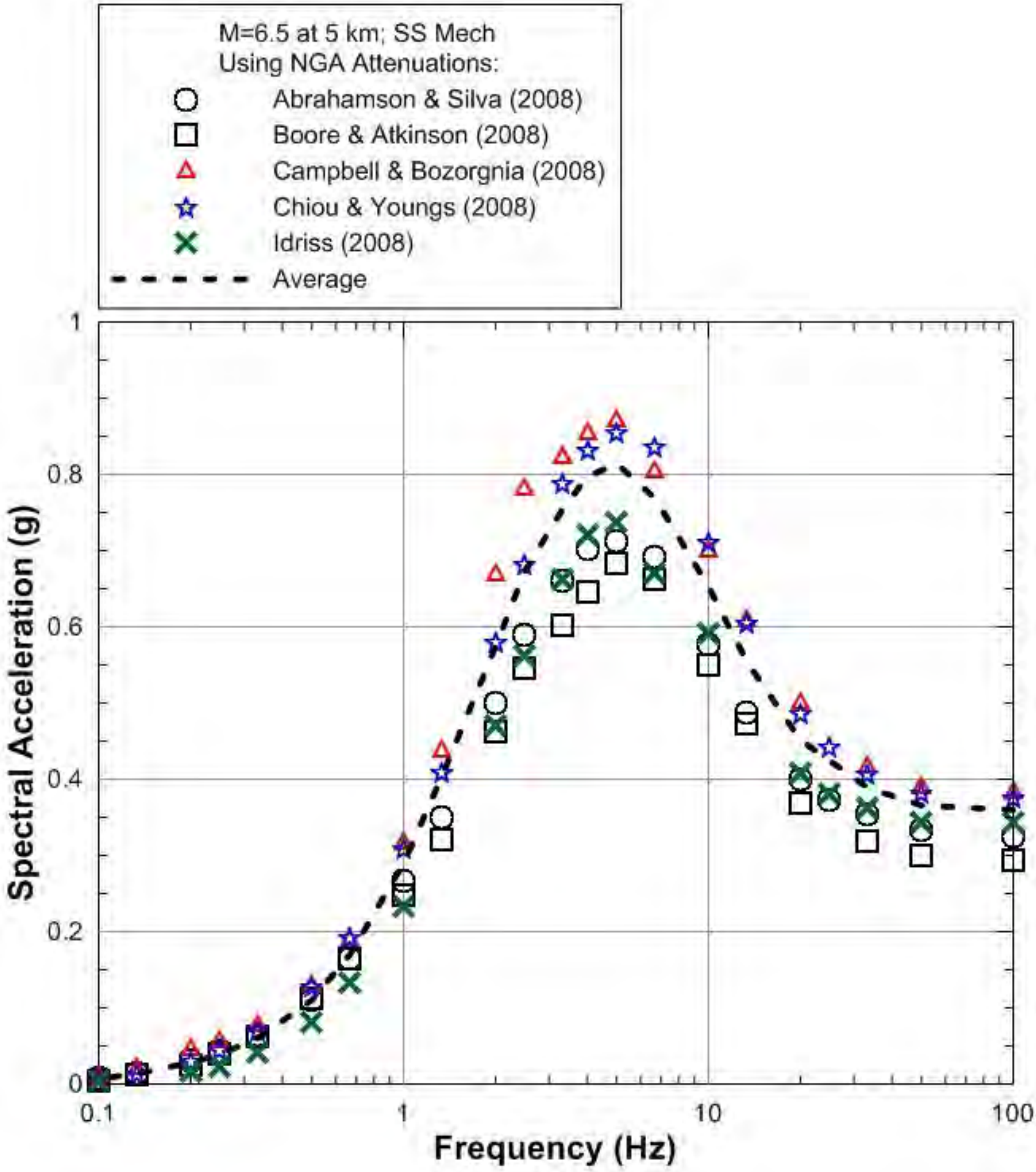

NOTE: Mw=6.5 at 5 km for strike-slip faulting mechanism

GeoPentech
Geotechnical & Geoscience Consultants

RESPONSE SPECTRA FOR THE 5 NGA ATTENUATION RELATIONSHIPS USED

FIGURE B-6

SAN ONOFRE NUCLEAR GENERATING STATION

SEISMIC HAZARD ASSESSMENT PROGRAM

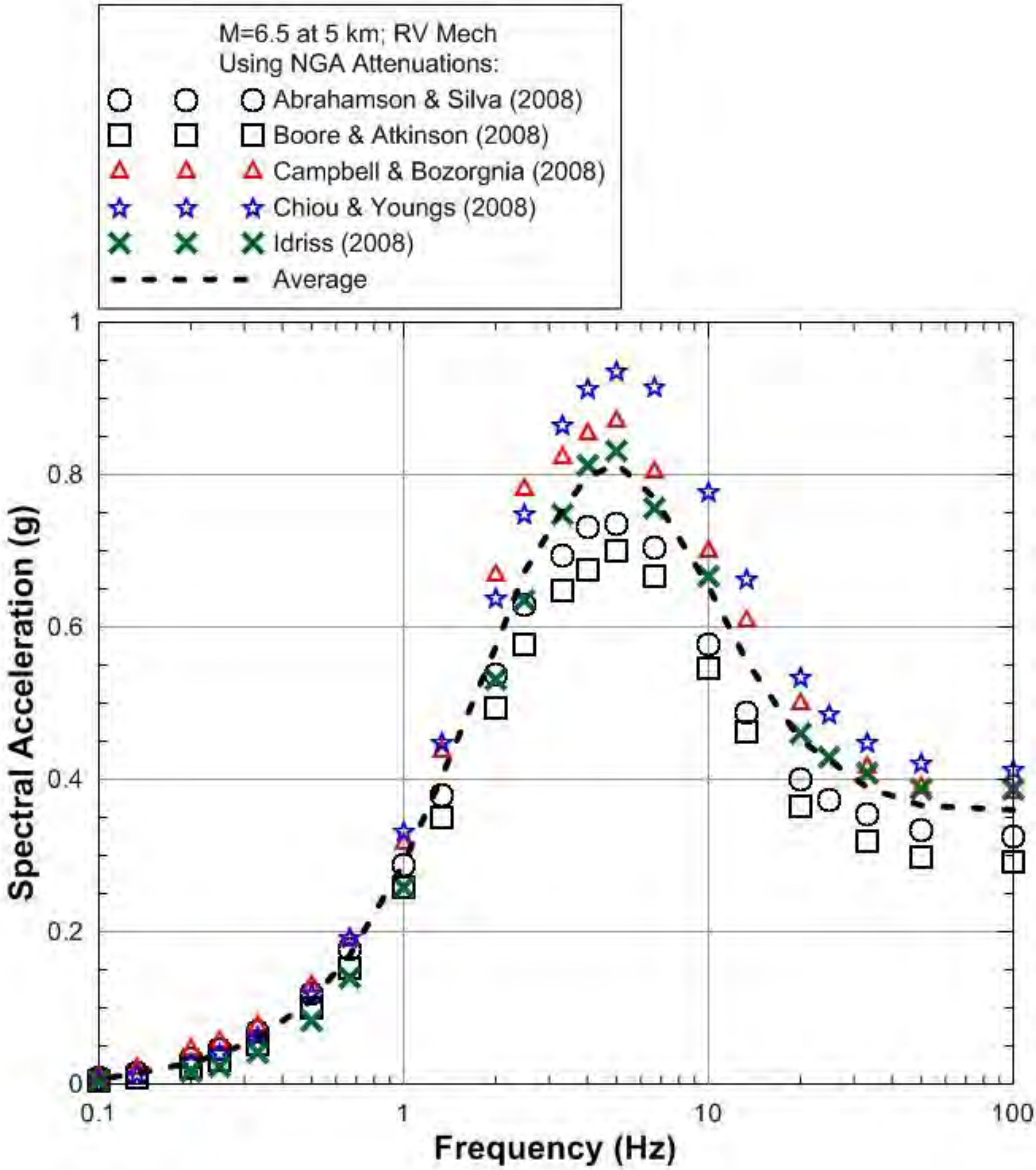

NOTE: Mw=6.5 at 5 km for reverse faulting mechanism

GeoPentech Geotechnical & Geoscience Consultants	RESPONSE SPECTRA FOR THE 5 NGA ATTENUATION RELATIONSHIPS USED	FIGURE B-7
	SAN ONOFRE NUCLEAR GENERATING STATION SEISMIC HAZARD ASSESSMENT PROGRAM	

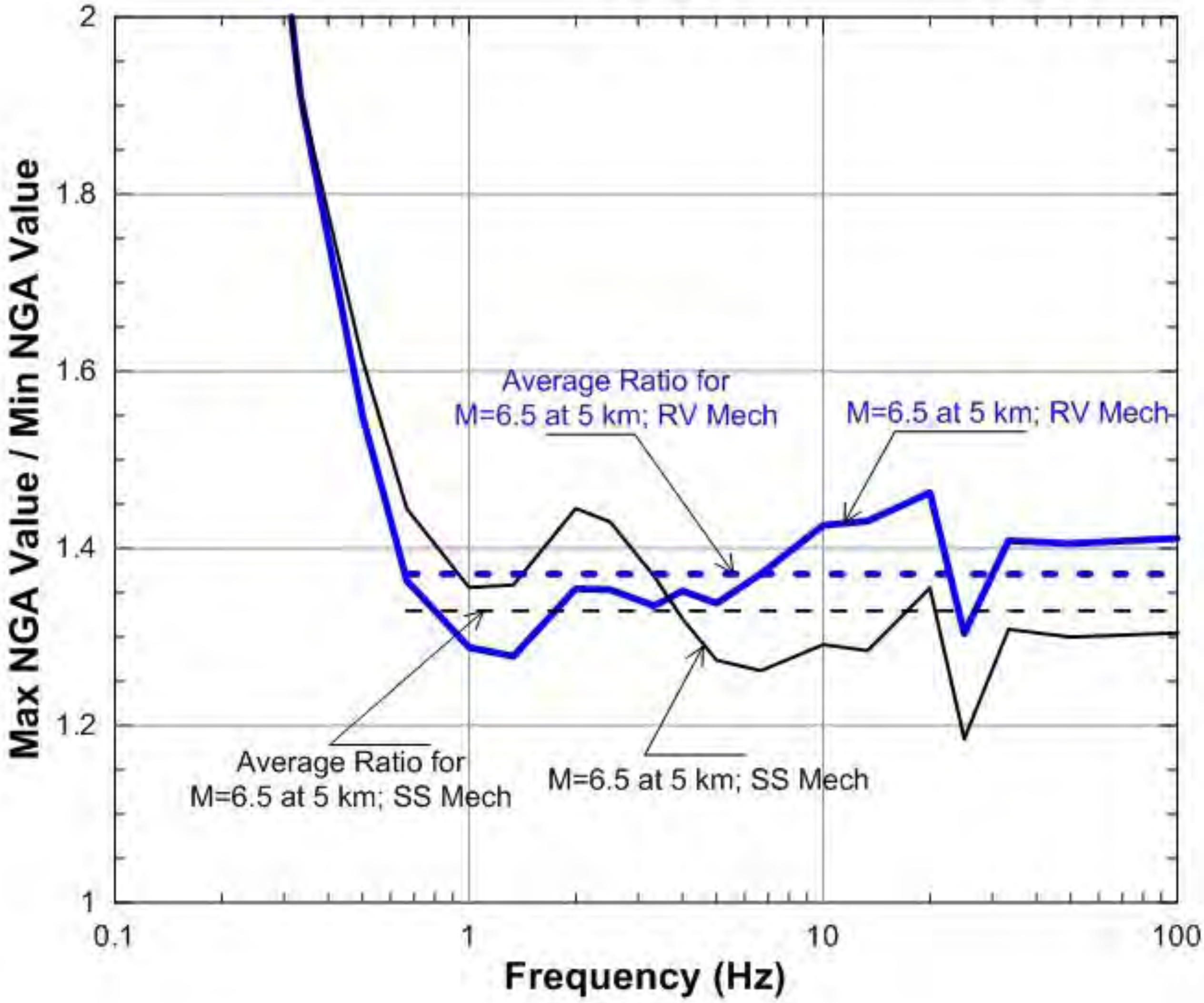

NOTE: Mw=6.5 at 5 km for strike-slip and reverse faulting mechanism

GeoPentech Geotechnical & Geoscience Consultants	**RATIOS OF MAXIMUM TO MINIMUM SPECTRAL ACCELERATIONS**	FIGURE B-8
	SAN ONOFRE NUCLEAR GENERATING STATION SEISMIC HAZARD ASSESSMENT PROGRAM	

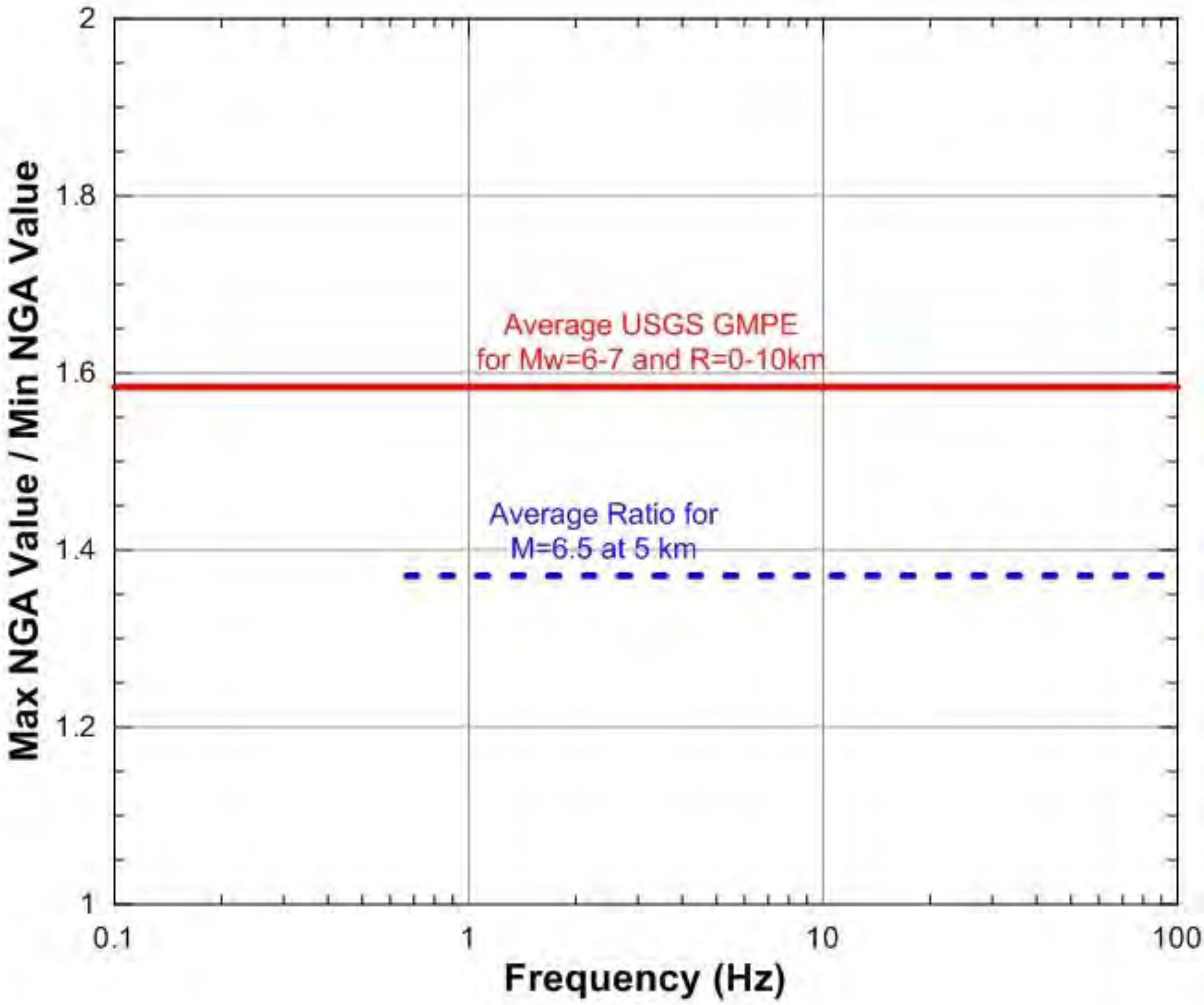

NOTE: Mw=6-7, R=0-10 km

GeoPentech Geotechnical & Geoscience Consultants	**COMPARISON OF USGS EPISTEMIC UNCERTAINTY AND ATTENUATION RELATIONSHIP EPISTEMIC UNCERTAINTY**	FIGURE B-9
	SAN ONOFRE NUCLEAR GENERATING STATION SEISMIC HAZARD ASSESSMENT PROGRAM	

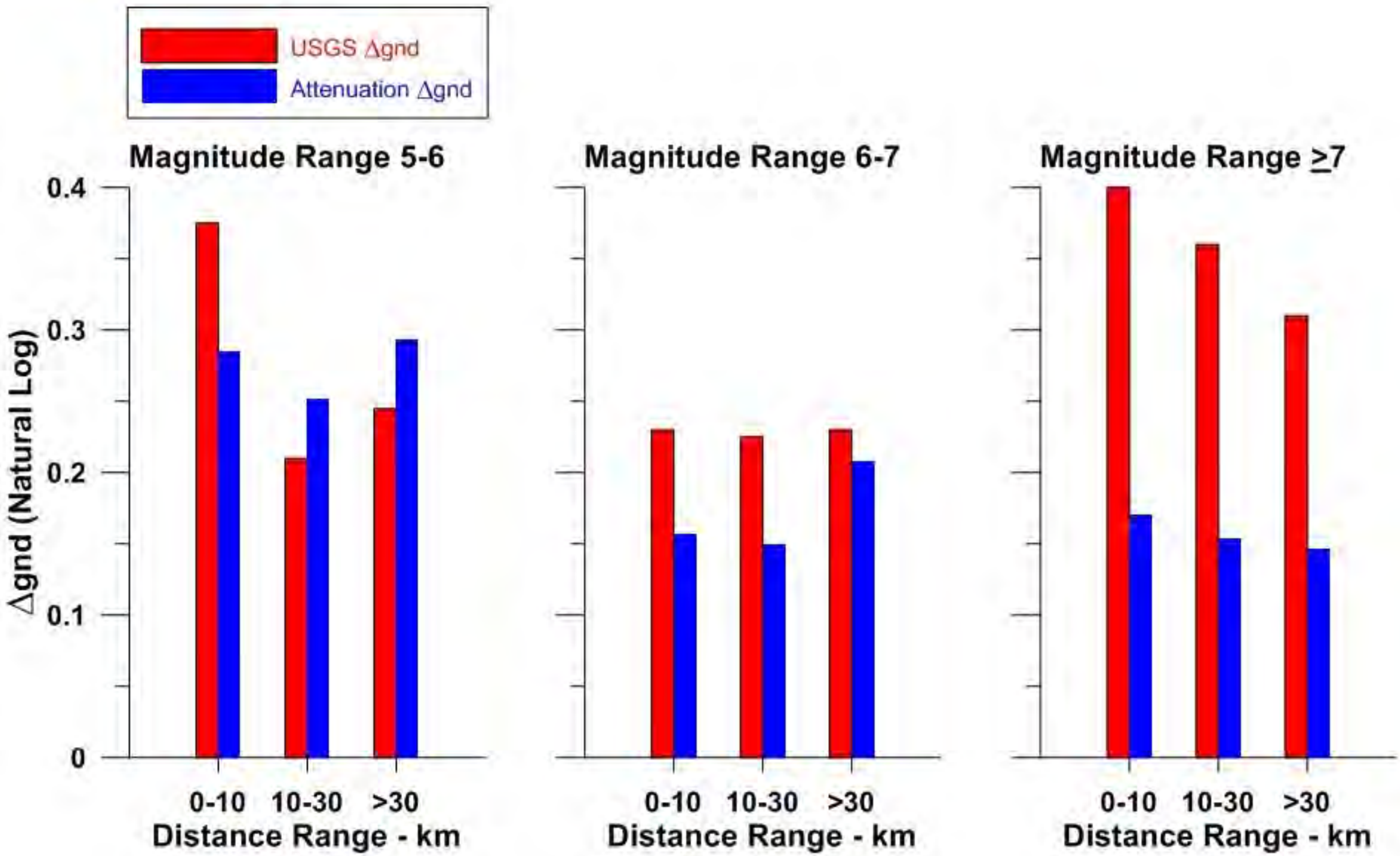

GeoPentech
Geotechnical & Geoscience Consultants

SAN ONOFRE NUCLEAR GENERATING STATION
SEISMIC HAZARD ASSESSMENT PROGRAM

COMPARISON OF THE dgnd TERM FOR THE 9 BINS CONSIDERED

FIGURE B-10

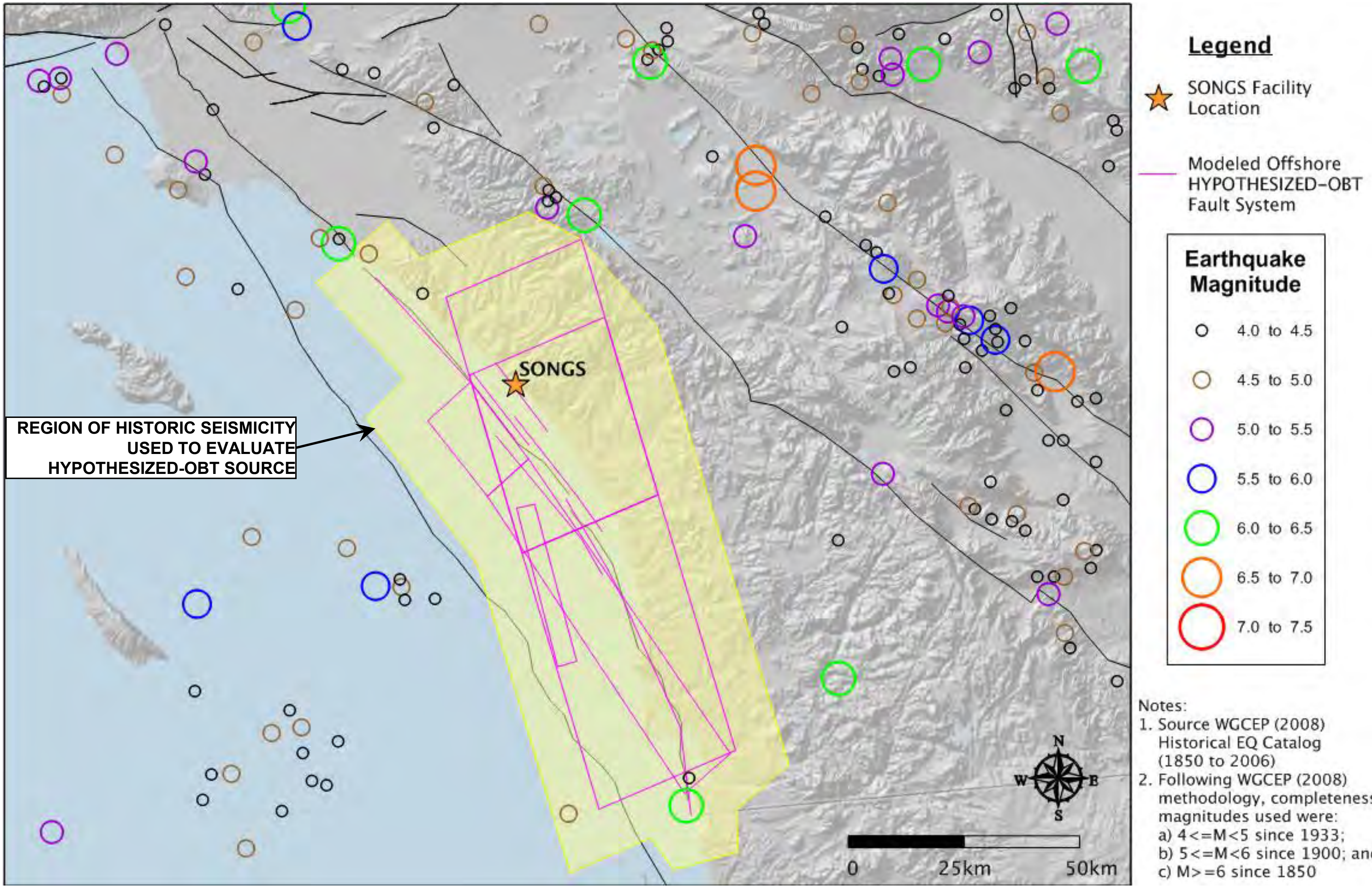

GeoPentech
Geotechnical & Geoscience Consultants

SAN ONOFRE NUCLEAR GENERATING STATION
SEISMIC HAZARD ASSESSMENT PROGRAM

HISTORIC SEISMICITY IN SONGS AREA AND REGION OF HISTORIC SEISMICITY USED TO EVALUATE OBT SOURCE

FIGURE B-11

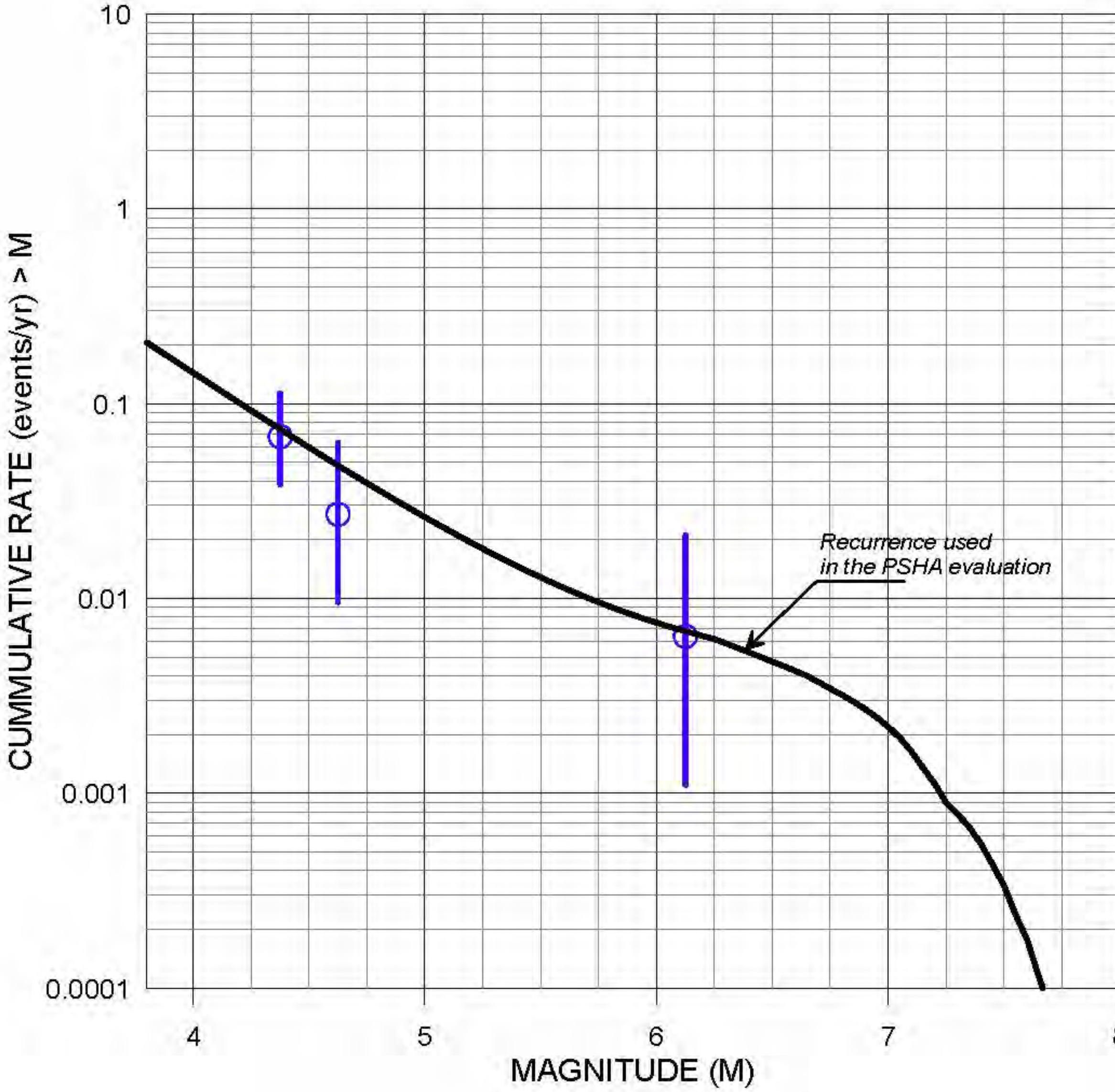

GeoPentech
Geotechnical & Geoscience Consultants

COMPARISON OF HISTORICAL AND MODEL RECURRENCES

FIGURE B-12

SAN ONOFRE NUCLEAR GENERATING STATION

SEISMIC HAZARD ASSESSMENT PROGRAM

From: Steve Rosansky
To: Energy@Coastal
Cc: Melinda Andrade
Subject: SONGS NUHOMS CDP - Application #E-00-014-A2
Date: Monday, October 3, 2022 10:37:03 AM
Attachments: image002.png

Dear California Coastal Commissioners:

I am writing to you on behalf of the Newport Beach Chamber of Commerce. We recently received a briefing from Public Information Officer, John Dobken, with San Onofre Nuclear Generating Station (SONGS). During that presentation, our members saw the various storage systems at SONGS for spent nuclear fuel. I am writing to urge your approval of the Coastal Development Permit (CDP) before you to extend the term for the NUHOMS waste storage facility at SONGS.

The Newport Beach Chamber is a member of the Action for Spent Fuel Solutions Now, and we believe it is of the utmost importance for our community and local businesses that we provide SONGS all the tools they need to continue to safely store spent nuclear fuel on site. We would like to see the federal government fulfill its obligation to provide a permanent facility to dispose of spent fuel but until action is taken, we have no other option.

Renewal of the CDP is an important interim step to facilitate continued onsite storage and we ask for you to vote “yes” and approve CDP application E-00-014-A2 at your meeting next week.

Sincerely,

Steve Rosansky
President and C.E.O.

Newport Beach Chamber of Commerce
The Business and Community Resource

4343 Von Karman Ave., Ste. 150-W
Newport Beach, CA 92660

PH: (949) 729-4404
FX: (949) 729-4417

www.NewportBeach.com

Click to sign up for eMail updates
Privacy by SafeSubscribe℠

From:	Juliann Harkness
To:	Energy@Coastal
Subject:	SONGS NUHOMS CDP - Application #E-00-014-A2
Date:	Monday, October 3, 2022 10:35:47 AM

Dear California Coastal Commissioners:

On behalf of the Costa Mesa Chamber of Commerce, I am writing to urge your approval of the Coastal Development Permit (CDP) to extend the term for the NUHOMS waste storage facility to provide for the continued safe storage of spent nuclear fuel at the San Onofre Nuclear Generating Station (SONGS).

As a member of the Action for Spent Fuel Solutions Now, we are frustrated by the federal government's failure to provide an offsite facility to dispose of spent fuel from nuclear plants like SONGS. Despite nuclear utility customers having pre-paid more than $40 billion for disposal, today all-American taxpayers are saddled with $2 million per day and $9 billion to date to reimburse utilities for on-site storage of spent fuel that the federal government was supposed to start picking up in 1998.

We are grateful for utilities like Southern California Edison, who have stepped in and are providing safe onsite storage of the spent fuel. Renewal of the CDP is an important interim step to facilitate continued onsite storage. There is no other immediate option.

We applaud the efforts of the team at SONGS and ask that at your meeting on Oct. 13, please vote "yes" and approve CDP application E-00-014-A2.

Sincerely,

Juliann Harkness
Vice President of Member Services

(714) 885-9090 | jharkness@costamesachamber.com
http://www.costamesachamber.com/ [costamesachamber.com]
1870 Harbor Blvd. Suite 105, Costa Mesa, CA 92627

Like and follow us!
Facebook: Costa Mesa Chamber of Commerce [facebook.com]
Instagram: costamesa_commerce [instagram.com]
LinkedIn: Costa Mesa Chamber of Commerce [linkedin.com]
Twitter: @ CM_chamber [twitter.com]

ORANGE COUNTY COASTKEEPER®

3151 Airway Ave, Suite F-110
Costa Mesa, CA 92626
714-850-1965
www.coastkeeper.org

To: EORFC@coastal.ca.gov
From: Garry Brown, Founder & President
Orange County Coastkeeper
Subject: **The Coast and SONGS CDP - Application #E-00-014-A2**
Date: October 4, 2022

Dear California, Coastal Commissioners:

As the founder of Coastkeeper, I have worked for decades on issues related to marine habitats throughout California and served as a volunteer member of the Community Engagement Panel for SONGS decommissioning since 2014. In short, I urge you to approve the application to extend the CDP for the SONGS NUHOMS storage system through 2035.

I have toured SONGS, seen the NUHOMS system up close, and I have had the opportunity to talk to the team at SONGS that manages the dry storage system. Without a federal solution for disposal of spent fuel, continued storage at SONGS is the only safe option.

In the interest of stimulating federal action, I joined the Advisory Council for Action for Spent Fuel Solutions Now, which is advocating for offsite solutions for spent nuclear fuel storage and/or disposal. We as a country must make this issue a priority.

I share the Coastal Commission's commitment to thoughtful land use planning in the Coastal Zone and I believe that the careful and active storage of spent fuel at San Onofre is consistent with the Coastal Act. I understand that Southern California Edison plans to complete decommissioning and restore the site for other uses once the spent fuel is removed from the site.

Please vote in favor of approval of CDP application E-00-014-A2 at your October meeting.

Sincerely,

Garry Brown

Garry Brown
Founder and President, Orange County Coastkeeper
Advisory Council Member, Action for Spent Fuel Solutions Now
Member, SONGS Community Engagement Panel

E-00-014-A2 (SONGS)

OCTOBER 13, 2022

CORRESPONDENCE:

Individual Emails

Th12a (amendment to Coastal Development Permit E-00-014)

Ace Hoffman <rhoffman@animatedsoftware.com>

Tue 10/4/2022 8:44 PM

To: SanOnofreComments@Coastal <SanOnofreComments@coastal.ca.gov>

From: Ace Hoffman
To: California Coastal Commission
Re: Th12a (amendment to Coastal Development Permit E-00-014)
Date: October 4, 2022

To: The California Coastal Commission:

The California Coastal Commission (CCC) staff report makes the following claim:

"When the Commission considered the waste storage facility in 2001, the information available at the time indicated that the U.S. Department of Energy would establish a federal repository for spent nuclear fuel and would begin accepting spent fuel from commercial facilities, including SONGS, by 2010."

What "information" was the California Coastal Commission going on in 2001 to make that claim? Yucca Mountain was far from a decided thing then (it has since been cancelled compelely). There were hundreds of known problems with it (California alone has dozens of significant objections). Only whimsey and fantasy would have allowed anyone to think it was "the information available."

The nuclear industry has survived on waste management promises for decades (see link below to the author's review of waste management attempts in America over the past half century, as well as the attached page from a 1970s book called the Anti-Nuclear Handbook).

Page 23 of the CCC staff report claims to have analyzed (or had analyzed for them) a 7.5 earthquake (elsewhere up to 7.44 (an oddly specific number for such an inexact science) was indicated). But a 7.8 magnitude earthquake is three times stronger than a 7.5 earthquake, and perhaps one even stronger than that will strike the Independent Spent Fuel Storage Installation (ISFSI) at San Onofre.

The CCC staff report repeatedly refers to a "design basis earthquake" and a "design basis tsunami". This conveniently ignores "beyond design basis earthquakes" and "beyond design basis tsunamis" which are certainly possible -- nor does the staff report give any indication of the odds for anything: Instead, they just describe things as "unlikely" or "extremely unlikely."

Even if these events are "unlikely" or "extremely unlikely" their impacts could be so devastating that the events must be considered.

Beyond Design Basis events are not only possible, but additionally: Even the Nuclear Regulatory Commission (NRC) occasionally considers them and regulates the nuclear industry regarding them. So why can't the California Coastal Commission do so?

But what really galls me about the CCC staff report is that they completely ignore consequences of accidents. Not just that they are unlikely, but no consideration of how damaging to SoCal an accident -- however unlikely -- would be. They do this with the excuse that that would be strictly the purview of the Nuclear Regulatory Commission -- which is absurd. The NRC might "regulate" nuclear reactor safety and spent fuel safety, but the consequences will be OUR problem -- not theirs.

Another point: The CCC staff report says the containers should be "transportable" so that at some future time they can be moved to either a safer location on the SoCal Edison (SCE) site (which is actually leased from Camp Pendleton (Marine Corps)) or to a permanent repository somewhere. Yet the enormous number of fuel assemblies allowed in each cask -- to save money by using fewer casks -- makes them extremely heavy and to move them away from San Onofre will require them going over (and under) numerous bridges where a far greater fall than the canisters are designed to withstand might occur (the NRC only requires the casks to withstand a drop of 30 feet, and even then, a "back breaker" accident is not considered (where the middle of the cask takes all the force of the impact with a solid object)).

So really, the CCC isn't making sure the canisters can be transported even as far as across the bridge that goes over the (eroding) train tracks and the busy I-5 highway to store them further away from the coast on (borrowed) SCE land slightly further inland. If a bridge fails (perhaps because a truck or train crashes into a bridge abutment just when one of the 123 canisters is being moved) then the fall could exceed the drop height the casks are designed to (possibly) withstand.

The CCC staff report earthquake estimates are based on a maximum 7.5 magnitude earthquake. But experts now believe the Palos Verdes Fault (PVF) is capable of producing a 7.8 magnitude earthquake. PVF is nearly 70 miles long and the tip is within about 10 miles of San Onofre.

The staff report's sea rise estimates and tsunami estimates could also be way off -- and in instance after instance in the Th12a staff report, the NUHOMS horizontal cask system is just barely safe from their estimated worst case scenario.

The CCC staff report's beach erosion estimates might be way off too. Especially note that this week, Surfliner has suddenly been cancelled indefinitely between Mission Viejo and San Diego due to coastal erosion in San Clemente. These tracks were the 2nd busiest route in the country -- until suddenly they weren't available and thousands of people are suddenly severely inconvenienced for who-knows-for-how-long, including both commuter and freight traffic.

It is expected that sooner or later the tracks will be repaired. Compare this to what would happen from even a "small" accident involving just one of the 123 dry casks stored at San Onofre: The entire area, including the Cities of San Clemente and Oceanside, Camp Pendleton, I-5 AND the vital rail line would all be permanently unavailable, just over 1,000 square miles are permanently unavailable around Chernobyl for the foreseeable future from an accident that occurred nearly 40 years ago. It should be noted that EACH dry cask at San Onofre contains as much radiation as was released in the Chernobyl accident. This figure has been admitted in a published letter to the editor by the SCE spokesperson, who claimed there needs to be a "motive force" to release it to the environment.

Let me suggest a few "motive forces" that might cause a large dispersal of the nuclear waste at San Onofre: An airplane strike, either intentional or accidental. A large ship settling on the cask structure after being washed inland during a tsunami. A high-powered weapon (even a shoulder-fired weapon could go through both the concrete overpack and the dry cask itself, and that's just ONE trigger pull. There is almost no defensive guard requirements for the ISFSI. It is unlikely that ONE guard with ONE pistol would be able to stop even a small group of well-prepared terrorists). An earthquake that bursts open one or more casks during a rainstorm, or followed by a tsunami, would be particularly disastrous.

There are many other ways the spent fuel canister can be breached. A breach can cause the fuel to self-ignite by exposing the canisters to air and water. The zirconium cladding, being pyrophoric (self-igniting) could/would entirely burn off, releasing all the fission products currently held in the "gap" between the uranium/plutonium pellets and the zirconium cladding.

This would be a local, state, and global disaster, but it might not, in and of itself, cause the uranium/plutonium/fission/product-laden fuel pellets to also self-ignite since zirconium burns at a much lower temperature than uranium. But it would cause the fuel assemblies to disassemble. The fuel pellets would fall to the bottom of what's left of the canister, and then a self-sustaining criticality event could/would quickly reach a temperature which ignites the entire cask of spent fuel.

An American Chernobyl, because the California Coastal Commission didn't do its job.

Lastly, why is the Th12a staff report coming so late, just a month before the current San Onofre ISFSI license for the NUHOMS casks expires? Why does it cite a 2001 DOE waste management report that proves how poorly the DOE estimates nuclear waste management timelines as a reason that the DOE will (probably, hopefully, possibly) have a national repository by 2035 -- or any time?

I recommend the CCC staff report be thrown out, the relicensing stopped, and SCE be required to repack the fuel in much smaller quantities, and that all spent fuel canisters be moved away from the coast (and away from ANY earthquake zone in California (good luck with that)), and that all spent fuel canisters be separated from each other by a minimum of several hundred yards. Local fire departments need to be constantly trained and retrained about how to handle a fire at the spent fuel installation, and all other possibilities for what might happen at San Onofre should be covered. For example, the ability to dump many tons of sand on a spent fuel fire should be practiced by local/state government helicopter pilots on at least an annual basis if not more frequently.

All costs for more properly storing the spent fuel should be borne solely by the owners, Southern California Edison (80%) and San Diego Gas and Electric (SDG&E) (20%), and their shareholders.

Ace Hoffman
Carlsbad, California

The author, an independent researcher and two-time cancer survivor, has studied nuclear issues for approximately 50 years and has interviewed and/or worked with dozens of technical experts in all related subjects. All views are his own.

Additional information:
Palos Verdes Fault: A serious issue for San Onofre; Recent history of fault research in California:
https://acehoffman.blogspot.com/2022/09/palos-verdes-fault-serious-issue-for.html

Extending Diablo Canyon's operating license: A fiasco waiting to happen (contains additional discussion about dry cask accident issues):
https://acehoffman.blogspot.com/2022/08/extending-diablo-canyons-operating.html

Nuclear Waste Management: The view through the years:
https://acehoffman.blogspot.com/2017/10/nuclear-waste-management-view-through.html

Different types of nuclear radiation and why they are all dangerous (a backgrounder on radiation dangers):
https://acehoffman.blogspot.com/2022/07/different-types-of-nuclear-radiation.html

FW: Letter of Support to CCC for SONGS CDP 09/28/2022 from Ted Quinn

Energy@Coastal <EORFC@coastal.ca.gov>
Wed 9/28/2022 6:19 PM
To: SanOnofreComments@Coastal <SanOnofreComments@coastal.ca.gov>

From: tedquinn@cox.net <tedquinn@cox.net>
Sent: Wednesday, September 28, 2022 9:52 AM
To: Energy@Coastal <EORFC@coastal.ca.gov>
Cc: tedquinn@cox.net
Subject: Letter of Support to CCC for SONGS CDP 09/28/2022 from Ted Quinn

To: EORFC@coastal.ca.gov
From: Ted Quinn
Subject: **SONGS NUHOMS System CDP Renewal (Application No. E-00-014-A2)**
Date: 09/28/2022

To California Coastal Commission:

This e-mail is to offer a vote of support for your approval of SCE's application number E-00-014-A2 and extend the lease of the NUHOMS Independent Spent Fuel Storage Installation (ISFSI) out to 2035.

I am very familiar with ISFSIs in general as well as the particular NUHOMS dry storage facility that has been in service at SONGS for nearly 20 years. I am former president of the American Nuclear Society and a member of the SONGS Community Engagement Panel.

In the history of dry cask storage of spent nuclear fuel in the United States, there has never been an accident that caused a radiological disaster. These concrete and rebar reinforced structures are very robust.

As you know, SCE—the decommissioning agent for SONGS—has a detailed and thoughtful Aging Management Program for the NUHOMS facility that takes into account industry experience as well as research and development by third party entities such as the Electric Power Research Institute. SCE also has demonstrated a repair method that accelerates nickel to supersonic speeds and create a strong metallurgical bond without introducing excess heat into the canister, which can create a new issue with a canister that requires attention.

As a career-long nuclear professional, I urge you to approve the coastal development permit for the NUHOMS dry cask storage system at SONGS during your upcoming meeting.

Thank you for your attention to this important issue. I hope you approve the application.

Best regards,

Sincerely,

Ted Quinn
Past President, American Nuclear Society
IEC SC45A WGA9 Convenor
Vice Chair, ISA S67 Committee

Vice President, Licensing
Paragon Energy Solutions
www.paragones.com
(949) 632-1369
23292 Pompeii Drive

Dana Point, CA 92629

FW: Lou Bosch letter of support to CCC for SONGS NUHOMS System CDP Renewal (Application No. E-00-014-A2)

Energy@Coastal <EORFC@coastal.ca.gov>
Wed 9/28/2022 3:38 PM
To: SanOnofreComments@Coastal <SanOnofreComments@coastal.ca.gov>

From: Louis Bosch <louis45@sbcglobal.net>
Sent: Wednesday, September 28, 2022 7:52 AM
To: Energy@Coastal <EORFC@coastal.ca.gov>
Subject: Lou Bosch letter of support to CCC for SONGS NUHOMS System CDP Renewal (Application No. E-00-014-A2)

To: EORFC@coastal.ca.gov

From: Lou Bosch P.E.

Subject: **SONGS NUHOMS System CDP Renewal (Application No. E-00-014-A2)**

Date: 9/28/2022

Dear Coastal Commissioners,

As a career-long nuclear professional, I urge you to approve the coastal development permit for the NUHOMS dry cask storage system at SONGS during your upcoming meeting.

I worked at SONGS for 34 years in a range of capacities, including Plant Manager for the final six years, before retiring in 2021. Through the decades, I learned firsthand what it means to work as a nuclear professional here in the U.S. It means continuous improvement, a commitment to the highest levels of performance, regulatory compliance, and cultivating a culture of open communication and trust.

I was working at SONGS in 2003 when some of my colleagues loaded the first multipurpose canisters of spent fuel from Unit 1 into the NUHOMS ISFSI for temporary, on-site storage. The design basis for the NUHOMS facility took into account natural events such as earthquakes and tsunamis as well as considerable man-made threats (terrorism).

The aging management program for the NUHOMS system is designed for early detection of the onset of chloride induced stress corrosion cracking such that indications can be addressed well before they can pose a threat to the containment function provided by the canisters.

Based on my personal experience, I have full confidence that the team at SONGS will continue to ensure the safe and secure storage of spent fuel in the NUHOMS system.

Please vote “yes” to approve application E-00-014-A2 and provide for the continued safe storage of spent fuel in the NUHOMS system at SONGS through at least 2035.

Best regards,

Sincerely,

Lou Bosch P.E.

Oceanside Ca.

The California Coastal Commission

10/07/2022

Regarding: CPD, E-00-014-A2 (Southern California Edison) 10/13/22
agenda item 12a

Honorable California Coastal Commission members,

"Better late than never"….The Th12a Staff Report finally recognizes the existing geological hazards and their affects on Marine Resources, water quality, the environment and environment justice and visual impacts from SONGS, that activists and nuclear experts have been warning you about.

In fact, the Staff report is an admission of Failure to Plan ahead.

Now what? Another permit for storage time extensions and more un-enforceable conditions which can be waived or exempted upon request by the industry?

To be consistent with Coastal Act, the CCC must vote NO! More time means more foot dragging and lack of action.

The CCC must NOW demand that all means be taken to keep the 1800 tons of highly radioactive nuclear waste as safe as scientifically possible while stranded here. See how the Swiss do it.

In addition to condition #7, The CCC must add irrevocable CONDITION #8; to immediately study and provide funding to build a Dry Transfer Facility (Hot Cell) onsite, paid for by the SCE and the billions of dollars recently given to the Nuclear industry by Gov. Newsom. (Hot Cell cost estimate, by Chris Hansen of the NRC, is a meager 10 million dollars)
Secondly, that all storage CASKS meet ASME 3N standards so that they actually can be transported. Handling of fuel can only be done safely with a Dry Transfer Facility.

The narrative, that the Nuclear industry sets to calm the public, is that "Nuclear is safe".
Show us that the CCC will no, longer buy into this myth.

Alice McNally
1332 Stratford Ct.
Del Mar, CA 92014
858-342-3244

Comments for the CCC regarding the thousands of tons of uranium on the beach

RJohnson <r66nj@yahoo.com>

Fri 10/7/2022 8:51 PM

To: SanOnofreComments@Coastal <SanOnofreComments@coastal.ca.gov>

To the Coastal Commission:

It is essential that the Coastal Commission weigh in strongly on the future of San Onofre, by far the biggest threat to the southern California coast and the 15.4 million people who live within 100 km. Please do not hide behind bureaucratic issues of jurisdiction and instead come out forcefully to declare that the 1,773 ton nuclear waste dump must be relocated to a safer interim or permanent site ASAP. Those 123 thin temporary canisters hold over 300 million uranium/plutonium pellets which will be lethal for over 100 million years. In a few decades, it will be too dangerous to move the canisters.

I wonder if you read the *New York Times* Op Ed a few weeks ago opposing nuclear power:

https://www.nytimes.com/2022/09/16/opinion/nuclear-power-still-doesnt-make-much-sense.html

The author noted that the cost of the Fukushima debacle is approaching a trillion dollars. Who will be to blame if the waste is allowed to remain here and we have a similar disaster? “Holding your nose” and going along with keeping it here (which was mentioned at one of your previous meetings) might prove to be a huge embarrassment for the Coastal Commission.

Last Sunday the NYTimes devoted a half page to readers who weighed in about this article. Mine was among them: ***Does Nuclear Power Deserve a Bad Rap?*** *Readers debate safety, cost, reliability and environmental issues.*

To the Editor:

Re “Nuclear Power Still Doesn’t Make Much Sense,” by Farhad Manjoo (column, Sept. 17):

It is alarming to hear someone outside the nuclear industry casually assert, “Nuclear power is relatively safe, reliable and clean.”

Nuclear power is safe? There have been over 100 serious nuclear power accidents, including the Fukushima debacle, which could end up costing $1 trillion.

Reliable? According to the Nuclear Regulatory Commission, the Diablo Canyon Power Plant, which insiders want to keep open, has been down 40 percent of the time over the last three years.

Clean? On the front end of the nuclear cycle, many have died and towns have been bulldozed because of radioactive contamination from the mining and milling of uranium. Nuclear power plants regularly discharge radioactivity into the atmosphere and pump billions of gallons of radioactive waste into rivers and oceans.

On the back end of the cycle, after half a century the nation still has no solution for how to safely store about 100,000 tons of highly radioactive civilian nuclear waste, which will remain lethal for millions of years.

Yes, nuclear power does not make sense, but for more powerful reasons than the claims that it is slow to build and not cost-efficient.

Roger Johnson
San Clemente, Calif.

Now may I ask you to consider some recent important events. First, you must be aware that the coastal train that connects Los Angeles to San Diego has been shut down indefinitely at the Orange and San Diego county border because of beach erosion and coastal instability. The breakdown occurred in south San Clemente, only about 2 miles from the San Onofre nuclear waste ISFSI. If simple structures like railroad tracks next to the beach are in danger, how could anyone assume that thousands of tons of uranium two miles away (and 108 feet from the Pacific Ocean) are safe? See the diagram below and the photo of waves already crashing near the top of the seawall.

Sea Levels at the San Onofre Nuclear Waste Dump

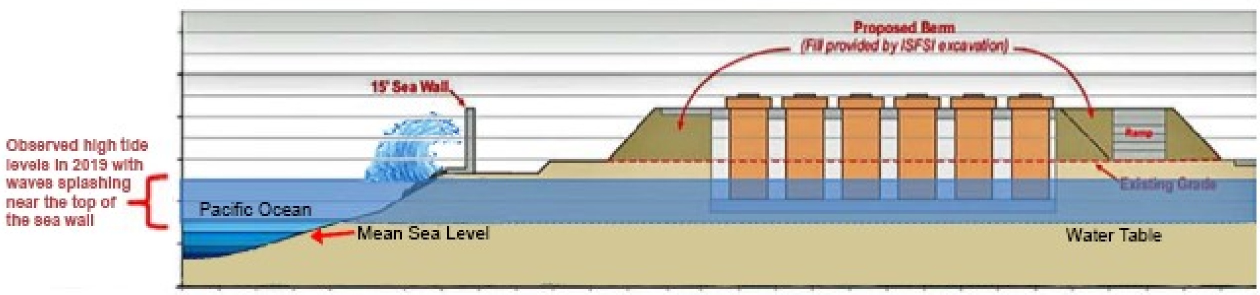

1,773 tons of highly-radioactive nuclear waste are stored 108 feet from the ocean.

Next, may I call your attention to an important recent paper in the scientific journal *Bulletin of the Seismological Society of America:* https://pubs.geoscienceworld.org/ssa/bssa/article-abstract/112/5/2689/615140/Origin-of-the-Palos-Verdes-Restraining-Bend-and For easier reading, here is the LATimes report about it: https://www.latimes.com/california/story/2022-09-23/palos-verdes-fault-could-produce-quake-san-andreas-level-quake-study-shows

This research studied in great detail the Palos Verdes Fault Zone which runs only about 13 miles from San Onofre. New calculations reveal that a major quake is overdue and that it will be 4 times more powerful than previously believed (7.8 vs. 7.4). It warns of possible massive destruction up and down the coast. Keep in mind that San Onofre was designed to withstand a mere 6.5 quake, then retrofitted for a possible 7.0 quake. Is it safe to assume that this will get your attention? Perhaps this is by far the biggest threat ever to coastal California?

Everyone in California looks forward to your leadership and decisive statements and actions.

Roger Johnson, PhD

Professor Emeritus

San Clemente, CA

Oct. 7, 2022

Wyer, Holly@Coastal

From: Bart Ziegler <bziegler@toxco.net>
Sent: Friday, October 7, 2022 4:47 PM
To: SanOnofreComments@Coastal
Cc: Hannah Burns SLF
Subject: CCC hearing notice on permit amendment, San Onofre

Dear Commissioners,

The California Coastal Commission (CCC) is created to protect the coastline for the people of California, and the Coastal Commission does not address nuclear safety and nuclear radiation. With respect to CCC purview, we will not talk about nuclear safety or nuclear radiation, but we well understand the link between a natural or man made event to render the sacred California coast inaccessible forever.

The Coastal Commission report we address below speaks to aging management of the nuclear waste dump site's sea level rise, tsunami, seismic earthquakes, bluff erosion, el nino, and more. We restrict our written comments below to the CCC per view and these factual points:

1. Seismic risks from the original San Onofre 2010 study spoke of 0.77 G force design basis earthquake. The 53 casks the NUHOMS storage system are built to withstand 1.5 G. The recent Harvard earthquake study suggests proximal fault lines can reach a 7.8 magnitude earthquake, versus the 7.4G of the original San Onofre design. This is a 4x increase in severity from the original design base. At 0.77 G x 4 = 3.08 G force is greater than the G force the NUHOMS canisters were designed. The potential earthquake damage is so huge as to present a significant problem for stewards of our California coast. The latest CCC report analysis gave no report on the depth of the earthquake faults. Also a 7.4 magnitude seismic modeling program ought to address underlying assumptions. A seismologist can better interpret seismic forces involved, with respect to depth of earthquake, the condition of the geology, in light of the recent seismological study.

2. The NUHOMS Aging Management Program called for periodic inspections, with most recent completed in November 2021 of the coolest and oldest canister, with the most potential salt air condensation, longest exposure to the corrosion of the marine air. No sign of pitting or corrosion was found, and AMO is up for rereview again in 2024. The public has no idea how well it was inspected. A third party detailed review of the process and video is requested of the CCC.

3. As mentioned in the CCC report, should the canisters not be moved by 2035 then other locations you say are available for this radioactive waste. Your report says the other waste sites "on site, nearby" are +30 to 80 feet more elevated, which will protect the metal cans from sea level rise. A) Can the NUHOMS canisters even be removed from their storage. Has one ever been pulled out of storage? B) Where is that nearby site located? C) Is transportation even possible? If it is across the freeway then will the roadways which are old and of questionable condition for such tremendous weight actually allow for transportation, nearby?

Certainly there must be a link between seismic earthquake risk and safety when it comes to radioactivity and catastrophe. We do not agree with approval of this study report until a third party is called in to review. Thank you for your attention and concern.

Bart Ziegler, PhD

Bart Ziegler PhD, Community and Environmental Medicine
President, The Samuel Lawrence Foundation
P.O. Box F, Del Mar, CA 92014 USA
Office 858.481.1673 | Mobile 619.300.1097
Website | Instagram | Twitter | Facebook | LinkedIn
Read about SLF's impact in our 2020 Annual Report

Samuel Lawrence Foundation is a 501(c)(3) organization, Tax ID 27-1030462